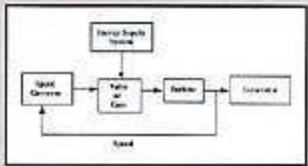


Electric Systems, Dynamics, and Stability with Artificial Intelligence Applications



James A. Momoh
Mohamed E. El-Hawary

Electric Systems, Dynamics, and Stability with Artificial Intelligence Applications

James A. Momoh

*Howard University
Washington, D.C.*

Mohamed E. El-Hawary

*Dalhousie University
Halifax, Nova Scotia, Canada*



MARCEL DEKKER, INC.

NEW YORK • BASEL

ISBN: 0-8247-0233-6

This book is printed on acid-free paper.

Headquarters

Marcel Dekker, Inc.
270 Madison Avenue, New York, NY 10016
tel: 212-696-9000; fax: 212-685-4540

Eastern Hemisphere Distribution

Marcel Dekker AG
Hutgasse 4, Postfach 812, CH-4001 Basel, Switzerland
tel: 41-61-261-8482; fax: 41-61-261-8896

World Wide Web

<http://www.dekker.com>

The publisher offers discounts on this book when ordered in bulk quantities. For more information, write to Special Sales/Professional Marketing at the headquarters address above.

Copyright © 2000 by Marcel Dekker, Inc. All Rights Reserved.

Neither this book nor any part may be reproduced or transmitted in any form or by any means, electronic or mechanical, including photocopying, microfilming, and recording, or by any information storage and retrieval system, without permission in writing from the publisher.

Current printing (last digit):

10 9 8 7 6 5 4 3 2 1

PRINTED IN THE UNITED STATES OF AMERICA

To Felicia, for the amazing grace, and Omeiza.
Ojirese, Eshovo, and Toyin, joy of life.

—JAM

To Ferial, thanks for your company.
Bob, Ron, and Betty, you make me happy.

—MEE

This page intentionally left blank

Series Introduction

Power engineering is the oldest and most traditional of the various areas within electrical engineering, yet no other facet of modern technology is currently undergoing a more dramatic revolution in both technology and industry structure. Among the most exciting changes are those where new solutions are being applied to classical problem areas.

System dynamics and stability engineering have been crucial elements of power system engineering since early in the twentieth century. Smooth, continuous operation of modern power supply systems depends greatly on the accurate anticipation of interconnected equipment, dynamic behavior, and correct identification of the system's operating limits. Proper engineering requires precise methods that can manage that knowledge and direct it to the design of economical and secure power systems. Artificial intelligence offers an exciting new basis for performing dynamic modeling and stability analysis, one that can provide considerable value and new insight to these often difficult aspects of power system performance.

Electric Systems, Dynamics, and Stability with Artificial Intelligence Applications is an exceedingly comprehensive and practical guide to both power system dynamics and stability concepts, and to the use of artificial intelligence in their modeling and engineering. Drs. Momoh and El-Hawary provide a comprehensive introduction to power system dynamics and stability, along with a thorough discussion of recently developed concepts such as transient energy func-

tions. Their book is rich in its appreciation of the intricate operating constraints and issues that real-world power system engineers and operators must face every day. But what sets this book apart is its application of artificial intelligence to these long-recognized power system engineering challenges. Chapters 7–9 explain how neural networks, expert systems using knowledge-based frameworks, and fuzzy logic can be applied to the solution of some of the thorniest problems in power system dynamics.

Like all books in Marcel Dekker's Power Engineering series, *Electric Systems, Dynamics, and Stability with Artificial Intelligence Applications* presents modern power technology in a context of proven, practical applications; useful as a reference book as well as for self-study and classroom use. Marcel Dekker's Power Engineering series will eventually include books covering the entire field of power engineering, in all of its specialties and sub-genres, all aimed at providing practicing power engineers with the knowledge and techniques they need to meet the electric industry's challenges in the twenty-first century.

H. Lee Willis

Preface

The intention of this book is to offer the reader a firm foundation for understanding and analyzing power system dynamics and stability problems as well as the application of artificial intelligence technology to these problems. Issues in this area are extremely important not only for real-time operational considerations, but also in planning, design, and operational scheduling. The significance of dynamics and stability studies grows as interconnected systems evolve to meet the requirements of a competitive and deregulated operational environment. The complexities introduced give rise to new types of control strategies based on advances in modeling and simulation of the power system.

The material presented in this book combines the experience of the authors in teaching and research at a number of schools and professional development venues. The work reported here draws on experience gained in conducting research sponsored by the Electric Power Research Institute, the National Science Foundation, the Department of Energy, and NASA for Dr. Momoh. Dr. El-Hawary's work was supported by the Natural Sciences and Engineering Research Council of Canada and Canadian Utilities Funding.

This book is intended to meet the needs of practicing engineers involved in the electric power utility business, as well as graduate students and researchers. It provides necessary fundamentals, by explaining the practical aspects of artificial intelligence applications and offering an integrated treatment of the evolution of modeling techniques and analytical tools.

Chapter 1 discusses the structure of interconnected power systems, foundations of system dynamics, and definitions for stability and security assessment. Chapter 2 deals with static electric network models and synchronous machine representation and its dynamics. Limits for operations of a synchronous machine and static load models are discussed as well. Chapter 3 deals with dynamic models of the electric network including the excitation, and prime mover and governing system models. The chapter concludes with a discussion of dynamic load models.

Chapter 4 covers concepts of dynamic security assessment based on transient stability evaluation. This chapter includes both conventional and extended formulations of the problem. Chapter 5, a complement to Chapter 4, treats the more recent approach of angle stability assessment via the transient energy function idea. Chapter 6 introduces the idea of voltage stability and discusses techniques for its assessment.

Chapters 7 through 9 are devoted to an exposé of artificial intelligence technology and its application to problems of system stability, from both the angle and the voltage sides. In Chapter 7, we introduce basic concepts of artificial neural networks, knowledge-based systems, and fuzzy logic. In Chapter 8, we deal with the application of artificial intelligence to angle stability problems, and the extension to voltage stability is presented in Chapter 9. Chapter 10 offers conclusions and directions for future work in this field.

In developing this book, we have benefited from input from many of our students, colleagues, and associates. While they are too many to count, we wish to mention specifically encouragement by H. Lee Willis, the editor of the Power Engineering Series for Marcel Dekker, Inc. The continual counsel and prodding of B. J. Clark was extremely helpful. We acknowledge the able administrative support of Linda Schonberg and the assistance of our respective deans.

We are grateful to Dr. Chieh for the great inspiration and generous contributions, and to many others, whose names are not included, in the development of this volume. Our students, both present and former, contributed their time and many valuable suggestions. Many thanks to them and especially to the young research assistants at the Center for Energy Systems and Control for putting up with the burdensome challenge of producing this book just in time.

Finally, the book would not have been published without the help of our Creator and the support of our families.

*James A. Momoh
Mohamed E. El-Hawary*

Contents

| | | |
|--|---------------|-----------|
| <i>Series Introduction</i> | H. Lee Willis | v |
| <i>Preface</i> | | vii |
| 1 Introduction | | 1 |
| 1.1 Historical Background | | 1 |
| 1.2 Structure at a Generic Electric Power System | | 3 |
| 1.3 Power System Security Assessment | | 7 |
| 2 Static Electric Network Models | | 10 |
| Introduction | | 10 |
| 2.1 Complex Power Concepts | | 11 |
| 2.2 Three-Phase Systems | | 14 |
| 2.3 Synchronous Machine Modeling | | 21 |
| 2.4 Reactive Capability Limits | | 31 |
| 2.5 Static Load Models | | 32 |
| Conclusions | | 35 |
| 3 Dynamic Electric Network Models | | 36 |
| Introduction | | 36 |
| 3.1 Excitation System Model | | 36 |
| 3.2 Prime Mover and Governing System Models | | 40 |

| | |
|--|------------|
| 3.3 Modeling of Loads | 43 |
| Conclusions | 44 |
| 4 Philosophy of Security Assessment | 45 |
| Introduction | 45 |
| 4.1 The Swing Equation | 46 |
| 4.2 Some Alternative Forms | 47 |
| 4.3 Transient and Subtransient Reactances | 50 |
| 4.4 Synchronous Machine Model in Stability Analysis | 55 |
| 4.5 Subtransient Equations | 59 |
| 4.6 Machine Models | 59 |
| 4.7 Groups of Machines and the Infinite Bus | 63 |
| 4.8 Stability Assessment | 63 |
| 4.9 Concepts in Transient Stability | 68 |
| 4.10 A Method for Stability Assessment | 71 |
| 4.11 Mathematical Models and Solution Methods in Transient Stability Assessment for General Networks | 82 |
| 4.12 Integration Techniques | 89 |
| 4.13 The Transient Stability Algorithm | 98 |
| Conclusions | 108 |
| 5 Assessing Angle Stability via Transient Energy Function | 109 |
| Introduction | 109 |
| 5.1 Stability Concepts | 110 |
| 5.2 System Model Description | 117 |
| 5.3 Stability of a Single-Machine System | 118 |
| 5.4 Stability Assessment for n -Generator System by the TEF Method | 121 |
| 5.5 Application to a Practical Power System | 125 |
| 5.6 Boundary of the Region of Stability | 127 |
| Conclusion | 131 |
| 6 Voltage Stability Assessment | 132 |
| Introduction | 132 |
| 6.1 Working Definition of Voltage Collapse Study Terms | 134 |
| 6.2 Typical Scenario of Voltage Collapse | 135 |
| 6.3 Time-Frame Voltage Stability | 136 |
| 6.4 Modeling for Voltage Stability Studies | 136 |
| 6.5 Voltage Collapse Prediction Methods | 138 |
| 6.6 Classification of Voltage Stability Problems | 138 |
| 6.7 Voltage Stability Assessment Techniques | 140 |

| | | |
|-----------|---|------------|
| 6.8 | Analysis Techniques for Steady-State Voltage Stability Studies | 145 |
| 6.9 | Parameterization | 151 |
| 6.10 | The Technique of Modal Analysis | 156 |
| 6.11 | Analysis Techniques for Dynamic Voltage Stability Studies | 157 |
| | Conclusion | 169 |
| | Modal Analysis: Worked Example | 170 |
| 7 | Technology of Intelligent Systems | 175 |
| | Introduction | 175 |
| 7.1 | Fuzzy Logic and Decision Trees | 177 |
| 7.2 | Artificial Neural Networks | 177 |
| 7.3 | Robust Artificial Neural Network | 184 |
| 7.4 | Expert Systems | 191 |
| 7.5 | Fuzzy Sets and Systems | 206 |
| 7.6 | Expert Reasoning and Approximate Reasoning | 214 |
| | Conclusion | 220 |
| 8 | Application of Artificial Intelligence to Angle Stability Studies | 221 |
| | Introduction | 221 |
| 8.1 | ANN Application in Transient Stability Assessment | 222 |
| 8.2 | A Knowledge-Based System for Direct Stability Analysis | 238 |
| | Conclusions | 257 |
| 9 | Application of Artificial Intelligence to Voltage Stability Assessment and Enhancement to Electrical Power Systems | 259 |
| | Introduction | 259 |
| 9.1 | ANN-Based Voltage Stability Assessment | 260 |
| 9.2 | ANN-Based Voltage Stability Enhancement | 265 |
| 9.3 | A Knowledge-Based Support System for Voltage Collapse Detection and Prevention | 272 |
| 9.4 | Implementation for KBVCDP | 278 |
| 9.5 | Utility Environment Application | 287 |
| | Conclusion | 287 |
| 10 | Epilogue and Conclusions | 289 |
| | <i>Glossary</i> | 298 |
| | <i>Appendix: Chapter Problems</i> | 311 |
| | <i>Bibliography</i> | 332 |
| | <i>Index</i> | 351 |

This page intentionally left blank

Electric Systems, Dynamics, and Stability with Artificial Intelligence Applications

This page intentionally left blank

1

Introduction

1.1 HISTORICAL BACKGROUND

Electric power has shaped and contributed to the progress and technological advances of humans over the past century. It is not surprising then that the growth of electric energy consumption in the world has been nothing but phenomenal. In the United States, for example, electric energy sales have grown to well over 400 times in the period between the turn of the century and the early 1970s. This growth rate was 50 times as much as the growth rate in all other energy forms used during the same period.

Edison Electric of New York pioneered the central station electric power generation by opening of the Pearl Street station in 1881. This station had a capacity of four 250-hp boilers supplying steam to six engine-dynamo sets. Edison's system used a 110-dc underground distribution network with copper conductors insulated with a jute wrapping. The *low voltage of the circuit* limited the service area of a central station, and consequently central stations proliferated throughout metropolitan areas.

The invention of the transformer, then known as the "inductorium," made ac systems possible. The first practical ac distribution system in the United States was installed by W. Stanley at Great Barrington, Massachusetts, in 1866 for Westinghouse, who acquired the American rights to the transformer from its

British investors Gaulard and Gibbs. Early ac distribution utilized 1000 V overhead lines.

By 1895, Philadelphia had about twenty electric companies with distribution systems operating at 100 V and 500 V two-wire dc and 220 V three-wire dc; single-phase, two-phase, and three-phase ac; with frequencies of 60, 66, 125, and 133 cycles per second; and feeders at 1000–1200 V and 2000–2400 V.

The consolidation of electric companies enabled the realization of economies of scale in generating facilities, the introduction of a certain degree of equipment standardization, and the utilization of the load diversity between areas. Generating unit sizes of up to 1300 MW are in service, an era that was started in 1973 by the Cumberland Station of the Tennessee Valley Authority.

Underground distribution of voltages up to 5 kV was made possible by the development of rubber-base insulated cables and paper insulated, lead-covered cables in the early 1900s. Since that time higher distribution voltages have been necessitated by load growth that would otherwise overload low-voltage circuits and by the requirement to transmit large blocks of power over great distances. Common distribution voltages in today's systems are in 5, 15, 25, 35, and 69 kV voltage classes.

The growth in size of power plants and in the higher voltage equipment was accompanied by interconnections of the generating facilities. These interconnections decreased the probability of service interruptions, made the utilization of the most economical units possible, and decreased the total reserve capacity required to meet equipment-forced outages. This growth was also accompanied by the use of sophisticated analytical tools. Central control of the interconnected systems was introduced for reasons of economy and safety. The advent of the load dispatcher heralded the dawn of power systems engineering, whose objective is to provide the best system to meet the load demand reliably, safely, and economically, utilizing state-of-the-art computer facilities.

Extra high voltage (EHV) has become the dominant factor in the transmission of electric power over great distances. By 1896, an 11 kV three-phase line was transmitting 10 MW from Niagara Falls to Buffalo over a distance of 20 miles. Today, transmission voltages of 230 kV, 287 kV, 345 kV, 500 kV, 735 kV, and 765 kV are commonplace, with the first 1100 kV line scheduled for energization in the early 1990s. One prototype is the 1200 kV transmission tower. The trend is possible, resulting in more efficient use of right-of-way, lower transmission losses, and reduced environmental impact.

The preference for ac was first challenged in 1954 when the Swedish State Power Board energized the 60-mile, 100 kV dc submarine cable utilizing U. Lamm's Mercury Arc valves at the sending and receiving ends of the world's first high-voltage direct current (HVDC) link connecting the Baltic island of Gotland and the Swedish mainland. Today, numerous installations with voltages up to 800 kV dc have become operational around the globe. Solid-state technol-

ogy advances have also enabled the use of the silicon-controlled rectifiers (SCR) of thyristor for HVDC applications since the late 1960s. Whenever cable transmission is required (underwater or in a metropolitan area), HVDC is more economically attractive than ac.

Protecting isolated systems has been a relatively simple task, which is carried out using overcurrent directional relays with selectivity being obtained by time grading. High-speed relays have been developed to meet the increased short-circuit currents due to the larger size units and the complex interconnections.

For reliable service, an electric power system must remain intact and be capable of withstanding a wide variety of disturbances. It is essential that the system be operated so that the more probable contingencies can be sustained without loss of load (except that connected to the faulted element) and so that the most adverse possible contingencies do not result in widespread and cascading power interruptions.

The November 1965 blackout in the northeastern part of the United States and Ontario had a profound impact on the electric utility industry. Many questions were raised and led to the formation of the National Electric Reliability Council in 1968. The name was later changed to the North American Electric Reliability Council (NERC). Its purpose is to augment the reliability and adequacy of bulk power supply in the electricity systems of North America. NERC is composed of nine regional reliability councils and encompasses virtually all the power systems in the United States and Canada. Reliability criteria for system design and operation have been established by each regional council. Since differences exist in geography, load pattern, and power sources, criteria for the various regions differ to some extent.

Design and operating criteria play an essential role in preventing major system disturbances following severe contingencies. The use of criteria ensures that, for all frequently occurring contingencies, the system will, at worst, transmit from the normal state to the alert state, rather than to a more severe state such as the emergency state or the *in extremis* state. When the alert state is entered following a contingency, operators can take action to return the system to the normal state.

1.2 STRUCTURE OF A GENERIC ELECTRIC POWER SYSTEM

While no two electric power systems are alike, all share some common fundamental characteristics including:

1. Electric power is generated using synchronous machines that are driven by turbines (steam, hydraulic, diesel, or internal combustion).

2. Generated power is transmitted from the generating sites over long distances to load centers that are spread over wide areas.
3. Three phase ac systems comprise the main means of generation, transmission and distribution of electric power.
4. Voltage and frequency levels are required to remain within tight tolerance levels to assure a high quality product.

The basic elements of a generic electric power system are displayed in Figure 1.1. Electric power is produced at generating stations (GS) and transmitted to consumers through an intricate network of apparatus including transmission lines, transformers, and switching devices.

Transmission network is classified as the following:

1. Transmission system
2. Subtransmission system
3. Distribution system

The *transmission system* interconnects all major generating stations and main load centers in the system. It forms the backbone of the integrated power system and operates at the highest voltage levels (typically, 230 kV and above). The generator voltages are usually in the range of 11–35 kV. These are stepped up to the transmission voltage level, and power is transmitted to transmission substations where the voltages are stepped down to the subtransmission level (typically, 69 kV to 138 kV). The generation and transmission subsystems are often referred to as the *bulk power system*.

The *subtransmission system* transmits power at a lower voltage and in smaller quantities from the transmission substation to the distribution substations. Large industrial customers are commonly supplied directly from the subtransmission system. In some systems, there expansion and higher voltage levels becoming necessary for transmission, the older transmission lines are often relegated to subtransmission function.

The *distribution system* is the final stage in the transfer of power to the individual customers. The primary distribution voltage is typically between 4.0 kV and 34.5 kV. Small industrial customers are supplied by primary feeders at this voltage level. The secondary distribution feeders supply residential and commercial customers at 120/240 V.

The function of an electric power system is to convert energy from one of the naturally available forms to the electrical form and to transport it to the points of consumption. Energy is seldom consumed in electrical form but is rather converted to other forms such as heat, light, and mechanical energy. The advantage of the electrical form of energy is that it can be transported and controlled with relative ease and with a high degree of efficiency and reliability. A properly designed and operated power system should, therefore, meet the following fundamental requirements:

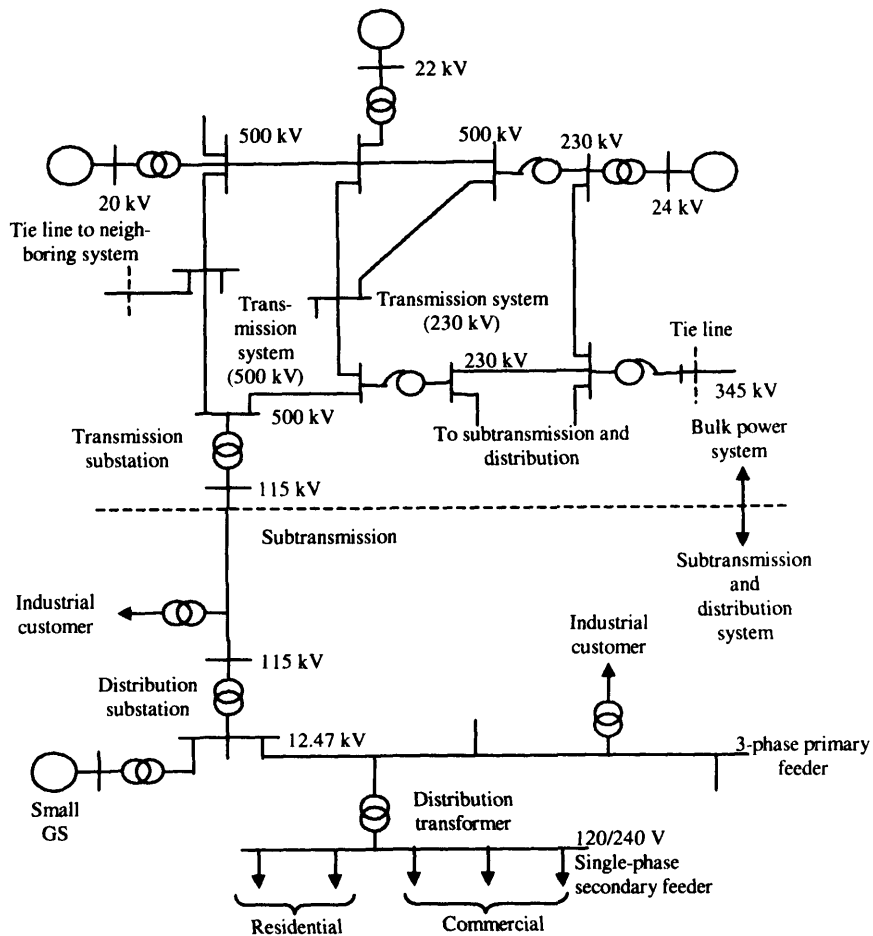


Figure 1.1 Basic elements of a power system.

1. The system must be able to meet the continually changing load demand for active and reactive power. Unlike other types of energy, electricity cannot be conveniently stored in sufficient quantities. Therefore, adequate “spinning” reserve of active and reactive power should be maintained and appropriately controlled at all times.
2. The system should supply energy at minimum cost and with minimum ecological impact.
3. The “quality” of power supply must meet certain minimum standards

with regard to the following factors: (1) constancy of frequency; (2.) constancy of voltage; and (3) level of reliability.

Several levels of controls involving a complex array of devices are used to meet the above requirements. These are depicted in Figure 1.2, which identifies the various subsystems of a power system and the associated controls. In this overall structure, there are controllers operating directly on individual system elements. In a generating unit these consist of prime mover controls and excitation controls. The prime mover controls are concerned with speed regulation and control of energy supply system variables such as boiler pressures, temperatures, and flows. The function of the excitation control is to regulate generator voltage and reactive power output. The desired MW outputs of the individual generating units are determined by the system-generation control.

The primary purpose of the system-generation control is to balance the total system generation against system load and losses so that the desired frequency and power interchange with neighboring systems (tie flows) is maintained.

The transmission controls include power and voltage control devices, such as static var compensators, synchronous condensers, switched capacitors and

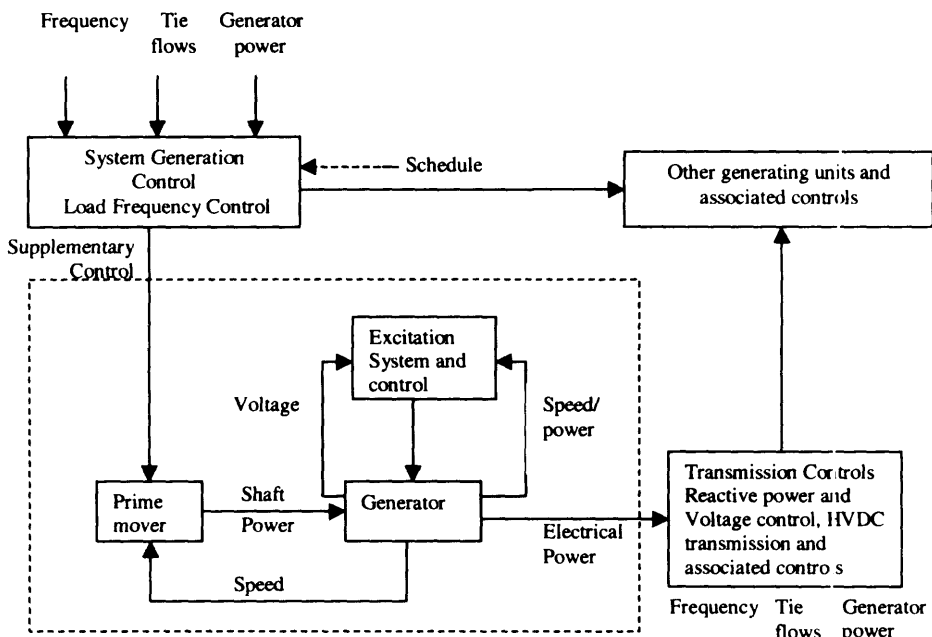


Figure 1.2 Subsystems of a power system and associated controls.

reactors, tap-changing transformers, phase-shifting transformers, and HVDC transmission controls.

These controls described above contribute to the satisfactory operation of the power system by maintaining system voltages and frequency and other system variables within their acceptable limits. They also have a profound effect on the dynamic performance of the power system and on its ability to cope with disturbances.

The control objectives are dependent on the operating state of the power system. Under normal conditions, the control objective is to operate as efficiently as possible with voltages and frequency close to nominal values. When an abnormal condition develops, new objectives must be met to restore the system to normal operation.

Major system failures are rarely the result of a single catastrophic disturbance causing collapse of an apparently secure system. Such failures are usually brought about by a combination of circumstances that stress the network beyond its capability. Severe natural disturbances (such as a tornado, severe storm, or freezing rain), equipment malfunction, human error, and inadequate design combine to weaken the power system and eventually lead to its breakdown. This may result in cascading outages that must be contained within a small part of the system if a major blackout is to be prevented.

1.3 POWER SYSTEM SECURITY ASSESSMENT

The term *Power System Stability* is used to define “the ability of the bulk power electric power system to withstand sudden disturbances such as electric short circuits or unanticipated loss of system components.” In terms of the requirements for the proper planning and operation of the power system, it means that following the occurrence of a sudden disturbance, the power system will:

1. Survive the ensuing transient and move into an acceptable steady-state condition, and
2. In this new steady state condition, all power system components are operating within established limits.

Electric utilities require security analysis to ensure that, for a defined set of contingencies, the above two requirements are met. The analysis required to survive a transient is complex, because of increased system size, greater dependence on controls, and more interconnections. Additional complicating factors include the operation of the interconnected system with greater interdependence among its member systems, heavier transmission loadings, and the concentration of the generation among few large units at light loads.

The second requirement is verified using steady state analysis in what is

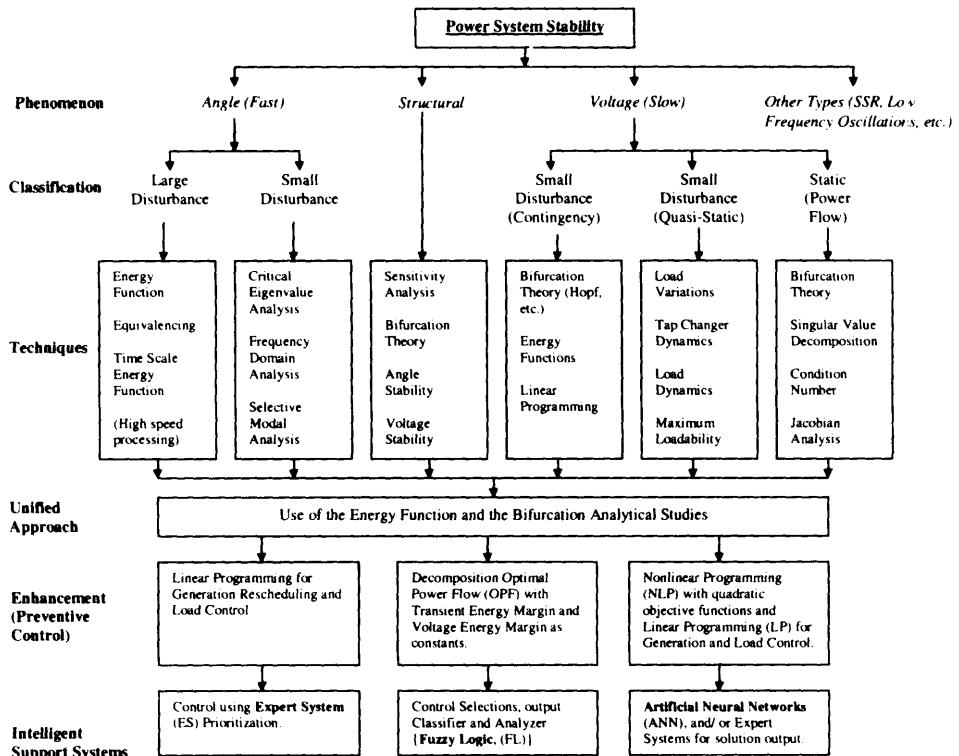


Figure 1.3 Overview of power system stability.

referred to as “static security assessment.” The first requirement is the subject dealt with in “dynamic security assessment.” Dynamic security studies are broadly classified as being either “angle stability studies” or “voltage stability” as depicted in Figure 1.3.

In “angle stability studies,” problems are classified as either “large disturbance” for transient evaluation, or “small disturbance” for steady state stability evaluation. A similar classification for voltage problems is indicated in Figure 1.3. Solution techniques for transient angle stability evaluation include:

- Time domain simulation
- Direct methods
- Hybrid methods
- Probabilistic methods, pattern recognition
- Computational intelligence

Time domain simulation techniques involve judicious use of integration methods such as Runge-Kutta, trapezoidal rule of integration, and waveform relaxation. These methods are particularly useful for off-line transient stability analysis.

On the other hand, in “voltage stability studies,” the problems are classified as “large disturbance” in some contingency cases, “small disturbance” in quasi-static cases, and “static,” which requires solutions to the general power flow (algebraic) equations only. It is as a result of this classification that the solution techniques and requirements are derived. The bifurcation theory, Linear Programming applications, and the use of the energy function are but a few such techniques. Again, the time domain simulations that are involved take advantage of various numerical integration methods mentioned earlier. (The machine dynamics lead to differential equations that are inherently nonlinear.)

The unified approach as indicated on Figure 1.3 is aimed at encompassing the similarities and differences that distinguishes the various techniques used in assessing the stability of the electric power system. This is whether or not the problems are a result of voltage or angle instability. The resulting enhancement that is brought forth by this approach, measurable as a benefit-to-cost index, lies in the development and use of more robust tools for solving present and long-range problems. In this light, various programming and optimization schemes that are applicable include decomposition *Optimal Power Flow* (OPF), *Linear Programming* (LP), and *Quadratic Programming* (QP), with the necessary and sufficient system and network constraints.

Finally, this book introduces three fundamental types of intelligence support systems that truly adds the rigor, value, and robustness to the desired enhancement schemes. These support systems include expert systems (ES), fuzzy logic (FL), and artificial neural network (ANN). Each have their unique characteristics (decision-support, classifiers, learning capabilities, etc.) and are adaptable in providing viable solutions to a variety of voltage/angle instability problems associated with the electric power system. The discussion on this area of artificial intelligence applications to power system stability and dynamics is presented in the final few chapters of this book.

2

Static Electric Network Models

INTRODUCTION

The power industry in the United States has engaged in a changing business environment for some time, by moving away from a centrally planned system to one in which players operate in a decentralized fashion with little knowledge of the full-state of the network, and where decision-making is likely to be market driven rather than through technical considerations alone. This new environment is quite different from the one in which the system operated in the past. This leads to the requirement of new techniques and analysis methods for functions of system operation, operational planning, and long-term planning.

Electrical power systems vary in size, topography and structural components. However, what is consistent is that the overall system can be divided into three subsystems, namely, the generation, transmission, and distribution subsystems. System behavior is affected by the characteristics of each of the major elements of the system. The representation of these elements by means of appropriate mathematical models is critical to successful analysis of system behavior. Due to computational efficiency considerations for each different problem, the system is modeled in a different way. This chapter describes some system models for analysis purposes.

We begin in Section 2.1 by introducing concepts of power expressed as active, reactive, and apparent. This is followed in Section 2.2 by a brief review

of three phase systems. Section 2.3 deals with modeling the synchronous machine from an electric network standpoint. Reactive capability curves are examined in Section 2.4. Static and dynamic load models are discussed in Section 2.5 to conclude the chapter.

2.1 COMPLEX POWER CONCEPTS

In electrical power systems one is mainly concerned with the flow of electrical power in the circuit rather than the currents. As the power into an element is basically the product of the voltage across and current through it, it is reasonable to exchange the current for power without losing any information. In treating sinusoidal steady-state behavior of an electric circuit, some further definitions are necessary. To illustrate, we use a cosine representation of the sinusoidal waveforms involved.

Consider an impedance element $\bar{Z} = Z\angle\phi$. For a sinusoidal voltage, $v(t)$ is given by

$$v(t) = V_m \cos\omega t$$

The instantaneous current in the circuit shown in Fig. 2.1 is

$$i(t) = I_m \cos(\omega t - \phi)$$

where the current magnitude is:

$$I_m = \frac{V_m}{|Z|} = \frac{V_m}{Z}$$

The instantaneous power is given by

$$p(t) = v(t)i(t) = V_m I_m [\cos(\omega t)\cos(\omega t - \phi)]$$

Using the trigonometric identity

$$\cos\alpha \cos\beta = \frac{1}{2}[\cos(\alpha - \beta) + \cos(\alpha + \beta)]$$

we can write the instantaneous power as

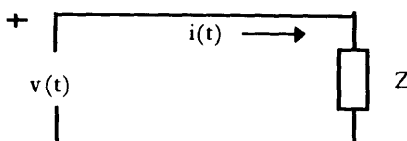


Figure 2.1 Instantaneous current in a circuit.

$$p(t) = \frac{V_m I_m}{2} [\cos\phi + \cos(2\omega t - \phi)]$$

The average power p_{av} is seen to be

$$p_{av} = \frac{V_m I_m}{2} \cos\phi \quad (2.1)$$

Since through 1 cycle, the average of $\cos(2\omega t - \phi)$ is zero, this term contributes nothing to the average of p .

It is more convenient to use the effective (rms) values of voltage and current than the maximum values. Substituting $V_m = \sqrt{2}(V_{rms})$, and $I_m = \sqrt{2}(I_{rms})$, we get

$$p_{av} = V_{rms} I_{rms} \cos\phi \quad (2.2)$$

Thus the power entering any network is the product of the effective values of terminal voltage and current and the cosine of the phase angle between the voltage and current which is called the *power factor* (PF). This applies to sinusoidal voltages and currents only. For a purely resistive load, $\cos\phi = 1$, and the current in the circuit is fully engaged in conveying power from the source to the load resistance. When reactance (inductive or capacitive) as well as resistance are present, a component of the current in the circuit is engaged in conveying energy that is periodically stored in and discharged from the reactance. This stored energy, being shuttled into and out of the magnetic field of an inductance or the electric field of a capacitance, adds to the magnitude of the current in the circuit but does not add to the average power.

The average power in a circuit is called active power, and loosely speaking the power that supplies the stored energy in reactive elements is called reactive power. Active power is denoted by P , and the reactive power, is designated as Q . They are expressed as

$$P = VI\cos\phi \quad (2.3)$$

$$Q = VI\sin\phi \quad (2.4)$$

In both equations, V and I are rms values of terminal voltage and current, and ϕ is the phase angle by which the current lags the voltage.

Both P and Q are of the same dimension, that is in (Joules/s) Watts. However, to emphasize the fact that Q represents the nonactive power, it is measured in reactive voltampere units (var). Larger and more practical units are kilovars and megavars, related to the basic unit by

$$1 M \text{ var} = 10^3 k \text{ var} = 10^6 \text{ var}$$

Assume that V , $V \cos\phi$, and $V \sin\phi$, all shown in Fig. 2.2, are each multiplied by I , the rms value of the current. When the components of voltage $V \cos\phi$

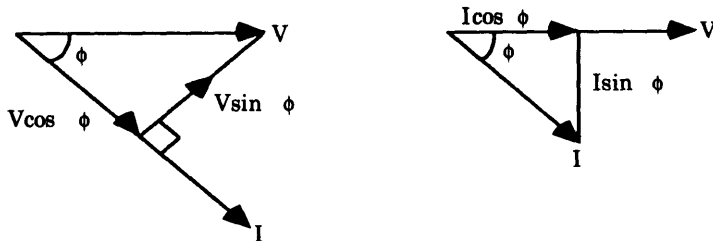


Figure 2.2 Phasor diagrams leading to power triangles.

and $V \sin\phi$ are multiplied by current, they become P and Q respectively. Similarly, if I , $I \cos\phi$, and $I \sin\phi$ are each multiplied by V , they become VI , P , and Q respectively. This defines a power triangle.

We define a quantity called the complex or apparent power, designated S , of which P and Q are orthogonal components. By definition,

$$\begin{aligned} S &= P + jQ = \bar{V}I^* \\ &= VI \cos\phi + jVI \sin\phi \\ &= VI (\cos\phi + j \sin\phi) \end{aligned}$$

Using Euler's identity, we thus have

$$S = VIe^{j\phi}$$

or

$$S = VI\angle\phi$$

If we introduce the conjugate current defined by the asterisk (*)

$$I^* = |I| \angle -\phi$$

it becomes obvious that an equivalent definition of complex or apparent power is

$$S = VI^* \quad (2.5)$$

We can write the complex power in two alternative forms by using the relationships $\bar{V} = Z\bar{I}$ and $\bar{I} = Y\bar{V}$

This leads to

$$S = ZI I^* = Z|I|^2 \quad (2.6)$$

or

$$S = VY^*V^* = Y^*|V|^2 \quad (2.7)$$

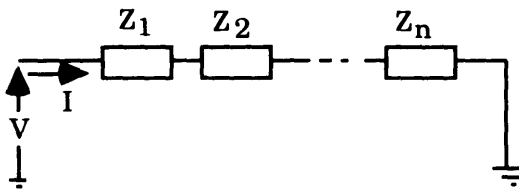


Figure 2.3 Series circuit of n impedances.

Consider the series circuit shown in Fig. 2.3. Here the applied voltage is equal to the sum of the voltage drops:

$$V = I(Z_1 + Z_2 + \dots + Z_n)$$

Multiplying both sides of this relation by I^* results in

$$S = VI^* = II^*(Z_1 + Z_2 + \dots + Z_n)$$

or

$$S = \sum_{i=1}^n S_i \quad (2.8)$$

with

$$S_i = |I|^2 Z_i \quad (2.9)$$

being the individual element's complex power. Equation (2.8) is known as the summation rule for complex powers. The summation rule also applies to parallel circuits. The use of the summation rule and concepts of complex power are advantageous in solving problems of power system analysis.

The phasor diagrams shown in Fig. 2.2 can be converted into complex power diagrams by simply following the definitions relating complex power to voltage and current. Consider the situation with an inductive circuit in which the current lags the voltage by the angle ϕ . The complex conjugate of the current will be in the first quadrant in the complex plane as shown in Fig. 2.4(a).

Multiplying the phasors by V , we obtain the complex power diagram in Fig. 2.4(b). Inspection of the diagram as well as previous development leads to a relation for the power factor of the circuit:

$$\cos\phi = \frac{P}{|S|}$$

2.2 THREE-PHASE SYSTEMS

A significant portion of all the electric power presently used is generated, transmitted, and distributed using balanced three-phase voltage systems. The single-

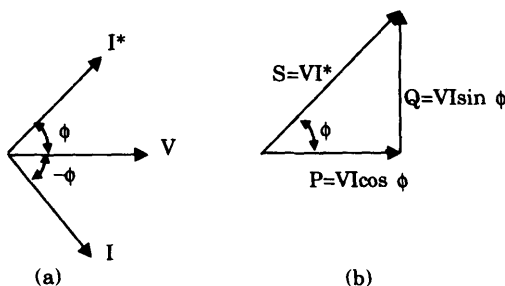


Figure 2.4 Complex power diagram showing the relationship among voltage, current, and power components.

phase voltage sources referred to in the preceding section originate in many instances as part of the three-phase system. Three-phase operation is preferable to single-phase because a three-phase winding makes more efficient use of generator copper and iron. Power flow in single-phase circuits is known to be pulsating. This drawback is not present in a three-phase system as will be shown later. Also, three-phase motors start more conveniently and, having constant torque, run more satisfactorily than single-phase motors. However, the complications of additional phases are not compensated for by the slight increase of operating efficiency when polyphase systems of order higher than three-phase are used.

A balanced three-phase voltage system consists of three single-phase voltages having the same magnitude and frequency but time-displaced from one another by 120° . Figure 2.5(a) shows a schematic representation where the sin-

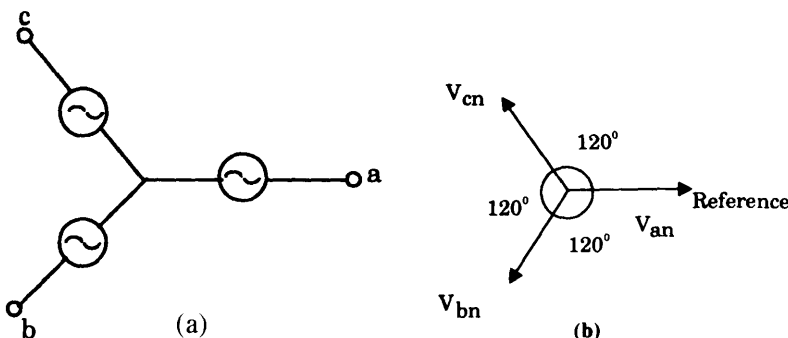


Figure 2.5 (a) A Y-connected three-phase system and (b) the corresponding phasor diagram.

gle-phase voltage sources appear in a wye or Y-connection; a delta or Δ configuration is also possible, as discussed later. A phasor diagram showing each of the phase voltages is also given in Figure 2.5(b). As the phasors rotate at the angular frequency ω with respect to the reference line in the counterclockwise (designated as positive) direction, the positive maximum value first occurs for phase a and then in succession for phases b and c . Stated in a different way, to an observer in the phasor space, the voltage of phase a arrives first followed by that of b and then that of c . For this reason the three-phase voltage of Fig. 2.5 is said to have the phase sequence abc (order, phase sequence, or rotation all mean the same thing). This is important for certain applications. For example, in three-phase induction motors, the phase sequence determines whether the motor rotates clockwise or counterclockwise.

2.2.1 Current and Voltage Relations

Balanced three-phase systems can be studied using techniques developed for single-phase circuits. The arrangement of the three single-phase voltages into a Y or a Δ configuration requires some modifications in dealing with the overall system.

2.2.2 Y-Connection

With reference to Fig. 2.6, the common terminal n is called the neutral or star (Y) point. The voltages appearing between any two of the line terminals a , b , and c have different relationships in magnitude and phase to the voltages appearing between any one line terminal and the neutral point n . The set of voltages V_{ab} , V_{bc} , and V_{ca} are called the line voltages, and the set of voltages V_{an} , V_{bn} , and V_{cn} are referred to as the phase voltages. Consideration of phasor diagrams provides the required relationships.

The effective values of the phase voltages are shown in Fig. 2.6 as V_{an} , V_{bn} , and V_{cn} . Each has the same magnitude, and each is displaced 120° from the other two phasors. To obtain the magnitude and phase angle of the line voltage from a to b (i.e., V_{ab}), we apply Kirchhoff's voltage law:

$$V_{ab} = V_{an} + V_{bn} \quad (2.10)$$

This equation states that the voltage existing from a to b is equal to the voltage from a to n (i.e., V_{an}) plus the voltage from n to b . Thus Eq. (2.10) can be rewritten as

$$V_{ab} = V_{an} - V_{bn} \quad (2.11)$$

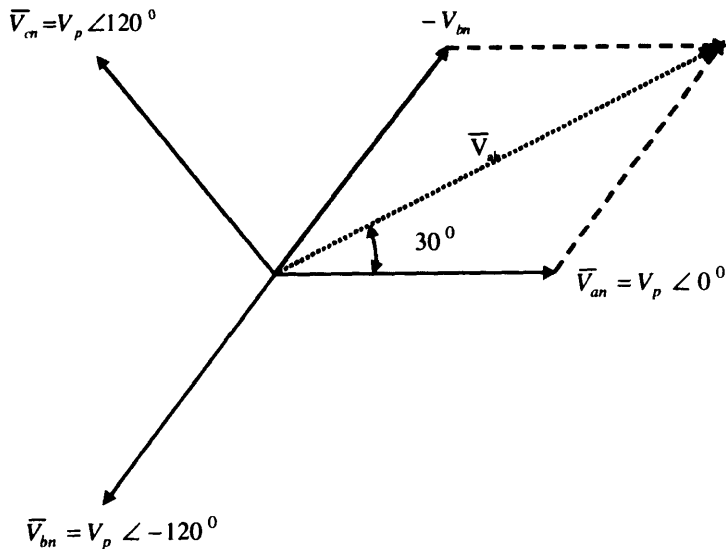


Figure 2.6 Illustration of the phase and magnitude relations between the phase and line voltage of a Y-connection.

Since for a balanced system, each phase voltage has the same magnitude, let us set

$$|V_{an}| = |V_{bn}| = |V_{cn}| = V_p \quad (2.12)$$

where V_p denotes the effective magnitude of the phase voltage. Accordingly we may write

$$V_{an} = V_p \angle 0^\circ \quad (2.13)$$

$$V_{bn} = V_p \angle -120^\circ \quad (2.14)$$

$$V_{cn} = V_p \angle -240^\circ = V_p \angle 120^\circ \quad (2.15)$$

Substituting Eqs. (2.13) and (2.14) in Eq. (2.11) yields

$$\begin{aligned} V_{ab} &= V_p (1 - 1 \angle -120^\circ) \\ &= \sqrt{3} V_p \angle 30^\circ \end{aligned} \quad (2.16)$$

Similarly we obtain

$$V_{bc} = \sqrt{3} V_p \angle -90^\circ \quad (2.17)$$

$$V_{ca} = \sqrt{3} V_p \angle 150^\circ \quad (2.18)$$

The expressions obtained above for the line voltages show that they constitute a balanced three-phase voltage system whose magnitudes are $\sqrt{3}$ times those of the phase voltages. Thus we write

$$V_L = \sqrt{3} V_p \quad (2.19)$$

A current flowing out of a line terminal a (or b or c) is the same as that flowing through the phase source voltage appearing between terminals n and a (or n and b or n and c). We can thus conclude that for a Y-connected three-phase source, the line current equals the phase current. Thus

$$I_L = I_p \quad (2.20)$$

In the above equation, I_L denotes the effective value of the line current and I_p denotes the effective value for the phase current.

2.2.3 Δ-Connection

We now consider the case when the three single-phase sources are rearranged to form a three-phase Δ -connection as shown in Fig. 2.7. It is clear from inspection of the circuit shown that the line and phase voltages have the same magnitude:

$$|V_L| = |V_p| \quad (2.21)$$

The phase and line currents, however are not identical, and the relationship between them can be obtained by using Kirchhoff's current law at one of the line terminals.

In a manner similar to that adopted for the Y-connected source, let us consider the phasor diagram shown in Fig. 2.8. Assume the phase currents to be

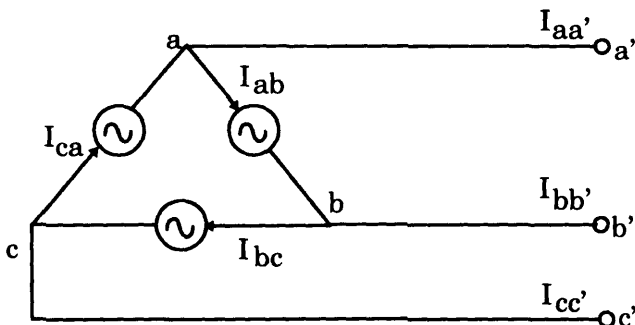


Figure 2.7 A Δ -connected three-phase source.

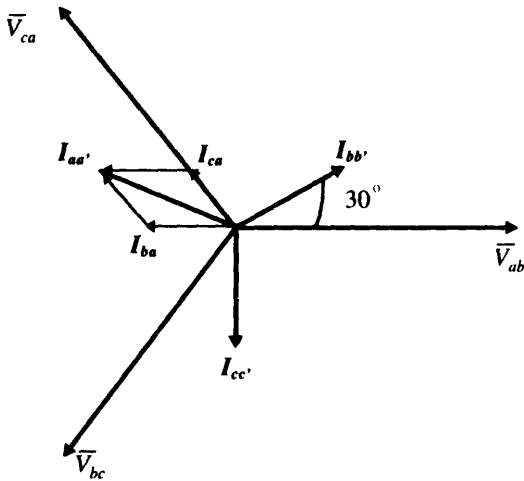


Figure 2.8 Illustration of the relation between phase and line currents in a Δ -connection.

$$I_{ab} = I_p \angle 0^\circ$$

$$I_{bc} = I_p \angle -120^\circ$$

$$I_{ca} = I_p \angle 120^\circ$$

The current that flows in the line joining a to a' is denoted by $I_{aa'}$ and is given by

$$I_{aa'} = I_{ca} - I_{ab}$$

As a result, we have

$$I_{aa'} = I_p [1 \angle 120^\circ - 1 \angle 0]$$

which simplifies to

$$I_{aa'} = \sqrt{3} I_p \angle 150^\circ$$

Similarly,

$$I_{bb'} = \sqrt{3} I_p \angle 30^\circ$$

$$I_{cc'} = \sqrt{3} I_p \angle -90^\circ$$

Note that a set of balanced three-phase currents yields a corresponding set of balanced line currents whose magnitudes are $\sqrt{3}$ times the magnitudes of the phase values:

$$I_L = \sqrt{3} I_p$$

where I_L denotes the magnitude of any of the three line currents.

2.2.4 Power Relationships

Assume that a three-phase generator is supplying a balanced load with the three sinusoidal phase voltages:

$$\begin{aligned} v_a(t) &= \sqrt{2} V_p \sin(\omega t) \\ v_b(t) &= \sqrt{2} V_p \sin(\omega t - 120^\circ) \\ v_c(t) &= \sqrt{2} V_p \sin(\omega t + 120^\circ) \end{aligned}$$

With the currents given by

$$\begin{aligned} i_a(t) &= \sqrt{2} I_p \sin(\omega t - \phi) \\ i_b(t) &= \sqrt{2} I_p \sin(\omega t - 120^\circ - \phi) \\ i_c(t) &= \sqrt{2} I_p \sin(\omega t + 120^\circ - \phi) \end{aligned}$$

where ϕ is the phase angle between the current and voltage in each phase. The total power in the load is

$$P_{\text{tot}}(t) = v_a(t)i_a(t) + v_b(t)i_b(t) + v_c(t)i_c(t)$$

This turns out to be expanded as:

$$\begin{aligned} P_{\text{tot}}(t) &= 2V_p I_p [\sin(\omega t)\sin(\omega t - \phi) \\ &\quad + \sin(\omega t - 120^\circ)\sin(\omega t - 120^\circ - \phi) \\ &\quad + \sin(\omega t + 120^\circ)\sin(\omega t + 120^\circ - \phi)] \end{aligned}$$

Using a trigonometric identity, we get

$$\begin{aligned} P_{\text{tot}}(t) &= V_p I_p \{ 3\cos\phi - [\cos(2\omega t - \phi) + \cos(2\omega t - 240^\circ - \phi) \\ &\quad + \cos(2\omega t + 240^\circ - \phi)] \} \end{aligned}$$

Note that the last three terms in the above equation add up to zero. Thus we obtain

$$P_{\text{tot}}(t) = 3V_p I_p \cos\phi$$

When referring to the voltage level of a three-phase system, by convention, one invariably understands the line voltages. From the above discussion, the relationship between the line and phase voltages in a Y-connected system is

$$|V_L| = \sqrt{3} |V|$$

The power equation thus reads in terms of line quantities:

$$P_{3\phi} = \sqrt{3} |V_L| |I_L| \cos \phi$$

We note that the total instantaneous power is constant, having a magnitude of three times the real power per phase.

We may be tempted to assume that the reactive power is of no importance in a three-phase system since the Q terms cancel out. However, this situation is analogous to the summation of balanced three-phase currents and voltages that also cancel out. Although the sum cancels out, these quantities are still very much in evidence within each phase.

We extend the concept of complex or apparent power (S) to three-phase systems by defining

$$S_{3\phi} = 3 V_L I_L^*$$

where the active and reactive powers are obtained from

$$S_{3\phi} = P_{3\phi} + j Q_{3\phi}$$

as

$$P_{3\phi} = 3 |V_L| |I_L| \cos \phi$$

$$Q_{3\phi} = 3 |V_L| |I_L| \sin \phi$$

In terms of line values, we can assert that

$$S_{3\phi} = \sqrt{3} V_L I_L^*$$

and

$$P_{3\phi} = \sqrt{3} |V_L| |I_L| \cos \phi$$

$$Q_{3\phi} = \sqrt{3} |V_L| |I_L| \sin \phi$$

2.3 SYNCHRONOUS MACHINE MODELING

In power system stability analysis, there are several types of models used for representing the dynamic behavior of the synchronous machine. These models are deduced by using some approximations to the basic machine equations. This section gives a brief introduction to synchronous machine equations.

2.3.1 Stator and Rotor Voltage Equations

In developing performance equations of a synchronous machine, the following assumptions are made:

1. The stator windings are sinusoidally distributed along the air-gap as far as the mutual inductance effects with the rotor are concerned.
2. The stator slots cause no appreciable variation of the rotor inductances with rotor position.
3. Magnetic hysteresis is negligible.
4. Magnetic saturation effects are negligible.

Based on these assumptions, a synchronous machine can be represented by six windings as shown in Fig. 2.9. The stator circuit consists of three-phase armature windings carrying alternating currents. The rotor circuit consists of field and amortisseur windings. The positive direction of a stator winding current is assumed to be into the machine.

The voltage equations of the three-phase armature windings are:

$$\begin{aligned} e_a &= \frac{d\Psi_a}{dt} - R_a i_a \\ e_b &= \frac{d\Psi_b}{dt} - R_b i_b \\ e_c &= \frac{d\Psi_c}{dt} - R_c i_c \end{aligned} \quad (2.22)$$

Rotation

ω_r elec. rad/s

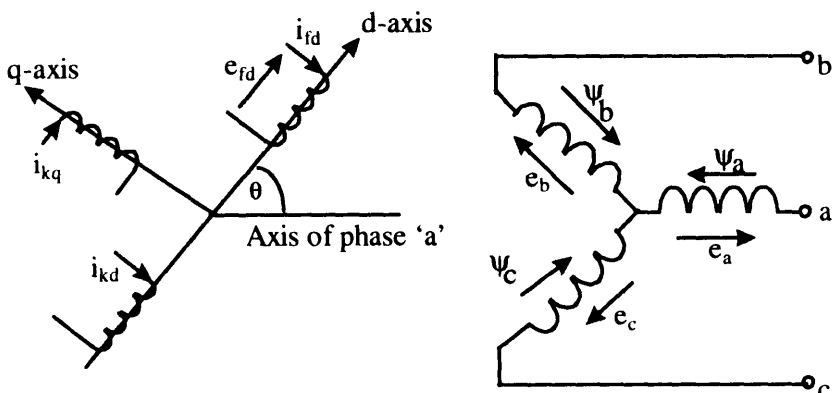


Figure 2.9 Stator and rotor circuits of a synchronous machine. a, b, c : Stator phase windings; fd : field winding; kd : d-axis armature circuit; kq : q-axis armature circuit; $k = 1, 2, \dots, n$; n = number of armature circuits; θ = angle by which d-axis leads the magnetic axis of phase a winding, electrical radians; ω_r = rotor angular velocity, electrical rad/s.

The flux linkages in the phase a, b, c windings at any instant are given by

$$\begin{aligned}\Psi_a &= L_{aa}i_a - L_{ab}i_b - L_{ac}i_c + L_{afd}i_{fd} + L_{akd}i_{kd} + L_{akq}i_{kq} \\ \Psi_b &= L_{ba}i_a - L_{bb}i_b - L_{bc}i_c + L_{bfd}i_{fd} + L_{bkd}i_{kd} + L_{bkq}i_{kq} \\ \Psi_c &= L_{ca}i_a - L_{cb}i_b - L_{cc}i_c + L_{cfi}i_{fd} + L_{ckd}i_{kd} + L_{ckq}i_{kq}\end{aligned}\quad (2.23)$$

where

L_{aa}, L_{bb}, L_{cc} are self-inductance of abc windings.

$L_{ab}, L_{ac}, L_{ba}, L_{bc}, L_{ca}, L_{cb}$ are mutual inductances between two stator winding (ab, bc, ac)

$L_{afd}, L_{bfd}, L_{cfi}$ are mutual inductances between stator and fields windings

$L_{akd}, L_{bkd}, L_{ckd}$ are mutual inductances between stator winding and d-axis armature circuit

$L_{akq}, L_{bkq}, L_{ckq}$ are mutual inductances between stator windings and q-axis armature circuit.

The rotor circuit voltage equations are given by:

$$\begin{aligned}e_{fd} &= \frac{d\Psi_{fd}}{dt} + R_{fd}i_{fd} \\ 0 &= \frac{d\Psi_{kd}}{dt} + R_{kd}i_{kd} \\ 0 &= \frac{d\Psi_{kq}}{dt} + R_{kq}i_{kq}\end{aligned}\quad (2.24)$$

The rotor circuit flux linkages are given by

$$\begin{aligned}\Psi_{fd} &= L_{ffd}i_{fd} + L_{fkd}i_{kd} - L_{akd}i_b - L_{bkd}i_b - L_{ckd}i_c \\ \Psi_{kd} &= L_{kfd}i_{fd} + L_{kkd}i_{kd} - L_{akd}i_a - L_{bkd}i_b - L_{ckd}i_c \\ \Psi_{kq} &= L_{kkq}i_{kq} - L_{akq}i_a - L_{bkq}i_b - L_{ckq}i_c\end{aligned}\quad (2.25)$$

Equations (2.22) and (2.23) associated with the stator circuits together with equations (2.24) and (2.25) associated with the rotor circuits completely describe the electrical performance of a synchronous machine.

The fact that mutual and self inductances of the stator circuits vary with rotor position q which in turn varies with time, complicates the synchronous machine Eqs. (2.22) to (2.25). The variations in inductances are caused by the variations in the permeance of the magnetic flux path due to nonuniform air gap. This is pronounced in a salient pole machine in which the permeances along the two axes are significantly different. Even in a round rotor machine there are differences between the two axes due mostly to the large number of slots associated with the field winding.

The self and mutual inductances of the stator circuits are given by

$$L_{d0} = L_{d0(0)} + L_{d0(2)} \cos 2\theta$$

$$L_{d0} = L_{d0(0)} + L_{d0(2)} \cos 2\left[\theta - \frac{2\pi}{3}\right]$$

$$L_{d0} = L_{d0(0)} + L_{d0(2)} \cos 2\left[\theta + \frac{2\pi}{3}\right]$$

$$L_{q0} = L_{q0(0)} = -L_{d0(0)} + L_{d0(2)} \cos\left[2\theta - \frac{2\pi}{3}\right]$$

$$L_{q0} = L_{q0(0)} = -L_{d0(0)} + L_{d0(2)} \cos\left[2\theta - \frac{2\pi}{3}\right]$$

$$L_{q0} = L_{q0(0)} = -L_{d0(0)} + L_{d0(2)} \cos\left[2\theta - \frac{2\pi}{3}\right] \quad (2.26)$$

2.3.2 The dq0 Transformation

The fact that the self and mutual inductances are not constant introduces considerable complexity in solving machine and power systems problems. A much simpler form leading to a clearer physical picture is obtained by appropriately transforming stator variables to an alternative form by introducing the dq0 transformation defined by

$$\begin{bmatrix} f_d \\ f_q \\ f_0 \end{bmatrix} = \frac{2}{3} \begin{bmatrix} \cos\theta & \cos\left(\theta - \frac{2\pi}{3}\right) & \cos\left(\theta + \frac{2\pi}{3}\right) \\ -\sin\theta & -\sin\left(\theta - \frac{2\pi}{3}\right) & -\sin\left(\theta + \frac{2\pi}{3}\right) \\ \frac{1}{2} & \frac{1}{2} & \frac{1}{2} \end{bmatrix} \begin{bmatrix} f_a \\ f_b \\ f_c \end{bmatrix} \quad (2.27)$$

The equations which describe the synchronous machine in dq0 components become

$$e_d = \frac{d\Phi_d}{dt} - \Phi_d \omega - R_d i_d$$

$$e_q = \frac{d\Phi_q}{dt} + \Phi_q \omega - R_q i_q$$

$$e_0 = \frac{d\Phi_0}{dt} - R_0 i_0 \quad (2.28)$$

$$\psi_d = -L_d i_d + L_{qd} i_{qd} + L_{q0d} i_{q0d}$$

$$\begin{aligned}\psi_q &= -L_q i_q + L_{oq} i_{kq} \\ \psi_0 &= -L_0 i_0\end{aligned}\quad (2.29)$$

where

$$\begin{aligned}L_d &= L_{ad0} + L_{abd} + \frac{3}{2} L_{aad2} \\ L_q &= L_{ad0} + L_{abd} - \frac{3}{2} L_{aad2} \\ L_0 &= L_{ad0} - 2 L_{abd} \\ \psi_{fd} &= L_{qfd} i_{fd} + L_{kfd} i_{kd} - \frac{3}{2} L_{ofd} i_d \\ \psi_{kd} &= L_{kld} i_{kd} + L_{kdl} i_{ld} - \frac{3}{2} L_{okd} i_d \\ \psi_{kq} &= L_{kkq} i_{kq} - \frac{3}{2} L_{okq} i_q\end{aligned}\quad (2.30)$$

All the inductances expressed as dq0 components are seen to be constant, i.e., they are independent of the rotor position. It is interesting to note that i_0 does not appear in the rotor flux linkage equation. This is because the zero sequence components of armature current do not produce net mmf across the air-gap.

While the dq0 transformation has resulted in constant inductances in Eqs. (2.28) to (2.30), the mutual inductances between stator and rotor quantities are not. For example, the mutual inductance associated with the flux linking the field winding due to current i_d flowing in the d-axis stator winding from equation (2.30) is $(3/2) L_{ofd}$, whereas from equation (2.29) the mutual inductance associated with flux in the d-axis stator winding due to field current is L_{ofd} . This difficulty is overcome by an appropriate choice of the per unit system for the rotor quantities.

2.3.3 Per Unit Representation

It is usually convenient to use a per unit system to normalize system variables, to offer computational simplicity by eliminating units and expressing system quantities as dimensionless ratios. Thus

$$\bar{X}_{(\text{in per unit})} = \frac{X_{(\text{actual quantity})}}{X_{(\text{base value of equation})}}$$

A well-chosen per unit system can minimize computational effort, simplify evaluation, and facilitate understanding of system characteristics. Some base quantities may be chosen independently and quite arbitrarily, while others fol-

low automatically depending on the fundamental relationships between system variables. Normally, the base values are chosen so that the principal variables will be equal to one per unit under rated operating conditions.

In the case of a synchronous machine, the per unit system may be used to remove arbitrary constants and simplify mathematical equations so that they may be expressed in terms of equivalent circuits. The basis for selecting the per unit system for the stator is straightforward, while it requires careful consideration for the rotor. The L_{au} -base reciprocal per unit system will be discussed here.

The following base quantities for the stator are chosen (denoted by subscripts)

$$e_{\text{base}} = \text{peak value of rated line-to-line voltage, V}$$

$$i_{\text{base}} = \text{peak value of rated line-to-line current, A}$$

$$f_{\text{base}} = \text{rated frequency, Hz}$$

The base value of each of the remaining quantities are automatically set and depend on the above as follows:

$$\omega_{\text{base}} = 2\pi f_{\text{base}}, \text{ electrical rad/s}$$

$$\omega_{\text{mibase}} = \psi_{\text{base}} \frac{2}{\pi f}, \text{ mechanical rad/s}$$

$$Z_{\text{base}} = \frac{e_{\text{base}}}{i_{\text{base}}}, \text{ ohms}$$

$$L_{\text{base}} = \frac{e_{\text{base}}}{\omega_{\text{base}}}, \text{ henrys}$$

$$\psi_{\text{base}} = L_{\text{base}} \times i_{\text{base}} = \frac{e_{\text{base}}}{\omega_{\text{mibase}}}, \text{ weber-turns}$$

$$VA_{3\phi,\text{base}} = 3E_{\text{RMS base}} I_{\text{RMS base}}$$

$$= \frac{3}{2} e_{\text{base}} \times i_{\text{base}} \text{ volt-amperes}$$

$$\text{Torque base} = \frac{VA_{3\phi,\text{base}}}{\omega_{\text{mibase}}}$$

$$\text{Time base } (t_{\text{base}}) = \frac{1}{\omega_{\text{base}}} = \frac{1}{2\pi f_{\text{base}}}$$

The stator voltage equations expressed in per unit notations are given by

$$e_d = \frac{d\bar{\Psi}_d}{dt} - \bar{\Psi}_d \bar{\omega} - \bar{R}_d \bar{i}_d$$

$$\bar{e}_q = \frac{d\bar{\Psi}_q}{dt} + \bar{\Psi}_q \bar{\omega} - \bar{R}_q \bar{i}_q$$

$$e_0 = \frac{d\bar{\Psi}_0}{dt} - \bar{R}_0 \bar{i}_0 \quad (2.51)$$

The corresponding flux linkage equations may be written as

$$\begin{aligned}\bar{\Psi}_d &= -\bar{L}_d \bar{i}_d + \bar{L}_{ad} \bar{i}_{fd} + \bar{L}_{akd} \bar{i}_{kd} \\ \bar{\Psi}_q &= -\bar{L}_q \bar{i}_q + \bar{L}_{aq} \bar{i}_q \\ \bar{\Psi}_0 &= -\bar{L}_0 \bar{i}_0\end{aligned}\quad (2.32)$$

The rotor circuit base quantities will be chosen so as to make the flux linkage equations simple by satisfying the following:

1. The per unit mutual inductances between different windings are to be reciprocal. This will allow the synchronous machine model to be represented by simple equivalent circuits.
2. All per unit mutual inductances between stator and rotor circuits in each axis are to be equal.
3. The following base quantities for the rotor are chosen, in view of the L_{ad} -base per unit system choose,

$$\begin{aligned}\bar{e}_d &= \frac{d\bar{\Psi}_d}{dt} - \bar{\Psi}_q \bar{\omega} - \bar{R}_d \bar{i}_d \\ \bar{e}_q &= \frac{d\bar{\Psi}_q}{dt} + \bar{\Psi}_d \bar{\omega} - \bar{R}_q \bar{i}_q \\ \bar{e}_0 &= \frac{d\bar{\Psi}_0}{dt} - \bar{R}_0 \bar{i}_0\end{aligned}\quad (2.33)$$

The per unit rotor flux linkage equations are given by

$$\begin{aligned}\bar{\Psi}_d &= -\bar{L}_d \bar{i}_d + \bar{L}_{ad} \bar{i}_{fd} + \bar{L}_{akd} \bar{i}_{kd} \\ \bar{\Psi}_q &= -\bar{L}_q \bar{i}_q + \bar{L}_{aq} \bar{i}_q \\ \bar{\Psi}_0 &= -\bar{L}_0 \bar{i}_0\end{aligned}\quad (2.34)$$

Since all quantities in Eqs. (2.31) to (2.34) are in per unit, we drop the overbar notation in subsequent discussion.

If the frequency of the stator quantities is equal to the base frequency, the per unit reactance of a winding reactance is numerically equal to the per unit inductance. For example:

$$X_d = 2\pi f L_d \quad (\Omega)$$

Dividing by $Z_{\text{base}} = 2\pi f_{\text{base}} L_{\text{base}}$, if $f = f_{\text{base}}$, then the per unit values of X_d and L_d are equal.

2.3.4 Classical Representation of the Synchronous Machine

The per unit equations completely describe the electrical and dynamic performance of a synchronous machine. However, except for the analysis of very

small systems, these equations cannot be used directly for system stability studies. Some simplifications and approximations are required to represent the synchronous machine in stability studies. For large systems, it is necessary to neglect the transformer voltage terms ψ_d and ψ_q and the effect of speed variations. Therefore, the machine equation described by Eqs. (2.33) and (2.34) become

$$\begin{aligned} e_d &= -\psi_q - R_d i_d \\ e_q &= \psi_d - R_q i_q \\ e_{qd} &= p\psi_{qd} + R_{qd} i_{qd} \end{aligned} \quad (2.35)$$

$$\begin{aligned} \psi_d &= -L_d i_d + L_{qd} i_{qd} \\ \psi_q &= -L_q i_q \\ \psi_{qd} &= -L_{qd} i_d + L_{qq} i_q \end{aligned} \quad (2.36)$$

By defining the following variables

$$E_d = L_{qd} i_{qd}, \quad E'_q = \frac{L_{qd}}{L_{qq}} \psi_{qd}, \quad E_{qd} = \frac{L_{qd}}{R_{qd}} e_{qd}, \quad T'_{qd} = \frac{L_{qd}}{R_{qd}}$$

the machine equations becomes

$$\begin{aligned} \psi_d &= -L_d i_d + E_d \\ \psi_q &= -L_q i_q \\ E'_q &= E_d - (L_d - L'_d) i_d \\ \dot{E}'_q &= \frac{1}{T'_{qd}} (E_{qd} - E_d) \end{aligned} \quad (2.37)$$

where E'_q is the q-axis component of the voltage behind transient reactance x'_d , T'_{qd} is the open-circuit transient time constant, E_d is the voltage proportional to i_{qd} , and e_{qd} is the voltage proportional to E_{qd} . Since per unit $x_d = L_d$, from equation (2.37) we have

$$\begin{aligned} \psi_d &= -x_d i_d + E_d \\ \psi_q &= -x_q i_q \\ E'_q &= E_d - (x_d - x'_d) i_d \\ \dot{E}'_q &= \frac{1}{T'_{qd}} (E_{qd} - E_d) \end{aligned} \quad (2.38)$$

For studies in which the period of analysis is small in comparison with T'_{qd} the machine model is often simplified by assuming that E'_q is constant throughout the study period. This assumption eliminates the only differential equation associated with the electrical characteristics of the machine. A further approximation is to ignore transient saliency by assuming that $x'_d = x'_q$ and to assume that the flux linkage also remains constant. With these assumptions, the voltage

behind the transient impedance $R_a + jx'_d$ has a constant magnitude. The equivalent circuit is shown in Fig. 2.10. The machine terminal voltage phasor is represented by

$$\tilde{V}_t = E' \angle \delta - (R_a + jx'_d) \tilde{I}_t$$

The machine dynamic model is represented by

$$T_f \frac{d\Psi}{dt} = M_m - M_e$$

$$\frac{d\delta}{dt} = \omega - \omega_0$$

$$M_e = \frac{P_c}{\omega_0}$$

$$P_c = R_e(\tilde{V}_t, \hat{\tilde{I}})$$

$$\tilde{V}_t = E' \angle \delta - (R_a + jx'_d) \tilde{I}_t, \quad (2.39)$$

where \tilde{V}_t is the machine terminal voltage phasor and can be calculated from power flow considerations. Then E' can be calculated. The machine swing equation can then be solved.

Equation (2.39) is the so-called classical model of the synchronous machine and is widely used in power system stability studies. This classical model is often used for three different time frames: subtransient, transient, and steady-state. Figure 2.11 summarizes these three simple synchronous machine models. The subtransient and transient assume constant rotor flux linkages, and the steady-state model assumes constant field current. These models neglect saliency effects and stator resistance and offer considerable structural and computational simplicity.

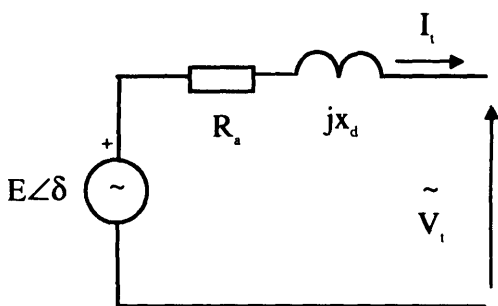
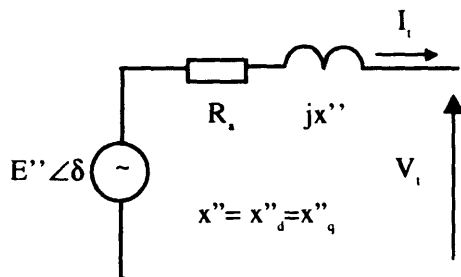
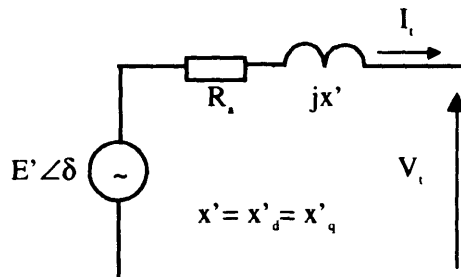


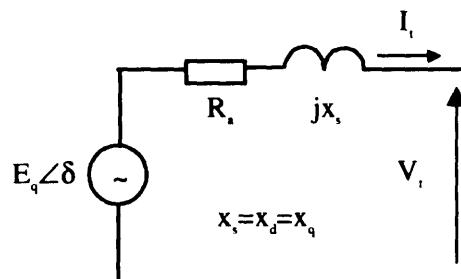
Figure 2.10 Equivalent circuit synchronous with $\chi'_d = \chi'_r$



(a) Subtransient model



(b) Transient model



(c) Steady-state model

Figure 2.11 Simple synchronous machine model.

2.4 REACTIVE CAPABILITY LIMITS

It is important in voltage stability and long-term stability studies to consider the reactive capability limits of synchronous machines. Synchronous machines are rated in terms of maximum MVA output at specified voltage and power factor (usually 0.85 or 0.9 lagging) which they can carry continuously without overheating. The active power output is limited by the prime mover capability to a value within the MVA rating. The continuous reactive power output capability is limited by three considerations: armature current limit, field current limit, and end region heating limit.

Figure 2.12 demonstrates a family of reactive capability areas for three different values of hydrogen coolant pressure. Note that the higher the pressure, the larger the capability curve. In Fig. 2.12, the region AB is the field current limited while the region BC is due to armature heating constraints.

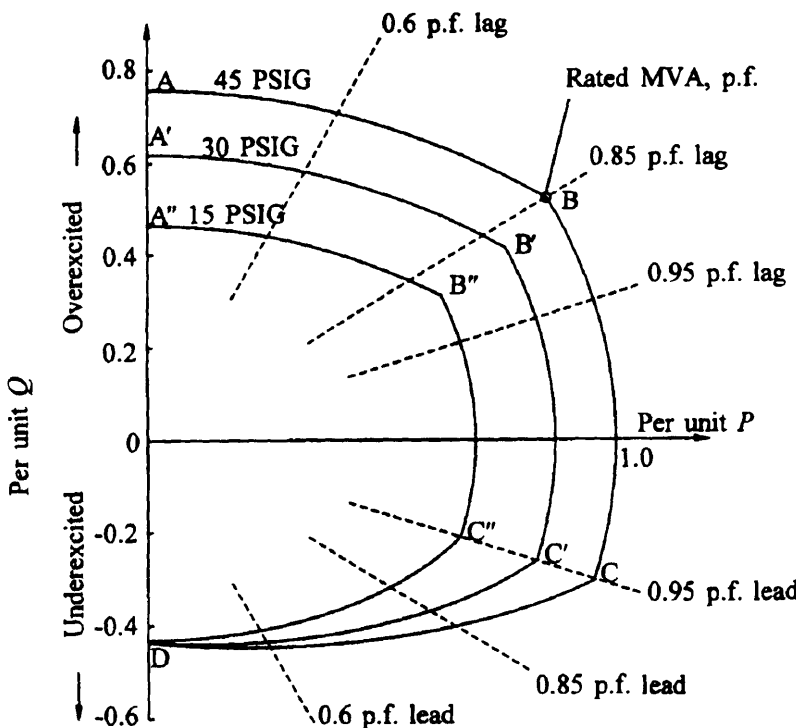


Figure 2.12 Reactive capability curves of a hydrogen-cooled generator at rated voltage.

2.5 STATIC LOAD MODELS

Conventional transient-stability studies were involved mainly with generator stability, and little importance was attached to loads. Recently, significant attention has been given to load modeling. Much of the domestic load and some industrial load consist of heating and lighting, particularly in the winter, and in early load models these were considered as constant impedances. Rotating equipment was often modeled as a simple form of synchronous machine and composite loads were simulated by a mixture of these two types of load. A lot of work has gone into the development of more accurate load models. These include some complex models of specific large loads. Most loads, however, consist of a large quantity of diverse equipment of varying levels and composition and some equivalent model is necessary.

A static load model expresses the characteristic of the load at any instant of time in terms of algebraic functions of the bus voltage magnitude and frequency at that instant. The active power component P and the reactive power component Q are considered separately.

A general load characteristic may be adopted such that the MVA loading at a particular bus is a function of voltage and frequency:

$$P = K_p V^m f^n$$

$$Q = K_q V^m f^n$$

where K_p and K_q are constants which depend upon the nominal value of the variables P and Q . For constant frequency operation, we write:

$$P = P_0 \left(\frac{V}{V_0} \right)^m$$

$$Q = Q_0 \left(\frac{V}{V_0} \right)^n \quad (2.40)$$

where P and Q are active and reactive components of the load when the bus voltage magnitude is V . The subscript 0 identifies the values of the respective variables at the initial or nominal operating condition.

Static loads are relatively unaffected by frequency changes, i.e., $m_f = n_f = 0$, and with constant impedance loads $m_i = n_i = 2$. The importance of accurate load models has been demonstrated for voltage sensitive loads. Figure 2.13 demonstrates the power and current characteristics of constant power, constant current, and constant impedance loads.

Many researchers identified the characteristic load parameters for various homogeneous loads, typical values are shown in Table 2.1. These characteristics

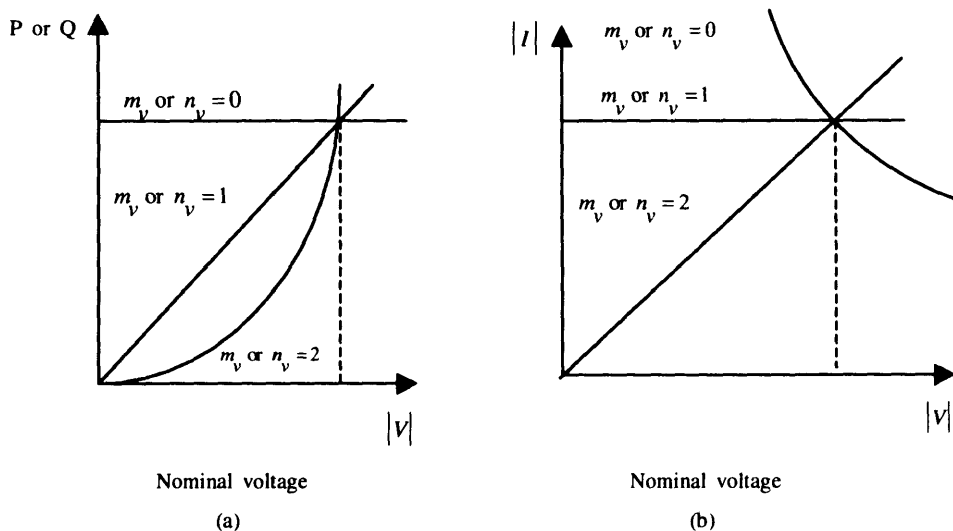


Figure 2.13 Characteristics of different load models. (a) Active and reactive power versus voltage. (b) Current versus voltage.

may be combined to give the overall load characteristic at a bus. For example, a group of homogeneous loads, each with a characteristic of m , j , and a nominal power of P_j may be combined to give an overall characteristic of:

$$m_{v_{eq}} = \frac{\sum_{j=1}^n m_j P_j}{\sum_{j=1}^n P_j}$$

Table 2.1 Typical Values of Characteristic Load Parameters

| Load | m_v | n_v | m_t | n_t |
|---------------------------|-------|-------|-------|-------|
| Filament lamp | 1.6 | 0 | 0 | 0 |
| Fluorescent lamp | 1.2 | 3.0 | -1.0 | -2.8 |
| Heater | 2.0 | 0 | 0 | 0 |
| Induction motor half load | 0.2 | 1.6 | 1.5 | -0.3 |
| Induction motor full load | 0.1 | 0.6 | 2.8 | 1.8 |
| Reduction furnace | 1.9 | 2.1 | -0.5 | 0 |
| Aluminum plant | 1.8 | 2.2 | -0.3 | 0.6 |

$$n_{v_{eq}} = \frac{\sum_{j=1}^n n_j P_j}{\sum_{j=1}^n P_j}$$

$$m_{I_{eq}} = \frac{\sum_{j=1}^n m_j P_j}{\sum_{j=1}^n P_j}$$

An alternative model which has been widely used to represent the voltage dependence of loads is the polynomial model:

$$\begin{aligned} P &= P_0 \left[p_1 \left(\frac{V}{V_0} \right)^a + p_2 \left(\frac{V}{V_0} \right) + p_3 \right] \\ Q &= Q_0 \left[q_1 \left(\frac{V}{V_0} \right)^b + q_2 \left(\frac{V}{V_0} \right) + q_3 \right] \end{aligned} \quad (2.41)$$

This model is commonly referred to as the ZIP model, since it is composed of constant impedance (Z), constant current (I), and constant power (P) components. The parameters of the model are the coefficients P_1 to P_3 and Q_1 to Q_3 , which define the proportion of each component.

When the load parameters m_v and n_v are less than or equal to unity, a problem can occur when the voltage drops to a low value. As the voltage magnitude decreases, the current magnitude does not decrease. In the limiting case with zero voltage magnitude, a load current flows which is clearly irrational, given the nondynamic nature of the load model. From a purely practical point of view, then the load characteristics are only valid for a small voltage deviation from nominal. Further, if the voltage is small, small errors in magnitude and phase produce large errors in current magnitude and phase. This results in loss of accuracy and with iterative solution methods of poor convergence. These effects can be overcome by using a constant impedance characteristic to represent loads where the voltage is below some predefined value, for example 0.8 pu.

The parameters of this model are exponents a and b . With these exponents equal to 0, 1, or 2, the model represents constant power, constant current, or constant impedance characteristics, respectively. For composite loads, their values depend on the aggregate characteristics of load components.

The frequency dependence of load characteristics is represented by multiplying the exponential model or the polynomial model by a factor as follows:

$$P = P_0 \left(\frac{V}{V_0} \right)^a (1 + K_{pr} \Delta f)$$

$$Q = Q_0 \left(\frac{V}{V_0} \right)^b (1 + K_{qf} \Delta f)$$

or

$$\begin{aligned} P &= P_0 \left[p_1 \left(\frac{V}{V_0} \right)^a + p_2 \left(\frac{V}{V_0} \right) + p_3 \right] (1 + K_{pf} \Delta f) \\ Q &= Q_0 \left[q_1 \left(\frac{V}{V_0} \right)^b + q_2 \left(\frac{V}{V_0} \right) + q_3 \right] (1 + K_{qf} \Delta f) \end{aligned} \quad (2.43)$$

where Δf is the frequency derivation ($f - f_0$).

CONCLUSIONS

In this chapter we offered a review of power concepts for single and three phase systems. We also treated the fundamentals of synchronous machine models for stability evaluation including the idea of a reactive capability curve and static load models. The per unit system was reviewed and extended to quantities not frequently encountered, such as time and frequency. Also, some modeling aspects of static loads, such as frequency dependent loads in typical electric power systems, were also discussed.

The reader is referred to the bibliography section for references dealing with materials in the chapter and contributions made by many other pioneers in the field. Please note that an annotated glossary of terms is given to summarize the key definitions and terminology employed in this chapter.

3

Dynamic Electric Network Models

INTRODUCTION

Chapter 2 focused on steady-state models to represent power system elements for the so called static analysis studies. We now turn our attention to models for transient or dynamic operational studies. This chapter describes some system models for analytical purposes. A model of an excitation system is studied in Section 3.1 and Section 3.2 gives a discussion of a model of the prime mover and governor system. Dynamic load models are discussed in Section 3.3 to conclude the chapter.

3.1 EXCITATION SYSTEM MODEL

The basic function of an excitation system is to provide a direct current to the synchronous machine field winding. In addition, the excitation system performs control and protective functions essential to the secure operation of the system by controlling the field voltage and hence the field current to be within acceptable levels under different operating conditions.

The control functions include the control of voltage and reactive power flow, thereby enhancing power system stability. The protective functions ensure that the capability limits of the synchronous machine, excitation system, and other equipment are not exceeded.

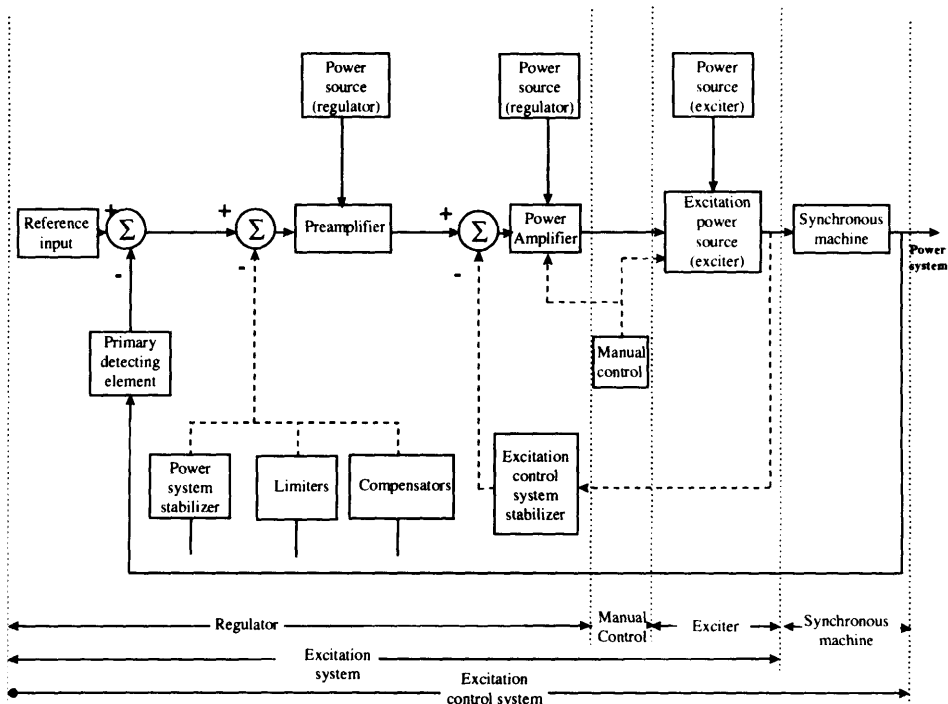


Figure 3.1 Functional block diagram of a synchronous excitation control system.

Figure 3.1 shows the functional block diagram of a typical excitation control system for a synchronous generator. The following is a brief description of the various subsystems identified in the figure. The exciter provides dc power to the synchronous machine field winding and constitutes the power stage of the excitation system. Usually an exciter is modeled by the first-order system as shown in Fig. 3.2. The effect of saturation is considered by introducing S_e and K_l , and thus the exciter model is given by

$$E_f = \frac{1}{1 + S_e + K_l + T_{e,S}} V_R \quad (3.1)$$

The voltage regulator processes and amplifies the input control signals to a level and form appropriate for the control of the exciter. This includes both regulating and excitation system stabilizing function (rate feedback or lead-lag compensation). Normally, the regulator is modeled by a first-order system as shown in Fig. 3.3. The regulator model is given by

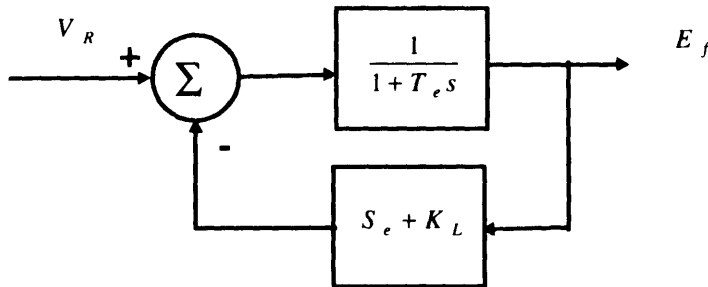


Figure 3.2 Block diagram model of exciter.

$$\frac{V_R}{\Delta V} = \frac{K_A}{1 + T_b s} \quad (3.2)$$

The terminal voltage transducer senses the generator terminal voltage, rectifies and filters it to dc, and compares it with a reference which represents the desired terminal voltage. Figure 3.4 shows the terminal voltage transducer model given by:

$$\Delta V = V_{ref} + V_t - V_r - \frac{1}{1 + T_b s} V_t \quad (3.3)$$

The power system stabilizer provides an additional input signal to the regulator to further damp power system oscillations. Some commonly used input signals are rotor speed deviation, accelerating power, and frequency deviation.

A power system stabilizer is modeled as shown in Fig. 3.5. The PSS model is given by

$$\Delta V = K_w G(s) \Delta \omega + K_p G(s) \Delta P_c \quad (3.4)$$

where

$$G(s) = K_p s \frac{T_2 s}{1 + T_2 s} \left(\frac{1 + T_1 s}{1 + T_2 s} \right)^2$$



Figure 3.3 Block diagram of the voltage regulator.

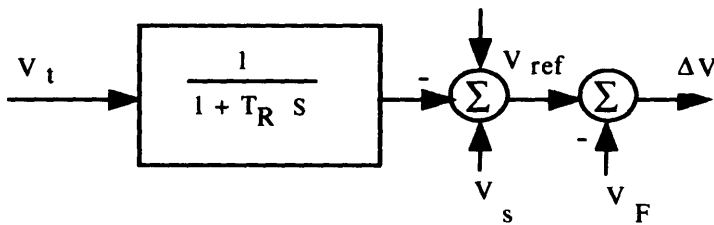


Figure 3.4 Block diagram of a terminal voltage transducer model.

Limiters and protective circuits ensure that the capability limits of excitor and synchronous generator are not exceeded.

The full excitation system is modeled as shown in Fig. 3.6. The system is represented by the following set of linear differential equations:

$$\begin{aligned}
 T_R \frac{dV_i}{dt} &= V_i - V_r \\
 T_A \frac{dV_k}{dt} &= -V_k - K(V_{ref} - V_i + V_s + V_f) \\
 T_e \frac{dE_t}{dt} &= V_k - (S_e + K_L + 1) E_t \\
 T_i \frac{dV_i}{dt} &= -V_i + \frac{K_E}{T_e} (V_k - (S_e + K_L + 1) E_t) \\
 T_S \frac{dX_1}{dt} &= K_{PSS} K_{\omega} \frac{d\Delta\omega}{dt} + K_{PSS} K_p \frac{d\Delta P_e}{dt} - X_1 \\
 T_1 \frac{dX_2}{dt} &= -X_2 + \frac{T_1}{T_5} \left(K_{PSS} K_{\omega} \frac{d\Delta\omega}{dt} + K_{PSS} K_p \frac{d\Delta P_e}{dt} \right) + \left(1 - \frac{T_1}{T_5} \right) X_1 \\
 T_2 \frac{dX_2}{dt} &= -V_s + \frac{T_1}{T_2} \left[\frac{T_1}{T_5} \left(K_{PSS} K_{\omega} \frac{d\Delta\omega}{dt} + K_{PSS} K_p \frac{d\Delta P_e}{dt} \right) + \left(1 - \frac{T_1}{T_5} \right) X_1 \right] + \left(1 - \frac{T_1}{T_2} \right) X_2 \quad (3.5)
 \end{aligned}$$

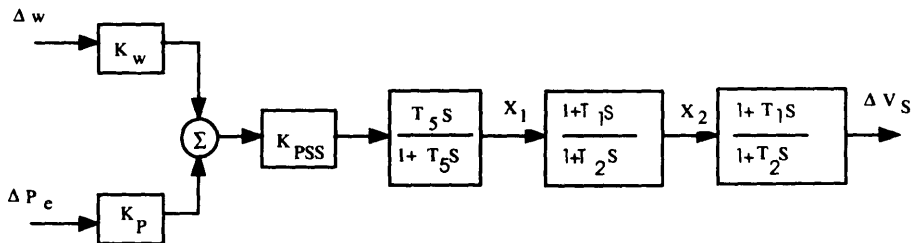


Figure 3.5 Block diagram of a typical Power System Stabilizer (PSS) model.

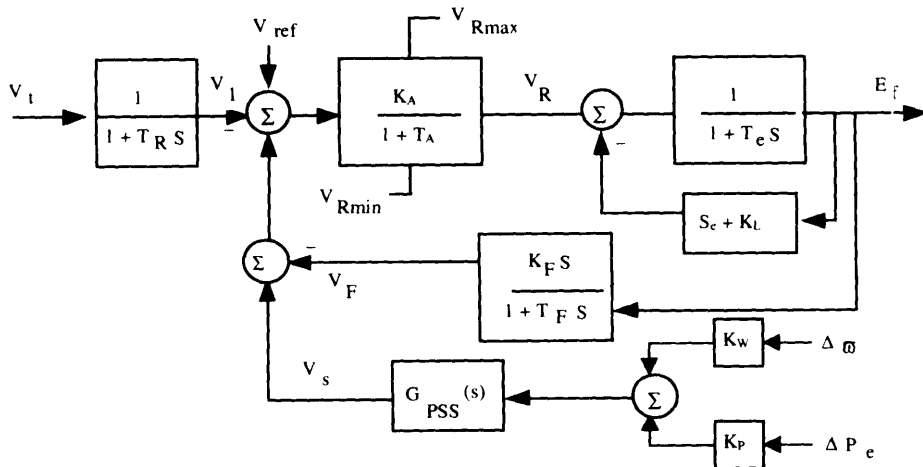


Figure 3.6 Integrated block diagram of a full excitation system.

3.2 PRIME MOVER AND GOVERNING SYSTEM MODELS

The prime sources of electrical energy supplied by utilities are the kinetic energy of water and the thermal energy derived from fossil fuels and nuclear fission. The prime movers convert these sources of energy into mechanical energy that, in turn, is converted to electrical form by the synchronous generator. The prime mover governing system provides a means of controlling power and frequency. The functional relationship between the basic elements associated with power generation and control is shown in Fig. 3.7. This section introduces the models for hydraulic turbines and governing systems as well as steam turbines and their governing systems.

3.2.1 Hydraulic Turbines and Governing System Model

The hydraulic turbine model describes the characteristics of gate opening μ and output mechanical power. In power system dynamic analysis, the hydraulic turbine is usually modeled by an ideal lossless turbine along with the consideration of “water hammer” effect caused by the water inertia, is given by

$$\frac{P_w}{\mu} = \frac{1 - T_{ws}}{1 + T_{ws}} \quad (3.6)$$

where T_{ws} is water starting time.

Because of the “water hammer” effect, a change in gate position produces

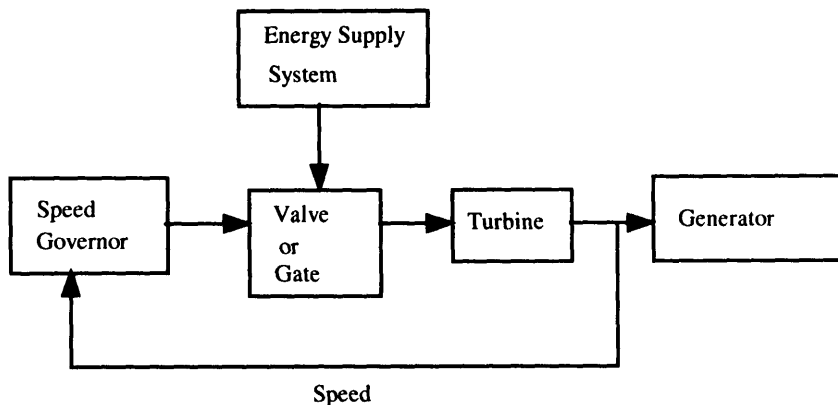


Figure 3.7 Functional block diagram of power generation and control.

an initial turbine power change which is opposite that which is desired. For stable control performance, a large transient (temporary) droop with a long re-setting time is therefore required. This is accomplished by introducing a transient gain reduction compensation in the governing system. The compensation retards or limits the gate movement until the water flow and power output have time to catch up. The governing system model is shown in Fig. 3.8.

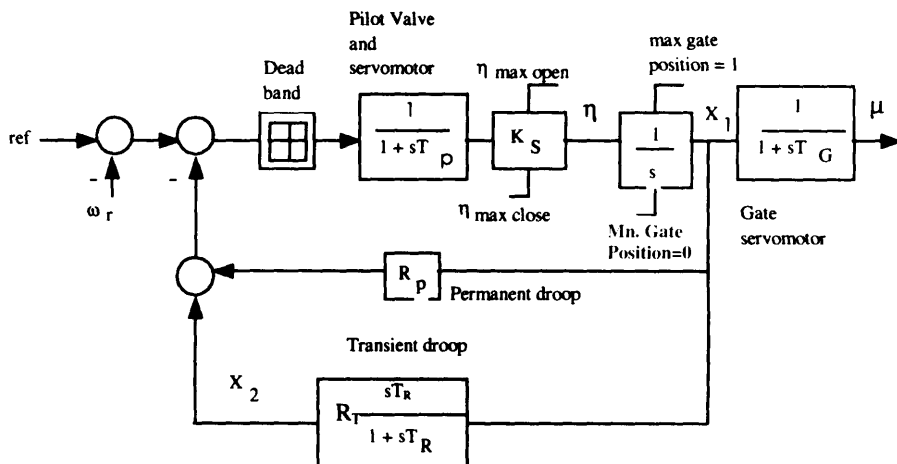


Figure 3.8 Block diagram of governing system for a hydraulic turbine.

The governing system model is given by

$$\begin{aligned}\frac{dX_1}{dt} &= \eta \\ T_c \frac{d\mu}{dt} &= -\mu + X_1 \\ T_k \frac{dX_2}{dt} &= -X_2 + R_I T_k \eta \\ T_p \frac{d\eta}{dt} &= -\eta + K_s (\omega_{ref} - \omega_r - R_p X_1 - X_2)\end{aligned}\quad (3.7)$$

where

T_p = pilot valve and servomotor time constant

K_s = servo gain

T_c = main servo time constant

R_p = permanent droop

R_I = temporary droop

T_R = reset time

$\eta_{max\ open}$ = maximum gate opening rate

$\eta_{max\ close}$ = maximum gate closing rate

μ = gate position

3.2.2 Steam Turbines and Governing System Model

A steam turbine converts stored energy of high pressure and high temperature steam into rotating energy. The input of the steam turbine is control valve position (ΔV_c), while its output is torque (ΔT_m). In power stability analysis, a first order model is used for steam turbine, i.e.,

$$\frac{\Delta T_m}{\Delta V_c} = \frac{1}{1 + sT_{ch}} \quad (3.8)$$

where T_{ch} = time constant

Comparing the turbine models for hydraulic turbine and steam turbine, it is clear that the response of a steam turbine has no peculiarity such as that exhibited by a hydraulic turbine due to water inertia. The governing requirements of steam turbines, in this respect, are more straightforward. There is no need for transient droop compensation.

The governing system model is given by

$$T_c \frac{d\Delta V_c}{dt} = -\Delta V_c + X_1$$

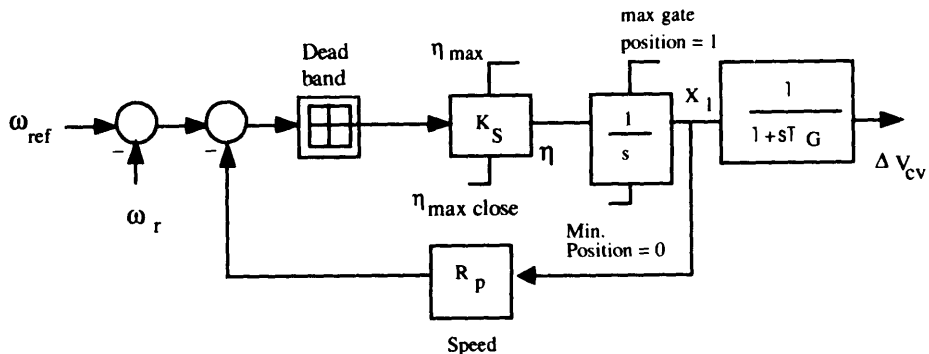


Figure 3.9 Typical block diagram of a steam turbine.

$$\frac{dX_1}{dt} = K_v (\omega_{ref} - \omega_r - R_p X_1) \quad (3.9)$$

A typical governing model for steam turbine is shown in Fig. 3.9.

3.3 MODELING OF LOADS

Load models are traditionally classified into two broad categories: static models and dynamic models. Earlier, we considered the static load models (Chap. 2). In this section, the dynamic load model is discussed.

3.3.1 Dynamic Load Models

Typically, motors consume 60 to 70% of the total energy supplied by a power system. Therefore, the dynamic effects due to motors are usually the most significant aspects of dynamic characteristics of system loads. Modeling of motors is discussed in this section.

An induction motor can be represented by the equivalent circuit shown in Fig. 3.10, which accounts for quantities in one phase.

In the equivalent circuit all quantities have been referred to the stator side. The directions of current shown are positive when operating as a motor, in which case the slip s is positive. The rotor equation of motion is given by

$$J \frac{d^2\delta}{dt^2} = T_m - T_e \quad (3.10)$$

The torque (T_e) is slip-dependent.

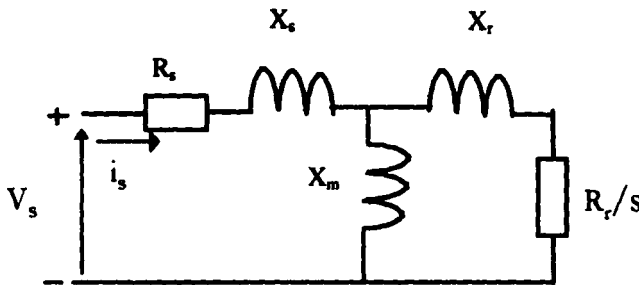


Figure 3.10 Equivalent circuit of a three-phase induction machine.

$$T = \frac{3}{2} P_t \left(\frac{R_i}{s \Omega_e} \right) \frac{V^2}{(R_i + R_s/s)^2 + (X_s + X_m)^2} \quad (3.11)$$

where P_t is the number of poles and s is the slip, defined as:

$$s = \frac{n_s - n_1}{n_s}$$

with n_s being the synchronous speed of the machine, where P is the number of poles, and f is the frequency. In Eq. (3.11) we have

$$V_s = \frac{j X_m V}{R_s + j (X_s + X_m)}$$

$$R_i + j X_i = \frac{j X_m (R_s + j X_s)}{R_s + j (X_s + X_m)}$$

It is noted that Eq. (3.10) represents a steady state performance model of the induction motor, with all quantities referred to the stator side. There are models that represent the transient performance of the motor that are based on flux linkages, voltages, and torque variations.

CONCLUSIONS

In this brief chapter we concentrated on models for power system stability in the time domain. We discussed electric excitation model as well as prime mover and governor system models. We concluded with a brief introduction to dynamic load model. For further reading on the topic, a reference list and an annotated glossary of terms is provided at the back of the book.

4

Philosophy of Security Assessment

INTRODUCTION

We are concerned with the implications of a major network disturbance such as a short circuit on a transmission line, the opening of a line or the switching on of a major load to name just a few. Here, we will consider the behavior of the system immediately following such a disturbance. Studies of this nature are called transient stability analysis. The tendency of a power system to react to disturbances in such a manner as to maintain its equilibrium (stay in synchronism) is referred to as stability. One way of classifying disturbances is through the categorization of small versus large. A disturbance is assumed to be small if the behavior of the system can be adequately represented through a linearization of the nonlinear system of dynamic equations of the system.

Stability considerations have been recognized to be among the essential tools in electric power system planning. The possible consequences of instability in an electric power system were dramatized by the northeast power failure of 1965. This is an example of a situation that arises when a severe disturbance is not cleared away quickly enough. The blackout began with a loss of a transmission corridor, which isolated a significant amount of generation from its load. More recently, a transmission tower in the Consolidated Edison system was hit by a severe lightning stroke in July 1977. The events that followed led to the

shutdown of power in New York City. Both events dramatized the consequences of an instability in an interconnected electric power system.

Our intention is to give an introduction to transient stability in electric power systems. We treat the case of a single machine operating to supply an infinite bus. The analysis of the more complex problem of large electric power networks with the interconnections taken into consideration is treated as well.

4.1 THE SWING EQUATION

In the power systems engineer's terminology, the dynamic equation relating the inertial torque to the net accelerating torque of the synchronous machine rotor is called the swing equation. This simply states

$$J \frac{d^2\theta}{dt^2} = T_a \quad (4.1)$$

The left-hand-side is the inertial torque which is the product of the inertia (in kg m^2) of all rotating masses attached to the rotor shaft and the angular acceleration. The accelerating torque T_a , is in Newton-meters and can be expressed as:

$$T_a = T_m - T_e \quad (4.2)$$

In the above, T_m is the driving mechanical torque and T_e is the retarding or load electrical torque. The angular position of the rotor θ may be expressed as the following sum of angles

$$\theta = \alpha + \omega_{rt}t + \delta \quad (4.3)$$

The angle α is a constant which is needed if the angle θ is measured from an axis different from the angular reference. The angle ω_{rt} is the result of the rotor angular motion at rated speed. The angle θ is time varying and represents deviations from the rated angular displacements. This gives the basis for our new relation

$$J \frac{d^2\theta}{dt^2} = T_m - T_e \quad (4.4)$$

We find it more convenient to substitute the dot notation

$$\ddot{\delta} = \frac{d^2\delta}{dt^2} = \frac{d^2\theta}{dt^2}$$

Therefore we have

$$J\ddot{\delta} = T_m - T_e \quad (4.5)$$

4.2 SOME ALTERNATIVE FORMS

Some useful alternative forms of Eq. (4.5) have been developed. The first is the power form which is obtained by multiplying both sides of by ω and recalling that the product of the torque T and angular velocity is the shaft power. This results in

$$J\omega\ddot{\delta} = P_m - P_e$$

The quantity $J\omega$ is called the inertia constant and is truly an angular momentum denoted by M (J.s/rad.):

$$M = J\omega \quad (4.6)$$

Thus the power form is:

$$M\ddot{\delta} = P_m - P_e \quad (4.7)$$

A normalized form of the swing equation can be obtained by dividing Eq. (4.5) by the rated torque T_R to obtain the dimensionless equation.

$$\frac{J}{T_R}\ddot{\delta} = \frac{T_m - T_e}{T_R}$$

The left-hand side of the above equation can be further manipulated to yield a form frequently used. Recall the definition of the kinetic energy of a rotating body. This gives the kinetic energy at rated speed as

$$W_k = \frac{1}{2} J\omega_R^2$$

then

$$\frac{J}{T_R} = \frac{2W_k}{\omega_R^2 T_R}$$

We know further that the rated power is

$$P_R = \omega_R T_R$$

Thus

$$\frac{J}{T_R} = \frac{2W_L}{\omega_R P_R}$$

Consequently we have

$$\frac{2W_L}{\omega_R P_R} \delta = \frac{T_m - T_r}{T_R}$$

A constant which has proved very useful is denoted by H , which is equal to the kinetic energy at rated speed divided by the rated power P_R

$$H = \frac{W_L}{P_R} \quad (4.8)$$

The units of H are in sec. As a result we write the per unit or normalized swing equation as

$$\frac{2H}{\omega_R} \delta = T_{m_{pu}} - T_{r_{pu}} \quad (4.9)$$

Observing that $T_{pu} = P_{pu}$, we can then write

$$\frac{2H}{\omega_R} \delta = P_m - P_r \quad (4.10)$$

where the equation is in pu.

4.2.1 Machine Inertia Constants

The angular momentum inertia constant M as defined by Eq. (4.6) can be obtained from manufacturer supplied machine data. The machine kinetic energy, N , may be written in terms of M as follows:

$$N = \frac{1}{2} M \omega_R^2 \quad (4.11)$$

where ω_R is the angular speed in electrical degrees per second. This in turn is related to the frequency by

$$\omega_R = 360 f$$

We can therefore conclude that

$$M = \frac{N}{180f} \quad (4.12)$$

The value of N is obtained from the moment of inertia of the machine usually denoted by WR^2 and traditionally given in lb-f \cdot f 2 . The conversion formula is:

$$N = 2.3097 \times 10^{-10} WR^2 n^2 \quad (4.13)$$

The relation between H and M can be obtained using Eq. (4.8) rewritten as

$$H = \frac{N}{G} \quad (4.14)$$

Here G is the machine rating. Thus

$$M = \frac{GH}{180f} \quad (4.15)$$

The quantity H does not vary greatly with the rated power and speed of the machine, but instead has a characteristic value or set of values for each class of machine. In the absence of definite information typical values of H may be used. The curves in Figs. 4.1, 4.2, and 4.3 give the general characteristic variation of H for existing and future large turbo generators.

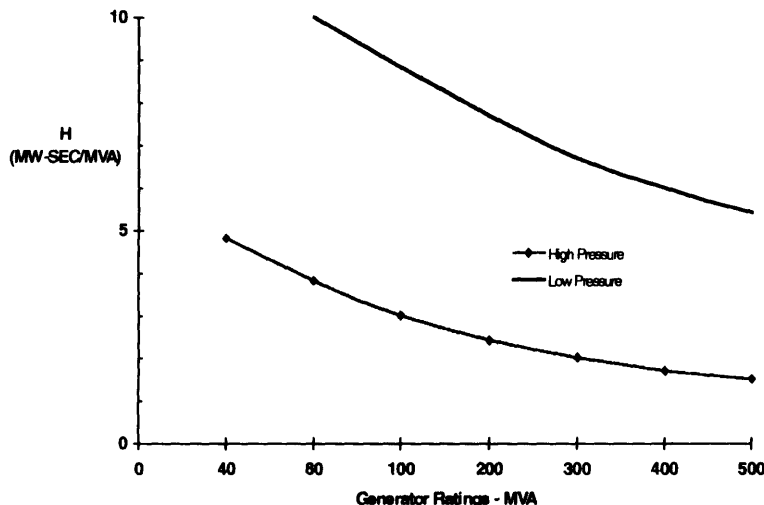


Figure 4.1 Inertia constants for large turbo generator rated 500 MVA and below.

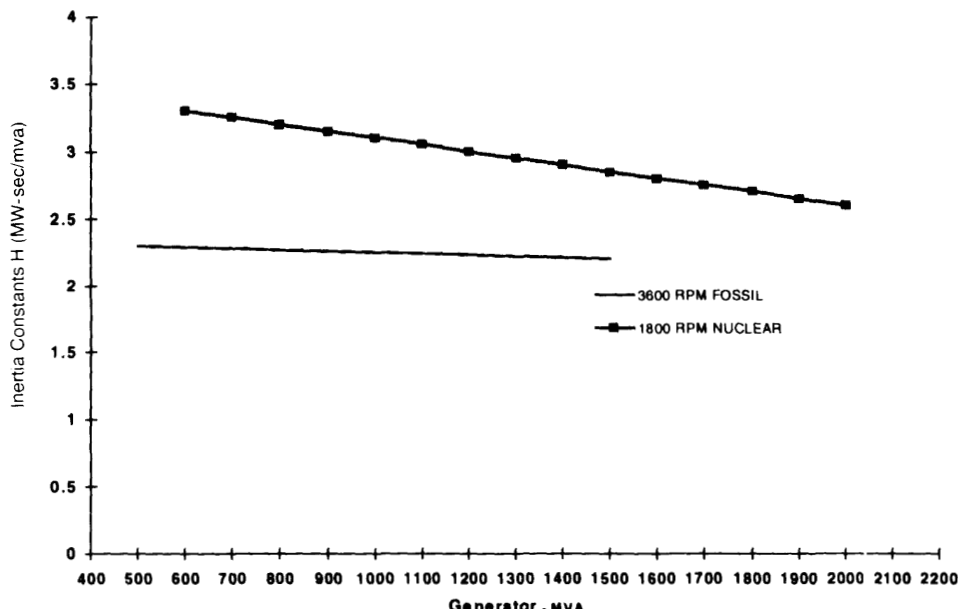


Figure 4.2 Expected inertia constants for future large turbo generators.

In system studies where several machines having different ratings are used, the H constant for each machine, given to a base of the machine rating, must be converted to the common system base by multiplying H in Eq. (4.14) by the ratio (machine base MVA/system base MVA).

4.3 TRANSIENT AND SUBTRANSIENT REACTANCES

In order to understand the concept of transient and subtransient reactances of a synchronous generator, let us consider the transient behavior during a balanced fault. The dependence of the value of the short circuit current in the electric power system on the instant in the cycle at which the short circuit occurs can be verified using a very simple model. The model is a generator with series resistance R and inductance L as shown in Fig. 4.4. The voltage of the generator is assumed to vary as:

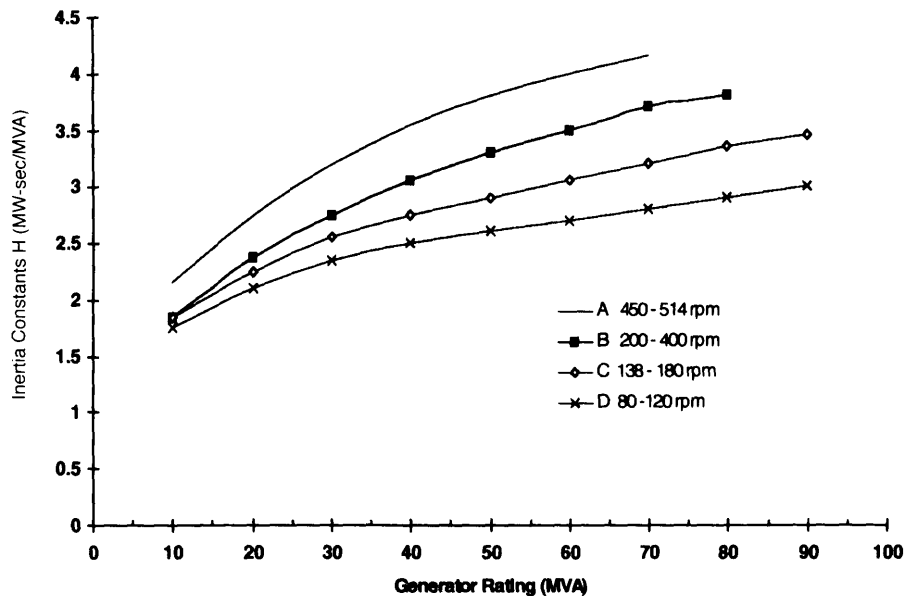


Figure 4.3 Inertia constants of large water wheel generators.

$$e(t) = E_m \sin(\omega t + \alpha)$$

With a balanced fault placed on the generator terminals at $t = 0$, then we can show that a dc term will in general exist. Its magnitude at $t = 0$ may be equal to the magnitude of the steady-state current term.

The transient current $i(t)$ is given by

$$i(t) = \frac{E_m}{Z} \left[\sin(\omega t + \alpha - \theta) - \sin(\alpha - \theta) e^{-\frac{t}{\tau}} \right]$$

where

$$Z = \sqrt{R^2 + \omega^2 L^2}$$

$$\theta = \tan^{-1} \omega \tau$$

$$\tau = \frac{L}{R}$$

The worst possible case occurs for the value of α given by:

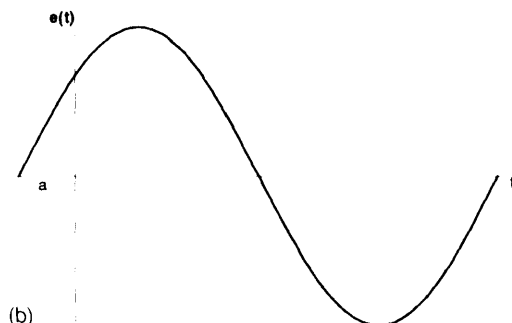
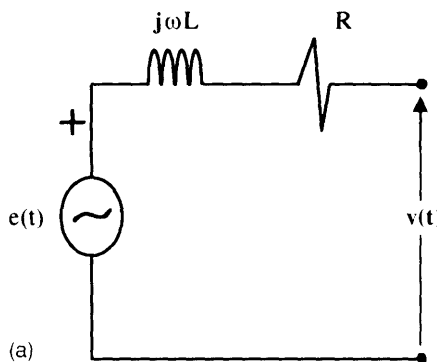


Figure 4.4 (a) Generator model. (b) Generated waveform.

$$\tan \alpha = -\frac{R}{\omega L}$$

In this case the current magnitude will approach twice the steady-state maximum value immediately after the short circuit. The transient current is given by the following for small t ($e^{\frac{t}{\tau}} \approx 1$):

$$i(t) = \frac{E_{\text{m}}}{Z} \left[-\cos \omega t + e^{-\frac{t}{\tau}} \right]$$

Thus:

$$i(t) = \frac{E_m}{Z} [1 - \cos\omega t]$$

It is clear that the maximum of $i(t)$ is twice that of E_m/Z . This waveform is shown in Fig. 4.5a.

For the case $\tan\alpha = \omega\tau$ we have $i(t) = \frac{E_m}{Z} \sin\omega t$. This waveform is shown in

Fig. 4.5b.

It is clear from inspection of either the expression for the short circuit current or the response waveform given in Fig. 4.6 that the reactance of the machine appears to be time varying. This is so if we assume a fixed voltage source E . For our power system purposes we let the reactance vary in a step-wise fashion X''_d , X'_d and X_d as shown in Fig. 4.6.

The current history $i(t)$ can be approximated in three time zones by three different expressions. In the first, denoted the subtransient interval, lasting up to 2 cycles, the current is I'' . This defines the direct axis subtransient reactance

$$X''_d = \frac{E}{I''}$$

The second denoted the transient gives rise to

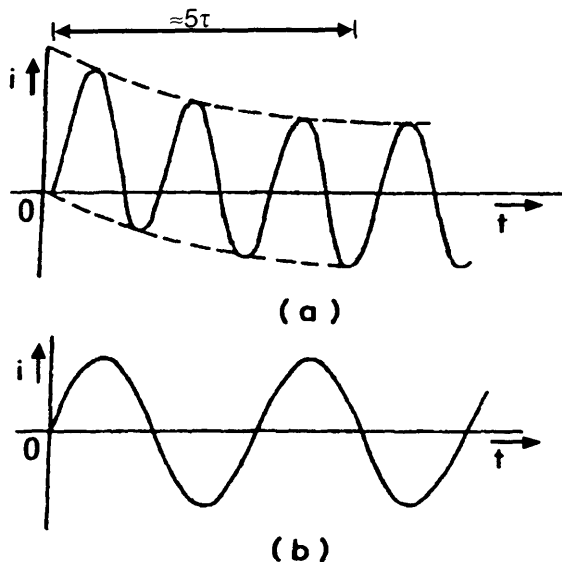


Figure 4.5 Short circuit current waveforms.

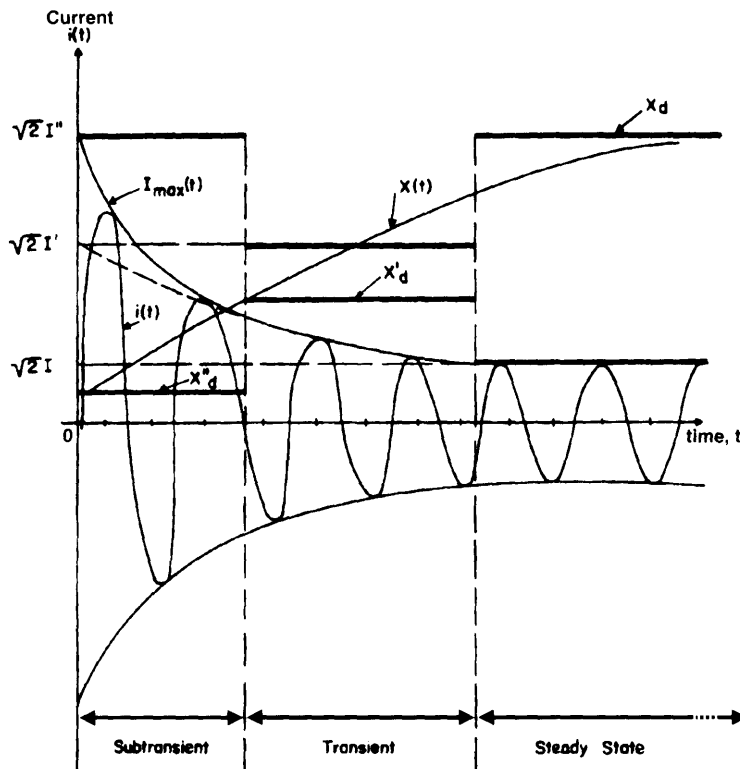


Figure 4.6 Symmetrical short circuit current and reactances for a synchronous machine.

$$X'_d = \frac{E}{I'}$$

where I' is the transient current and X'_d is the direct axis transient reactance. The transient interval lasts for about 30 cycles. The steady-state condition gives the direct axis synchronous reactance.

$$X_d = \frac{E}{I}$$

Note that the subtransient reactance can be as low as 7% of the synchronous reactance.

4.4 SYNCHRONOUS MACHINE MODEL IN STABILITY ANALYSIS

A brief outline of equations to account for flux changes in a synchronous machine is given to define various electrical quantities and to construct phasor diagrams. The following approximations are involved in the models discussed:

1. The rotor speed is sufficiently near 1.0 pu and may be considered a constant.
2. All inductances are independent of current. The effects due to saturation of iron are not considered.
3. Machine winding inductances can be represented as constants plus sinusoidal harmonics of the rotor angle.
4. Distributed windings may be represented as concentrated windings.
5. The machine may be represented by a voltage behind an impedance.
6. There are no hysteresis losses in the iron, and eddy currents are only accounted for by equivalent windings on the rotor.
7. Leakage reactance only exists in the stator.

Under these assumptions, classical theory allows constructing a model of the synchronous machine in the steady-state, transient, and subtransient states.

The per unit system adopted is normalized, although the term “proportional” should be used instead of “equal” when comparing quantities. Note that one pu field voltage produces 1.0 pu field current and 1.0 pu open-circuit terminal voltage at rated speed.

4.4.1 Steady-State Equations

Figure 4.7 shows the flux and voltage phasor diagram for a cylindrical rotor synchronous machine ignoring all saturation effects.

The following comments explain the construction:

1. The flux Φ_f is proportional to the field current I_f and the applied field voltage and acts in the direct axis of the machine.
2. The stator open-circuit terminal voltage E_i is proportional to Φ_f , which is located on the quadrature axis.
3. The voltage E_i is proportional to the applied field voltage and may be referred to as E_r .
4. When the synchronous machine is loaded, a flux Φ proportional to and in phase with the stator current I and when added vectorially to the field flux Φ_f , gives an effective flux Φ_e .
5. The effective internal stator voltage E_i is due to Φ_e and lags it by 90° .
6. The terminal voltage V is found from the voltage E_i by considering the

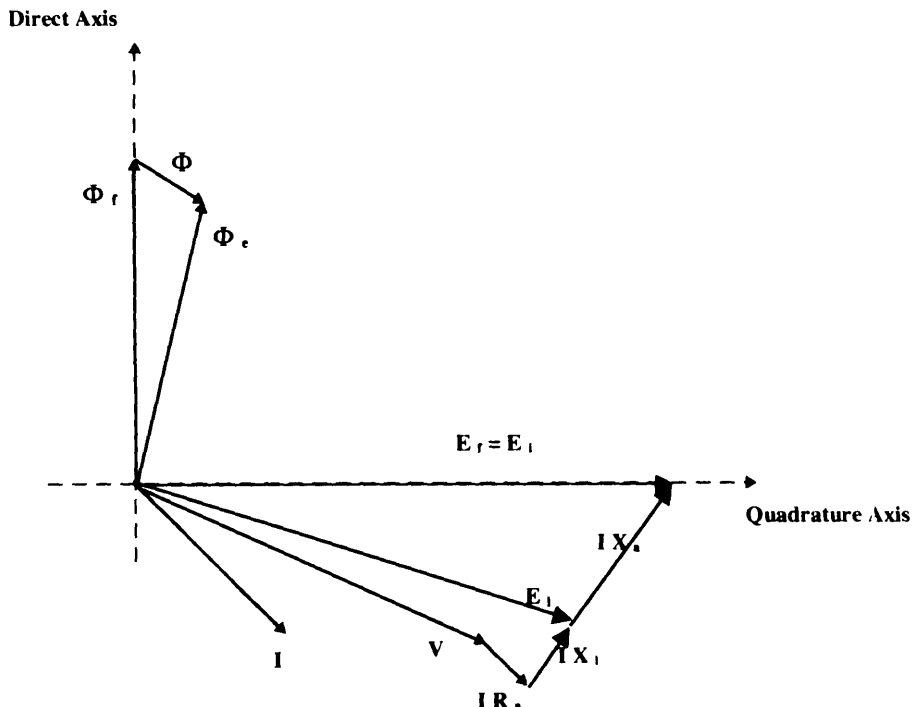


Figure 4.7 Phasor diagram of a cylindrical rotor synchronous machine in the steady state.

voltage drops due to the leakage reactance X_s and armature resistance R_s .

- By similarity of triangles, the difference between E_r and E_i is in phase with the IX_s voltage drop and is proportional to I . Therefore the voltage difference may be treated as a voltage drop across an armature reactance X_a .

The sum of X_a and X_s is termed the synchronous reactance, χ_s .

For the salient pole synchronous machine, the phasor diagram is more complex. Because the rotor is symmetrical about both the d and q axes it is convenient to resolve many phasor quantities into components in these axes. The stator current may be treated in this manner. Although Φ_d will be proportional to I_d and Φ_q will be proportional to I_q , because the iron paths in the two axes are different, the total armature reaction flux Φ will not be proportional to I nor necessarily be in phase with it. Retaining our earlier normalizing assumptions,

it may be assumed that the proportionality between I_d and Φ_{d*} is unity but the proportionality between I_q and Φ_{q*} is less than unity and is a function of the saliency.

4.4.2 Salient Pole Synchronous Machine

Figure 4.8 shows the phasor diagram of the salient pole synchronous machine. The d and q axes armature reactances are developed as in the cylindrical rotor case. Direct and quadrature synchronous reactances X_d and X_q can be established. i.e.,

$$X_d = X_i + X_{ad}$$

$$X_q = X_i + X_{aq}$$

From the phasor diagram we have:

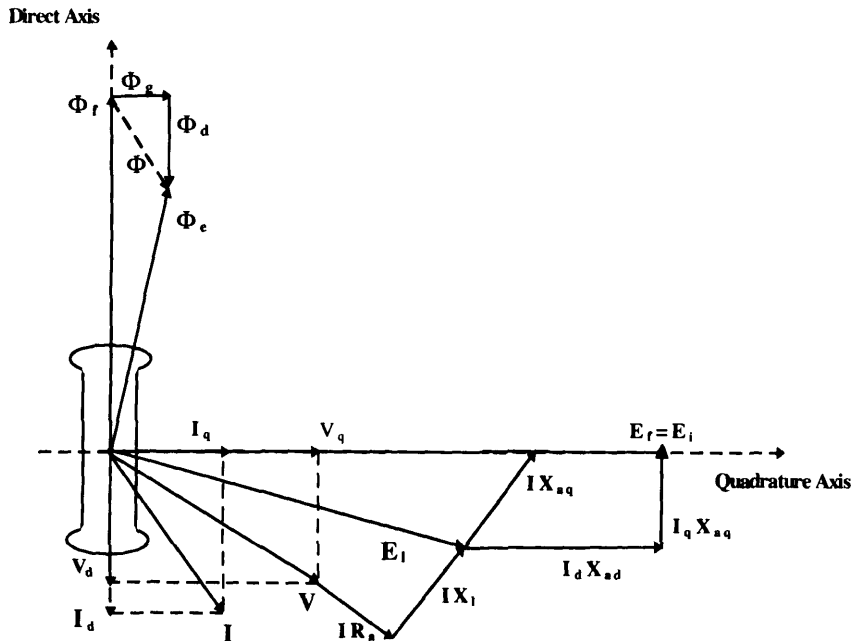


Figure 4.8 Phasor diagram of a salient rotor synchronous machine in steady state.

$$E_t = V_d + R_d I_q - I_d X_d$$

$$0 = V_d + R_d I_d + I_q X_q$$

where V_d and V_q are the axial components of the terminal voltage V .

In steady-state conditions it is reasonable to use the field voltage E , or the voltage equivalent to field current E , behind the synchronous reactances as the machine model. In this case the rotor position (quadrature axis) with respect to the synchronously rotating frame of reference is given by the angular position of E_r .

As the cylindrical rotor model may be regarded as a special case of a salient machine ($X_d = X_q$), we will consider only the salient pole machine.

4.4.3 Transient Equations

For faster changes in the conditions external to the synchronous machine, the steady-state model is no longer appropriate. Due to the inertia of the flux linkages these changes cannot be introduced throughout the whole of the model immediately. It is essential to establish new fictitious voltages E'_d and E'_q , representing the flux linkages of the rotor windings. These transient voltages can be shown to exist behind the transient reactances X'_d and X'_q ,

$$E'_q = V_q + R_d I_q - I_d X'_d$$

$$E'_d = V_d + R_d I_d + I_q X'_q$$

The voltage E_t is now considered as the sum of two voltages, E_d and E_q and is the voltage behind synchronous reactance. In steady-state, current flows only in the field winding and hence, in that case, $E_d = 0$ and $E_q = 0$.

Allowing for the rotor flux linkages change with time requires using the following ordinary differential equations:

$$\begin{aligned} sE'_q &= \frac{E_t - E_d}{\tau'_{dq}} \\ &= \frac{[E_t - E'_d + (X_d - X'_d)I_d]}{\tau'_{dq}} \end{aligned}$$

$$\begin{aligned} sE'_d &= \frac{-E_d}{\tau'_{qp}} \\ &= \frac{[-E'_d - (X_q - X'_q)I_q]}{\tau'_{qp}} \end{aligned}$$

The phasor diagram of the machine operating in the transient state is shown in Fig. 4.9.

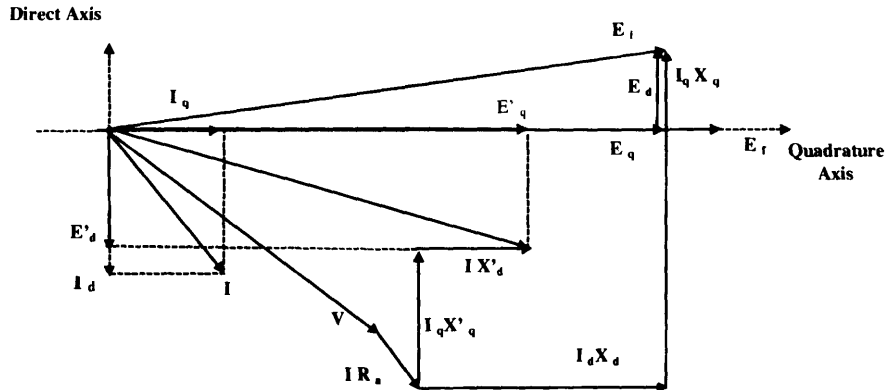


Figure 4.9 Phasor diagram of a salient pole synchronous machine in the transient state.

4.5 SUBTRANSIENT EQUATIONS

Other circuits exist in the rotor, either intentionally, as in the case of damper windings, or unavoidably. These circuits are taken into account if a more exact model is required. The reactances and time constants involved are small and can often be practically disregarded. When required, the development of these equations is identical to that for transients and yields:

$$\begin{aligned} E''_q &= V_q + R_d I_q - I_d X''_d \\ E''_d &= V_d + R_d I_d + I_q X'_q \\ sE''_q &= \frac{[E'_q - E''_q + (X'_d - X''_d)I_d]}{\tau''_{do}} \\ sE''_d &= \frac{[E'_d - E''_d - (X'_q - X''_q)I_q]}{\tau''_{qo}} \end{aligned}$$

The equations are developed assuming that the transient time constants are large compared with the subtransient time constants. A phasor diagram of the synchronous machine operating in the subtransient state is shown in Fig. 4.10.

4.6 MACHINE MODELS

It is feasible to expand the model even further than the subtransient level but this is rarely done in multi-machine stability programs. Investigations using a

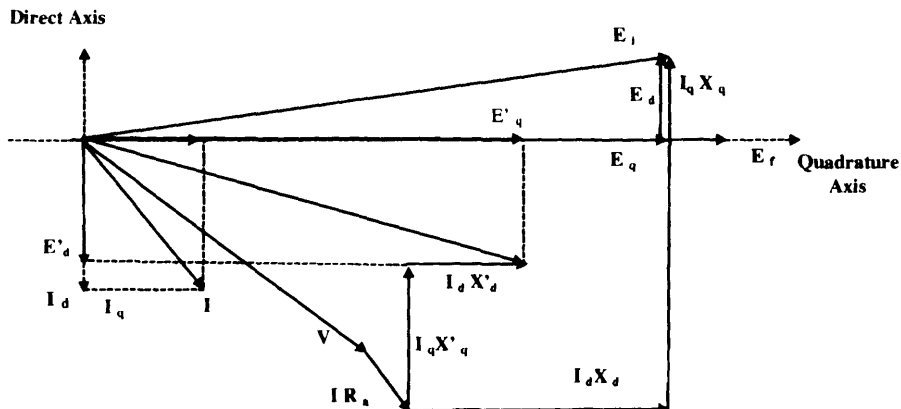


Figure 4.10 Phasor diagram of a salient pole synchronous machine in the subtransient state.

generator model with up to seven rotor windings, have shown that using the standard machine data, the more complex models do not necessarily yield accurate results. However, improved results can be obtained if the data, especially the time constants, are appropriately modified.

The most convenient method of treating synchronous machines of differing complexity is to allow each machine the maximum possible number of equations and then let the actual model used be determined automatically according to the data presented. Thus, five models are possible for a four-winding rotor

4.6.1 Model 1

Constant voltage magnitude behind d -axis transient reactance (X_d'). This requires no differential equations. Only the following algebraic equations are used.

$$E'_q = V_q + R_d I_q - I_d X_d'$$

$$E'_d = V_d + R_d I_d + I_q X_d'$$

4.6.2 Model 2

d -axis transient effects requiring one differential equation (sE'_q). The following equations are used.

$$E'_q = V_q + R_d I_q - I_d X_d'$$

$$\begin{aligned}
 E'_d &= V_d + R_d I_d + I_q X'_q \\
 sE'_q &= \frac{E_f - E_q}{\tau'_{do}} \\
 &= \frac{[E_f - E_q + (X_d - X'_d) I_d]}{\tau'_{do}}
 \end{aligned}$$

4.6.3 Model 3

d- and *q*-axis transient effects requiring two differential equations (sE'_q , and sE'_d). The following equations are used. A block diagram is shown in Fig. 4.11.

$$E'_q = V_q + R_d I_q - I_d X'_d$$

$$E'_d = V_d + R_d I_d + I_q X'_q$$

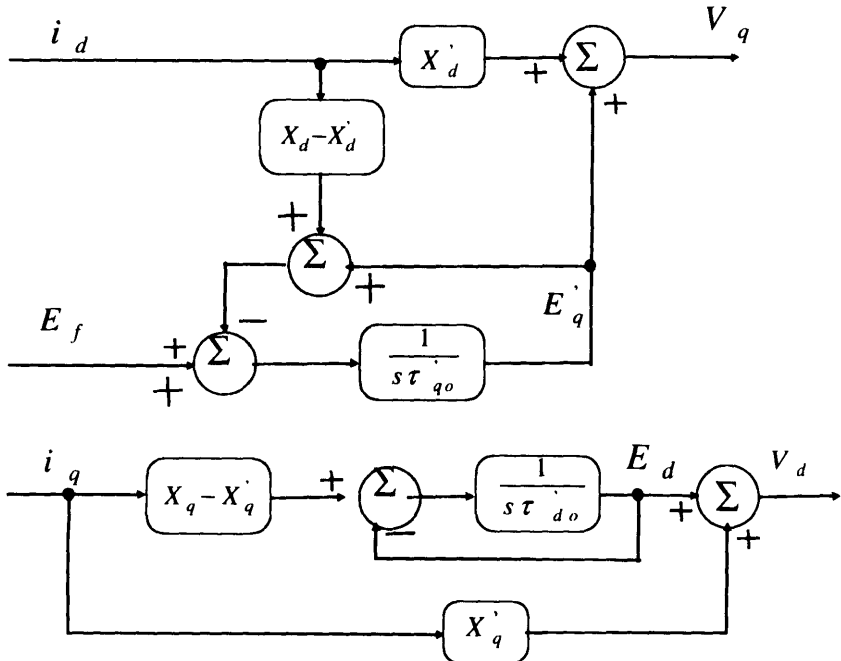


Figure 4.11 Block diagram representation for model 3.

$$\begin{aligned}
 sE'_q &= \frac{E_d - E_q}{\tau'_{dq}} \\
 &= \frac{[E_d - E'_q + [X_d - X'_d]I_d]}{\tau'_{dq}} \\
 sE'_d &= \frac{-E_d}{\tau'_{qd}} \\
 &= \frac{[-E'_d - [X_d - X'_d]I_d]}{\tau'_{qd}}
 \end{aligned}$$

4.6.4 Model 4

d- and *q*-axis subtransient effects requiring three differential equations (sE'_q , sE''_q , and sE''_d). The following equations are used.

$$\begin{aligned}
 sE'_q &= \frac{E_d - E_q}{\tau'_{dq}} \\
 &= \frac{[E_d - E'_q + [X_d - X'_d]I_d]}{\tau'_{dq}} \\
 E''_q &= V_q + R_d I_q - R_d X''_d \\
 E''_d &= V_d + R_d I_d + I_q X''_q \\
 sE''_q &= \frac{[E'_d - E''_q + [X'_d - X''_d]I_d]}{\tau''_{dq}} \\
 sE''_d &= \frac{[E'_d - E''_d - [X'_d - X''_d]I_d]}{\tau''_{qd}}
 \end{aligned}$$

4.6.5 Model 5

d- and *q*-axis subtransient effects requiring four differential equations (sE'_q , sE'_d , sE''_q , and sE''_d). The following equations are used.

$$\begin{aligned}
 sE'_q &= \frac{E_d - E_q}{\tau'_{dq}} \\
 &= \frac{[E_d - E'_q + [X_d - X'_d]I_d]}{\tau'_{dq}} \\
 sE'_d &= \frac{-E_d}{\tau'_{qd}} \\
 &= \frac{[-E'_d - [X_d - X'_d]I_d]}{\tau'_{qd}}
 \end{aligned}$$

$$\begin{aligned} E''_q &= V_q + R_a I_q - I_d X''_d \\ E''_d &= V_d + R_a I_d + I_q X''_q \\ sE''_q &= \frac{[E'_q - E''_q + [X'_d - X''_d]I_d]}{\tau_{do}} \\ sE''_d &= \frac{[E'_d - E''_d - [X'_q - X''_q]I_d]}{\tau_{qo}} \end{aligned}$$

The following mechanical equations need to be solved for all these models

$$s\omega = \frac{P_m - P_e - D_a(\omega - \omega_R)}{M}$$

$$s\delta = \omega - \omega_R$$

4.7 GROUPS OF MACHINES AND THE INFINITE BUS

Groups of synchronous machines or parts of the system may be represented by a single synchronous machine model. An infinite busbar, representing a large stiff system, may be similarly modeled as a single machine represented by model 1, with the simplification that the mechanical equations are not required. This sixth model is thus defined as:

4.7.1 Model 0

Infinite machine-constant voltage (phase and magnitude) behind d -axis transient reactance (X'_d). Only the following equations are used.

$$\begin{aligned} E'_q &= V_q + R_a I_q - I_d X'_d \\ E'_d &= V_d + R_a I_d + I_q X'_q \end{aligned}$$

4.8 STABILITY ASSESSMENT

In this section, we discuss the conventional approach to stability assessment applicable to a single machine against an infinite bus. The method leads to the equal area criterion.

We concluded that a simple representation of the salient pole machine is offered by the model 0 given by:

$$\begin{aligned} E'_q &= V_q + R_a I_q - I_d X'_d \\ E'_d &= V_d + R_a I_d + I_q X'_q \end{aligned}$$

We will make the following additional assumptions:

1. Neglect armature resistance R_a
2. Assume that only a direct axis rotor winding is considered. Thus $E'_d = 0$ and that $E' = E'_q$

As a result:

$$E' = V_q - I_d X_d'$$

$$0 = V_d + I_q X_q'$$

The direct axis and quadrature axis currents are thus given by:

$$I_d = \frac{V_q - E'}{X_d'}$$

$$I_q = -\frac{V_d}{X_q'}$$

The output power of the machine is given by:

$$P_e = V_d I_d + V_q I_q$$

As a result:

$$\begin{aligned} P_e &= V_d \frac{V_q - E'}{X_d'} - V_q \frac{V_d}{X_q'} \\ &= V_d V_q \left[\frac{1}{X_q'} - \frac{1}{X_d'} \right] - \frac{E' V_d}{X_d'} \end{aligned}$$

We will take the machine terminal voltage as the reference, and assume that E' leads V_t by an angle δ and hence

$$V_q = V_t \cos \delta$$

$$V_d = -V_t \sin \delta$$

The phasor diagram is shown in Fig. 4.12.

The electric power output of the salient pole machine is therefore given by:

$$P_e = \frac{E' V_t}{X_d'} \sin \delta + \frac{V_t^2}{2} \left[\frac{1}{X_q'} - \frac{1}{X_d'} \right] \sin 2\delta$$

The variation of the output for salient pole machine with the torque or power angle δ is shown in Fig. 4.13.

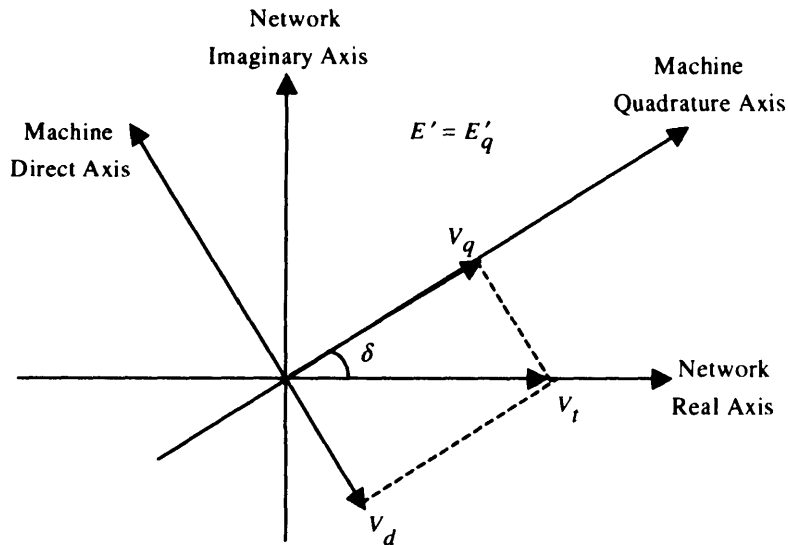


Figure 4.12 Synchronous machine and network frames of reference for developing electric power output formula.

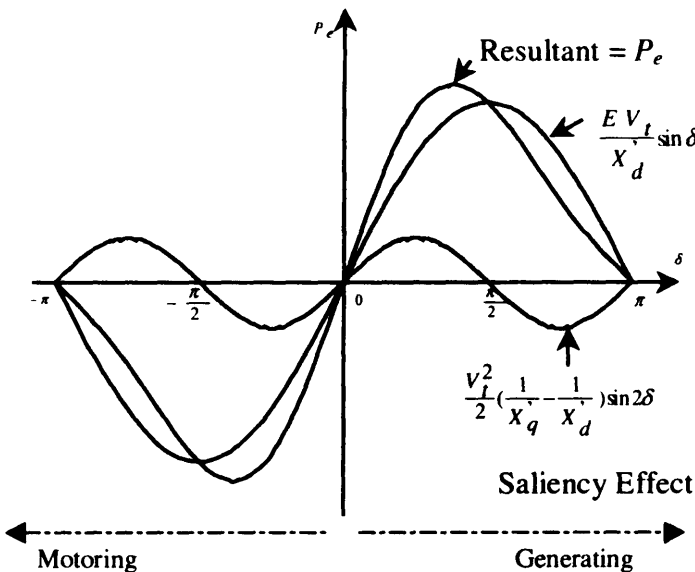


Figure 4.13 Power angle characteristics for a salient pole machine.

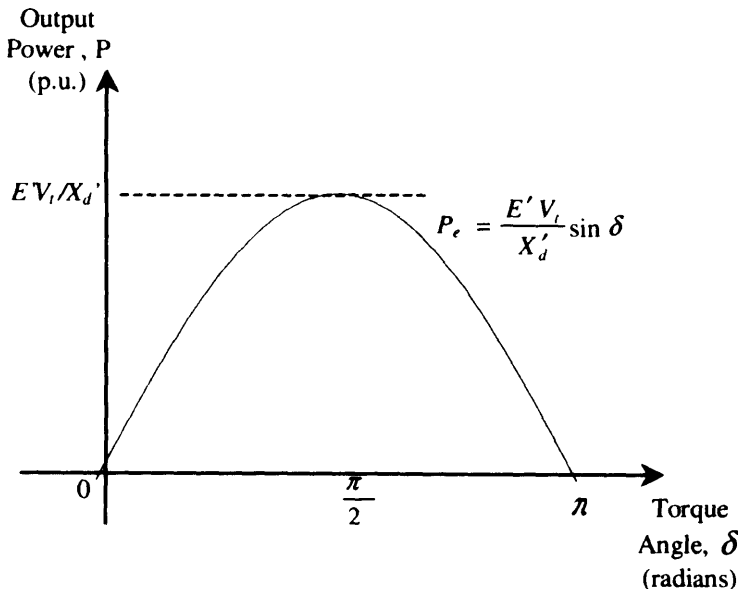


Figure 4.14 Power angle characteristics for a round rotor machine.

In the case of a round rotor machine, we have $X_d' = X_q'$ and hence

$$P_e = \frac{E' V_t}{X_d'} \sin \delta$$

The variation of the output power for a round rotor machine with the angle δ , (torque or power angle) is shown in Fig. 4.14.

Example 1

A synchronous machine is connected to an infinite bus through a transformer having a reactance of 0.1 pu and a double-circuit transmission line with 0.45 pu reactance for each circuit. The system is shown in Fig. 4.15. All reactances are given to a base of the machine rating. The direct-axis transient reactance of the machine is 0.15 pu . Determine the variation of the electrical power with angle δ . Assume $V = 1.0 \text{ pu}$.

Solution

An equivalent circuit of the above system is shown in Fig. 4.16. From this we have the following: $X_{eq} = 0.475 \text{ pu}$.

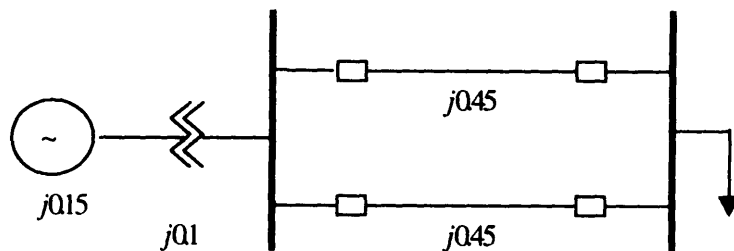


Figure 4.15 System for example 1.

Changes in the network configuration between the two sides (sending and receiving) will alter the value of X_{eq} and hence the expression for the electric power transfer. The following example illustrates this point.

Example 2

Assume for the system of Example 1 that only one circuit of the transmission line is available. Obtain the relation between the transmitted electric power and the angle δ . Assume other variables to remain unchanged.

Solution

The network configuration presently offers an equivalent circuit as shown in Fig. 4.17.

For the present we have

$$X_{eq} = 0.70 \text{ pu}$$

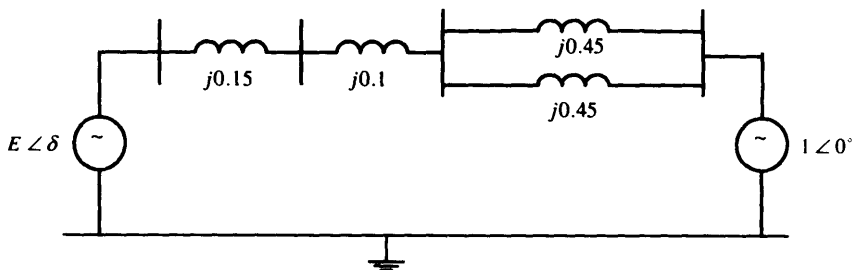


Figure 4.16 Equivalent circuit for example 1.

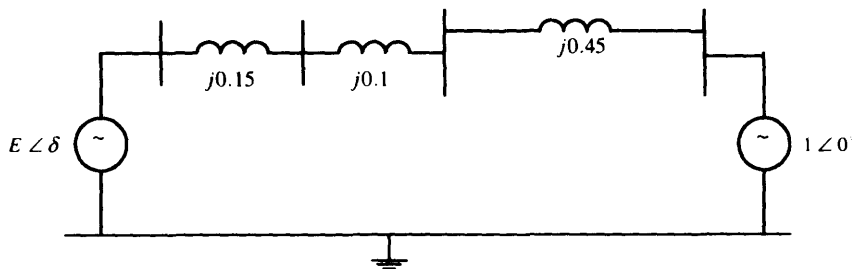


Figure 4.17 Equivalent circuit for example 2.

Therefore,

$$\begin{aligned} P_c &= \frac{EV}{X} \sin\delta \\ \Rightarrow P_c &= 1.43 \sin\delta \end{aligned}$$

Observe that the maximum value of the new curve is lower than the one corresponding to the previous example.

4.9 CONCEPTS IN TRANSIENT STABILITY

In order to gain an understanding of the concepts involved in transient stability prediction, we will concentrate on the simplified network consisting of a series reactance connecting the machine and the infinite bus. Under these conditions our power expression reduces to

$$P_c = \frac{VE}{X_{eq}} \sin\delta$$

For simplicity of notation we will assume steady-state values. An important assumption that we adopt is that the electric changes involved are much faster than the resulting mechanical changes produced by the generator/turbine speed control. Thus we assume that the mechanical power is a constant for the purpose of transient stability calculations. The functions P_m and P_c are plotted in Fig. 4.18.

The intersection of the two functions defines two values for δ . The lower value is denoted by δ_0 . Consequently, the higher is $\pi - \delta_0$ according to the symmetry of the curve. At both points $P_m = P_c$, that is $d^2\delta/dt^2 = 0$ and we say that the system is in equilibrium.

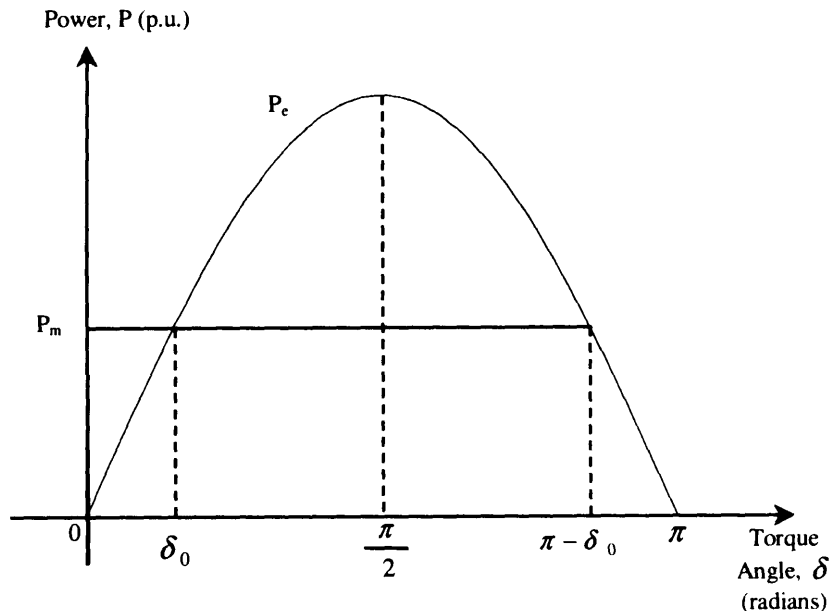


Figure 4.18 Power-angle curve.

Assume that a change in the operation of the system occurs such that δ is increased by a small amount $\Delta\delta$. Now for operation near δ_0 , $P_e > P_m$ and $d^2\delta/dt^2$ becomes negative according to the swing equation. Thus δ is decreased, and the system responds by returning to its stable operating or equilibrium point. We refer to this as a stable operating point. On the other hand, operating at $\pi - \delta_0$ results in a system response that will increase δ and move further from $\pi - \delta_0$. For this reason, we call $\pi - \delta_0$ an unstable equilibrium point.

If the system is operating in an equilibrium state supplying an electric power P_{e0} with the corresponding mechanical power input P_{m0} , then the corresponding rotor angle is δ_0 . Suppose the mechanical power P_m is changed to P_{m1} at a fast rate, which the angle δ cannot follow as shown in Fig. 4.19. In this case $P_m > P_e$ and acceleration occurs so that δ increases. This goes on until the point δ_1 where $P_m = P_e$ and the acceleration is zero. The speed, however, is not zero at that point, and δ continues to increase beyond δ_1 . In this region $P_m < P_e$ and rotor retardation takes place.

The rotor will stop at δ where the speed is zero and retardation will bring δ down. This process continues on as oscillations around the new equilibrium point δ_1 . This serves to illustrate what happens when the system is subjected to a sudden change in the power balance of the right-hand side of the swing equa-

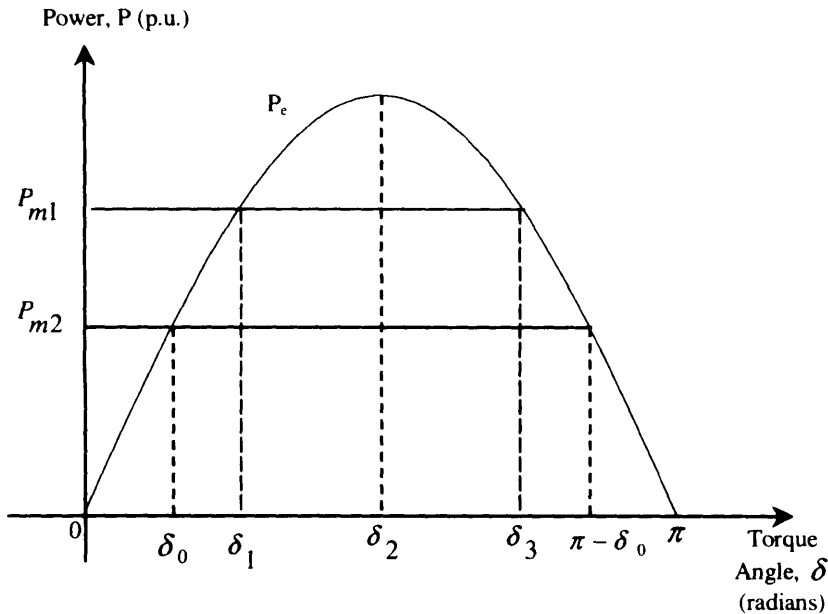


Figure 4.19 Power angle curve.

tion. The situation described above will occur for sudden changes in P , as well. The system discussed in Examples 1 and 2 serves to illustrate this point, which we discuss further in the next example.

Example 3

The system of example 1 is delivering an apparent power of 1.1 pu at 0.85 PF lagging with two circuits of the line in service. Obtain the source voltage (excitation voltage) E and the angle δ under these conditions. With the second circuit open as in Example 2, a new equilibrium m angle can be reached. Sketch the power angle curves for the two conditions. Find the angle δ_0 and the electric power that can be transferred immediately following the circuit opening, as well as δ_1 . Assume that the excitation voltage remains unchanged.

Solution

The power delivered is $P_0 = S \cos \phi$, $P_0 = 1.1 \times 0.85 = 0.94$ pu

Using $P = VI \cos \phi$, then the current in the circuit is $I = \frac{1}{1.1} / \cos^{-1} 0.85$

Thus we can write

$$\begin{aligned}
 E &= V + jXI \\
 &= 1 + (1.1 \angle -31.79^\circ)(0.475 \angle 90^\circ) \\
 &= 1.28 + j0.44 = 1.35 \angle 19.20^\circ \text{ pu}
 \end{aligned}$$

Therefore, $E = 1.35$ p.u., $\delta_0 = 19.20^\circ$

The power angle curve for the line with two circuits according to Example 1, is

$$P_{e0} = 2.1053 \times 1.35 \sin \delta = 2.84 \sin \delta$$

With one circuit open, the new power angle curve is obtained as in Example 2, thus

$$\begin{aligned}
 P_{el} &= \frac{EV}{X_{eq}} \sin \delta \\
 \Rightarrow P_{el} &= 1.43 \times 1.35 \sin \delta = 1.93 \sin \delta
 \end{aligned}$$

The two power angle curves are shown in Fig. 4.20.

From inspection of the curves, we can deduce that the angle δ_1 , can be obtained from

$$\begin{aligned}
 P_m &= P_e \sin \delta, \text{ (curve B)} \\
 0.93 &= 1.93 \sin \delta_1 \\
 \delta_1 &= 29.15^\circ
 \end{aligned}$$

We can obtain the value of electric power corresponding to δ_0 , with one line open as

$$\begin{aligned}
 P_{e10} &= 1.93 \sin 19.2^\circ \\
 &= 0.63 \text{ pu}
 \end{aligned}$$

4.10 A METHOD FOR STABILITY ASSESSMENT

To predict whether a particular system is stable after a disturbance it is necessary to solve the dynamic equation describing the behavior of the angle δ immediately following an imbalance or a disturbance to the system. The system is said to be unstable if the angle between any two machines tends to increase without limit. On the other hand if under disturbance effects, the angles between every possible pair reach maximum value and decrease thereafter, the system is deemed stable.

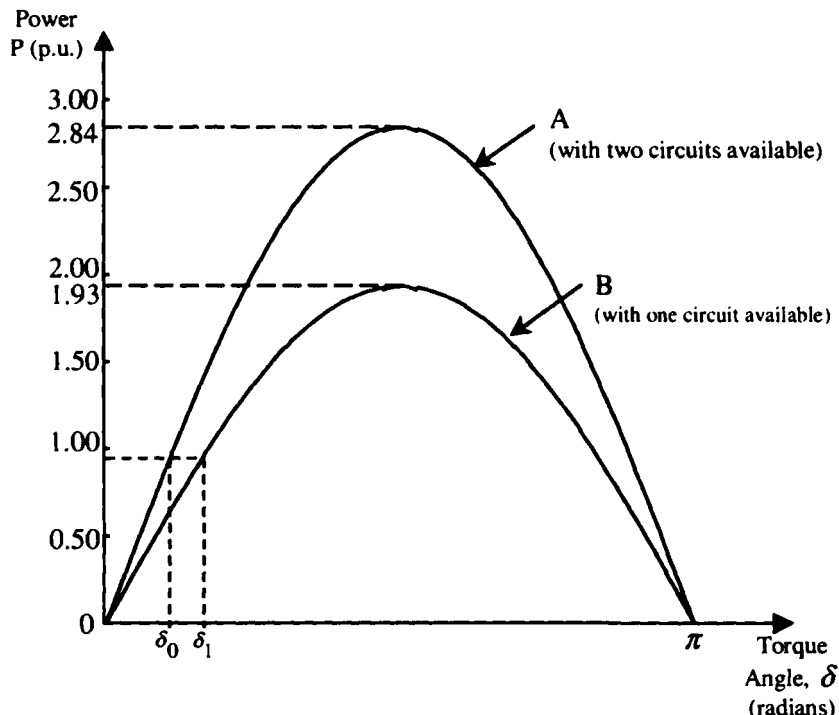


Figure 4.20 Power angle curves for example 3.

Assuming as we have already done that the input is constant, negligible damping and constant source voltage behind the transient reactance, the angle between two machines either increase indefinitely or oscillates after all disturbances have occurred. Therefore, in the case of two machines, these will either fall out of step on the first swing or never. Here the observation that the machines angular differences stay constant can be taken as an indication of system stability. A simple method for determining stability known as the equal-area method is available. We will discuss this here.

The swing equation for a machine connected to an infinite bus can be written as

$$\frac{d\omega}{dt} = \frac{P_a}{M}$$

where $\omega = \frac{d\delta}{dt}$ and P_a is the accelerating power.

We obtain an expression for the variation of the angular speed ω with P_a , by noting the alternative form

$$\omega d\omega = \frac{P_a}{M} d\delta$$

Integrating, assuming $\omega = 0$ and integrating the above equation, we obtain

$$\omega^2 = \frac{2}{M} \int_{\delta_0}^{\delta_1} P_a d\delta$$

or

$$\frac{d\delta}{dt} = \sqrt{\frac{2}{M} \int_{\delta_0}^{\delta_1} P_a d\delta}$$

The above equation gives the relative speed of the machine with respect to a reference frame moving at a constant speed (by definition of the angle δ). If the system is stable, then the speed must be zero when the acceleration is either zero or is opposing the rotor motion. Thus for a rotor which is accelerating, the condition for stability is that a value of δ_s exists such that

$$P_a(\delta_s) \leq 0 \quad \text{and} \quad \int_{\delta_0}^{\delta_1} P_a d\delta = 0$$

This condition is applied graphically in Fig. 4.21 where the net area under the $P_a - \delta$ curve reaches zero at the angle δ as shown. Observe that at δ_0 , P_a is negative and consequently the system is stable. Observe that the area A_1 equals A_2 as indicated.

The accelerating power need not be plotted to assess stability. Instead, the same information can be obtained from a plot of electrical and mechanical powers. The former is the power angle curve and the latter is assumed constant. In this case the integral may be interpreted as the area between the P_e curve and the curve of P_m both plotted versus δ . The area to be equal to zero, must consist of a positive portion A_1 , for which an equal and opposite negative portion of A_2 must exist, for which $P_m < P_e$. This explains the term equal-area criterion for stability. This situation is shown in Fig. 4.22.

If the accelerating power reverses sign before the two areas A_1 and A_2 are equal, synchronism is lost. This situation is illustrated in Fig. 4.23. The area A_2 is smaller than A_1 and as δ increases beyond the value where P_a reverses sign again, the area A_3 is added to A_1 .

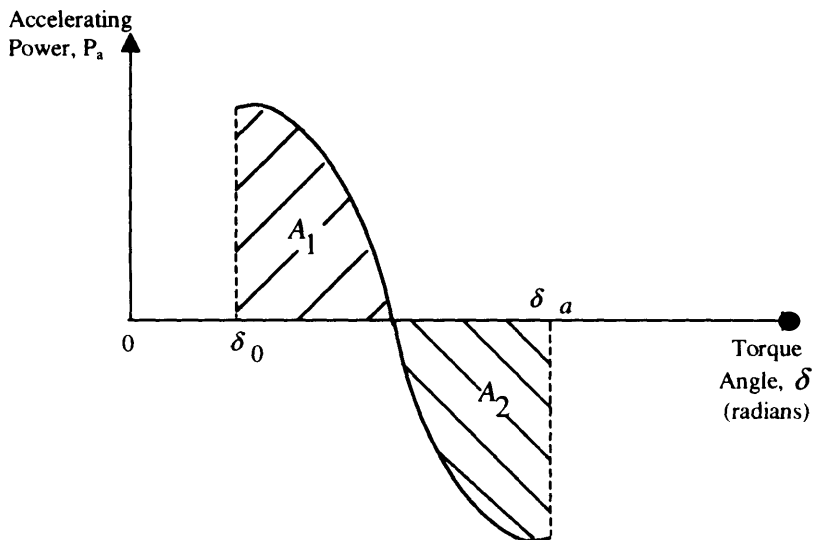


Figure 4.21 Stability condition for accelerating rotor.

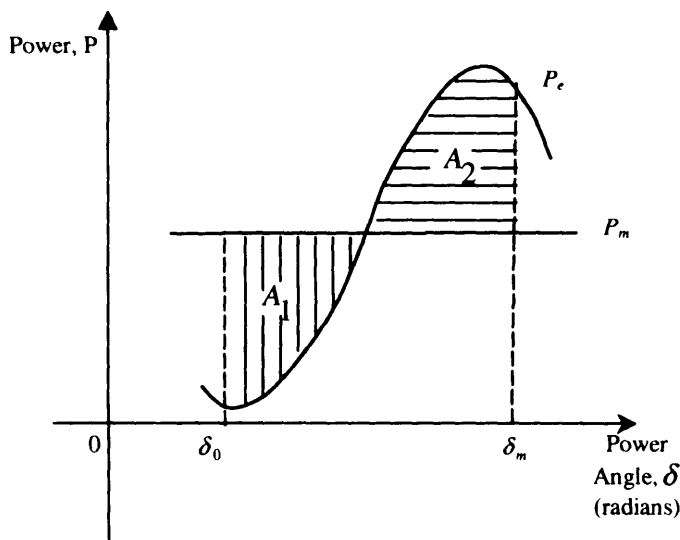


Figure 4.22 Equal-area criterion for stability.

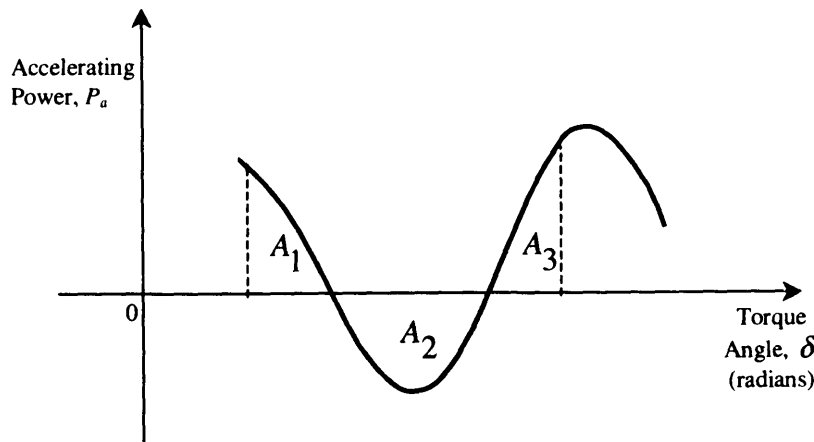


Figure 4.23 Accelerating power as a function of the torque angle.

Example 4

Consider the system of the previous three examples. Determine whether the system is stable for the fault of an open circuit on the second line. If the system is stable, determine δ_s , the maximum swing.

Solution

From the examples given above we have

$$\delta_0 = 19.2^\circ$$

$$\delta_1 = 29.50^\circ$$

The geometry of the problem is shown in Fig. 4.24. We can calculate the area A_1 immediately:

$$A_1 = 0.94 [29.15 - 19.20] \frac{\pi}{180} - \int_{19.20}^{29.15} 1.93 \sin \delta \, d\delta$$

Observe that the angles δ_1 and δ_0 are substituted for in radians. The result is:

$$A_1 = 0.0262$$

The angle δ_s is

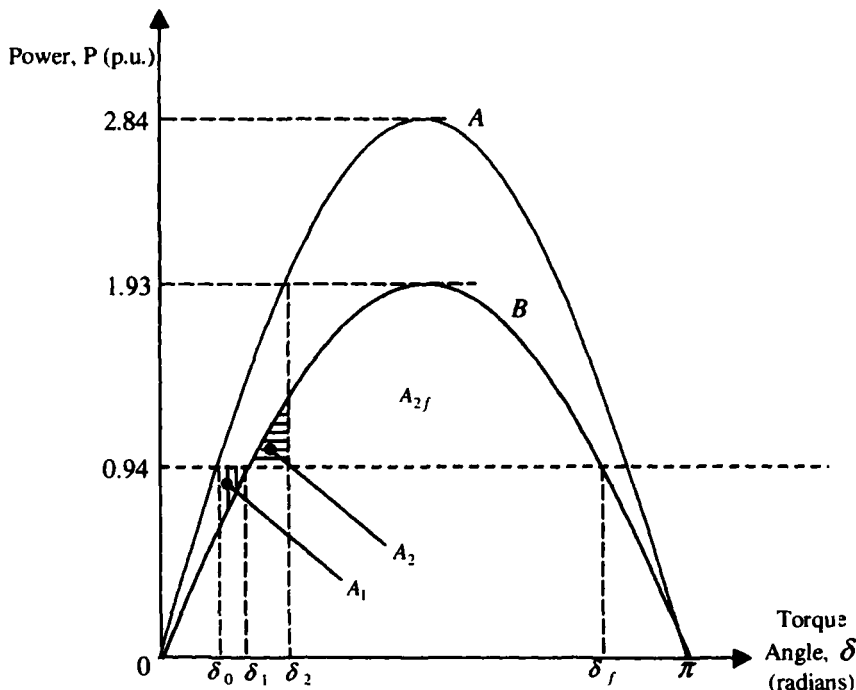


Figure 4.24 Power angle curves for example 4.

$$\delta_f = 180 - \delta_1 = 150.85^\circ$$

If the area enclosed by the power angle curve for one circuit and the fixed $P_m = 0.94$ line between δ_1 and δ_f denoted by A_2 is larger than A_1 then the system is stable. To ascertain this we have

$$A_2 = 2 \int_{\delta_1}^{\pi} 1.93 \sin \delta d\delta = 3.37$$

This clearly gives

$$A_2 > A_1$$

and the system is stable.

The angle δ_c is obtained by solving for $A_2 = A_1$. Here we get:

$$0.0262 = \int_{\delta_1}^{\delta_s} 1.93 \sin \delta \, d\delta - 0.94[\delta_s - \delta_1] \frac{\pi}{180}$$

This gives some algebra

$$1.93 \cos \delta_s + 0.0164 \delta_s = 2.1376$$

The solution is obtained iteratively as $\delta_s = 39.39^\circ$

This example shows the application of the equal area criterion to the case of a generator supplying power to an infinite bus over two parallel transmission lines. For the loading indicated above the system is stable. The opening of one of the lines may cause the generator to lose synchronism even though the load could be supplied over a single line. The following example illustrates this point.

Example 5

Assume that the system in Example 3 is delivering an active power of 1.8 pu using the same source, voltage E , as before. Determine whether the system will remain stable after one circuit of the line is opened.

Solution

We have for the initial angle δ_0

$$1.8 = 2.84 \sin \delta_0$$

$$\delta_0 = 39.33^\circ$$

The angle δ_1 , is obtained from

$$1.8 = 1.93 \sin \delta_1$$

$$\delta_1 = 68.85^\circ$$

The area A_1 is thus:

$$A_1 = 1.8[68.85 - 39.33] \frac{\pi}{180} - \int_{39.33}^{68.85} 1.93 \sin \delta \, d\delta = 0.13$$

The area A_2 is obtained as:

$$A_2 = \int_{\delta_1}^{\frac{\pi}{2}} 3.86 \sin \delta \, d\delta - 1.8[\delta_2 - \delta_1] \frac{\pi}{180} = 0.06$$

We note that $A_1 > A_2$ and the system is therefore unstable.

If a three-phase short circuit took place at a point on the extreme end of the line, there is some impedance between the generator bus and the load (infinite) bus. Therefore, some power is transmitted while the fault is still on. The situation is similar to the ones analyzed above and we use the following example to illustrate the point.

Example 6

A generator is delivering 25% of P_{\max} to an infinite bus through a transmission line. A fault occurs such that the reactance between the generator and the bus is increased to two times its prefault value.

1. Find the δ_0 before the fault.
2. Show graphically what happens when the fault is sustained.
3. Find the maximum value of δ swing in case of a sustained fault.

Solution

Figure 4.25 illustrates the situation for this example. The amplitude of the power angle curve with the fault sustained is half of the original value.

Before the fault we have

$$0.25 = 1.0 \sin \delta_0$$

$$\delta_0 = 18.48^\circ$$

At the fault instant, we get

$$0.25 = 0.5 \sin \delta_1$$

$$\delta_1 = 30^\circ$$

$$A_1 = 0.25[30 - 14.48] \frac{\pi}{180} - \int_{14.48}^{30} 0.5 \sin \delta d\delta = 0.0166$$

As before, the stability condition yields

$$0.0166 = \int_{\delta_1}^{\delta_s} 0.5 \sin \delta d\delta - 0.25[\delta_s - \delta_1] \frac{\pi}{180}$$

Hence

$$0.5 \cos \delta_s + \frac{\pi}{72^\circ} \delta_s = 0.5473$$

By trial and error

$$\delta_s = 46.3^\circ$$

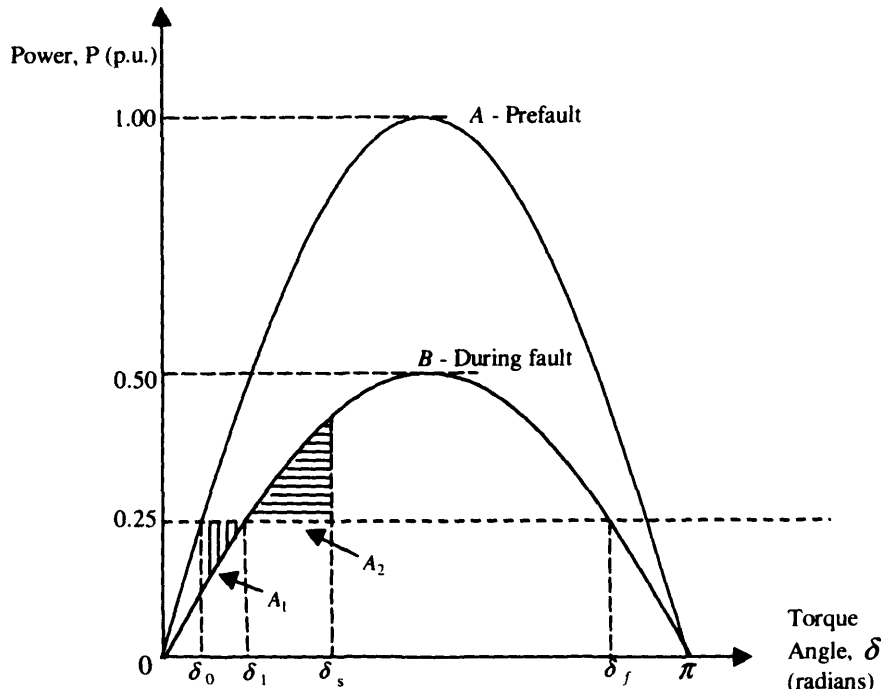


Figure 4.25 Power angle curves for example 6.

The following example illustrates the effects of short circuits on the network from a stability point of view.

Example 7

The system of the previous examples delivers a power of 1.0 pu when subjected to a three-phase short circuit in the middle of one of the transmission circuits. This fault is cleared by opening the breakers at both ends of the faulted circuit. If the fault is cleared for $\delta_c = 50^\circ$, determine whether the system will be stable or not. Assume the same source voltage E is maintained as before. If the system is stable, find the maximum angle of swing.

Solution

The power angle curves have been determined for the prefault network in Example 1 and for the postfault network in Example 2. In Example 3 we obtained

$$E = 1.35 \text{ pu}$$

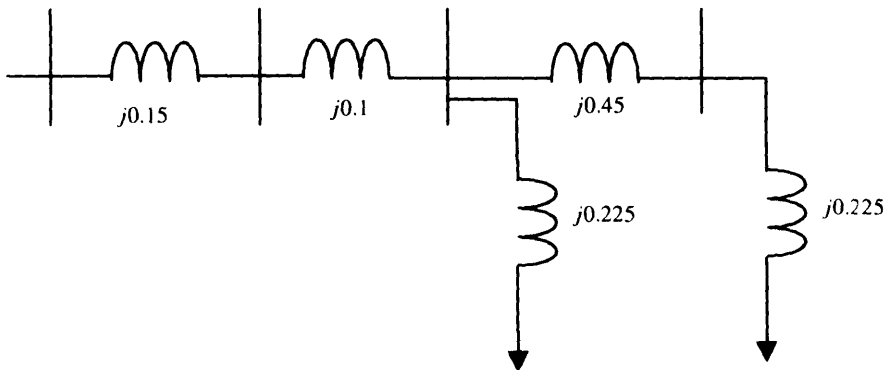


Figure 4.26 Network configuration during the fault.

Therefore

$$\text{Prefault: } P = 2.84 \sin\delta$$

$$\text{Postfault: } P = 1.93 \sin\delta$$

During the fault the network offers a different configuration, which is shown in Fig. 4.26. We will need to reduce the network in such a way as to obtain a clear path from the source to the infinite bus. We do this by using a $Y - \Delta$ transformation as indicated in Fig. 4.27.

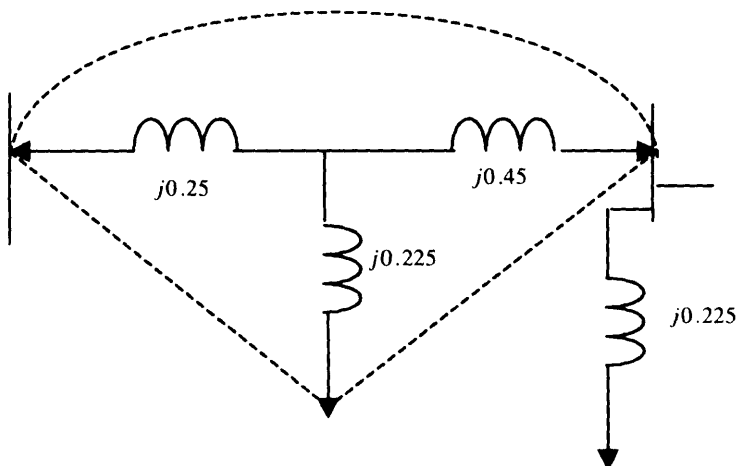


Figure 4.27 $Y - \Delta$ transformation for the reduced network of example 7.

Consequently

$$X = 0.45 + 0.25 + \frac{(0.45)(0.25)}{0.225} = 1.2$$

and fault power angle curve is given by

$$P = 1.13 \sin\delta$$

The three power angle curves are shown in Fig. 4.28.

The initial angle is given by the equation

$$1.0 = 2.84 \sin\delta_0$$

$$\delta_0 = 20.62^\circ$$

The clearing angle is $\delta_c = 50^\circ$

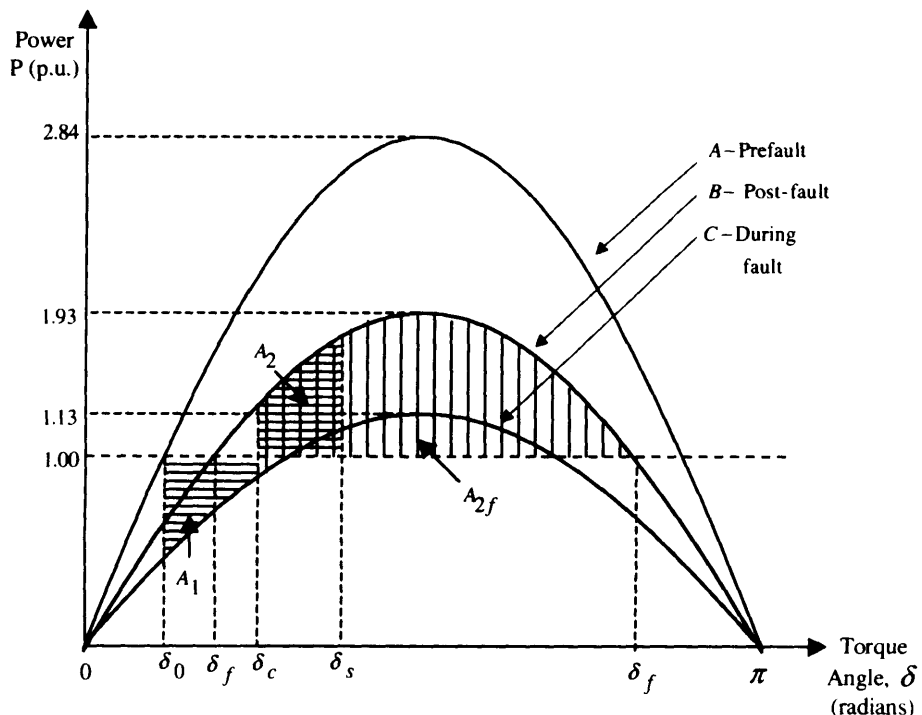


Figure 4.28 Pre-fault, during fault, and post-fault power angle curves for example 7.

The area A_1 can thus be calculated as:

$$A_1 = [50 - 20.62] \frac{\pi}{180} - \int_{20.62}^{50} 1.13 \sin\delta d\delta = 0.18$$

The maximum area A_2 is obtained using the angle δ_i'

$$1 = 1.93 \sin\delta_i'$$

$$\delta_i' = 31.21^\circ$$

$$\delta_i = 180 - \delta_i' = 148.79^\circ$$

Now

$$A_{2i} = \int_{\delta_i}^{\delta_i'} 1.93 \sin\delta d\delta - 1.0[\delta_i - \delta_i] \frac{\pi}{180} = 1.17$$

We note that $A_1 > A_{2i}$ and the system is therefore stable.
To calculate the angle of maximum swing we have

$$A_1 = A_{2i}$$

Thus

$$0.18 = \int_{\delta_i}^{\delta_s} 1.93 \sin\delta d\delta - [\delta_s - \delta_i] \frac{\pi}{180}$$

Hence

$$1.93 \cos\delta_s + 1.7453 \times 10^{-2}\delta_s = 1.19332$$

By trial and error

$$\delta_s \cong 66.3^\circ$$

4.11 MATHEMATICAL MODELS AND SOLUTION METHODS IN TRANSIENT STABILITY ASSESSMENT FOR GENERAL NETWORKS

It is common practice to model static equipment in the transmission system by lumped equivalent pi parameters independent of the changes arising in the generating and load equipment. This approach is employed in multimachine stability programs because the inclusion of time varying parameters would pro-

duce major computational difficulties. Moreover, frequency, the most obvious variable in the network, usually varies by only a small amount and thus, the errors involved are insignificant. Additionally, the rates of change of network variables are assumed to avoid the introduction of differential equations into the network solution. The transmission network can thus be represented in the same manner as in the load-flow or short-circuit programs, that is, by a square complex admittance matrix.

The behavior of the network is described by the matrix equation:

$$I_{nj} = YV$$

where I_{nj} is the vector of injected currents into the network due to generators and loads Y is the admittance matrix of the network, and V is the vector of nodal voltages.

Any loads represented by constant impedances may be directly included in the network admittance matrix with the injected currents due to these loads set to zero. Their effect is thus accounted for directly by the network solution.

4.11.1 System Representation

Two alternative solution methods are possible. The preferred method uses the nodal matrix approach, while the alternative is the mesh matrix method. Matrix reduction techniques can be used if specific network information is not required, but this gives little advantage as the sparsity of the reduced matrix is usually very much less.

Nodal Matrix Method

In this method, all network loads are converted into Norton equivalents of injected currents in parallel with admittances. The admittances can be included in the network admittance matrix to form a modified admittance matrix which is then inverted, or preferably factorized by some technique so that solution at each stage is straight forward.

The following solution process applies:

1. For each network load, determine the injected currents into the modified admittance matrix by solving the relevant differential and algebraic equations.
2. Determine network voltages from the injected currents using the Z -matrix or factors.

As the network voltages affect the loads, an iterative process is often required, although good approximations can be used to avoid this.

With the Nodal Matrix method, bus voltages are available directly and branch currents can be calculated if necessary.

4.11.2 Synchronous Machine Representation in the Network

The equations representing a synchronous machine are given in the form of Thevenin voltages behind its impedances. This must be modified to a current source in parallel with an admittance using Norton's theorem. The admittance of the machine thus formed may be added to the shunt admittance of the machine bus and treated as a network parameter. The vector I_{nj} thus contains the Norton equivalent currents of the synchronous machines. The synchronous machine equations are written in a frame of reference rotating with its own rotor. The real and imaginary components of the network equations, as given in Fig. 4.29, are obtained from the following transformation

$$V_r = V_d \cos\delta - V_q \sin\delta$$

$$V_m = V_d \sin\delta + V_q \cos\delta$$

The inverse relation is

$$V_d = V_r \cos\delta + V_m \sin\delta$$

$$V_q = -V_r \sin\delta + V_m \cos\delta$$

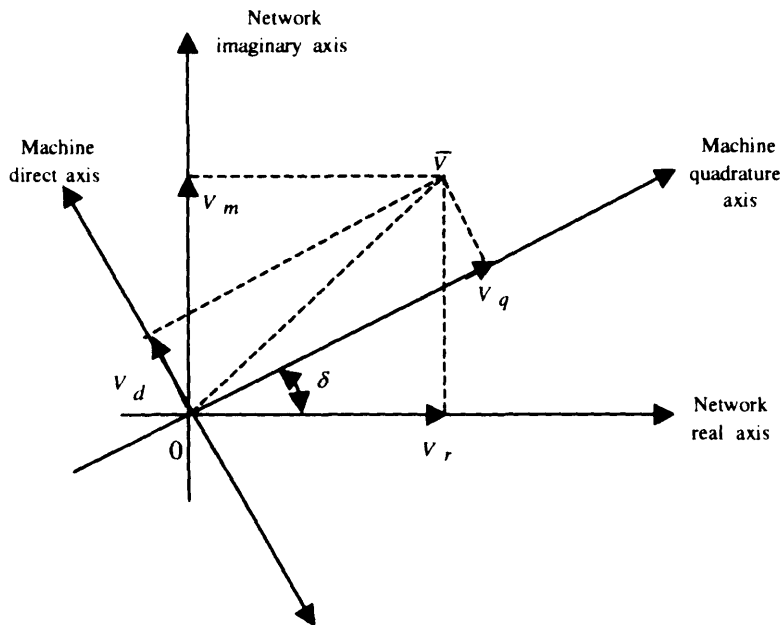


Figure 4.29 Synchronous machine and network frames of reference.

The transformation also applies to currents.

When saliency is accounted for, the subtransient and transient reactances in direct and quadrature axes frames are different, and the Norton shunt admittance will have a different value in each axis, and when transformed into the network frame of reference, will be time varying. To circumvent this difficulty, a constant impedance is used while modifying the injected current.

4.11.3 Load Representation in the Network

To be suitable for representation in the overall solution method, loads must be transformed into injected currents into the transmission network from which the terminal voltages can be calculated. A Norton equivalent model of each load must therefore be introduced. In a similar way to that adopted for synchronous machines, the Norton admittance may be included directly in the network admittance matrix.

A constant impedance load is therefore included in the network admittance matrix and its injected current is zero. This representation is extremely simple to implement, causes no computational problems, and improves the accuracy of the network solution by strengthening the diagonal elements in the admittance matrix. Nonimpedance loads may be treated similarly. In this case the steady-state values of voltage and complex power obtained from the load flow are used to obtain a steady-state equivalent admittance (\bar{Y}_0) which is included in the network admittance matrix [Y]. During the stability run, each load is solved sequentially along with the generators, etc., to obtain a new admittance (\bar{Y}), i.e.:

$$\bar{Y} = \frac{\bar{S}^*}{|V|^2}$$

The current injected into the network thus represents the deviation of the load characteristic from an impedance characteristic.

$$I_{inj} = [Y_0 - Y]V$$

By converting the load characteristic to that of a constant impedance, when the voltage drops below some predetermined value (V_{min}), the injected current is kept relatively small. An example of a load characteristic and its corresponding injected current is shown in Fig. 4.30.

In an alternative model the low-voltage impedance is added to the network and the injected current compensates for the deviation from the actual characteristic. In this case, there is a nonzero injected current in the initial steady-state operational condition.

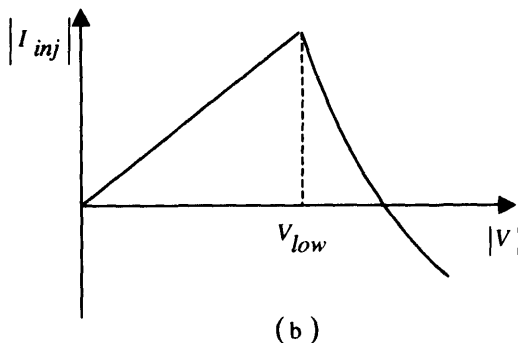
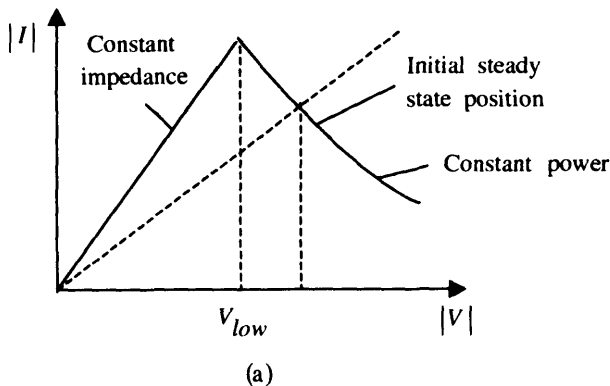


Figure 4.30 Load and injected currents for a constant type load with low voltage adjustment. (a) Load current. (b) Injected current.

4.11.4 System Faults and Switching

In general most power system disturbances to be studied will be caused by changes in the network, normally caused by faults and subsequent switching action. Occasionally the effect of branch or machine switching will be considered.

Although faults can occur anywhere in the system, it is much easier computationally to apply a fault to a bus. In this case, only the shunt admittance at the bus need be changed, that is, a modification to the relevant self-admittance of the Y matrix. Faults on branches require the construction of a dummy bus at the fault location and suitable modification of the branch data unless the distance between the fault position and the nearest bus is small enough to be ignored.

The worst case is a three-phase zero-impedance fault and this involves placing an infinite admittance in parallel with the existing shunt admittance. In practice, a nonzero but sufficiently low-fault impedance is used so that the bus voltage is effectively brought to zero. This is necessary to meet the requirements of the numerical solution method.

The application or removal of a fault at an existing bus does not affect the topology of the network and where the solution method is based on sparsity exploiting ordered elimination, the ordering remains unchanged and only the factors required for the forward and backward substitution need be modified. Alternatively the factors can remain constant and diakoptical techniques can be used to account for the network change.

4.11.5 Branch Switching

Branch switching can easily be carried out by either modifying the relevant mutual- and self-admittances of the Y matrix or by using diakoptical techniques. In either case, the topology of the network can remain unchanged, as an open branch is merely one with zero admittance. While this does not fully exploit sparsity, the gain in computation time by not reordering exceeds the loss by retaining zero elements, in almost all cases.

The only exception is the case of a branch switched into a network where no interconnections existed prior to that event. In this case, either diakoptical or reordering techniques become necessary. To avoid this problem, a dummy branch may be included with the steady-state data of sufficiently high impedance that the power flow is negligible under all conditions, or alternatively, the branch resistance may be set negative to represent an initial open circuit. A negative branch reactance should not be used as this is a valid parameter where a branch contains series capacitors.

Where a fault occurs on a branch but very close to a bus, non-unit protection at that bus will normally operate before that at the remote end. Therefore, there will be a period when the fault is still being supplied from the remote end. There are two methods of accounting for this type of fault.

The simplest method only requires data manipulation. The fault is initially assumed to exist at the local bus rather than on the branch. When the specified time for the protection and local circuit breaker to operate has elapsed, the fault is removed and the branch on which the fault is assumed to exist is opened. Simultaneously, the fault is applied at the remote bus, but in this case, with the fault impedance increased by the faulted branch impedance, similarly the fault is maintained until the time specified for the protection and remote circuit breaker to operate has elapsed.

The second method is generally more involved but it is better when protection schemes are modeled. In this case, a dummy bus is located at the fault

position, (even though it is close to the local bus) and a branch with a very small impedance is inserted between the dummy bus and the local bus. The faulted branch then connects the dummy bus to the remote bus and the branch shunt susceptance originally associated with the local bus is transferred to the dummy bus. This may all be done computationally at the time when the fault is being specified. The two branches can now be controlled independently by suitable protection systems. An advantage of this scheme is that the fault duration need not be specified as part of the input data. Opening both branches effectively isolates the fault, which can remain permanently attached to the dummy bus, or if auto-reclosing is required, it can be removed automatically after a suitable deionization period.

If the network is not being solved by a direct method, the second method will probably fail. During the iterative solution of the network, slight voltage errors will cause large currents to flow through a branch with a very small impedance. This will slow convergence and in extreme cases will cause divergence. With a direct method, based on ordered elimination, an exact solution of the bus voltages is obtained for the injected currents specified at that particular iteration. Thus, provided that the impedance is not so small that numerical problems occur when calculating the admittance, and the subsequent factors for the forward and backward substitution, then convergence of the overall solution between machines and network will be unaffected. The value of the low-impedance branch between the dummy and local bus may be set at a fraction of the total branch impedance, subject to a minimum value. If this fraction is under 0.001, the change in branch impedance is very small compared to the accuracy of the network data input and it is unnecessary to modify the impedance of the branch from the remote to the dummy bus.

4.11.6 Machine Switching

Machine switching may be considered, either as a network or machine operation. It is a network operation if a dummy bus is created to which the machine is connected. The dummy bus is then connected to the original machine bus by a low-impedance branch.

Alternatively, it may be treated as a machine operation by retaining the original network topology. When a machine is switched out, it is necessary to remove its injected current from the network solution. Also any shunt admittance included in the network Y matrix, which is due to the machine must be removed.

Although a disconnected machine can play no direct part in system stability, its response should still be calculated as before, with the machine stator current set to zero. Thus machine speeds, terminal voltages, etc., can be observed even

when disconnected from the system and in the event of reconnection, sensible results are obtained.

When an industrial system is being studied many machines may be disconnected and reconnected at different times as the voltage level changes. This process will require many recalculations of the factors involved in the forward and backward substitution solution method of the network. However, these can be avoided by using the method adopted earlier to account for synchronous machine saliency. That is, an appropriate current is injected at the relevant buses, which cancels out the effect of the shunt admittance.

4.12 INTEGRATION TECHNIQUES

Many integration methods have been applied to the power system transient stability problem, and the principal methods are discussed now.

4.12.1 Predictor Corrector Methods

These methods for the solution of the differential equation

$$\dot{Y} = F(Y, X) \text{ with } Y(0) = Y_0$$

$$\text{and } X(0) = X_0$$

have all been developed from the general k -step finite difference equation:

$$\sum_{i=0}^k \alpha_i Y(n-i+1) - h \sum_{i=0}^k \beta_i F(n-i+1) = 0$$

Basically the methods consist of a pair of equations, one being explicit ($\beta_0 = 0$) to give a prediction of the solution at $t(n+1)$ and the other being implicit ($\beta_0 \neq 0$) which corrects the predicted value. There are a great variety of methods available, such as hybrid methods, the choice of which being made by the requirements of the solution.

It is usual for simplicity to maintain a constant step length with these methods if $k > 2$. Each application of a corrector method improves the accuracy of the method by one order, up to a maximum given by the order of accuracy of the corrector. Therefore, if the corrector is not to be iterated, it is common to use a predictor with an order of accuracy one less than that of the corrector. The predictor is thus not essential as the value at the previous step may be used as a first crude estimate, but the number of iterations of the corrector may be large.

While for accuracy, there is a fixed number of relevant iterations, it is

desirable for stability purposes to iterate to some predetermined level of convergence. The characteristic root (z_i) of a predictor or corrector when applied to the single variable problem

$$sy = \lambda y \text{ with } y(0) = y_0$$

may be found from

$$\sum_{i=0}^k (\alpha_i - h\lambda\beta_i)z^{k-i} = 0$$

Applying a corrector to the problem defined and rearranging gives:

$$y(n+1) = \frac{-\sum_{i=1}^k (\alpha_i - h\lambda\beta_i)y(n-i+1)}{\alpha_0 - h\lambda\beta_0}$$

the solution to the problem becomes direct. The predictor is now not necessary as the solution only requires information of y at the previous steps, i.e., at $y(n-i+1)$, for $i = 1, 2, \dots, k$.

Where the problem contains two variables, one nonintegrable, such that:

$$sy = \lambda y + \mu x \text{ with } y(0) = y_0$$

$$x(0) = x_0$$

$$0 = g(x, y)$$

then

$$y(n+1) = c_{n+1} + m_{n+1}x(n+1)$$

where

$$c_{n+1} = \frac{-\sum_{i=1}^k (\alpha_i - h\lambda\beta_i)y(n-i+1) - h\mu\beta_r x(n+1)}{\alpha_0 - h\lambda\beta_0}$$

Although c_{n+1} and m_{n+1} are constant at a particular step, the solution is iterative.

Strictly in this simple case, $x(n+1)$ could be eliminated but in the general multivariable case this is not so. The convergence of the method is now a function of the nonlinearity of the system. Provided that the step length is sufficiently small, a simple Jacobian form of iteration gives convergence in only a few iterations. It is also possible to form a Jacobian matrix and obtain a solution by a Newton iterative process, although the storage necessary is much larger and the step length must be sufficiently small to ensure convergence.

For a multivariable system, the following two equations are coupled

$$sY = F(Y, X) \text{ with } Y(0) = Y_0 \text{ and } X(0) = X_0$$

and the solution of the integrable variables is given by the matrix equation.

The elements of the vector c_{n+1} are given by the vector form of

$$c_{n+1} = \frac{-\sum_{i=1}^k (\alpha_i - h\lambda\beta_i)y(n-i+1) - h\mu\beta_n x(n-i+1)}{\alpha_0 - h\lambda\beta_0}$$

and the elements of the sparse m_{n+1} matrix are given by

$$m_{n+1} = \frac{-h\mu\beta_0}{\alpha_0 - h\lambda\beta_0}$$

The iterative solution may be started at any point in the loop, if Jacobian iterations are used.

4.12.2 The Euler Method

Consider the following ordinary differential equation:

$$\dot{x}(t) = f[x(t), t]$$

Let $\mathbf{x}(t)$ be the state vector of this nonlinear differential equation, which is to be solved by an appropriate integration technique. The Euler method utilizes a predictor function based on the Taylor series expansion of $x(t + \Delta t)$, where Δt is the step size. As such, by neglecting the higher order terms in the series expansion, we obtain the generalized Euler's formula:

$$x(t + \Delta t) = x(t) + x(t) \cdot \Delta t \quad \text{where} \quad \dot{x}(t) = \frac{\partial x(t)}{\partial t}$$

The method is not often used for real-time applications in power systems, as it is computationally burdensome. Also, the accuracy of this model for integration is sacrificed by the truncation of $O[\Delta t]^2$ and higher order terms done in the Taylor series expansion. Figure 4.31 outlines an example of Euler's integration technique to power system dynamic stability assessment.

4.12.3 The Modified Euler Method

Reconsider the following problem to be solved:

$$\dot{x}(t) = f[x(t), t]$$

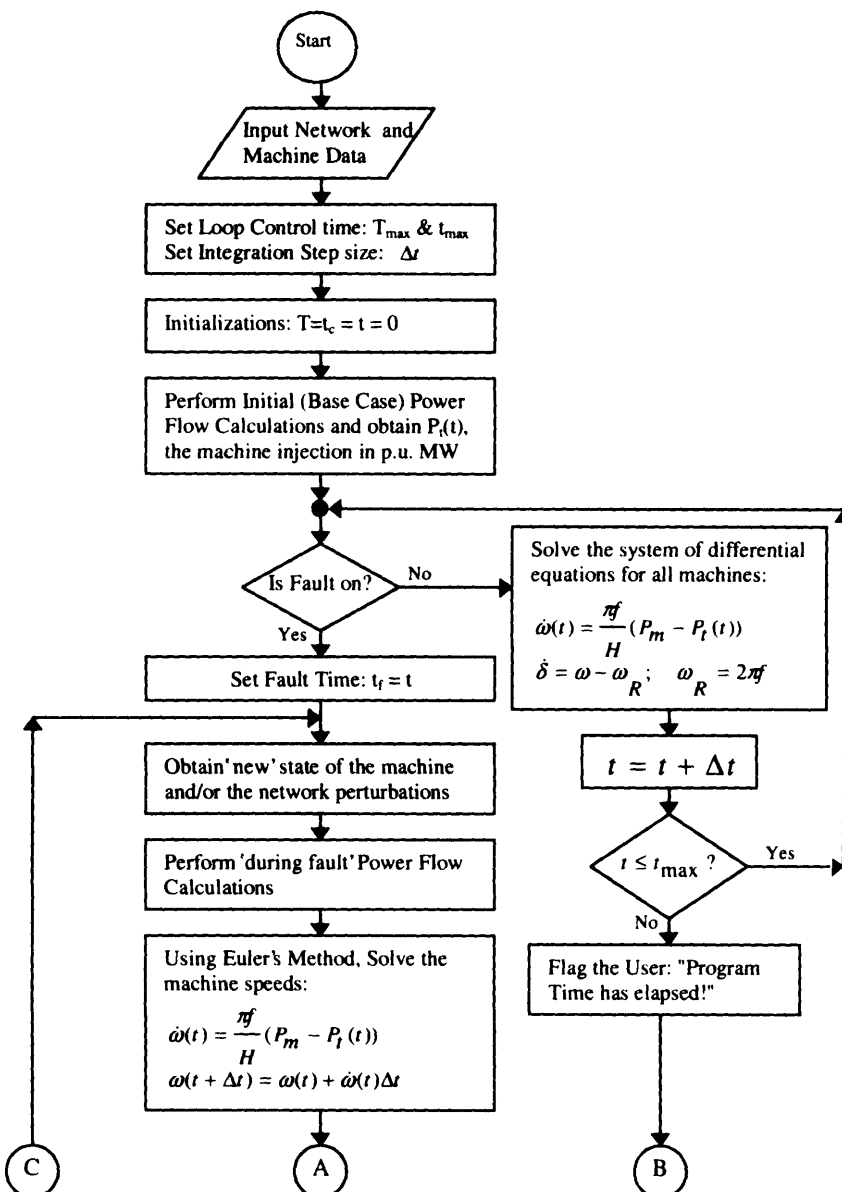
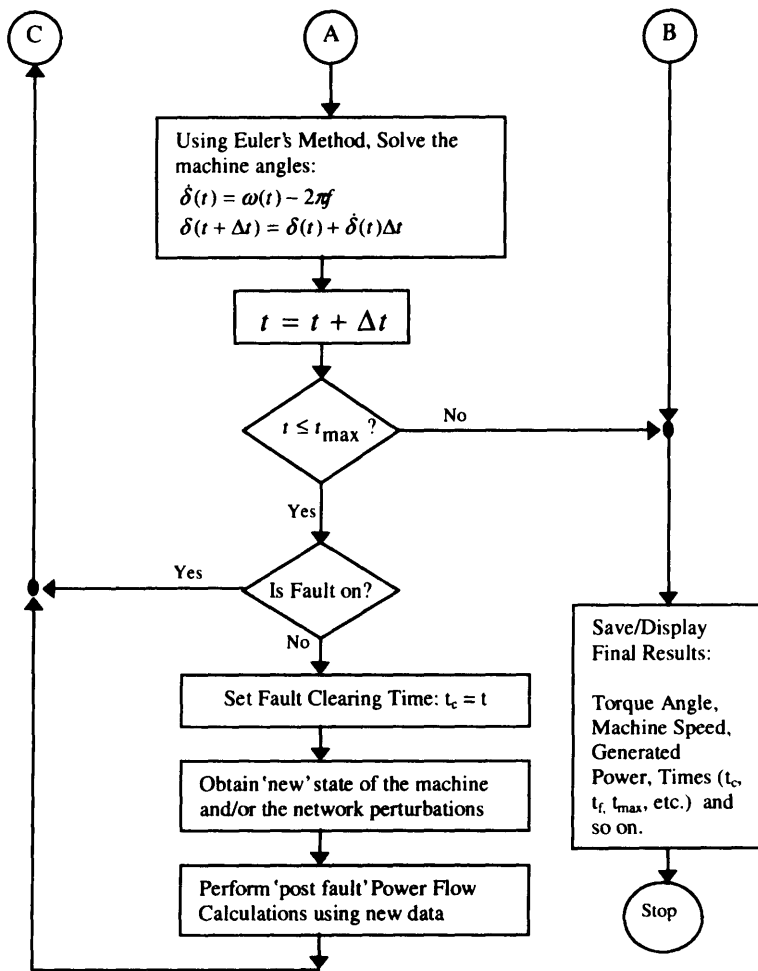


Figure 4.31 The transient stability algorithm.

**Figure 4.31** Continued.

where $x(t)$ and $f(x, t)$ are scalar or vector quantities. Expanding $x(t)$ to the right and left using the Taylor expansion yields:

$$x(t \pm \Delta t) = x(t) \pm \frac{\Delta t}{1!} \cdot \frac{\partial x(t)}{\partial t} + \frac{(\Delta t)^2}{2!} \cdot \frac{\partial^2 x(t)}{\partial t^2} \pm \frac{(\Delta t)^3}{3!} \cdot \frac{\partial^3 x(t)}{\partial t^3} + O[(\Delta t)^4]$$

If the $O[(\Delta t)^3]$ and higher order terms are truncated for a small step size, it can be shown that the modified Euler formula is obtained as follows:

$$x(t + \Delta t) - x(t - \Delta t) = 2\Delta t f[x(t), t]$$

Alternatively, we may write:

$$x_{n+1} = x_n + 2\Delta t f[x(t), t]_n$$

Note that the modified Euler method is not self-starting and thus requires an initial prediction on the state variables in the vector solution.

4.12.4 Trapezoidal Method

The trapezoidal rule is a nonself-starting integration technique that is somewhat related to the modified Euler method and is based on the geometric interpretation of the problem. The order of truncation in the Taylor series expansion of $x(t \pm \Delta t)$ is $O[(\Delta t)^2]$. The trapezoidal formula is:

$$x_{n+1} = x_n + \frac{\Delta t}{2} [f[x(t), t]_n + f[x(t), t]_{n+1}]$$

The merits of the trapezoidal method is evident in the accuracy brought forward as a result of the truncation of the $O[(\Delta t)^3]$ and higher order terms.

4.12.5 Runge-Kutta Methods

Runge-Kutta methods are able to achieve high accuracy while remaining single step methods. This is obtained by making further evaluation of the functions within the step. Here we present a class of self-starting prediction formulae, which are applicable in the assessment of transient analysis of rotating machines, in which case we are solving the swing equation of the generators.

The numerical integration of the ordinary differential equation given by:

$$\dot{x}(t) = f[x(t), t]$$

by a predictor generally involves calculation of x_{n+1} as a function of $x_n, x_{n-1}, x_{n-2}, \dots, f_n, f_{n-1}, f_{n-2}, \dots$, and t_n . If the predictor is self-starting, it must be free

of terms in $x_{n-1}, x_{n-2}, \dots, f_n, f_{n-1}, f_{n-2}$ and so forth. That is, the next state solution should be of the form: $x_{n+1} = F(x_n, f_n, t_n)$. Now, the equation below summarizes this requirement and is called the Runge-Kutta predictor formula.

$$y(n+1) = y(n) + \sum_{i=1}^m w_i k(i)$$

where $k(i) = hf \left\{ t(n) + c_i h, y(n) + \sum_{j=1}^m \alpha_{ij} k(j) \right\}$ for $i = 1, 2, \dots, m$

and the sum of all the weights equal to unity, i.e., $\sum_{i=1}^m w_i = 1$

The coefficients are uniquely determined, giving rise to various orders and associated approximate or accurate models of the Runge-Kutta predictor formula. Table 4.1 summarizes the 2nd, 3rd, and 4th order Runge-Kutta formulae.

Being single-step these methods are self starting and the step length need not be constant. If j is restricted so that $j < i$ then the method is explicit and c_1 must be zero. When j is permitted to exceed i , then the method is implicit and an iterative solution is necessary.

Table 4.1 Summary of the RK-2, RK-3, and RK-4 Predictor Formulae

| Runge-Kutta Predictor Formulae | Coefficients |
|--------------------------------|--|
| RK-2 | $k^{(1)} = F(x_n, t_n)$ $x_{n+1} = x_n + \frac{h}{2} [k^{(1)} + k^{(2)}]$ $k^{(2)} = F\left(x_n + \frac{h}{2} k^{(1)}, t_n + \frac{h}{2}\right)$ |
| RK-3 | $k^{(1)} = F(x_n, t_n)$ $x_{n+1} = x_n + \frac{h}{6} [k^{(1)} + 4k^{(2)} + k^{(3)}]$ $k^{(2)} = F\left(x_n + \frac{h}{2} k^{(1)}, t_n + \frac{h}{2}\right)$ $k^{(3)} = F(x_n + hk^{(1)}, t_n + h)$ |
| RK-4 | $k^{(1)} = F(x_n, t_n)$ $x_{n+1} = x_n + \frac{h}{6} [k^{(1)} + 2k^{(2)} + 2k^{(3)} + k^{(4)}]$ $k^{(2)} = F\left(x_n + \frac{h}{2} k^{(1)}, t_n + \frac{h}{2}\right)$ $k^{(3)} = F\left(x_n + \frac{h}{2} k^{(2)}, t_n + \frac{h}{2}\right)$ $k^{(4)} = F(x_n + hk^{(2)}, t_n + h)$ |

Explicit Runge-Kutta methods have been used extensively in transient stability studies. They have the advantage that a packaged integration method is usually available or quite readily constructed and the differential equations are incorporated with the method explicitly. It has only been with the introduction of more detailed system component models with very small time constants, that the problems of stability has caused interest in other methods.

Again, the advantage of the Runge-Kutta techniques is that they are all self-starting. The propagated error from one iteration to the next does not increase rapidly, thus the method is said to be stable. The exception is the solution to "stiff" problems, where the solution may diverge unless a small step size is used. (The stiffness of the ordinary differential equations of the system can be measured as a function of the ratio between the smallest to the largest eigenvalues of the linearized system or eigenvector analysis of the Jacobian matrix.) Nevertheless, they are not very attractive to power system engineers as k power flow calculations must be done at every iteration, where k is the order of the Runge-Kutta formula. The following example demonstrates the RK-4 application.

Example

Application of the 4th order Runge-Kutta integration technique to power system dynamic stability assessment. The algorithm is given below.

1. Start the RK-4 Subroutine.
2. Initialize all RK-4 dependencies.

| | |
|---------------------------|--------------------------|
| Count, d = 0; | Step Size, Δt |
| Time, $t = 0$; | Maximum Time, t_{\max} |
| Maximum iteration = itmax | |

3. Solve the initial power flow and the machine equations, and obtain the generator torque angle ($\delta(0)$), terminal voltages, bus injections $P_i^{(d)}(0)$, etc.
4. Initialize the RK-4 Coefficients: $k_i = l_i = 0$ for all $i \in /1,4/$
5. Set the *estimate index* to: $i = d + 1$.
6. Perform RK-4 calculations (obtaining the estimates).

$$k_i = \delta(t)\Delta t = (\omega(t) - 2\pi f)\Delta t$$

$$l_i = \omega(t) = \frac{2\pi f}{2H} (P_m - P_i^{(d)}(t))\Delta t$$

for all machines

7. Increment count: $d = d + 1$.
8. Increment the *estimate index* to: $i = i + 1$.
9. Update the torque angle delta to: $\delta(t) = \delta(t) + \frac{1}{2} k_i$ and solve the power flow for $|V_t|, P_t^{(d)}(t)$, etc.
10. Compute the new coefficients.

$$k_i = (\omega(0) + \frac{1}{2}l_{i-1} - 2\pi f)\Delta t$$

$$l_i = \frac{2\pi f}{2H} (P_m - P_t^{(d)}(t))\Delta t$$

for all machines

11. If $d < 3$, then go to step 7, otherwise continue.
12. Compute the final value of the power angle and the machine speed at $t = t + \Delta t$

$$\delta(t + \Delta t) = \delta(t) + \frac{1}{6}(k_1 + 2k_2 + 2k_3 + k_4)$$

$$\omega(t + \Delta t) = \omega(t) + \frac{1}{6}(l_1 + 2l_2 + 2l_3 + l_4)$$

13. Reset the count: $d = 0$
14. Compute the final power flow for this time interval to get $|V_t|, P_t^{(d)}(t)$, etc.
15. Increment the timer ($t = t + \Delta t$) and make the following comparisons:
 - If $(t < t_{max})$ and $(N \geq itmax)$ then flag the user: "Maximum Number of iteration reached!" and go to step 16.
 - Elseif $(t < t_{max})$ and $(N < itmax)$ then increment the iteration count to: $N = N + 1$ and go to step 4.
 - Else Flag the user: "Run time value of tmax reached!" and continue.
16. Display all results, power angle, machine speed, generator power, generator terminal voltage, etc.
17. End of subroutine.

4.12.6 The Sampling Method (James J. Ray; James A. Momoh, et al.)

Another promising development in this area is the sampling method. It was developed at Howard University with collaboration from the Energy Systems

Network Laboratory (ESNL) in 1989. The sampling method, also known as the “theta” method, takes advantage of the expanded Taylor Series in its formulation and approximations. It was incorporated in a stand-alone program capable of performing stability studies and fault analysis on a wide variety of electric power systems. The sampling method has been tested against the classical integration methods. A 4:1 speed advantage was observed, without sacrificing the accuracy brought forward in the results. Extended application of this method in power system stability studies is being developed for commercial purposes, both as a design tool and as a computational support system.

4.13 THE TRANSIENT STABILITY ALGORITHM

An overview of the structure of a transient stability program is given in Fig. 4.32. Only the main parts of the program have been included, and as can be seen, the same system may have several case studies performed on it by repeatedly specifying switching data when no further switching data is available. Control returns to the start to see if another system is to be studied. With care, the program can be divided into packages of subroutines each concerned with only one aspect of the system. This permits the removal of component models when not required and the easy addition of new models whenever necessary. Thus for example, the subroutines associated with the synchronous machine, the AVR, speed governors, etc., can be segregated from the network. Figure 4.32 shows a more detailed block diagram of the overall structure where this segregation is indicated. The diagram is subdivided into the five sections indicated in Fig. 4.33. While the block diagrams are intended to be self-evident several logic codes need to be explained. These are as follows:

KASE

This is the case study number for a particular system. It is initially set to zero and incremented by 1 at the end of the initialization and at the end of each case study.

KBIFAI

The sparse vectored inverse of the nodal network matrix is obtained using three bifactorization subroutines. The first and second subroutines are integer routines which determine bus ordering and nonzero element location. The code KBIFAI is set to unity if it is necessary to enter these two subroutines, otherwise it is set to zero.

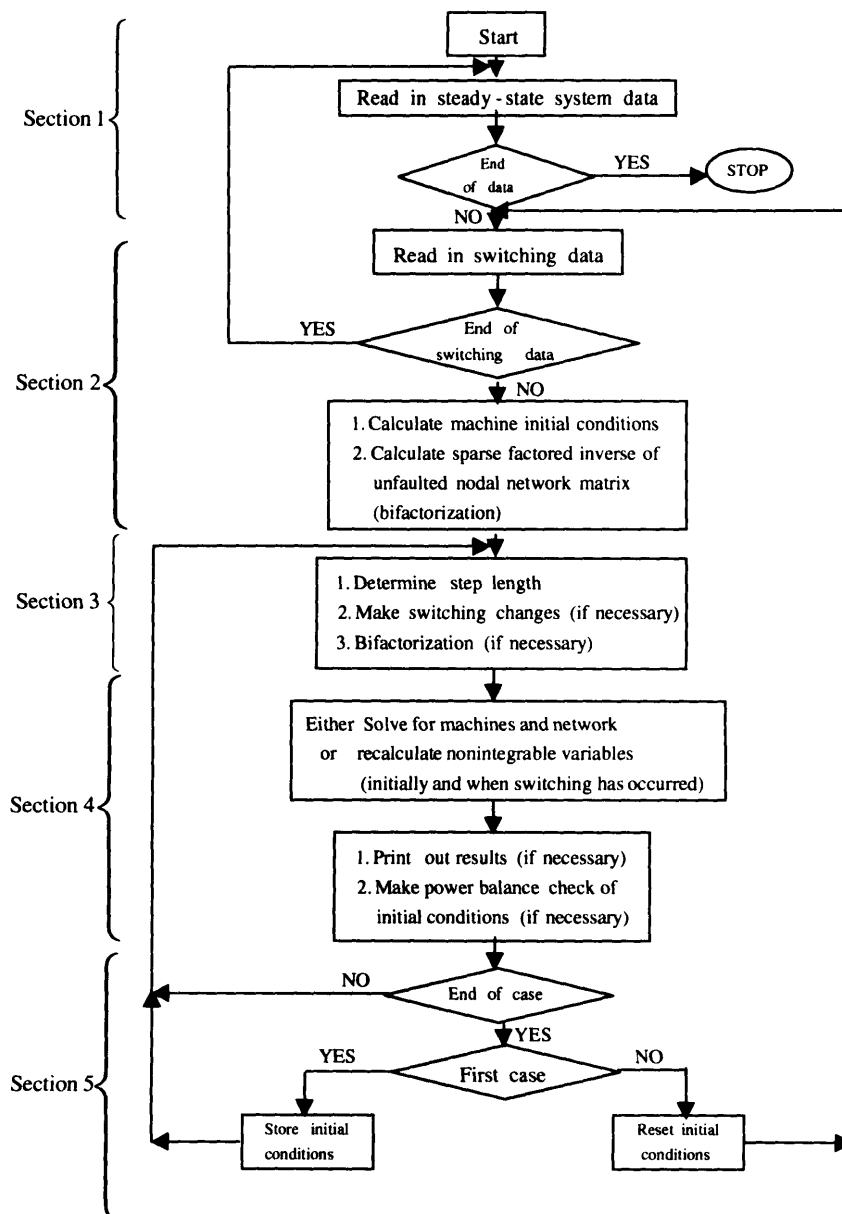


Figure 4.32 The transient stability algorithm.

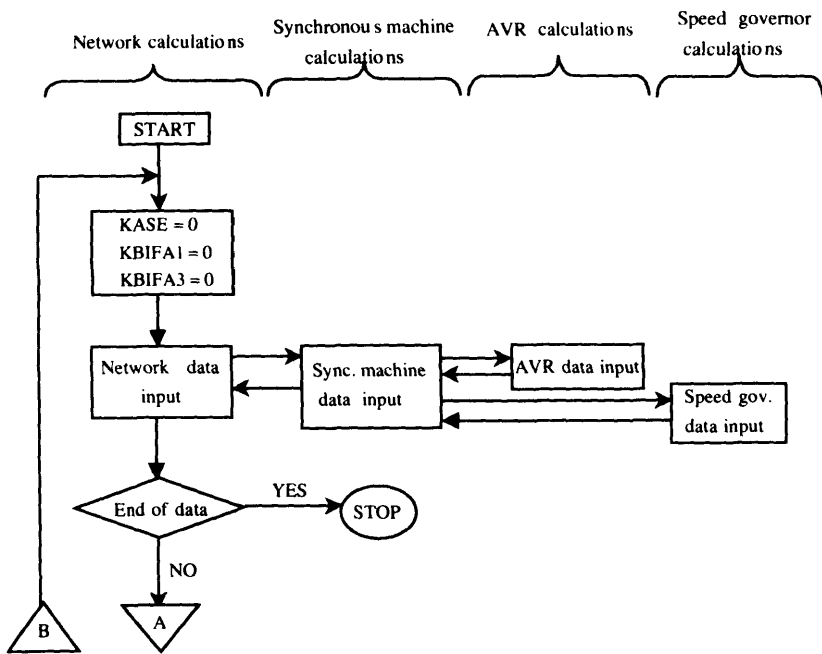


Figure 4.33a Section 1.

KBIFA3

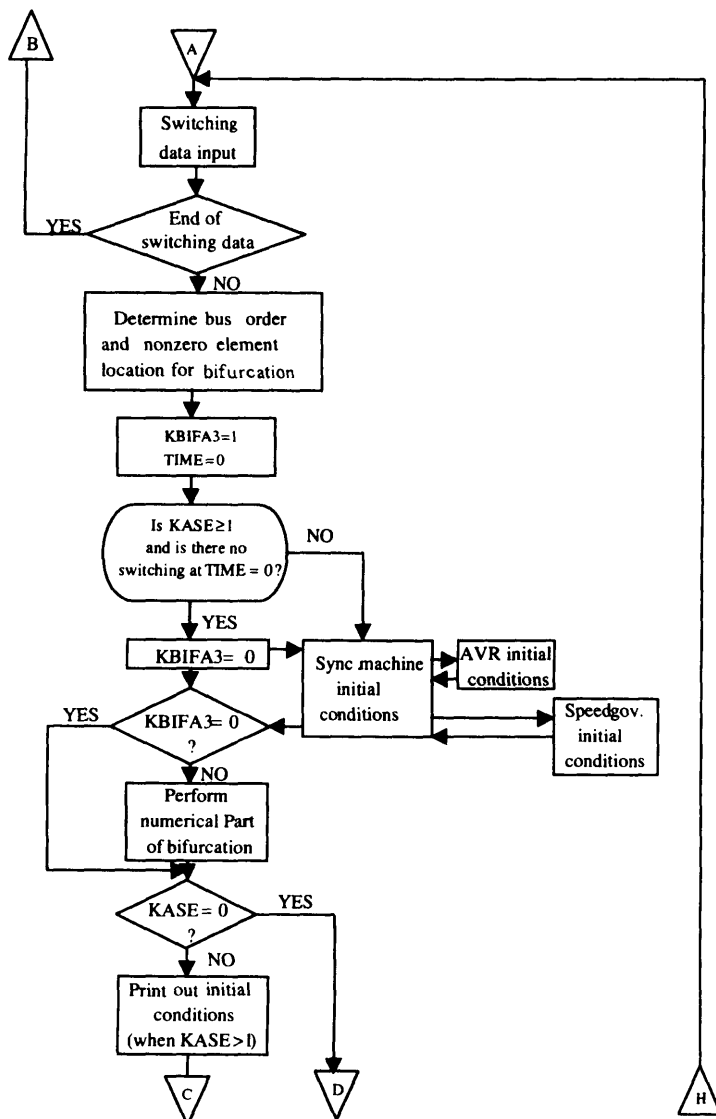
The elements of the sparse-vectored inverse are evaluated in the third bifactorization subroutine. The code KBIFA3 is set to unity if it is necessary to enter this subroutine, otherwise it is set to zero. When KBIFA3 is unity, it indicates that a network discontinuity has occurred and hence it is also used for this purpose.

Time

The integration time.

H

The integration step length. Like KBIFA3, it is also used to indicate a discontinuity when it is set to zero.

**Figure 4.33b** Section 2.

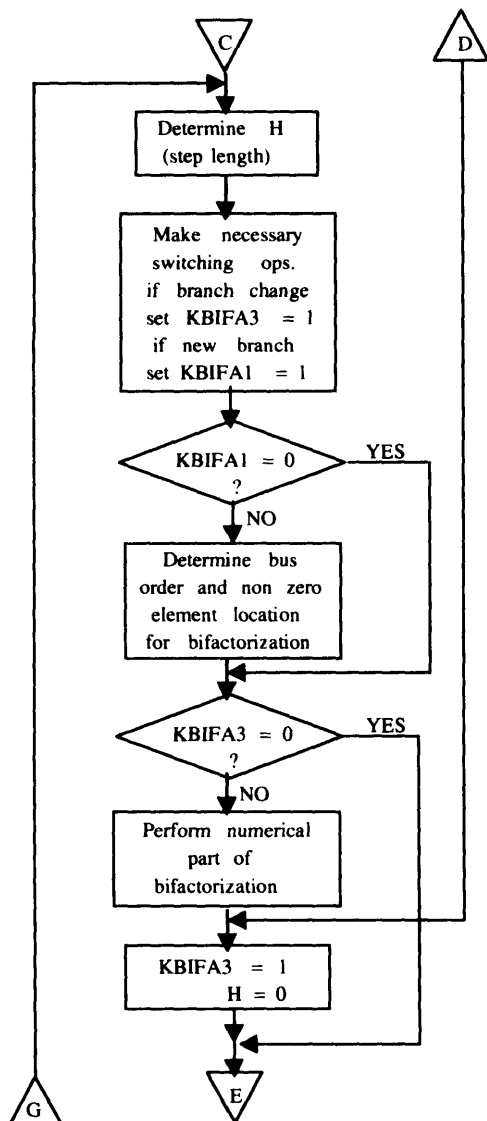
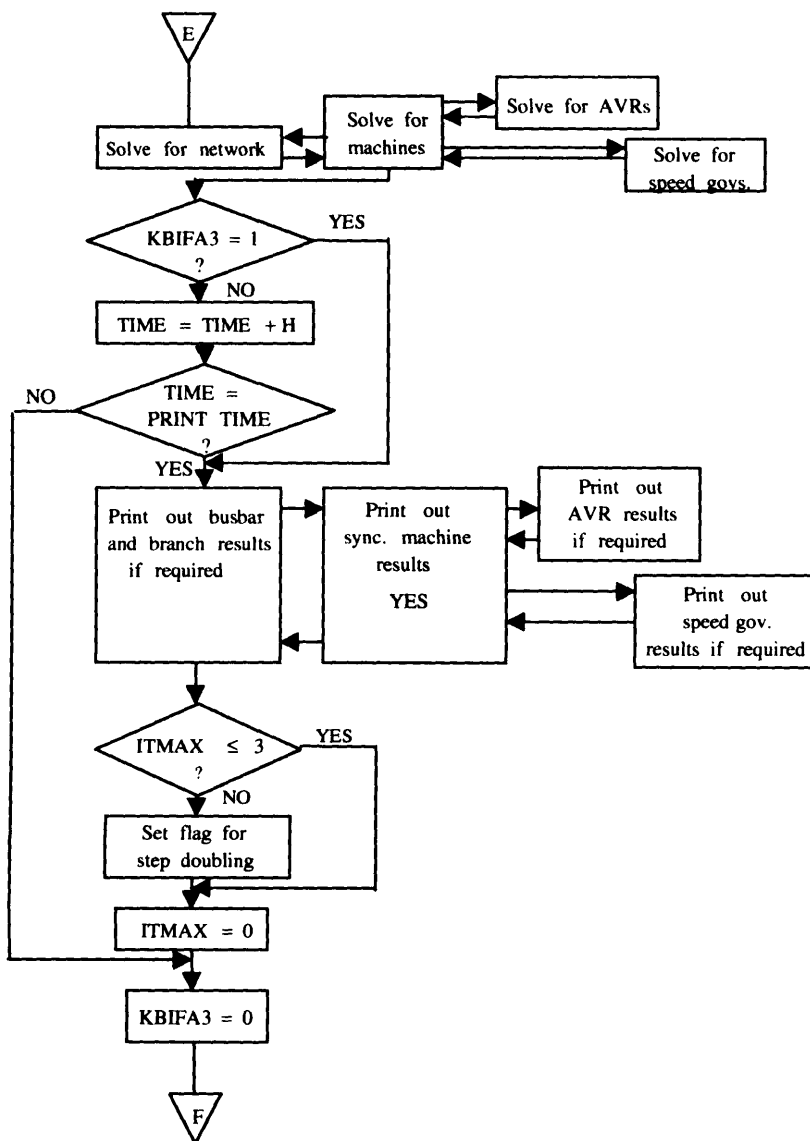


Figure 4.33c Section 3.

**Figure 4.33d** Section 4.

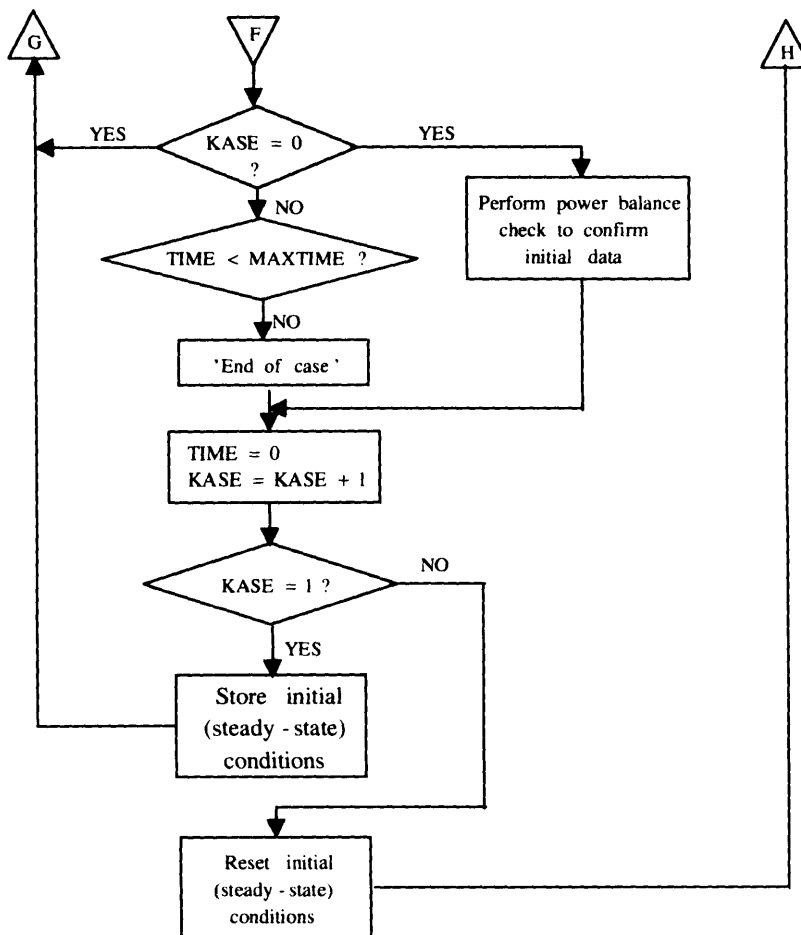


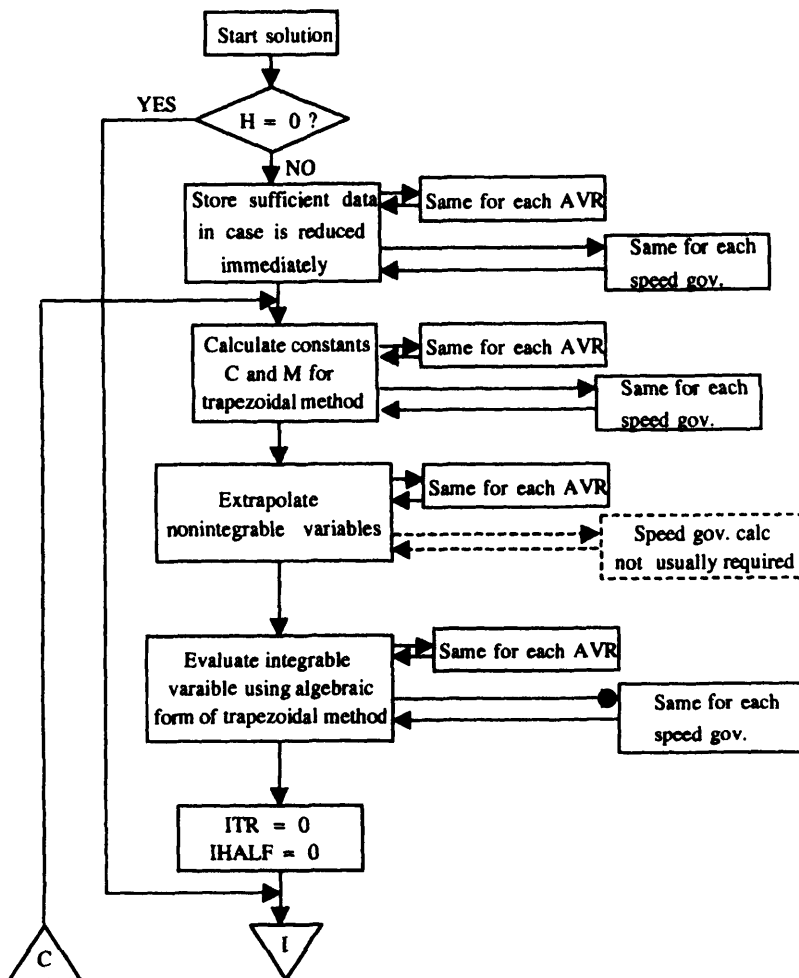
Figure 4.33e Section 5.

PRINTTIME

The integration time at which the next printout of results is required.

MAXTIME

The predefined maximum integration time for the case study.

**Figure 4.34a** Section 1.*ITMAX*

Maximum number of iterations per step since last printout of results.

Note that many data error checks are required in a program of this type but they have been omitted from the block diagram for clarity.

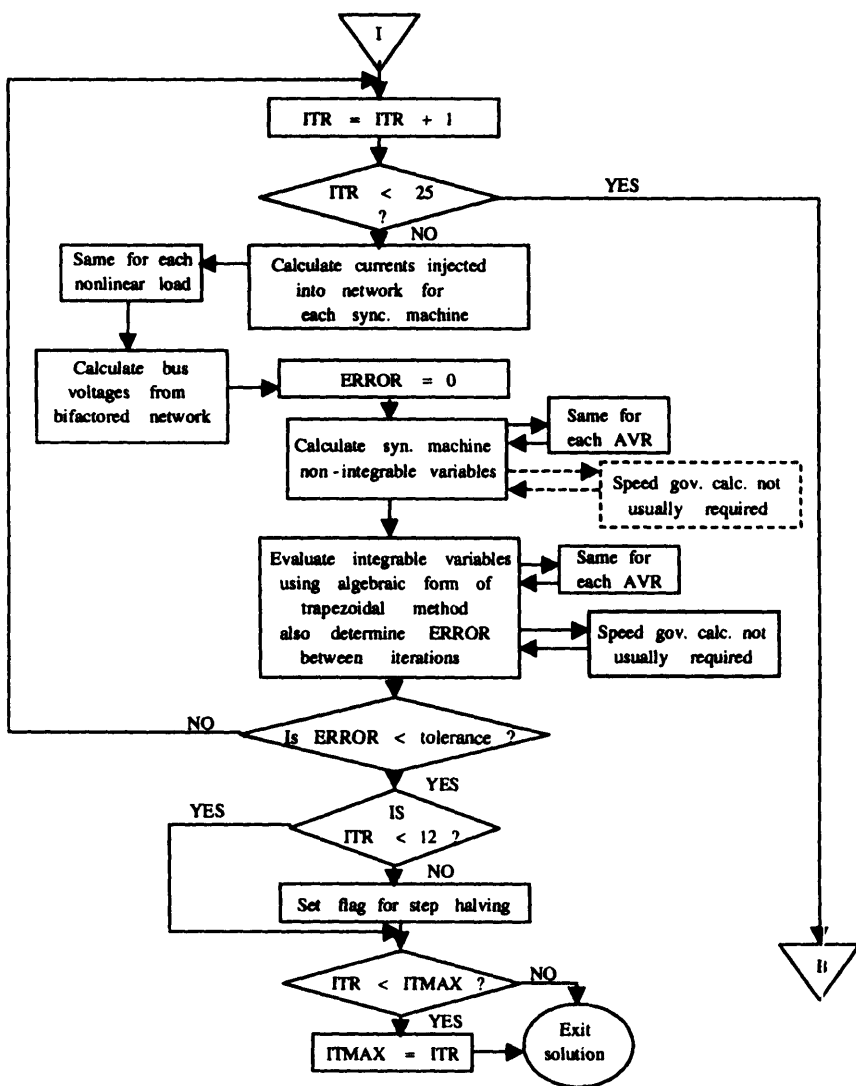


Figure 4.34b Section 2.

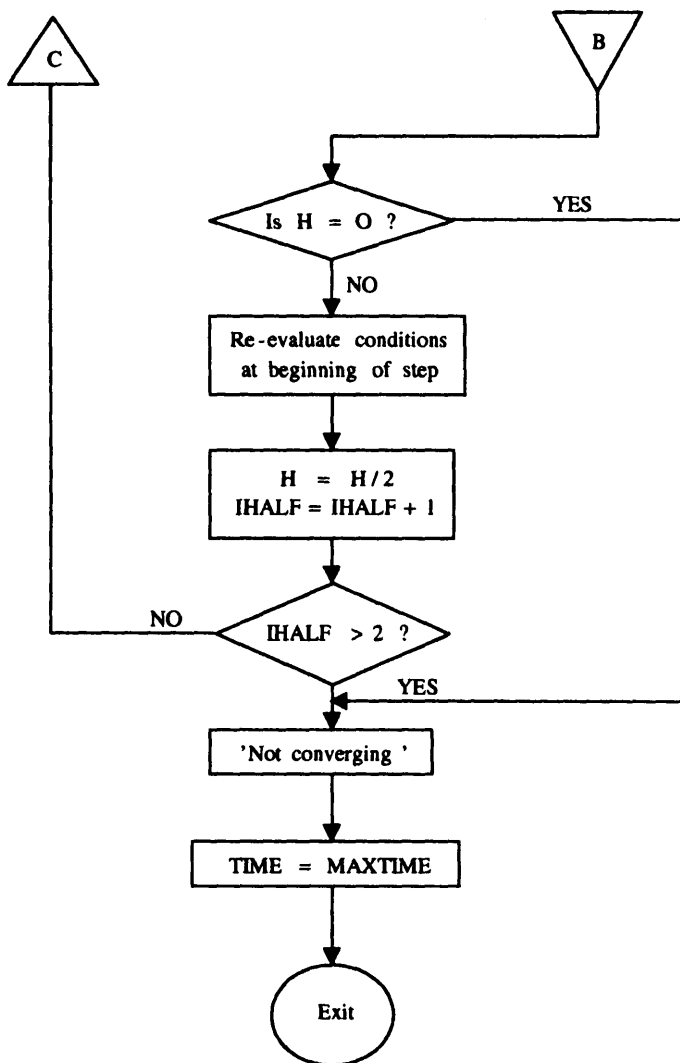


Figure 4.34c Section 3.

Structure of Machine and Network Iterative Solution

The structure of this part of the program requires further description. Two forms of solution are possible depending on whether an integration step is being evaluated or if the nonintegrable variables are being recalculated after a discontinuity. A block diagram is given in Fig. 4.33. The additional logic codes used in this part of the program are:

ERROR

The maximum difference between any integrable variable from one iteration to another.

ITR

Number of iterations required for solution.

IHALF

Number of immediate step halving required for the solution.

TOLERANCE

Specified maximum value of *ERROR* for convergence.

If convergence has not been achieved after a specified number of iterations the case study is terminated. This is done by setting the integration time equal to the maximum integration time. The latest results are thus printed out and a new case study is attempted.

CONCLUSION

This chapter dealt with the philosophy of security assessment based on frequency domain models and equal area criterion concepts. In particular, we define the conventional ingredients for power system stability including applications of the swing equation and its alternate forms.

Frequency domain models of synchronous machines introduced the idea of subtransient, transient, and steady state reactances. Models for a salient pole and round wound synchronous machines were discussed. The equal area criteria and its applications were discussed. The chapter concludes with the treatment of transient stability for the general network case, including a flowchart of a transient stability assessment program.

Again, the reader is reminded that additional information may be obtained from the list of references and the annotated glossary of terms.

5

Assessing Angle Stability via Transient Energy Function

INTRODUCTION

In the actual operation of an electric power system, the parameters and loading conditions are quite different from those assumed at the planning stage. As a result, to ensure power system security against possible abnormal conditions due to contingencies (disturbances), the system operator needs to simulate contingencies in advance, assess the results, and then take preventive control action if required. This whole process is called dynamic security assessment (DSA) and preventive control.

Simulation studies (called transient stability studies) can take up to an hour for a typical system with detailed modeling for a 500-bus, 100-machine system. Since it takes a long time to conduct a transient simulation even for a single contingency, direct methods of stability assessment such as those based on Lyapunov or energy functions offer attractive alternatives.

It should be noted that a transient stability study is often more than an investigation of whether the synchronous generators, following the occurrence of disturbance, will remain in synchronism. It can be a general-purpose transient analysis, in which the “quality” of the dynamic system behavior is investigated. The transient period of primary interest is the electromechanical transient, usually lasting up to a few seconds in duration. If growing oscillations are of con-

cern, or if the behavior of special controls is of interest, a longer transient period may be covered in the study.

For transient stability analysis, a nonlinear system model is used. The system is described by a set of differential equations and a set of algebraic equations. Generally, the differential equations are machine equations, control system equations, etc. The algebraic equations are system voltage equations involving the network admittance matrix. The time simulation method and direct method are often used for transient stability analysis. The former method determines transient stability by solving the system differential equation step by step, while the direct method determines the system transient stability without explicitly solving the system differential equations. This approach is appealing and has received considerable attention. Energy-based methods are a special case of the more general Lyapunov's second or direct method, the energy function being the possible Lyapunov function.

This chapter deals with transient stability by a specific direct method mainly the transient energy function (TEF) method. We begin by covering some basic concepts from the theory of nonlinear system stability.

5.1 STABILITY CONCEPTS

Consider an autonomous system described by the ordinary differential equation,

$$\dot{x} = F(x) \quad (5.1)$$

where $x = x(t)$, and $F(x)$ are n-vectors. $F(x)$ is generally a nonlinear function of x . Stability in the sense of Lyapunov is referred to an equilibrium state of Eq. (5.1). The equilibrium state is defined as the stage x_e at which $x(t)$ remains unchanged for all t . That is,

$$\dot{x}_e = F(x_e) = 0 \quad (5.2)$$

The solution for x_e from Eq. (5.2) is a fixed state since $F(x)$ is not an explicit function of t . For convenience, any nonzero x_e is to be translated to the origin ($x = 0$). That is, to replace x by $x + x_e$ in Eq. (5.1) to have

$$\frac{d}{dt}(x + x_e) = F(x + x_e) = f(x)$$

which gives

$$\dot{x} = F(x) \quad (5.3)$$

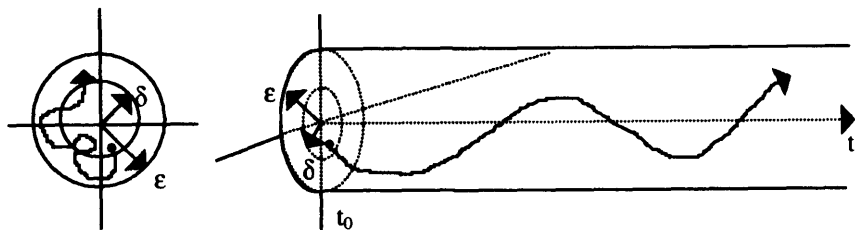


Figure 5.1 Illustration of local stability.

Note that the current x differs from the old one by x_ϵ . As can be seen later, from the definitions, this translation does not affect the stability of the system. Thus, the origin of Eq. (5.3) is always an equilibrium state. It should be noted that t in Eq. (5.3) may be any independent variable, including time.

5.1.1 Definitions and a Lemma

Stability (Local)

The origin of the system described by Eq. (5.3) is said to be stable if for any given $\epsilon > 0$, there exists a $\delta \leq \epsilon$ such that $\|x_0\| < \delta$ implies $\|x(t)\| < \epsilon$ for all t where x_0 is an initial state. The origin is called unstable if it is not stable.

The concept is illustrated in Fig. 5.1 where the initial state x_0 has a magnitude less than δ , and the trajectory of x remains within the cylinder of radius ϵ .

Asymptotic Stability (Local)

The origin of the system described by Eq. (5.3) is said to be asymptotically stable if it is stable and also if given $\|x_0\| < \delta$ implies $x \rightarrow 0$, as $t \rightarrow \infty$. The arrow is used to mean “approach.”

Figure 5.2 demonstrates the idea of asymptotic stability where the trajectory tends to 0 as time tends to infinity.

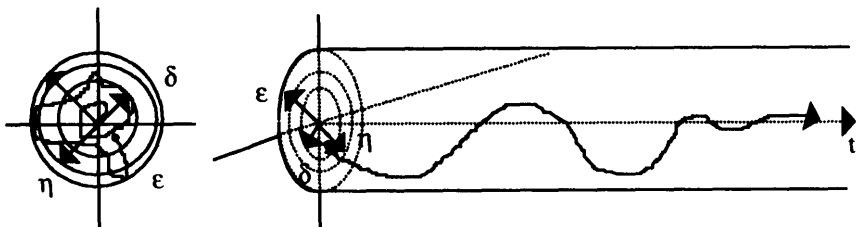


Figure 5.2 Illustration of asymptotic stability.

Globally Asymptotic Stability

The origin of the system described by Eq. (5.3) is said to be globally asymptotically stable if it is stable and also implies $\|x_0\| \rightarrow 0$ as $t \rightarrow \infty$, for any x_0 in the whole space.

Positive Definite Function

A uniquely defined, scalar and continuous function $V(x)$ is said to be positive definite in a region R if $V(x) > 0$ for $x \neq 0$ and $V(0) = 0$.

A space surface formed by all x satisfying $V(x) = 0$ is called a contour. Obviously, contours with different values cannot intersect one another. If they do, $V(x)$ has two values at the intersection. We need the following lemma required for the proof of a Lyapunov theorem.

Lemma

There exists a sphere defined by $\|x\| = N$ in which $V(x)$ increases monotonically along radial vectors emanating from the origin. That is, $V(\beta_u)$ increases monotonically with β in $0 \leq \beta \leq N$ for any unit vector u started from the origin.

This can be shown using the assumption of positive definiteness. First, continuity, $V(x) > 0$ and $V(0) = 0$, assume that $V(\beta_u)$ increases monotonically with β in an interval $0 \leq \beta \leq \beta_u$ and begins to decrease after $\beta = \beta_u$. Given a u , there is an associated β_u which may be unbounded $\beta_u (= \infty)$. Let w among all the u 's that has the smallest β_u , then $\|\beta_u w\| = \beta_u \|w\| = \beta_u \leq \beta_u$. Since $V(\beta_u)$ increases monotonically with β in the interval $0 \leq \beta \leq \beta_u \leq \beta_u$, we are able to identify the positive number to be $N = \beta_u$.

Lyapunov Theorem

There are three important theorems on stability developed by Lyapunov. We include these here to form the theorem given below. In the theorem, $\dot{V}(x)$ is the total derivative of $V(x)$ on the trajectory specified by Eq. (5.3). That is,

$$\dot{V}(x) = \frac{dV}{dt} = V_i(x)\dot{x} = V_i(x)f(x)$$

$$\text{where } V_i = \frac{\partial V}{\partial x}$$

where $V_i(x)$ is the row vector formed by the partial derivatives of $V(x)$.

Regions R , R_1 , R_2

All the regions are assumed to contain the origin as an interior point. R_2 is a subregion of R_1 which is a subregion of R : $R_2 \subseteq R_1 \subseteq R$.

Theorem

Let $V(x)$ be a positive definite function with continuous partial derivatives in a region R , then

1. The origin of the system described by Eq. (5.3) is stable if $\dot{V}(x) \leq 0$ in a subregion $R_1 \subseteq R$.
2. The system is asymptotically stable in the region if it is stable and $\dot{V}(x) \equiv 0$ (identically zero) takes place only at the region in a subregion $R_2 \subseteq R_1$.
3. The origin is globally asymptotically stable if the system is asymptotically stable, R_2 is the whole space and $V(x) \rightarrow \infty$ as $\|x\| \rightarrow 0$.

Proof

- (a) Let r be the smaller one between a given ϵ and N specified in the lemma. That is, $r = \min [\epsilon, N]$.
- (b) Continuity of $V(x)$ assures that there is a minimum of $V(x)$ on the sphere $\|x\| = r$. Let y be among all the u 's that yield the minimum, $V(r_u) = m$, then $V(r_u) \geq m$ must hold for any u . Monotonicity tells that $V(\beta_u) = m$ for a β in the interval $0 \leq \beta \leq r$, and hence $V(x = \beta_u) = m$ is enclosed by the sphere $\|x\| = r$, and also it is a closed contour since u is any unit vector.
- (c) Let δ be the minimum norm of the points on the closed contour $V(x) = m$, then since $\|x_0\| < \delta$ is enclosed by the contour, $V(x_0) < m$ follows by monotonicity. Thus, any trajectory initiated from x_0 cannot possibly cross the sphere $\|x\| = r \leq \epsilon$ due to the fact that $V(x)$ is non-increasing and $V(x) \geq m$ on the sphere $\|x\| = r$.

This completes the proof of part 1 of the theorem.

Part 2 can be shown by observing $\dot{V}(x)$ can be identically zero only at the origin. Hence, $V(x)$ keeps on decreasing except at a countable number of points at which it stops decreasing momentarily. This implies that $x \rightarrow 0$ as $t \rightarrow \infty$ since $V(0) = 0$ only when $x = 0$ in R_2 .

It seems obvious to have part 3 verified by the same reasoning used in part 2. This is true except for the case when $V(x)$ approaches a finite value as $\|x\| \rightarrow \infty$ when x_0 is allowed to be any point in the whole space. The assumption that $V(x) \rightarrow \infty$ as $\|x\| \rightarrow \infty$ excludes this possibility which completes the proof of the theorem.

Except for relying on experience, there is no systematic method to find the Lyapunov function as required by the theorem. It has been shown that any stable and constant linear system has a $V(x)$ but no one has yet shown its existence in general for nonlinear systems.

It can be shown that instability and asymptotic stability of the system described by Eq. (5.3) are the same as its linearized system at the origin, which is

$$\dot{x} = f(0) + f_i(0)x = 0 + Ax$$

where $A = f_i(0)$ is a constant and n-square matrix. That is, the system described by Eq. (5.3) is unstable if at least one eigenvalue of A has a positive real part and is asymptotically stable if all eigenvalues have negative real parts.

Asymptotic stability as judged from the linearized system is simple but of less practical use. It is valid only in a sufficiently small region which is not easily known. The Lyapunov function contains more information on stability in the regions R_1 and R_2 . For instance, global asymptotic stability tells us that the trajectory initiated from anywhere in the whole space, converges to the origin.

5.1.2 Application of Lyapunov's Method to the Simple Pendulum

We consider the dynamics of a pendulum as a prototype for exploring stability of an electric power system.

The motion of a pendulum with friction is described by

$$\ddot{\theta} + a\dot{\theta} + b \sin\theta = 0$$

where $-\pi < \theta < \pi$ is the angle, a is the damping constant and \sqrt{b} is the undamped angular velocity. We regard the problem as a mathematical one without restriction on θ . To convert the system to the standard form of Eq. (5.3), we define that $x_1 = \theta$ and $\dot{x}_1 = x_2$ to get:

$$\dot{x} = \begin{bmatrix} \dot{x}_1 \\ \dot{x}_2 \end{bmatrix} = \begin{bmatrix} x_2 \\ -ax_2 - b \sin x_1 \end{bmatrix} = f(x)$$

First, we want to check if it is possible to find a Lyapunov function for the problem. The matrix A for the linearized system is:

$$A = f_i(0) = \begin{bmatrix} 0 & 1 \\ -b \cos x_1 & -a \end{bmatrix} \Big|_{x=0} = \begin{bmatrix} 0 & 1 \\ -b & -a \end{bmatrix} \quad \text{where } f_i(x) = \frac{\partial f(x)}{\partial x} \Big|_{x_1, x_2}$$

Both eigenvalues of A have negative and real parts when $a > 0$. This suggests a possibility of finding a Lyapunov function.

The Lyapunov function is sometimes referred to as a generalized energy function. The name comes from the fact that it has an initial positive value and does not increase as time goes on. This is the case of physical systems that move without interference from the outside such as the pendulum system. To see this,

let M , J , μ and l be the mass, inertia, damping constant and the length of the pendulum, then one dynamic equation becomes

$$J\ddot{\theta} + \mu l \dot{\theta} + Mgl \sin\theta = 0$$

Multiply by v and then integrate with respect to t :

$$\frac{1}{2} J\dot{\theta}^2 + \mu l \int \dot{\theta}^2 dt + Mgl(-\cos\theta) = C$$

The total energy of the pendulum (sum of kinetic and potential energy) is

$$E = \frac{1}{2} J\dot{\theta}^2 + Mgl(-\cos\theta) = C + Mgl - \mu l \int \dot{\theta}^2 dt > 0$$

The time derivative is

$$\dot{E} = \dot{\theta}(J\ddot{\theta} + Mgl \sin\theta) = -\mu l \dot{\theta}^2 \leq 0$$

Therefore, the proposed Lyapunov function is given by

$$V(x) = \frac{1}{J} E = \frac{1}{2} \dot{\theta}^2 + b(1 - \cos\theta) = \frac{1}{2} x_2^2 + b(1 - \cos x_1)$$

with

$$\dot{V}(x) = -ax_2^2$$

Thus, the Lyapunov function is actually the total energy per unit inertia of the pendulum system.

Now, we have

$$V(x) = b(1 - \cos x_1) + \frac{1}{2} x_2^2$$

in the region

$$R = \{-2\pi < x < 2\pi; \text{free } x_2\}$$

The derivative of v is

$$\dot{V}(x) = [b \sin x_1, x_2] \begin{bmatrix} x_2 \\ -ax_2 - b \sin x_1 \end{bmatrix} = ax_2^2$$

1. The origin is stable since the condition of part 1 is satisfied by choosing $R_1 = R$. This is also true for the choice $a = 0$, which is the case of a frictionless pendulum.
2. $\dot{V}(x) = -ax_2^2 \equiv 0$ implies that $x_2 \equiv 0$ and hence $\dot{x}_2 = 0$. This makes $\ddot{x}_2 = -ax_2 - b \sin x_1 = 0$ which yields $\sin x_1 = 0$ or $x_1 = n\pi$. Therefore, $\dot{V}(x) \equiv 0$ only at the origin by choosing $R_2 = \{-\pi < x_1 < \pi; \text{free } x_2\}$. Thus, the origin is asymptotically stable since the condition of part 2 of the theorem is satisfied in R_2 .
3. Part 3 is not applicable for the following two reasons:
 - (i) $V(x) = 0$ at $x_1 = 2n\pi$ in the whole space,
 - (ii) $x_1 \rightarrow \infty$ with $x_2 = 0$ makes $V(x) = b(1 - \cos x_1) \leq 2b$ which does not approach infinity as required.

For demonstration purposes, we employ the proposed $V(x)$ to find a $\delta \leq \epsilon$ as required by the definition of stability. To this end, let $u = [u_1, u_2]^\top$ be any unit vector started from the origin, then

$$V(\beta u) = b(1 - \cos \beta u_1) + \frac{1}{2} \beta^2 u_2^2$$

and $dV/d\beta = bu_1 \sin \beta u_1 + \beta u_2^2 > 0$ for any $-\pi \leq \beta u_1 \leq \pi$ and $u_2 \neq 0$.

Since $V(\beta u)$ begins to decrease after $\beta = \pi$ for $u_1 = \pm 1$ and $u_2 = 0$, we identify $w = [\pm 1, 0]^\top$ and $N = \beta_w = \pi < \beta u$ for any u .

$$(a) r = \min \{\epsilon, N\} = \min \{\epsilon, \pi\}$$

$$(b) V(x) = b(1 - \cos x_1) + \frac{1}{2} x_2^2 = b(1 - \cos x_1) + \frac{1}{2}(r^2 - x_1^2)$$

on the circle $x_1^2 + x_2^2 = r^2$ or $\|x\| = r$. $dV/dx_1 = b \sin x_1 - x_1 < 0$ for $b \leq 1$ and $x_1 > 0$. Since $V(x)$ is a decreasing function, it has a minimum at $x_1 = \pm r$ and $x_2 = 0$. Therefore, $m = b(1 - \cos r)$. The expression for the minimum becomes complicated for $b > 1$.

$$(c) B = x_1^2 + x_2^2 = x_1^2 + 2(m - b + b \cos x_1)$$

on the contour $V(x) = m$. $db/dx_1 = 2(x_1 - b \sin x_1) > 0$ for $x_1 > 0$ and $b \leq 1$.

Since the minimum occurs at $x_1 = 0$ and $x_2 = \pm\sqrt{2m}$, we have the minimum norm

$$\delta = \sqrt{2m} = \sqrt{2b(1 - \cos r)} \leq \epsilon.$$

The inequality holds for the reason that

$$\sqrt{2b(1 - \cos r)} \leq \sqrt{2b(1 - \cos r)} \leq 2\sin\frac{r}{2} \leq 2\left(\frac{r}{2}\right) = r \leq \varepsilon$$

For the case $b > 1$, we may choose an independent variable $\alpha = \omega t$ with $\omega^2 = b$. Thus, the original dynamic equation becomes

$$\ddot{\theta} + a'\dot{\theta} + \sin\theta = 0$$

where $\dot{\theta} = d\theta/d\alpha$ and $a' = a/\omega$. Hence, the results of (b) and (c) are valid because $b = 1$. Probably, there exists a better $V(x)$ to yield the same results of (b) and (c) without considering $b \leq 1$ and $b > 1$ separately. Although different Lyapunov functions may serve the same purpose on stability, they may be different from other points of view such as estimating δ and other control applications.

4. The condition of part 2 guarantees that the closed contour

$$V(x) = b(1 - \cos x_1) + \frac{1}{2}x_2^2 = C$$

keeps on decreasing in R_2 , as time goes on until $C = 0$ as a limit. Being nonnegative, each term of $V(x)$ must be zero simultaneously when $C = 0$. This suggests that $x_1 \rightarrow 0$ and $x_2 \rightarrow 0$ as $C = 0$ and hence asymptotic stability for the origin is established.

5.2. SYSTEM MODEL DESCRIPTION

5.2.1 Real Power Supplied by a Generator

For a power network consisting of n -generators connected together by mutual admittances as shown in Fig. 5.3, we may write in matrix form:

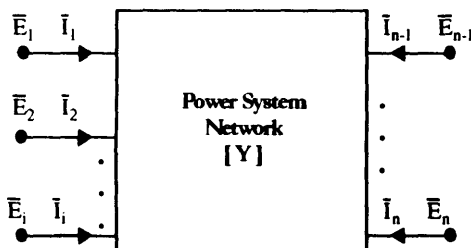


Figure 5.3 A general n -Generator system.

$$[I] = [Y][E] \quad (5.4)$$

where $[I]$ is the injected current vector, $[E]$ is generator internal voltage vector, and $[Y]$ is the system admittance matrix in which the generator impedances are included.

$$\bar{I}_i = \sum_{j=1}^n Y_{ij} \bar{E}_j \quad (5.5)$$

for all $i, j = 1, 2, \dots, n$. The matrix element and complex voltage are specified by

$$Y_{ij} = G_{ij} + jB_{ij} \text{ and } \bar{E}_i = E_i / \delta_i \quad (5.6)$$

The real power supplied by generator i to the network is

$$\begin{aligned} P_{ii} &= \operatorname{Re}[\bar{E}_i \bar{I}_i^*] = \operatorname{Re} \sum_{j=1}^n [\bar{E}_i \bar{E}_j^* Y_{ij}^*] \\ &= \operatorname{Re} \sum_{j=1}^n E_i E_j / (\delta_i - \delta_j) [G_{ij} - jB_{ij}] \\ &= \sum_{j=1}^n E_i E_j \operatorname{Re}[\cos(\delta_i - \delta_j) + j \sin(\delta_i - \delta_j)] [G_{ij} - jB_{ij}] \\ &= \sum_{j=1}^n P_{ij} \end{aligned} \quad (5.7)$$

where

$$P_{ij} = C_{ij} \sin(\delta_i - \delta_j) + D_{ij} \cos(\delta_i - \delta_j)$$

with $C_{ij} = E_i E_j B_{ij}$ and $D_{ij} = E_i E_j G_{ij}$ (5.8)

The power P_{ij} is the real power delivered by generator i to j ; it may be positive or negative. $P_{ii} = E_i^2 G_{ii}$ is the power delivered to the local load at generator i .

From Eq. (5.8) it is clear that P_{ij} depends on differences between phase angles rather than individual phase angles. This result suggests that one may choose an arbitrary reference for the angles without affecting the resulting P_{ij} . Indeed, we will first choose a reference rotating at synchronous speed to describe rotor dynamics and then a center of inertia to minimize the value of rotor kinetic energy.

5.3 STABILITY OF A SINGLE-MACHINE SYSTEM

Consider a generator connected to an infinite bus with voltage $\bar{V} \angle 0^\circ$ through a pure reactance X as shown in Fig. 5.4. If the internal reactance and EMF of

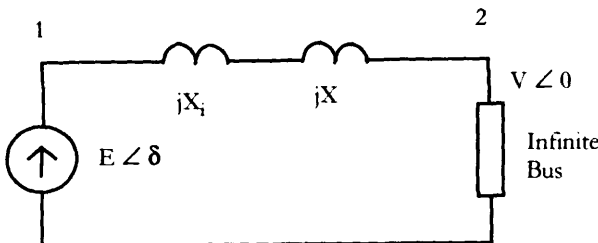


Figure 5.4 Single generator and infinite bus system.

the generator are given by X_i and $E \angle \delta$ respectively, we have from Eq. (4.7) that

$$P_e = A(x) \sin \delta$$

with

$$A(x) = \frac{E \bar{V}}{X_i + X}$$

Multiply on both sides (4-7) by $\omega \delta t = d\delta$ gives

$$M\omega d\omega = (P_m - P_e) d\delta \quad (5.9)$$

Let $S_o = (\delta_o, 0)$, $S_c = (\delta_c, \omega_c)$ and $S_m = (\delta_m, 0)$ be the start, fault clearing and maximum states of the fault respectively as shown in Fig. 5.5. Let $S = (\delta, \omega)$ be any state on the $P-\delta$ curve generated by X , then integration of Eq. (5.9) from S to S_c yields

$$\frac{1}{2} M\omega^2 - \frac{1}{2} M\omega_c^2 = P_m(\delta - \delta_c) - A(X)(\cos \delta_c - \cos \delta) \quad (5.10)$$

(a) During the fault: $X = X_f$

For $S = S_o$, we obtain from the above equation

$$\frac{1}{2} M\omega_c^2 = P_m(\delta_0 - \delta_c) - A(X_f)(\cos \delta_c - \cos \delta_0) = A_1 \quad (5.11)$$

(b) After the clearance: $X = X_c$

For $S = S_m$, we have from Eq. (5.11) that

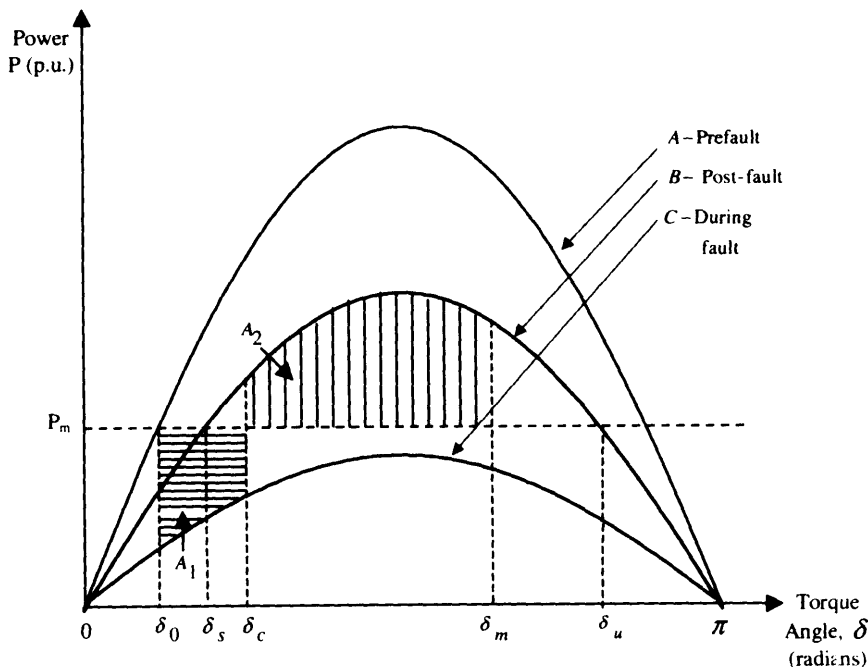


Figure 5.5 Prefault, during fault, and post-fault power angle curves.

$$\frac{1}{2} M \dot{\omega}_c^2 = A(X_c)(\cos \delta_c - \cos \delta_m) - P_m(\delta_m - \delta_c) = A_2$$

Thus, we conclude from (a) and (b) that

$$A_1 = A_2 \quad (5.12)$$

Therefore, δ_m can be found by solving the nonlinear algebraic Eq. (5.12) or graphically from Fig. 5.5 to judge stability. This is known as the equal-area criterion for stability study of power systems.

It is important to note that the excessive energy A_1 created during fault is converted to rotor kinetic energy at clearance. This result inspires the use of the transient energy function (TEF) after clearing. That is, to obtain from Eq. (5.12) with $X = X_c$

$$E - \nabla = \frac{1}{2} M \dot{\omega}^2$$

where

$$E = \frac{1}{2} M\omega_i^2 + P_m(\delta - \delta_i) \quad (5.13)$$

and

$$\nabla = A(X_i)(\cos\delta_i - \cos\delta)$$

5.3.1 Transient Swing

Let $a = d\omega/dt$ denote the acceleration of the system, then Eq. (5.13) together with Fig. 5.5 show that $a < 0$ above the P_m line and that $a > 0$ below it after fault clearance. There are two angles: $\delta_c = \sin^{-1} P_m/A(X_i)$ and $\delta_u = \pi - \delta_c$ that correspond to $a = 0$. Figure (5.5) reveals that δ increases from δ_0 with $\omega = 0$ due to $a > 0$ until reaching $\delta_m < \delta_u$ at which $\omega = 0$. Since $a < 0$ at δ_m , δ begins to decrease until $\omega = 0$ at an angle less than δ_c and then comes back because $a > 0$. As such, the power angle swings back and forth around δ_c . This is the case for $E - V < 0$ at δ_u because δ_u is unreachable (ω is imaginary). However, delayed fault clearance may result in large A_1 which makes δ cross δ_u with $\omega \geq 0$. Then, δ increases further without return due to $a > 0$. This is the case for $(E - \nabla) \geq 0$.

We will consider the transient to be stable if the power angle swings around δ_c and is otherwise unstable. This definition makes it possible to assess the stability by means of the (TEF) as follows:

- (a) The transient is stable if $(E - \nabla) < 0$ at δ_u ; large magnitude yields better stability.
- (b) The transient is unstable if $(E - \nabla) \geq 0$ at δ_u .

5.4 STABILITY ASSESSMENT FOR n -GENERATOR SYSTEM BY THE TEF METHOD

Consider a power system consisting of n -generators. The dynamics of each is described by Eq. (5.11). We have

$$M_i \frac{d\omega_i}{dt} = P_{mi} - P_{ci}(\delta_i) \quad (5.14a)$$

$$\frac{d\theta_i}{dt} = \omega_i \quad (5.14b)$$

for $i = 1, 2, \dots, n$. The dynamics are second order and nonlinear differential equations coupled together through the phase angles contained in the expression

of P_{ei} . Although the numerical solution can be determined, a closed form of solution is impossible to obtain. We need not discuss the solution of the system of equations as stability that does not require the exact solution.

Another reference with velocity ω_0 is to be chosen to minimize the integral-square error

$$ISE = \int_{t_1}^{t_2} \sum_{i=1}^n \frac{1}{2} M_i (\omega_i - \omega_0)^2 dt$$

for any t_1 and t_2 . The necessary and sufficient condition for this purpose is

$$M_T \omega_0 = \sum_{i=1}^n M_i \omega_i, \quad \text{with } M_T = \sum_{i=1}^n M_i$$

which indicates that the reference is the center of inertia (COI). The COI has a phase angle δ_0 satisfying

$$M_T \delta_0 = \sum_{i=1}^n M_i \delta_i \text{ and } \frac{d\delta_0}{dt} = \omega_0$$

With respect to δ_0 , all generators have phase angles

$$\theta_i = \delta_i - \delta_0$$

In terms of θ_i , Eq. (5.14) is now expressed by

$$M_i \frac{d\dot{\theta}_i}{dt} + M_i \frac{d\omega_0}{dt} = P_{mi} - P_{ei} = P_i - P'_{ei} \quad (5.15)$$

with

$$P_i = P_{mi} - D_{ii}$$

and

$$P'_{ei} = \sum_{j \neq i} P_{ej} \quad (5.16)$$

where $j \neq i$ signifies summation of j from 1 to n except i . All the angles $\delta_i - \delta_j$ in P_{ei} may be replaced by $\theta_{ij} = \theta_i - \theta_j$ because

$$\theta_{ij} = \theta_i - \theta_j = (\delta_i - \delta_0) - (\delta_j - \delta_0) = \delta_i - \delta_j$$

Multiply Eq. (5.11) by θ_i and then sum i from 1 to n :

$$\sum_{i=1}^n M_i \frac{d\dot{\theta}_i}{dt} + \frac{d\omega_0}{dt} \sum_{i=1}^n M_i \dot{\theta}_i = \sum_{i=1}^n (P_i - P_{ei}) \dot{\theta}_i \quad (5.17)$$

The second term of Eq. (5.17) is zero because

$$\sum_{i=1}^n M_i \dot{\theta}_i = \sum_{i=1}^n M_i (\dot{\delta}_i - \dot{\delta}_0) = \sum_{i=1}^n M_i \dot{\delta}_i - M_T \omega_0 = 0$$

The states at clearance angle δ_c and unstable equilibrium δ_u are to be specified by n pairs of (angle, velocity), that is,

$$S_c = \{(\theta_{ic}, \dot{\theta}_{ic})\} \text{ and } S_u = \{(\theta_{iu}, \dot{\theta}_{iu})\}$$

Integration of Eq. (5.15) with dt from S_c to S_u gives

$$E - \nabla = \sum_{i=1}^n \frac{1}{2} M_i \dot{\theta}_{ii}^2 \quad (5.18)$$

where

$$E = \sum_{i=1}^n \frac{1}{2} M_i \dot{\theta}_{ic}^2 + \sum_{i=1}^n P_i (\theta_{iu} - \theta_{ic}) \quad (5.19)$$

and

$$\nabla = \sum_{i=1}^n \int_c^u P'_{ei} \dot{\theta}_i dt \quad (5.20)$$

with c and u denoting S_c and S_u .

We know from Eq. (5.19) that E is the total energy input plus kinetic energy of rotors. The electrical energy stored and dissipated in the system is V given by Eq. (5.20). The energy here is referred to power integration with respect to phase angle (not time).

The stored energy in ∇ is path independent but the dissipated energy in ∇ is path dependent. To show this, we multiply Eq. (5.17) by $\dot{\theta}_i$ and then sum from $i = 1$ to n to obtain:

$$\sum_{i=1}^n P_{ei} \dot{\theta}_i = \sum_{i=1}^n \sum_{j \neq i} P_{ij} \dot{\theta}_i = \sum_{i=1}^{n-1} \sum_{j=i+1}^n (Q_{ij} \dot{\theta}_i + Q_{ji} \dot{\theta}_j) \quad (5.21)$$

The preceding equation can be verified by carrying out the summation. Substitutions of P_{ij} from Eq. (5.8) gives

$$P_{ij} \dot{\theta}_i + Q_{ji} \dot{\theta}_j = C_{ij} \sin \theta_{ij} \dot{\theta}_{ij} + D_{ij} \cos(\dot{\theta}_{ij} + \dot{\theta}_i) \quad (5.22)$$

Therefore, the integration of Eq. (5.21) results in

$$V = \sum_{i=1}^{n-1} \sum_{j=i+1}^n C_i [\cos(\theta_u - \theta_i) - \cos(\theta_u - \theta_j)] + I \quad (5.23)$$

with

$$I = \sum_{i=1}^{n-1} \sum_{j=i+1}^n D_i \int_{t_i}^u \cos \theta_i (d\theta_i + d\theta_j) \quad (5.24)$$

We can see from Eq. (5.23) that the first part is the stored energy and is independent of the path of integration. But, the second part denoted by I depends on the path of θ_i . Some kind of approximation has to be used to evaluate I since $\theta_i(t)$ cannot be found analytically.

Let θ_i be approximated for all $i = 1, 2, \dots, n$, by

$$\theta_i = C_i + K_i f(t)$$

where C_i and K_i are constants but may change with i and $f(t)$ is the only one for all i . For convenience, we use a parameter u to make

$$t = t_c + (t_u - t_c)u$$

where t_c and t_u are the times at the clearance and unstable equilibrium. Then

$$\begin{aligned} \theta_i &= C_i + K_i f(t) = C_i + K_i f[t_c + (t_u - t_c)u] \\ &= C_i + K_i g(u) \end{aligned}$$

for $t_c \leq t \leq t_u$ and $0 \leq u \leq 1$. The two constants are required to meet the boundary conditions

$$\theta_u = C_i + K_i g(0) \text{ and } \theta_c = C_i + K_i g(1)$$

Solving the two constants gives

$$K_i = \frac{\theta_u - \theta_c}{g(1) - g(0)} \quad (5.25)$$

$$C_i = \frac{\theta_u g(1) - \theta_c g(0)}{g(1) - g(0)} \quad (5.26)$$

Based on this approximation, we have

$$d(\theta_i + \theta_j) = (K_i + K_j)g'(u)du$$

$$d(\theta_i - \theta_j) = (K_i - K_j)g'(u)du = d\theta_{ij}$$

and hence it follows that

$$d(\theta_i + \theta_j) = \frac{K_i + K_j}{K_i - K_j} d\theta_{ij} = F_{ij} d\theta_{ij}$$

with

$$F_{ij} = \frac{\theta_m + \theta_n - \theta_w - \theta_h}{\theta_m - \theta_n - \theta_w + \theta_h} \quad (5.27)$$

This result makes it possible to integrate I as

$$I = \sum_{i=1}^{n-1} \sum_{j=i+1}^n D_{ij} F_{ij} [\sin(\theta_m - \theta_m) - \sin(\theta_w - \theta_h)] \quad (5.28)$$

It is interesting to note that $f(t)$ or $g(u)$ need not be known and that any $f(t)$ yields the same approximation for I as indicated by Eq. (5.28). Thus, one may perceive $f(t)$ to be the COI:

$$M_I f(t) = \sum_{i=1}^n M_i \theta_i(t)$$

which naturally minimizes the integral-square error $\int_{t_0}^{t_u} [M_i(\theta_i - f)]^2 dt$. This is probably the best choice of the f s. For example, if $g(u)$ is chosen as the combination:

$$g(u) = \alpha u + \beta \sin\left(\frac{\pi}{2}u\right) + \gamma \cos\left(\frac{\pi}{2}u\right)$$

then $g(0) = g$, $g(1) = \alpha + \beta$ and

$$K_i = \frac{\theta_m - \theta_w}{\alpha + \beta - \gamma}, \quad C_i = \frac{(\alpha + \beta)\theta_m - \gamma\theta_h}{\alpha + \beta - \gamma}$$

In concept, one may regard a system as stable if the kinetic energy accumulated at the instant of clearance can be absorbed by the electrical components of the system. Thus, it is the kinetic energy that determines the stability. It is usually during the fault that some generators are affected and tend to separate from the rest that are coherent with the system COI. So far as the kinetic energy is concerned, the gross motion of the separating generators (say the first k) may

be considered as a single generator with inertia and velocity the same as that of their COI. That is,

$$M_s = \sum_{i=1}^k M_i \text{ and } M\dot{\Omega} = \sum_{i=1}^k M_i \dot{\theta}_i$$

To be coherent with the system's COI, the rest of the generators must have zero velocity; $\dot{\theta}_i = 0$ for all $i = k+1, k+2, \dots, n$. Coherence suggests that the rest of the generators may be regarded as an infinite bus. As such, the whole system behaves like a single generator and an infinite bus and hence the result obtained before may be applied to the multiple generator system.

We modify Eqs. (5.18) and (5.19) according to the conclusion and update of Eq. (5.19) below.

$$\begin{aligned} E - \nabla &= \frac{1}{2} M_s \Omega_u^2 \\ E &= \frac{1}{2} M_s \Omega_c^2 + \sum_{i=1}^n P_i (\theta_{iu} - \theta_{ic}) \\ \nabla &= \sum_{i=1}^n \sum_{j \neq i+1}^n (A_{ij} - B_{ij}) \end{aligned} \quad (5.29)$$

where

$$A_{ij} = C_{ij} [\cos(\theta_{ij})_c - \cos(\theta_{ij})_u]$$

and

$$B_{ij} = D_{ij} [\sin(\theta_{ij})_c - \sin(\theta_{ij})_u]$$

Note that Ω_c , Ω_u , $(\theta_{ij})_c$ and $(\theta_{ij})_u$ denote the velocities and angles at the clearance and unstable state.

Comparing Eq. (5.26) with Eq. (5.11) enables us to draw the same conclusion as being made for single generator systems. That is, the system is stable if $E < \nabla$ and unstable if $E > \nabla$. It is inconclusive to talk about $E = \nabla$ since we have made approximations in evaluating E and ∇ .

5.5 APPLICATION TO A PRACTICAL POWER SYSTEM

The application of the direct method to actual power systems is quite difficult. A number of simplifying assumptions are necessary. To date, the analysis has been mostly limited to power system representation with generators represented

by classical models and loads modeled as constant impedances. Recently, there have been several attempts to extend the method to include more detailed load models.

In a multi-machine power system, the energy function V describing the total system transient energy for the postdisturbance system is given by:

$$V = -\frac{1}{2} \sum_{i=1}^n J_i \omega_i^2 - \sum_{i=1}^n P'_m(\theta_i - \theta_i^*) - \sum_{i=1}^{n-1} \sum_{j=i+1}^n [C_{ij}(\cos\theta_{ij} - \cos\theta_{ij}^*) - \int_{\theta_i^* + \theta_j^*}^{\theta_i + \theta_j} D_{ij} \cos\theta_{ij} d(\theta_i + \theta_j)] \quad (5.30)$$

where

θ_i^* = angle of bus i at the postdisturbance SEP

$J_i = 2H_i\omega_0$ = per unit moment of inertia of the i^{th} generator

The transient energy function consists of the following four terms:

1. $1/2 \sum J_i \omega_i^2$: change in rotor kinetic energy of all generators in the COI reference frame
2. $\sum P'_m(\theta_i - \theta_i^*)$: change in rotor potential energy of all generators relative to COI
3. $\sum C_{ij}(\cos\theta_{ij} - \cos\theta_{ij}^*)$: change in stored magnetic energy of all branches
4. $\sum \int D_{ij} \cos\theta_{ij} d(\theta_i + \theta_j)$: change in dissipated energy of all branches

The first term is called the kinetic energy (E_{ke}) and is a function of only generator speeds. The sum of terms 2, 3, and 4 is called the potential energy (E_{pe}) and is a function of only generation angles.

The transient stability assessment procedure involves the following steps:

Step 1 Calculation of the critical energy V_{cr}

Step 2 Calculation of the total system energy at the instant of fault-clearing V_{cl}

Step 3 Calculation of stability index: $V_{cr} - V_{cl}$. The system is stable if the stability index is positive.

Time-domain simulation is run up to the instant of fault clearing to obtain the angles and speeds of all the generators. These are used to calculate the total system energy (V_{cl}) at fault clearing. The flowchart of TEF for transient stability analysis is shown in Fig. (5.6).

5.6 BOUNDARY OF THE REGION OF STABILITY

The calculation of the boundary of the region of stability, V_{cr} , is the most difficult step in applying the TEF method. Three different approaches are briefly described here.

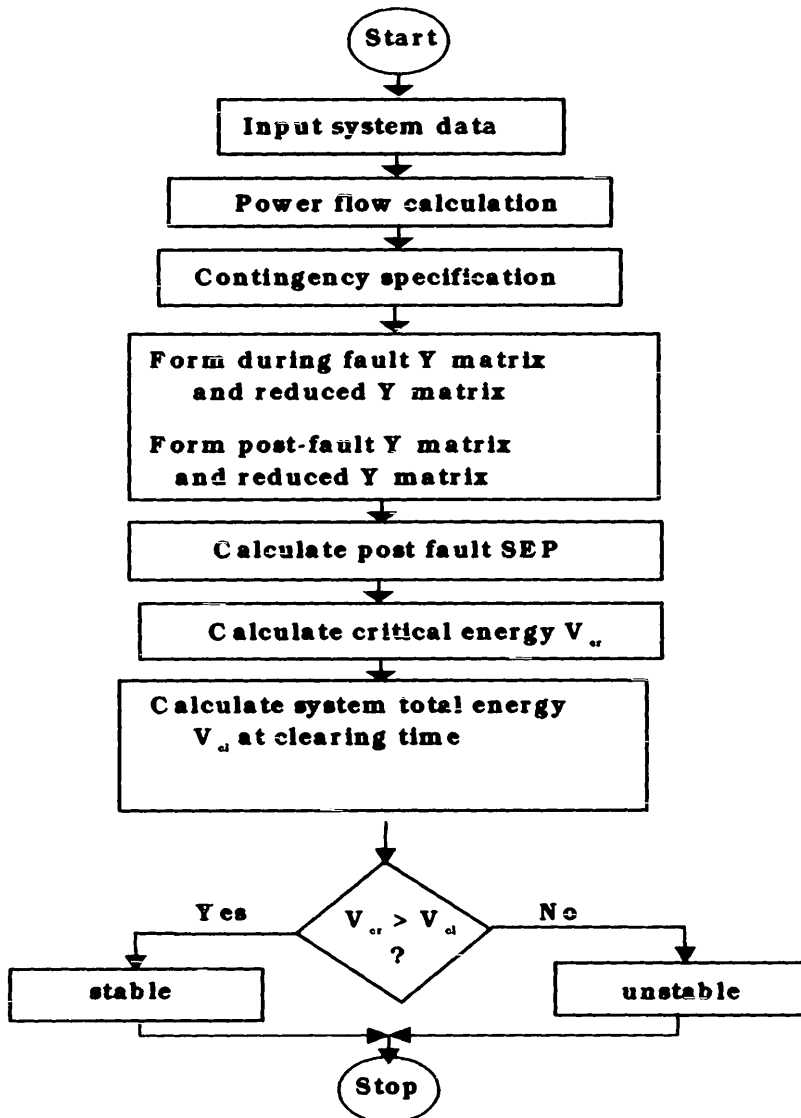


Figure 5.6 Flowchart of TEF for transient stability analysis.

1. The Closest Unstable Equilibrium Point (UEP) Approach

Early papers on the application of the TEF method for transient stability analysis used the following approach to determine the smallest V_c .

- Step 1** Determine all the UEPs. This is achieved by solving the postdisturbance system steady-state equations with different initial values of bus angles.
- Step 2** Calculate system potential energy at each of the UEPs obtained in step 1. The critical energy V_c is given by the system at the UEP, which results in the minimum potential energy.

This approach computes the critical energy by implicitly assuming the worst fault location, hence, the results are very conservative.

2. The Controlling UEP Approach

The degree of conservatism introduced by the closest UEP approach is such that the results are usually of little practical value. The controlling UEP approach removes much of this conservatism by computing the critical energy depending on the fault location. This approach is based on the observation that the system trajectories for all critically stable cases get close to those UEPs that are closely related to the boundary of system separation. The UEPs are called the controlling or relevant UEPs.

The essence of the controlling UEP method is to use the constant energy surface through the controlling UEP to approximate the relevant part of the stability boundary (stable manifold of the controlling UEP) to which the fault-on trajectory is heading.

For any fault-on trajectory $x_f(t)$ starting from a point $p \in A(x_s)$ with $V(p) < V(\hat{x})$, if the exit point of the fault-on trajectory lies in the stable manifold of \hat{x} , the fault-on trajectory must pass through the connected constant energy surface $\Delta V_c(\hat{x})$ before it passes through the stable manifold of $\hat{x}(W^s(\hat{x}))$ (thus exits the stability boundary $\Delta A(\hat{x}_s)$). Therefore, the connected constant energy surface $\Delta V_c(\hat{x})$ can be used to approximate the part of the stability boundary $\Delta A(\hat{x}_s)$ for the fault-on trajectory $x_f(t)$. The computation process in this approach consists of the following steps:

- Step 1** Determine the controlling UEP, x_{co} for the fault-on trajectory $x_f(t)$.
- Step 2** The critical energy V_c is the value of the energy function $V(\cdot)$ at the controlling UEP, that is, $V_c = V(x_{co})$.
- Step 3** Calculate the value of the energy function $V(\cdot)$ at the time of fault clearance (say, t_d) using the fault-on trajectory $V_f = V(x_f(t_d))$.
- Step 4** If $V_f < V_c$, then the postfault system is stable. Otherwise, it is unstable.

The key element of the controlling UEP method is how to find the controlling UEP for a fault-on trajectory. Much of the recent work in the controlling UEP method is based on heuristics and simulations. A theory-based algorithm to find the controlling UEP for the classical power system model with transfer conductance G_{ij} is presented now.

The energy function is of the form:

$$\begin{aligned}
 V(\delta, \omega) = & \sum_{i=1}^{n-1} \sum_{j=i+1}^n \left\{ \left(\frac{1}{2M_i} M_i M_j (\omega_m - \omega_{ji}) \right)^2 \right. \\
 & - \frac{1}{M_i} (P_i M_i - P_j M_j) (\delta_m - \delta_{ji} + \delta'_{ji}) \\
 & - V_i V_j B_{ij} \{ \cos(\delta_m - \delta_{ji}) - \cos(\delta'_m - \delta'_{ji}) \} \\
 & - V_i V_j G_{ij} \frac{\delta_m + \delta_{ji} - (\delta'_{ji} + \delta'_{ji})}{\delta_m - \delta_{ji} - (\delta'_m - \delta'_{ji})} \{ \sin(\delta_m - \delta_{ji}) - \sin(\delta'_m - \delta'_{ji}) \} \\
 & \left. = V_f(\delta) + \frac{1}{2M_f} \sum_{i=1}^{n-1} \sum_{j=i+1}^n M_i M_j (\omega_m - \omega_{ji})^2 \right\} \quad (5.3-1)
 \end{aligned}$$

where $M_f = \sum_{i=1}^n M_i$, $x^S = (\delta^*, 0)$ is the stable equilibrium point (SEP) under consideration.

Algorithm to Find the Controlling UEP

The reduced system is

$$\begin{aligned}
 \dot{\delta}_m &= \frac{1}{M_i} (P_i - P_c) - \frac{M_i}{M_n} (P_n - P_{cn}) \\
 &= f_i(\delta) \quad i = 1, 2, \dots, n-1
 \end{aligned}$$

The algorithm for finding the controlling UEP consists of the following steps:

- Step 1** From the fault-on trajectory $(\delta(t), \omega(t))$, detect the point δ^* at which the projected trajectory $\delta(t)$ reaches the first local maximum of $E_p(\cdot)$. Also, compute the point δ^- that is one step ahead of δ^* along $\delta(t)$, and the point δ^+ that is one step after δ^* .
- Step 2** Use the point δ^* as initial condition and integrate the postfault reduced system Eq. (5.31) to find the first local minimum of $\sum_{i=1}^n |f_i(\delta)|$, say at δ_0^* .
- Step 3** Use δ^- and δ^+ as initial conditions and repeat Step 2 to find the corresponding points, say δ_0^- and δ_0^+ respectively.
- Step 4** Compare the values of $|f_i(\delta)|$ at δ_0^- , δ_0^* , and δ_0^+ . The one with the smallest value is used as the initial guess to solve Eq. (5.31), $f_i(\delta) = 0$, say the solution is δ_{cv} .
- Step 5** The controlling UEP with respect to the fault-on trajectory is $(\delta_{cv}, 0)$.

The proposed algorithm finds the controlling UEP via the controlling UEP of the reduced system Eq. (5.31) with respect to the projected fault-on trajectory $\delta(t)$. Steps 1–4 find the controlling UEP of the reduced system and step 5 relates the controlling UEP of the reduced system to the controlling UEP of the original system. Theoretical justification of the proposed algorithm can be found in work done by Chiang.

3. The Boundary of Stability-Region-Based Controlling UEP (BCU) Method

Earlier UEP methods faced serious convergence problems when solving for the controlling UEP, especially when the system is highly stressed or highly unstressed, or when the mode of system instability is complex. These problems usually arise if the starting point for the UEP solution is not sufficiently close to the exact UEP. Some of the convergence problems can be overcome by the BCU method which has the capability of producing a much better starting point for the UEP solution.

CONCLUSION

One of the major innovations in stability assessment is based on the energy function concept, which is an offshoot of Lyapunov stability criteria. This chapter introduced the fundamental Lyapunov stability thought and the procedure of constructing Lyapunov stability function.

The main thrust of this chapter is to utilize concepts of system modeling to evaluate system stability using the energy function method. The reader is referred to the list of references and the annotated glossary of terms for further information on the subject matter.

6

Voltage Stability Assessment

INTRODUCTION

Voltage stability studies evaluate the ability of a power system to maintain acceptable voltages at all nodes under normal conditions and after being subjected to contingency conditions. A power system is said to have entered a state of voltage instability when a disturbance causes a progressive and uncontrollable decline in voltage values. Inadequate reactive power support from generators, reactive sources, and transmission lines can lead to voltage instability or even voltage collapse, which have resulted in several major system failures (black-outs) such as:

1. September 1910, New York Power pool.
2. Northern Belgium System and Florida System disturbances of 1982
3. Swedish system disturbance in December 1983.
4. French and Japanese system disturbances in 1987.
5. Recently, in the late nineties, in the U.S. and other parts of the world.

The literature and background studies reviewed indicate that voltage instability or collapse are characterized by a progressive fall of voltage which can take several forms. The main factor is the inability of the network to meet the demand of reactive power. The process of instability may be triggered by some form of disturbance, resulting in changes in the reactive power requirement. The

disturbance may either be small or large changes in essential load. The consequence of voltage instability may, however, have widespread impact on the system.

Power system voltage stability involves generation, transmission, and distribution. Voltage stability is closely associated with other aspects of power system steady-state and dynamic performance. Voltage control, reactive power compensation and management, rotor-angle stability, protective relaying, and control center operations all influence voltage stability.

Voltage stability studies involve a wide range of phenomena. Because of this, voltage stability means different things to different people. It is a fast phenomenon for engineers involved with the operation of induction motors, air conditioning loads, or HVDC links. It is a slow phenomenon (involving, for example, mechanical tap changing) for others. (Appropriate analysis methods have been discussed with the debate centering on whether the phenomena of voltage stability are static or dynamic). Voltage instability or collapse is a dynamic process. The term "stability" implies that a dynamic system is being discussed. A power system is a dynamic system. In contrast to rotor angle (synchronous) stability, the dynamics involve mainly the loads and the means for voltage control. Voltage stability has alternatively been called load stability.

The loss of lines or generators can sometimes cause voltage quality degradation. This phenomenon has equally been attributed to the lack of sufficient reactive reserve when the power system experiences a heavy load or a severe contingency. Thus, voltage instability is characterized in such a way that voltage magnitude of the power system decreases gradually and then rapidly near the collapsing point. Voltage stability is classified as either static voltage stability or dynamic voltage stability. The latter is further classified into small signal stability and large disturbance stability problems. A unified framework related to voltage stability problems will be shown in a proceeding section.

In dynamic voltage stability analysis, exact models of transformers, Static Voltage Compensating devices (SVCs), induction motors and other types of loads are usually included in problem formulations in addition to models of generators, excitors, and other controllers. Small signal voltage stability problems are formulated as a combination of differential and algebraic equations that are linearized about an equilibrium point. Eigen analysis methods are used to analyze system dynamic behavior. Small signal analysis can provide useful information on modes of voltage instability and is instructive in locating VAR compensations and in the design of controllers. Large disturbance voltage stability is approached mainly by using numerical simulation techniques. Since system dynamics are described by nonlinear differential and algebraic equations that cannot be linearized in nature. Voltage collapse is analyzed based on a center manifold voltage collapse model.

6.1 WORKING DEFINITION OF VOLTAGE COLLAPSE STUDY TERMS

Voltage stability has been viewed as a steady-state “viability” problem suitable for static analysis techniques. The ability to transfer reactive power from production sources to consumption sinks during steady operating conditions is a major aspect of voltage stability. The following definitions are often used in voltage stability studies.

Voltage collapse incidents in the U.S., Europe, and Japan have led to different explanations, interpretations, and concerns. To achieve a unifying framework, a working definition for detection and prevention of voltage collapse has been constructed (EPRI RP 2473-36).

6.1.1 Classification of Voltage Collapse Detection

Detection of VC is based on determination of imminence of power system voltage violating its limits which value may lead to system instability and consequently voltage collapse. The phenomenon in many instances is due to a deficit in reactive power generation, loss of critical lines or degradation of control on key buses.

6.1.2 Classification of Voltage Collapse Prevention

Voltage collapse prevention is any action taken to reduce the likelihood of power system degradation due to the violation of operating limits. Prevention scheme includes the use of optimal power flow strategy and other measures to minimize voltage deviations.

Other definitions of voltage collapse or stability are documented in the literature. For example, according to the IEEE working group in voltage stability, voltage collapse/stability is defined as follows:

Voltage stability is the *ability* of a system to maintain voltage so that when load admittances are increased, load power will increase, so that both power and voltage are controllable.

Voltage collapse is the *process* by which voltage instability leads to loss of voltage in a significant part of the system. Voltage degradation may also lead to “angle stability” as well, especially if the preventive measures are not enforced quickly enough. Sometimes only careful post incident analysis can discover the primary cause of voltage collapse.

6.2 TYPICAL SCENARIO OF VOLTAGE COLLAPSE

Assume that a power system undergoes a sudden increase of reactive power demand following a system contingency, the additional demand is met by the reactive power reserves carried by the generators and compensators. It is possible, because of a combination of events and system conditions, that the additional reactive power demand may lead to voltage collapse, causing a major breakdown of part or all of the system. A typical sequence of events leading to a voltage collapse can be as follows:

1. The power system is experiencing abnormal operating conditions with large generating units near the load centers being out of service. Some EHV lines are heavily loaded and reactive power resources are low.
2. A heavily loaded line is lost which causes additional loading on the remaining adjacent lines. This increases the reactive power losses in the lines causing a heavy reactive power demand on the system. (Reactive power absorbed by a line increases rapidly for loads above surge impedance loading).
3. Immediately following the loss of the line, a considerable reduction of voltage takes place at adjacent load centers due to extra reactive power demand. This causes a load reduction, and the resulting reduction in power flow through the lines would have a stabilizing effect. The generator AVRs would, however, quickly resolve terminal voltages by increasing excitation. The resulting additional reactive power flow through the inductances associated with generator transformers and lines would cause increased voltage drop across each of these elements. At this stage, generators are likely to be within the limits of P - Q output capabilities, i.e., within the armature and field current heating limits. The speed governors would regulate frequency by reducing MW output.
4. The EHV level voltage reduction at load centers would be reflected into the distribution system. The ULTCs of substation transformers would restore distribution voltages and loads to prefault levels in about 2 to 4 minutes. With each tap change operation, the resulting increment in load on EHV lines would increase the line XI^2 and RI^2 losses, which in turn would cause a greater drop in EHV lines. If the EHV line is loaded considerably above the SIL, each MVA increase in line flow would cause several MVAs of line losses.
5. As a result, with each tap-changing operation, the reactive output of generators throughout the system would increase. Gradually, the generators would exceed their reactive power capability limits (imposed by maximum allowable continuous field current) one by one. When the first generator reached its field current limit, its terminal voltage would drop. At the reduced terminal voltage for a fixed MW output, the armature current would increase. This may further limit reactive output to keep the armature current within allowable limits. Its share of reactive loading would be transferred to other generators, leading to overloading of more and more generators. With fewer generators on automatic

excitation control, the system would be much more prone to voltage instability. This would likely be compounded by the reduced effectiveness of shunt compensators at low voltages. The process will eventually lead to voltage collapse or avalanche, possibly leading to loss of synchronism of generating.

Sometimes, the term ‘voltage security’ is used. This means the ability of a system not only to operate in a stable mode but also to remain stable following credible contingencies or load increases. It often means the existence of a considerable margin from an operating point to the voltage instability point following credible contingencies.

6.3 TIME-FRAME VOLTAGE STABILITY

Voltage instability incidents in various places around the world has been described as a function of time. The time ranges from seconds to tenths of minutes. Three time frames and scenarios described by Carson Taylor are summarized as follows:

1. Transient voltage stability: This occurs between 0 to 10 seconds.
2. Classical Voltage Stability: This occurs between 1 to 5 minutes. This is the classic scenario involving automatic on-load tap changer, distribution voltage regulation, and generator current limiting. This scenario involves high loads, high power imports from a remote generator, and a large distribution. Tap changer action is also significant, if it can be beneficial or detrimental depending on load characteristics and location of the tap changer. Collapse in one area can affect a much larger area, thus, leading to a major black-out. This occurrence is typical on the East Coast, the Pacific West, and in Japan.
3. Long-term Voltage Stability: This involves several minutes. Several VC incidents (the Tokyo 1977 blackout, the Sweden blackout) are experiences of VC. The factors may include overload time, limit of transmission, loss load diversity due to low voltage (theoretically controlled loads), timeliness of applying reactive power, and other operating interventions such as load shedding.

Reported voltage instability incidents with and without voltage are summarized in Figure 6.1. For classical voltage instability, the phenomenon will occur at the onset of the voltage collapse. For long-term stability, the shorter-time frame phenomena will occur once voltage begins to sag leading to voltage collapse.

6.4 MODELING FOR VOLTAGE STABILITY STUDIES

Voltage stability studies involve the solution to algebraic and differential equations that map the system behavior under steady-state and transient states. Below are typical vectors encountered and the notation used.

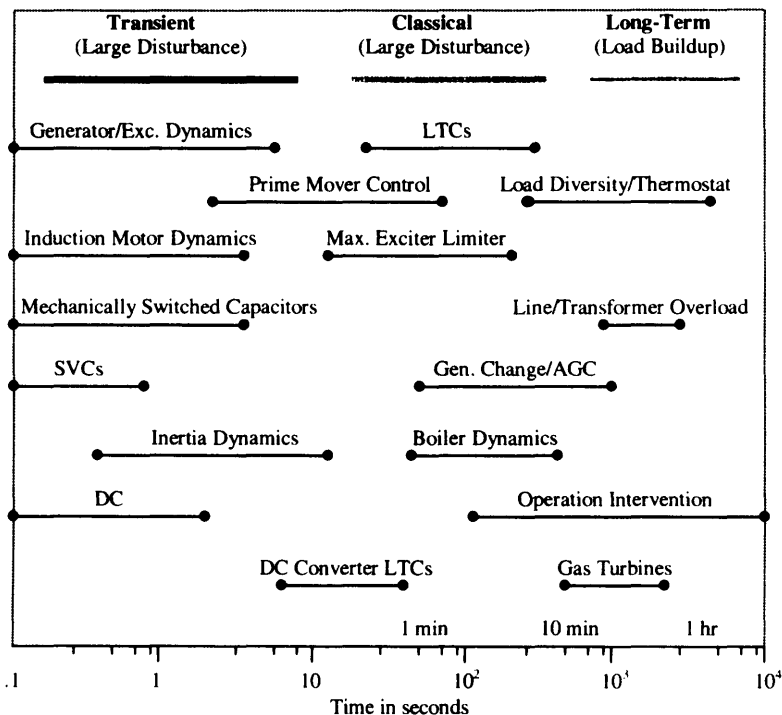


Figure 6.1 Time-frame of voltage stability (courtesy of Carson Taylor).

1. Dynamic state vector, $x(t)$

$$x(t) = [\theta(t), E'(t), S(t), \rho(t)]^T \quad (6.1)$$

where

$\theta(t)$ = Rotor angle

$E'(t)$ = Voltage components of synchronous machine

$S(t)$ = Dynamics in load bus

$\rho(t)$ = Other dynamic states (exciter, governor)

2. Algebraic state vector, $y(t)$

$$y(t) = [v(t), \delta(t), Q(t), \eta(t)]^T \quad (6.2)$$

where

$v(t), \delta(t)$ = Bus voltage magnitude and angle

- $Q(t)$ = Nonscheduled reactive power
 $\eta(t)$ = Other algebraic variables

3. Parameter vector, $p(t)$

$$p(t) = [P_s(t), P_l(t), Q_l(t), E_{ul}(t), \sigma(t)]^T \quad (6.3)$$

where

- $P_s(t)$ = Turbine shaft power
 $P_l(t), Q_l(t)$ = Scheduled load power
 $E_{ul}(t)$ = Controlled voltage or set points
 $\sigma(t)$ = Other similar parameters

6.5 VOLTAGE COLLAPSE PREDICTION METHODS

The framework for voltage stability studies can be simplified to fit the time span of the analysis. The categories of interest are as follows:

6.5.1 Static Stability

Assume all time derivatives equal zero at some operating point $H(x,y,p) = 0$

6.5.2 Dynamic Stability

At some operating point, small perturbations (local)

$$\dot{X}(t) = F(x, y, p) = Ax + By \quad (6.4)$$

6.5.3 Extended Stability

Simulation through time (up to hours)

$$\begin{aligned} \dot{X}(t) &= F(x(t), y(t), p(t)) \\ 0 &= H(x(t), y(t), p(t)) \\ 0 &\geq G(x(t), y(t), p(t)) \end{aligned} \quad (6.5)$$

6.6 CLASSIFICATION OF VOLTAGE STABILITY PROBLEMS

Voltage problems are distinguished in three categories:

1. Primary phenomena related to system structure. These reflect the autonomous response of the system to reactive supply/demand imbalances.

2. Secondary phenomena related to control actions. These reflect the counterproductive nature of some manual or automatic control actions.
3. Tertiary phenomena resulting from interaction of the above.

This classification of voltage quality problems implies that the problems involve both static and dynamic aspects of system components. Voltage collapse dynamics span a range in time from a fraction of a second to tens of minutes. Time frame charts are used to describe dynamic phenomena which show time responses from equipment that may affect voltage stability. The time frame chart is shown in Table 6.1, where x_t is a state vector representing transient dynamics, x_s is a state vector representing long-term dynamics.

Y is a state vector representing very fast transient dynamics related to network components and P is a system parameter vector. Then the time frames to be considered become very fast transient, transient, and long term. The main characteristics of the three time frames are as follows:

1. A very fast transient voltage collapse involves network RLC components having very fast response. The time range is from microseconds to milliseconds.
2. A transient voltage collapse involves a large disturbance and loads having a rapid response. Motor dynamics following a fault are often the main concern. The time frame is one to several seconds.
3. A long-term voltage collapse usually involves a load increase or a power transfer increase. Within this time frame, a voltage collapse shows load restoration by tap-changer and generator current limiting. Manual actions by system operators may be important. The time frame is usually 0.5 to 30 minutes. Since voltage stability is affected by various system components in a wide time range, in order to tackle this problem, one must consider proper modeling and analysis methods. Currently, voltage stability approaches mainly include static and dynamic, i.e., transient voltage collapse and long-term voltage collapse.

Table 6.1 Time Frame and Relevant Models in Voltage Stability Assessment

| Voltage stability models and time scale | | |
|---|-----------------------------------|---------------------------|
| Micro to milli seconds | A few seconds | Minutes |
| $\dot{x}_t = F_1[x_t, x_s, Y, P]$ | $\dot{x}_t = F_1[x_t, x_s, Y, P]$ | $0 = F_1[x_t, x_s, Y, P]$ |
| $\dot{x}_s = F_2[x_t, x_s, Y, P]$ | $\dot{x}_s = F_2[x_t, x_s, Y, P]$ | $0 = F_2[x_t, x_s, Y, P]$ |
| $Y = G[x_t, x_s, Y, P]$ | $0 = G[x_t, x_s, Y, P]$ | $0 = G[x_t, x_s, Y, P]$ |

6.7 VOLTAGE STABILITY ASSESSMENT TECHNIQUES

The loss of lines or generators can sometimes cause degradation in voltage. This phenomenon has equally been attributed to the lack of sufficient reactive reserve when the power system experiences a heavy load or severe contingency. Thus, voltage stability is characterized in such a way that voltage magnitude of the power system decreases gradually and then rapidly in the neighborhood of the collapsing point. Voltage stability is classified as static voltage stability and dynamic voltage stability. The latter is further divided into small signal stability and large disturbance stability problems.

In dynamic voltage stability analysis, exact modeling of transformers, SVCs, induction motors, and other types of loads are usually included in problem formulations in addition to models of generators, exciters, and other controllers. Small signal voltage stability problems are formulated as a combination of differential and algebraic equations that are linearized about an equilibrium point. Eigen analysis methods are used to analyze system dynamic behavior. Small signal analysis can provide useful information on modes of voltage instability and is instructive in locating VAR compensations and in the design of controllers. On the other hand, large disturbance voltage stability is mainly dealt with by numerical simulation techniques, since system dynamics are described by nonlinear differential and algebraic equations that cannot be linearized in nature. The mechanism of voltage collapse has been explained as saddle node bifurcation in some literature. Voltage collapse is analyzed based on a center manifold voltage collapse model.

Static voltage stability analysis is based on power system load flow equations. Indices characterizing the proximity of an operating state to the collapse point are developed. The degeneracy of the load flow Jacobian matrix has been used as an index of power system steady-state stability. Under certain conditions, a change in the sign of the determinant of the Jacobian matrix during continuous variations of parameters means that a real eigenvalue of the linearized swing equations crosses the imaginary axis into the right half of the complex plane and stability is lost. Various researchers have considered that a change in the sign of the Jacobian matrix may probably not indicate the loss of steady-state stability when even number eigenvalues whose real part cross the imaginary axis. Voltage stability is also related to multiple load flow solutions. A proximity indicator for voltage collapse (VCPI) was defined for a bus, an area, or the complete system as a vector of ratios of the incremental generated reactive power at a generator to a given reactive load demand increase. A different indicator (L index) is calculated from normal load flow results with reasonable computations. The minimum singular value of the Jacobian was proposed as a voltage security index, since the magnitude of the minimum singular value coincides with the degree of Jacobian ill-conditioning and the proximity to col-

lapse point. Based on a similar concept, the condition number of the Jacobian is also applied as an alternative voltage instability indicator by pioneers in the field.

Bifurcation theory is used to analyze static stability and voltage collapse. Static bifurcation of power flow equations were associated with either divergent-type instability or loss of casuality. Researchers have described necessary and sufficient conditions for steady-state stability based on the concept of feasibility regions of power flow maps and feasibility margins but with high computational efforts. A security measure is derived to indicate system vulnerability to voltage collapse using an energy function for system models that include voltage variation and reactive loads. It is concluded that the key to applications of the energy method is finding the appropriate *Type-I* low voltage solutions.

In addition to the above methods for direct computation of stability index, some indirect approaches, based on either the continuation method or optimization methods have been developed to compute the exact point of collapse. In applying the continuation methods, assumptions about load changing patterns are needed.

In summary, the methods for static voltage instability analysis are based on multiple load flow solutions (voltage instability proximity indicator [VIPI], energy method), load flow results (L index, VCPI), or eigenvalues of the Jacobian matrix (minimum singular value and condition number). While studies on dynamic voltage collapse shed light on control strategy design (off-line applications), static voltage stability analysis can provide operators with guideline information on the proximity of the current operating state to the collapse point (on-line applications). In this case, an index, which can give advance warning about the proximity to the collapse point, is useful.

The next discussion will be that of the formulation of selected voltage stability indices. Of the wide range of techniques available, we shall discuss the VIPI method, a method based on singular value decomposition, condition number of the Jacobian, and the method based on the Energy Margin.

6.7.1 Voltage Instability Proximity Indicator Method

The voltage instability proximity indicator (VIPI) was developed by Y. Tamura et al. based on the concept of multiple load flow solutions. A pair of load flow solutions x_1 and x_2 are represented by two vectors a and b as follows:

$$x_1 = a + b \quad (6.6)$$

$$x_2 = a - b \quad (6.7)$$

which are equivalent to:

$$a = \frac{x_1 + x_2}{2} \quad (6.8)$$

$$b = \frac{x_1 - x_2}{2} \quad (6.9)$$

where x_1 is the normal (high) power flow solution and x_2 its corresponding low voltage power flow solution; a is a singular vector in the space of node voltages and b is a margin vector in the same space.

We now define two other vectors Y_s and $Y(a)$, called singular vectors in the space of node specifications. The relationship between these vectors is shown in Figure 6.2.

VIPI is defined by the following equation:

$$\text{VIPI} = \cos^{-1} \left(\frac{Y_s^T \times Y(a)}{\|Y_s\| \times \|Y(a)\|} \right) \quad (6.10)$$

where vector Y_s consists of bus injections computed with respect to x_1 but the injection values corresponding to reactive powers of PV buses are replaced by the squared values of voltage magnitudes. $Y(a)$ consists of bus injections with respect to vector a : $\|x\|$ is the l_2 -norm of vector x . The computation of VIPI is easy once the relevant low voltage power flow solutions are obtained. Generally speaking, finding all the relevant low voltage solutions are time-consuming for practical size systems.

6.7.2 Minimum Singular Value (σ_{\min}) Method

When an operating state approaches the collapse point, the Jacobian matrix of the power flow equations (J), approaches singularity. The minimum singular

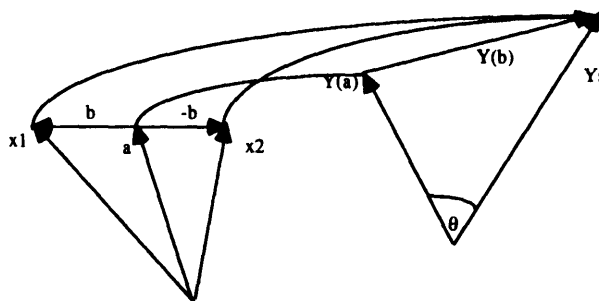


Figure 6.2 Concept of VIPI in the node specification space.

value of the Jacobian matrix expresses the closeness of Jacobian singularity. The singular value decomposition method is used to solve the minimum singular value for static voltage stability analysis.

According to the theory of singular value decomposition, power flow Jacobian can be decomposed as:

$$J = U\Sigma V^T \quad (6.11)$$

where: $J \in R^{2n \times 2n}$ is the power flow Jacobian matrix; $\Sigma = \text{diag}(\sigma_1, \sigma_2, \dots, \sigma_n)$ with $\sigma_{\max} = \sigma_1 \geq \sigma_2 \geq \dots \geq \sigma_n = \sigma_{\min} \geq 0$. If matrix J has rank r ($r \leq 2n$), its singular values are the square roots of the r positive eigenvalues of $A^T A$ (or AA^T). U and V are orthonormal matrices of order $2n$, and their columns contain the eigenvectors of AA^T and $A^T A$ respectively. From Eq. (6.9), it can be obtained that

$$AV_i = \sigma_i u_i \quad (6.12)$$

$$A^T u_i = \sigma_i V_i \quad (6.13)$$

We define

$$E_i = u_i V_i^T \quad (6.14)$$

Then Eq. (6.11) can be written as:

$$J = \sigma_1 E_1 + \sigma_2 E_2 + \dots + \sigma_n E_n \quad (6.15)$$

If we let

$$J' = \sigma_1 E_1 + \sigma_2 E_2 + \dots + \sigma_{n-1} E_{n-1} \quad (6.16)$$

then, as far as the l_2 -norm of the J matrix is concerned, J' is a matrix of rank $n - 1$ nearest to the J matrix of rank n . This means that the smallest singular value of a matrix is a measure of the distance between matrices J and J' . As for the power flow equations, its minimum singular value expresses the proximity of the Jacobian to singularity. It can be used as an index for static voltage stability.

6.7.3 Condition Number of the Jacobian Method

The condition number is used in numerical analysis to analyze the propagation of errors in matrix A or vector b in solving variable vector x for the linear equation $Ax = b$. If matrix A is ill-conditioned, even very small variations in vector b (or A) may result in significant changes in solution vector x .

For the linearized load flow equations, the condition number of the Jacobian matrix can be used to measure its conditioning and whether any small variations in vector b (or A) may result in significant changes in solution vector x .

For the linearized load flow equations, the condition number of the Jacobian matrix can be used to measure its conditioning and whether any small variations in loads may lead to large changes in bus voltages. If the condition number is greater than a specified threshold, this will mean that the current operating state is close to the collapsing point.

A precise measure of the sensitivity of a linear system solution with respect to matrix A or vector b can be defined as:

$$\text{Cond}_2(J) = \frac{(\text{max stretch of } A^T A)_2^{\frac{1}{2}}}{(\text{min stretch of } A^T A)_2^{\frac{1}{2}}} \quad (6.17)$$

If matrix A is symmetric with eigenvalues $\sigma_1, \sigma_2, \dots, \sigma_n$, then $\text{Cond}_2(A)$ is expressed as:

$$\text{Cond}_2(A) = \frac{\max |\sigma_i|}{\min |\sigma_i|} \quad (6.18)$$

For power flow Jacobian matrix J , the value of $\text{Cond}_2(J)$ can give an indication of the condition of J "with respect to inversion." A small value of $\text{Cond}_2(J)$ ($1 \sim 10$) refers to a well-conditioned Jacobian matrix (relatively large voltage stability margin); a large value of $\text{Cond}_2(J)$ (>100) means that the operating state is very close to the point of Jacobian singularity and has a low voltage stability margin. The extreme condition is that J is singular and $\text{Cond}_2(J)$ is infinite. Hence, the condition number $\text{Cond}_2(J)$ can be used to measure the proximity of the operating states to voltage collapse.

6.7.4 Energy Margin-Based Method

The energy method uses an energy function, derived from a closed form vector integration of the real and reactive mismatch equations between the operable power flow solution and a low voltage power flow solution, to provide a quantitative measure of how close the system is to voltage instability. The point of voltage instability corresponds to the saddle node bifurcation point defined by a singular power flow Jacobian with zero energy margin.

The energy function for voltage stability analysis is defined as:

$$V(x, x'') = -\frac{1}{2} \sum_{i=1}^{n-q} \sum_{j=1}^q B_{ij} V_i'' V_j'' \cos(\alpha_i'' - \alpha_j'') + \frac{1}{2} \sum_{i=1}^n \sum_{j=i+1}^n B_{ij} V_i' V_j' \cos(\alpha_i' - \alpha_j')$$

$$\begin{aligned}
& \sum_{i=1}^n \int_{x_t^s}^{x_t^n} Q_i(x) dx - P^T(\alpha'' - \alpha') - \frac{1}{2} \sum_{i=1}^n \sum_{j=1}^n G_{ij} V_i' V_j' \cos(\alpha'_i - \alpha'_j) (\alpha''_i - \alpha'_i) \\
& - \sum_{i=1}^n (V_i')^{-1} \sum_{j=1}^n G_{ij} V_i' V_j' \sin(\alpha'_i - \alpha'_j) (V''_i - V'_i)
\end{aligned} \tag{6.19}$$

with real and reactive mismatches defined as:

$$\begin{aligned}
f_i(\alpha, V) &= P_i - \sum_{j=1}^n B_{ij} V_i V_j \sin(\alpha_i - \alpha_j) + \sum_{j=1}^n G_{ij} V_i' V_j' \cos(\alpha'_i - \alpha'_j) \\
g_i(\alpha, V) &= (V_i')^{-1} [Q_i + \sum_{j=1}^n B_{ij} V_i V_j \cos(\alpha_i - \alpha_j) - (V_i')^{-1} \sum_{j=1}^n G_{ij} V_i' V_j' \sin(\alpha'_i - \alpha'_j)]
\end{aligned}$$

where: $x^* = (\alpha^*, V^*)$ is the normal operable power flow solution (or the stable equilibrium point, SEP); $x'' = (\alpha'', V'')$ is the relevant low voltage power flow solution with respect to x^* (or unstable equilibrium point, UEP).

A large energy value indicates a high degree of voltage stability while a small value indicates a low degree of voltage stability. In applying the energy method, the key is finding the relevant UEPs. Since the number of relevant low voltage power flow solutions is very large ($2^{n-1} - 1$) for a practical system, the exhaustive approach is not feasible. There is an improved technique to compute all the Type-1 UEPs based on the results that show for typical power systems, the system always loses steady-state stability by a saddle node bifurcation between the operable solution and a Type-1 low-voltage solution. That condition restricts the computation of relevant UEPs only corresponding to system PQ buses, or practically PQ load buses. After finding all the relevant UEPs, the buses corresponding to which the energy function has the lowest values are buses vulnerable to voltage instability. Similar to the VIPI method, the energy methods depend on the low-voltage power flow solutions, where the Newton-Raphson method with the optimal multiplier can be used.

6.8 ANALYSIS TECHNIQUES FOR STEADY-STATE VOLTAGE STABILITY STUDIES

6.8.1 Introduction to the Continuation Method

In its early stages, voltage collapse studies were mainly concerned with steady-state voltage behavior. The voltage collapse is often described as a problem that results when a transfer limit is exceeded. The transfer limit of an electrical power network is the maximal real or reactive power that the system can deliver from the generation sources to the load area. Specifically, the transfer limit is

the maximal amount of power that corresponds to at least one power-flow solution. From the well-known P - V or Q - V curves, one can observe that the voltage gradually decreases as the power transfer amount is increased. Beyond the maximum power transfer limit, the power-flow solution does not exist, which implies that the system has lost its steady-state equilibrium point. From an analytical point of view, the criteria for detecting the point of voltage collapse is the point where Jacobian of power-flow equations become singular.

The steady-state operation of the power system network is represented by power-flow equations given in equation (6.20).

$$F(\theta, V, \lambda) = 0 \quad (6.20)$$

where θ represents the vector of bus voltage angles and V represents the vector of bus voltage magnitudes. λ is a parameter of interest we wish to vary. In general the dimension of F will be $2n_{PV} + n_{PQ}$, where n_{PQ} and n_{PV} are the number of PQ and PV buses, respectively.

From equation (6.20) one obtains the fundamental equation of sensitivity analysis

$$dF = \frac{\partial F}{\partial \theta} d\theta + \frac{\partial F}{\partial V} dV + \frac{\partial F}{\partial \lambda} d\lambda = 0 \quad (6.21)$$

Let $x' = [\theta, V]'$. From Eq. (6.21), one can obtain an ODE system

$$\frac{dx}{d\lambda} = \left[\frac{\partial F}{\partial x} \right]^{-1} \frac{\partial F}{\partial \lambda} \quad (6.22)$$

For a specific variation of the parameter λ , the corresponding variation to the solution x is calculated by evaluating the Jacobian $[\partial F / \partial x]$. It should be emphasized that the singularity of the power flow Jacobian $\partial F / \partial x$ is necessary but not a sufficient condition to indicate voltage instability. The method proposed to observe the voltage instability phenomenon is closely related to multiple power flow solutions, which are caused by the nonlinearity of power flow solutions.

The drawback of the method is that it relies on the Newton–Raphson method of power flow analysis, which is unreliable in the vicinity of the voltage stability limit. As such, researchers have developed a technique known as the continuation method.

6.8.2 Continuation Method and Its Application to Voltages Stability Assessment

Consider the power flow equation defined in Eq. (6.20). The vector function F consists of n scalar equations defining a curve in the $n+1$ dimensional (x, λ) space. Continuation means tracing this curve. For a convenient graphical representation of the solution (x, λ) of Eq. (6.20) we need a one-dimensional measure of x . The frequently used measures are:

- (i) $|x| = \sum_{i=1}^n x_i^2$ (square of the Euclidean norm),
- (ii) $|x| = \max_{i=1,n} |x_i|$ (maximum norm),
- (iii) $|x| = x_k$ for some index k , $1 \leq k \leq n$.

In power systems generally we use the measure of (iii). As can be seen from Fig. 6.3 we have a type of critical solution for $\lambda = \lambda^*$, where for $\lambda > \lambda^*$ there are no solutions. For $\lambda < \lambda^*$ we have two solutions (one is the high voltage

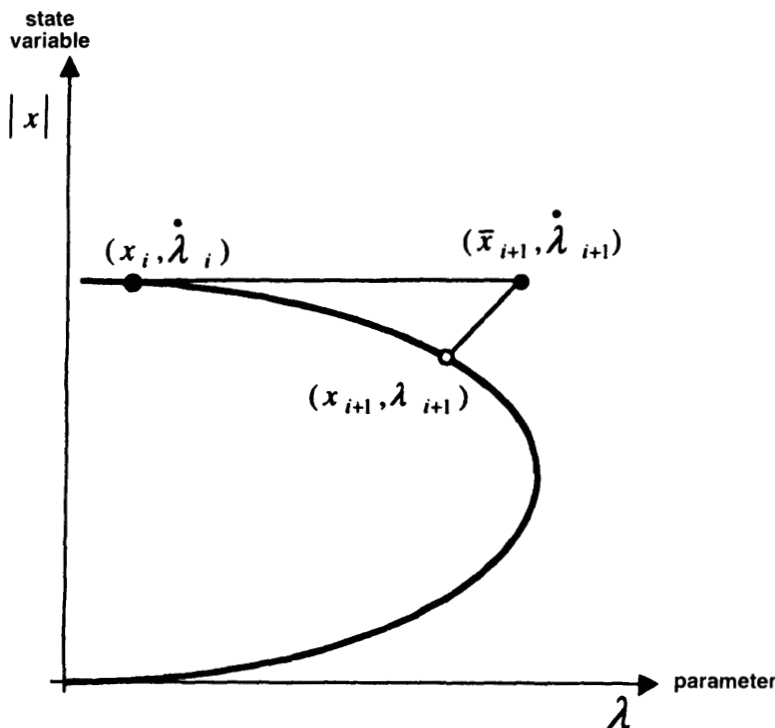


Figure 6.3 The fold type curve including predictor-corrector step.

solution and the other is the low voltage solution). When λ approaches $\lambda^*(\lambda < \lambda^*)$, both solutions merge. At this point the Jacobian of the power flow solution is singular. In the mathematical literature these points are called turning points, fold points, or bifurcation points. An algebraic feature of the turning point is given by F_λ below

$F_\lambda(x^*, \lambda^*)$ is singular for rank $< n$.

$F_\lambda(x^*, \lambda^*)/F_{\lambda\lambda}(x^*, \lambda^*)$ has a full rank n and satisfies some nondegeneracy conditions.

Several techniques have been proposed to calculate these points. These methods based their analysis on two approaches referred to as direct and indirect methods.

6.8.3 Detection of Voltage Collapse Points Using the Continuation Method

Direct Methods

This approach tries to find the maximum allowable variation of λ : that is, an operating point (x^*, λ^*) of the equation:

$$F(x, \lambda) = 0 \quad (6.23)$$

such that the Jacobian at this point is singular. It solves the following system of equations

$$G(y) = \begin{bmatrix} F(x, \lambda) \\ F'_\lambda(x, \lambda)h \\ h_k - 1 \end{bmatrix} = 0 \quad (6.24)$$

This procedure basically augments the original set of power flow equations $F(x, \lambda) = 0$ by $F'_\lambda(x, \lambda)h = 0$ where λ is an n -vector with $h_k = 1$. The disadvantages of this approach are:

The dimension of the nonlinear set of equations to be solved is twice that for the conventional power flow.

The approach requires good estimate of the vector λ .

The advantage is that, convergence of the direct method is very fast if the initial operating point is close to the turning point. The enlarged system is solved in such a way that it requires the solution of four $n \times n$ (n is the dimension of the Jacobian $F_\lambda(x, \lambda)$) linear systems, each with the same matrix, requiring only one LU decomposition.

Indirect Method (Continuation Methods)

Assuming that the first solution (x_0, λ_0) of $F(x, \lambda) = 0$, is available, the continuation problem is to calculate further solutions, (x_1, λ_1) , (x_2, λ_2) , until one reaches a target point, say at $\lambda = \lambda^*$. The i th continuation step starts from an approximation of (x_i, λ_i) and attempts to calculate the next solution. However, there is an intermediate step in between. With predictor, corrector type continuation, the step $i \rightarrow i + 1$ is split into two parts. The first part tries to predict a solution, and the second part tries to make this predicted part to converge to the required solution:

$$\text{Predictor } (x_i, \lambda_i) \rightarrow (\bar{x}_{i+1}, \bar{\lambda}_{i+1})$$

$$\text{Corrector } (\bar{x}_{i+1}, \bar{\lambda}_{i+1}) \rightarrow (x_{i+1}, \lambda_{i+1})$$

Continuation methods differ among other things, in the following: (1) choice of predictor, (2) type of the parameterization strategy, (3) type of corrector method, (4) step length control. All four aspects will be explained through the formulation of the power flow equations.

In order to apply the continuation method to the power flow problem, the power flow equations must be reformulated to include a load parameter (λ). This can be done by expressing the load and the generation at a bus as a function of the load parameter (λ). The general form of the new equations associated with each bus i is:

$$\begin{aligned} \Delta P_i &= P_{G_i}(\lambda) - P_{L_i}(\lambda) - P_{T_i} = 0 \\ \Delta Q_i &= Q_{G_i}(\lambda) - Q_{L_i}(\lambda) - Q_{T_i} = 0 \\ P_{T_i} &= \sum_{j=1}^n V_i V_j Y_{ij} \cos(\theta_i - \theta_j - \alpha_{ij}) \\ Q_{T_i} &= \sum_{j=1}^n V_i V_j Y_{ij} \sin(\theta_i - \theta_j - \alpha_{ij}) \end{aligned} \quad (6.25)$$

where the subscripts L_i , G_i , and T_i denote bus load, generation, and power out of a bus respectively. The voltage at bus i is $V_i \angle \theta_i$ and $Y_{ij} \angle \alpha_{ij}$ is the (i,j) th element of the system admittance matrix $[Y_{\text{BUS}}]$. $P_{L_i}(\lambda)$ and $Q_{L_i}(\lambda)$ terms depend on the type of load model. For example for the constant power load:

$$\begin{aligned} P_{L_i} &= P_{L_{\text{ref}}} + \lambda (K_{L_i} S_{\Delta_{\text{BASE}}} \cos(\psi_i)) \\ Q_{L_i} &= Q_{L_{\text{ref}}} + \lambda (K_{L_i} S_{\Delta_{\text{BASE}}} \sin(\psi_i)) \end{aligned} \quad (6.26)$$

For the nonlinear model

$$\begin{aligned}
 P_{L_i}(\lambda) &= (1 + K_{L_i}\lambda)P_{L_{\text{in}}} \left[P_{a_i} \left(\frac{V_i}{V_{o_i}} \right)^{KPV_1} + (1 - P_{a_i}) \left(\frac{V_i}{V_{o_i}} \right)^{KPV_2} \right] \\
 Q_{L_i}(\lambda) &= (1 + K_{L_i}\lambda) \left[P_{L_{\text{in}}} Q_{a_i} \left(\frac{V_i}{V_{o_i}} \right)^{KQV_1} + (Q_{L_{\text{in}}} - P_{L_{\text{in}}} Q_{a_i}) \left(\frac{V_i}{V_{o_i}} \right)^{KQV_2} \right]
 \end{aligned} \quad (6.27)$$

In addition, for any type of load model, the active power generation term can be modified to obtain

$$P_{G_i}(\lambda) = P_{G_{\text{in}}} (1 + \lambda_{G_i})$$

where the following definitions are made

$P_{L_{\text{in}}}$, $Q_{L_{\text{in}}}$ = Original load at bus i , active and reactive respectively

- K_{L_i} = Multiplier to designate the rate of load change at bus i as λ changes
- ψ_i = Power factor angle of load change at bus i
- $S_{\lambda_{\text{BASE}}}$ = Apparent power which is chosen to provide appropriate scaling of λ
- $P_{G_{\text{in}}}$ = Active generation at bus i in the base case
- K_{G_i} = Constant to specify the rate of change in generation as λ varies
- V_{o_i} = Initial voltage at the bus
- P_{a_i} = Frequency dependent fraction of active power load
- KPV_1 = Voltage exponent for frequency-dependent active power load
- KPV_2 = Voltage exponent for nonfrequency-dependent active power load
- Q_{a_i} = Ratio of uncompensated reactive power load to active power load
- KQV_1 = Voltage exponent for uncompensated reactive power load
- KQV_2 = Voltage exponent for reactive power compensation

Now if F is used to denote the whole set of equations, then the problem can be expressed as a set of nonlinear algebraic equations given by Eq. (6.20). The predictor, corrector continuation process can then be applied to those equations.

The first task in the predictor step is to calculate the tangent vector. This vector can be obtained from factorizing Eq. (6.21), i.e.,

$$[F_\theta, F_v, F_\lambda] \begin{bmatrix} d\theta \\ dV \\ d\lambda \end{bmatrix} = 0 \quad (6.28)$$

On the left side of the equation is a matrix of partial derivatives multiplied by vector of differentials. The former is the conventional power flow Jacobian

augmented by one column (F_λ), while the latter $t = [d\theta, dV, d\lambda]^T$ is the tangent vector being sought. A normalization has to be imposed in order to give t a nonzero length. One can use for example

$$e_k^T t = t_k = 1 \quad (6.29)$$

where e_k is an appropriately dimensioned row vector with all elements equal to zero except the k^{th} one, which equals one. If the index k is chosen properly, letting $t_k = \pm 1.0$ imposes a nonzero norm on the tangent vector which guarantees that the augmented Jacobian will be nonsingular at the point of maximum possible system load. Thus the tangent vector is determined as the solution of the linear system

$$\begin{bmatrix} F_\theta & F_V & F_\lambda \\ e_k \end{bmatrix} [t] = \begin{bmatrix} 0 \\ \pm 1 \end{bmatrix} \quad (6.30)$$

Once the tangent vector has been found by solving Eq. (6.30), the prediction can be made as follows:

$$\begin{bmatrix} \theta^* \\ V^* \\ \lambda^* \end{bmatrix} = \begin{bmatrix} \theta \\ V \\ \lambda \end{bmatrix} + \sigma \begin{bmatrix} d\theta \\ dV \\ d\lambda \end{bmatrix} \quad (6.31)$$

where “*” denotes the predicted solution and σ is a scalar that designates the step size.

6.9 PARAMETERIZATION

The branch consisting of solutions of Eq. (6.20) forming a curve in the (x, λ) space has to be parameterized. A parameterization is a mathematical way of identifying each solution on a branch. A parameterization is a kind of measure along the branch. There are many different kinds of parameterization. For instance, by looking at a PV curve, one sees that the voltage is continually decreasing as the load nears maximum. Thus, the voltage magnitude at some particular bus could be changed by small amounts and the solution is found for each given value of the voltage. Here the load parameter would be free to take on any value it needed to satisfy the equations. This is called local parameterization. In local parameterization the original set of equations is augmented by one equation that specifies the value of one of the state variables. In equation form this can be expressed as follows:

$$\begin{bmatrix} F(y) \\ y_k - \eta \end{bmatrix} = 0, \quad y = \begin{bmatrix} \theta \\ V \\ \lambda \end{bmatrix} \quad (6.32)$$

where η is an appropriate value for the k th element of y . Now once a suitable index k and the value of η are chosen, a slightly modified Newton-Raphson (N-R) power flow method (altered only in that one additional equation and one additional state variable are involved) can be used to solve the set of equations. This provides the corrector needed to modify the predicted solution found in the previous section.

The algorithm for static assessment is shown in Figure 6.4. We can use a simple example to explain the static analysis procedure.

6.9.1 Static Assessment: A Worked Example

Consider a system is represented by

$$\begin{cases} x^2 - y = 3 \\ 2x + y = \lambda \end{cases}$$

where λ is a variation parameter from $\lambda_o = 0$ to $\lambda_k = \lambda_{k,o}$

To begin, solve the system equations at $\lambda = 0$, we have

$$\begin{cases} x_o = 1 \\ y_o = -2 \\ \lambda_o = 0 \end{cases} \quad \text{or} \quad \begin{cases} x_o = -3 \\ y_o = 6 \\ \lambda_o = 0 \end{cases}$$

$$F(x,y,\lambda) = 0 \Rightarrow \begin{cases} x^2 - y - 3 = 0 \\ 2x + y - \lambda = 0 \end{cases}$$

$$F_1x = 2x, \quad F_1y = -1, \quad F_1\lambda = 0$$

$$F_2x = 2, \quad F_2y = 1, \quad F_2\lambda = -1$$

$$\therefore [F_x, F_y, F_\lambda] \begin{bmatrix} dx \\ dy \\ d\lambda \end{bmatrix} = \begin{bmatrix} 2x & -1 \\ 0 & 2 \\ 1 & -1 \end{bmatrix} \begin{bmatrix} dx \\ dy \\ d\lambda \end{bmatrix} = 0$$

Choose $k = 2$ and $c_k = [0 \quad 1 \quad 0]$, then the augmented equations are given by

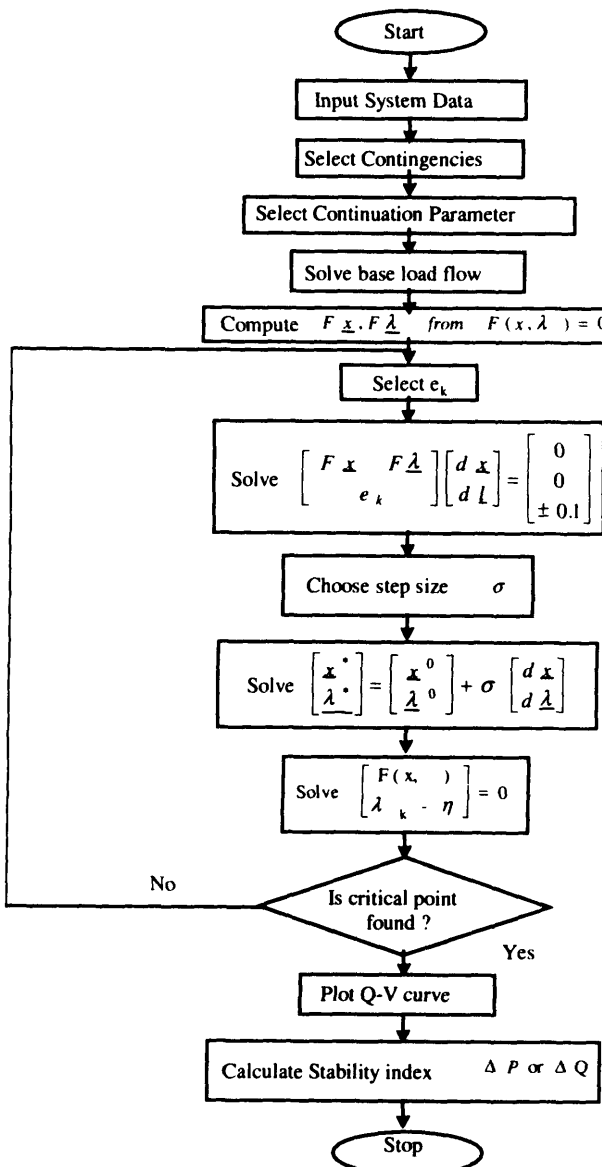


Figure 6.4 The algorithm for static assessment.

$$\begin{bmatrix} 2x & -1 & 0 \\ 2 & 1 & -1 \\ 0 & 1 & 0 \end{bmatrix} \begin{bmatrix} dx \\ dy \\ d\lambda \end{bmatrix} = 0$$

Since $x_0 = 1$, substituting into the above equation we have:

$$\begin{bmatrix} 2 & -1 & 0 \\ 2 & 1 & -1 \\ 0 & 1 & 0 \end{bmatrix} \begin{bmatrix} dx \\ dy \\ d\lambda \end{bmatrix} = 0$$

and

$$\begin{bmatrix} dx \\ dy \\ d\lambda \end{bmatrix} = \begin{bmatrix} 0.5 \\ 1.0 \\ 2.0 \end{bmatrix}$$

Therefore,

$$\begin{bmatrix} x^* \\ y^* \\ \lambda^* \end{bmatrix} = \begin{bmatrix} x_0 \\ y_0 \\ \lambda_0 \end{bmatrix} + \sigma \begin{bmatrix} dx \\ dy \\ d\lambda \end{bmatrix}$$

Choosing $\sigma = 0.1$, one gets

$$\hat{x}_1 = x^* = 1.0 + 0.05 = 1.05$$

$$\hat{y}_1 = y^* = -2 + 0.1 = -1.9$$

$$\hat{\lambda}_1 = \lambda^* = 0 + 0.2 = 0.2$$

where \hat{x}, \hat{y} , and $\hat{\lambda}$ are the approximated solutions.

In order to find the solution of $F(x, y, \lambda) = 0$, we need to solve the equation

$$\begin{bmatrix} F(x, y, \lambda) \\ y - \eta \end{bmatrix} = 0$$

where η is an appropriate value of y .

Choose $\eta = y^* = -1.9$, we have the solution of

$$\begin{cases} x_1 = 1.05 \\ y_1 = -1.9 \\ \lambda_1 = 0.2 \end{cases}$$

Based on the solution of (x, y, λ) , we can get the solution of (x_2, y_2, λ_2) . we have

$$\begin{bmatrix} x^* \\ y^* \\ \lambda^* \end{bmatrix} = \begin{bmatrix} x_1 \\ y_1 \\ \lambda_1 \end{bmatrix} + \sigma \begin{bmatrix} dx \\ dy \\ d\lambda \end{bmatrix}$$

Choose $\sigma = 0.1$, one gets

$$\begin{bmatrix} x^* \\ y^* \\ \lambda^* \end{bmatrix} = \begin{bmatrix} 1.05 + \frac{1}{21} \\ -1.8 \\ 0.2 + \frac{4.1}{21} \end{bmatrix}$$

Choose $\eta = -1.8$, we have the solution of

$$\begin{cases} x_1 = \sqrt{1.2} \\ y_1 = -1.8 \\ \lambda_1 = 2\sqrt{1.2} - 1.8 \end{cases}$$

Using the same procedure until the target system is reached. The modal analysis procedure is given in the following. System linearization equation is given by

$$\begin{bmatrix} 2x_o & -1 \\ 2 & 1 \end{bmatrix} \begin{bmatrix} \Delta x \\ \Delta y \end{bmatrix} = \begin{bmatrix} 0 \\ \Delta p \end{bmatrix}$$

where p represents the variation parameter.

At $x_o = 1$, $y_o = -2$, $p_o = 0$, the above equation can be reduced to

$$\begin{aligned} \Delta x &= J_k^{-1} \Delta p = \frac{1}{2 + 2x_o} \Delta p = \frac{1}{4} \Delta p \\ \therefore J &= 1, \quad \lambda = 4, \quad \eta = 1 \end{aligned}$$

6.10 THE TECHNIQUE OF MODAL ANALYSIS

The modal or eigenvalue analysis method is a kind of sensitivity analysis but the modal separation provides additional insight. The system partitioned matrix equations of the Newton–Raphson method can be rewritten as

$$\begin{bmatrix} \Delta P \\ \Delta Q \end{bmatrix} = \begin{bmatrix} J_{P_u} & J_{P_v} \\ J_{Q_u} & J_{Q_v} \end{bmatrix} \begin{bmatrix} \Delta \theta \\ \Delta V \end{bmatrix} \quad (6.33)$$

where the partitioned Jacobian reflects a solved power flow condition and includes enhanced device modeling. By letting $\Delta P = 0$, we can write

$$\Delta Q = [J_{Q_u} - J_{Q_v} J_{P_v}^{-1} J_{P_u}] \Delta V = J_R \Delta V \quad (6.34)$$

where J_R is a reduced Jacobian matrix of the system. J_R directly relates the bus voltage magnitude and bus reactive power injection.

Let λ_i be the i th eigenvalue of J_R with ξ_i and η_i being the corresponding column right eigenvector and row left eigenvector, respectively.

The i th modal reactive power variation is

$$\Delta Q_{im} = K_i \xi_i \quad (6.35)$$

where $K_i^2 \sum_j \xi_{ji}^2 = 1$ with ξ_{ji} the j th element of ξ_i . The corresponding i th modal voltage variation is

$$\Delta V_{im} = \frac{1}{\lambda_i} \Delta Q_{im} \quad (6.36)$$

The magnitude of each eigenvalue λ_i determines the weakness of the corresponding modal voltage. The smaller the magnitude of λ_i , the weaker the corresponding modal voltage. If $\lambda_i = 0$, the i th modal voltage will collapse because any change in that modal power will cause infinite modal voltage variation.

If all eigenvalues are positive, the system is considered voltage stable. This is a different dynamic system where eigenvalues with negative real parts are stable. The relationship between system voltage stability and eigenvalues of the J_R matrix is best understood by relating the eigenvalues with Q – V sensitivity of each bus. J_R can be taken as a symmetric matrix and therefore the eigenvalues

of J_R are close to being purely real. If all the eigenvalues are positive, J_R is positive definite and the V - Q sensitivities are also positive, indicating that the system is voltage stable.

The system is considered voltage unstable if at least one of the eigenvalues is positive. A zero eigenvalue of J_R means that the system is on the verge of voltage instability. Furthermore, small eigenvalues of J_R determine the proximity of the system to be voltage unstable.

The participation factor of bus k to mode i is defined as

$$P_{ki} = \xi_k \eta_{ik} \quad (6.37)$$

For all the small eigenvalues, bus participation factors determine the areas close to voltage instability. In addition to the bus participations, modal analysis also calculates branch and generator participations. Branch participations indicate which branches are important in the stability of a given mode. This provides insight into possible remedial actions as well as contingencies, which may result in loss of voltage stability. Generator participations depict which machines must retain reactive reserves to ensure stability of a given mode. Figure 6.5 depicts the technique static voltage stability assessment using modal analysis.

For a practical system with several thousand buses it is impractical and unnecessary to calculate all the eigenvalues. Calculating only the minimum eigenvalue of J_R is not sufficient because there are usually more than one weak modes associated with different parts of the system, and the mode associated with the minimum eigenvalue may not be the most troublesome mode as the system is stressed. The m smallest eigenvalues of J_R are the m least stable modes of the system. If the biggest of the m eigenvalues, say mode m , is a strong enough mode, the modes that are not computed can be neglected because they are known to be stronger than mode m . An implicit inverse lopsided simultaneous iteration technique is used to compute the m smallest eigenvalues of J_R and the associated right and left eigenvectors.

Similar to sensitivity analysis, modal analysis (see the worked example at the end of this chapter) is only valid for the linearized model. Modal analysis can, for example, be applied at points along P - V curves or at points in time of a dynamic simulation.

6.11 ANALYSIS TECHNIQUES FOR DYNAMIC VOLTAGE STABILITY STUDIES

It is only recently that the effects of system and load dynamics are being investigated in the context of voltage collapse. The dynamics that are being considered are:

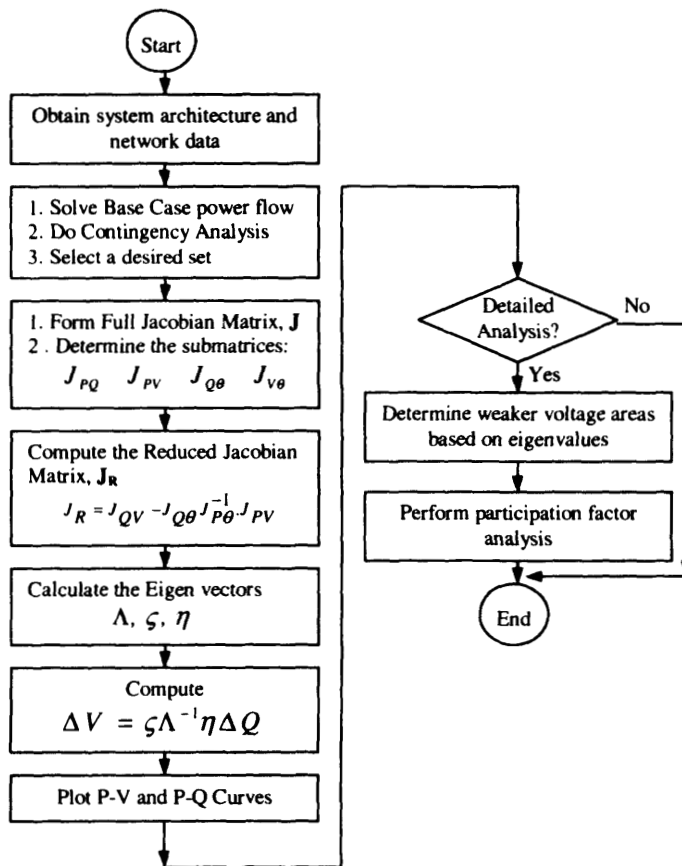


Figure 6.5 Static voltage stability assessment using modal analysis.

1. Machine and excitation system dynamics including power system stabilizer (PSS).
2. Load dynamics.
3. Dynamics of SVC controls and FACTS devices.
4. Tap-changer dynamics.
5. Dynamics due to load frequency control, AGC, etc.

While 1, 2, and 3 involve fast dynamics, 4 and 5 represent slow dynamics. A classification process of dynamic voltage stability vis-a-vis static stability is shown in Figure 6.6. Here "load" implies demand and " u " represents set points of LFC, AGC, and voltage/VAr controls at substations. x , represents the slow

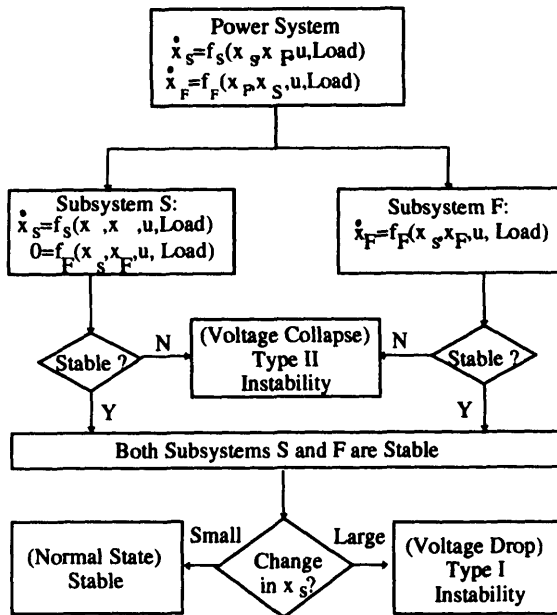


Figure 6.6 Classification of voltage instabilities.

variables such as the state variables belonging to tap-changing transformers, AGC loop and center of angle variables in the case of a multi-area representation. x_F represents the fast variables belonging to the generating unit including PSS and governor, induction motor load dynamics, SVC dynamics, and so forth.

The overall mathematical model is of the form:

$$\dot{x}_S = g_S(\hat{V}, u) \quad (6.38)$$

$$\dot{x}_F = g_F(x_S, x_F, \hat{V}, y, I_g, u, p_L) \quad (6.39)$$

$$0 = h_F(x_S, x_F, \hat{V}, I_g, u, p_L) \quad (6.40)$$

$$y = h_N(x_S, x_F, \hat{V}, u) \quad (6.41)$$

Ignoring the more slower AGC dynamics and the faster network transients (60 Hz) we can categorize the variables appearing in Eq. (6.38)–(6.41).

$$x_S = [n_i] \quad i = 1, \dots, p$$

where

n_i = transformer tap ratio

| | |
|---------------------------------|--|
| δ_i | |
| ω_i | rotor angle of i th machine |
| E'_{qp} | rotor velocity of i th machine |
| $x_t = \frac{E'_{di}}{E'_{td}}$ | rotor electrical variables $i = 1, \dots, m$ |
| V_R | excitation system variables |
| R_p | |

$$\hat{V}_i = \begin{bmatrix} V_{D_i} \\ V_{Q_i} \end{bmatrix} \text{ rectangular variables of } i\text{th bus voltage or } \begin{bmatrix} \theta_i \\ V_i \end{bmatrix}$$

$$y = \begin{bmatrix} P_{G_i} + P_{T_i} \\ Q_{G_i} + Q_{T_i} \end{bmatrix} \text{ injected real and reactive power } i = 1, 2, \dots, n$$

$$I_\psi = \begin{bmatrix} I_{d_i} \\ I_{q_i} \end{bmatrix} \text{ machine terminal currents in machine reference frame } i = 1, \dots, m$$

$$u = \begin{bmatrix} T_{ib} \\ V_{i_{ref}} \\ V_{i_t} \end{bmatrix} \quad \begin{array}{l} \text{desired real power of } i\text{th generator} \\ \text{desired voltage at } i\text{th generator bus} \\ \text{desired voltage at the bus controlled by tap-changer } i \end{array}$$

$$i = 1, 2, \dots, m$$

$$i = 1, 2, \dots, m$$

p_L = vector of load parameters to be defined.

The state variables of the static VAr system (SVC) control and induction motor will appear in x_t if included in the overall model. As an example we give below the equations for a m machine n bus system having p tap-changing transformers. Only the synchronous machine and tap-changer dynamics are included.

6.11.1 Equations of Slow and Fast Subsystems

For an m -machine, n -bus system having r tap-changing transformers, the following equations are applicable

Slow Subsystem

$$\frac{dn_i}{dt} = -\frac{1}{T_{ni}}(V_i - V_{ni}), \quad i = 1, \dots, p \quad (6.42)$$

Fast Subsystem

$$\begin{aligned}
 \frac{d\delta_i}{dt} &= \omega_i - \omega_s & i = 1, \dots, p \\
 M_i \frac{d\omega_i}{dt} &= T_{M_i} - [E'_{qi} - X'_{di} I_{di}] I_{qi} - [E'_{di} + X'_{qi} I_{qi}] I_{di} - D_i(\omega_i - \omega_s) & i = 1, \dots, m \\
 T'_{dq} \frac{dE'_{qi}}{dt} &= -E'_{qi} - (X_{di} - X'_{di}) I_{di} + E_{fdi} & i = 1, \dots, m \\
 T'_{qo} \frac{dE'_{di}}{dt} &= -E'_{di} + (X_{qi} - X'_{qi}) I_{qi} & i = 1, \dots, m \\
 T_{L_i} \frac{dE_{fdi}}{dt} &= -(K_{Ei} + S_L(E_{fdi})) E_{fdi} + V_{Ri} & i = 1, \dots, m \\
 T_{A_i} \frac{dV_{Ri}}{dt} &= -V_{Ri} + K_{Ai} R_{fi} - \frac{K_{Ai} K_{Ei}}{T_{Ei}} E_{fdi} + K_{Ai}(V_{ref,i} - V_i) & i = 1, \dots, m \\
 T_{Ei} \frac{dR_{fi}}{dt} &= -R_{fi} + \frac{K_{Ei}}{T_{Ei}} E_{fdi} & i = 1, \dots, m
 \end{aligned} \tag{6.43}$$

The algebraic equations for the stator and network can be used to analyze the system

$$\begin{aligned}
 E'_{di} - V_i \sin(\delta_i - \theta_i) - R_{si} I_{di} + X'_{qi} I_{qi} &= 0 \\
 E'_{qi} - V_i \cos(\delta_i - \theta_i) - R_{si} I_{qi} + X'_{di} I_{di} &= 0 \quad i = 1, 2, \dots, m \\
 I_{di} V_i \sin(\delta_i - \theta_i) + I_{qi} V_i \cos(\delta_i - \theta_i) + P_{Li}(V_i) \\
 - \sum_{k=1}^n V_i V_k Y_{ik} \cos(\theta_i - \theta_k - \alpha_{ik}) &= 0 \\
 I_{di} V_i \cos(\delta_i - \theta_i) + I_{qi} V_i \sin(\delta_i - \theta_i) + Q_{Li}(V_i) \\
 - \sum_{k=1}^n V_i V_k Y_{ik} \sin(\theta_i - \theta_k - \alpha_{ik}) &= 0 \quad i = 1, \dots, m \\
 P_{Li}(V_i) - \sum_{k=1}^n V_i V_k Y_{ik} \cos(\theta_i - \theta_k - \alpha_{ik}) &= 0 \\
 Q_{Li}(V_i) - \sum_{k=1}^n V_i V_k Y_{ik} \sin(\theta_i - \theta_k - \alpha_{ik}) &= 0 \quad i = m+1, \dots, n
 \end{aligned} \tag{6.44}$$

6.11.2 Load Flow and Equilibrium Point

The equilibrium point is calculated for a given set of reference points, $V_{ref,i}, T_{mi}, V_{oi}$ and a given demand P_{Li} and Q_{Li} and then solving the following equations for the variables $\theta_2, \dots, \theta_n, V_{m+1}, \dots, V_n$.

We may alternatively combine Eq. (6.44) in a compact way as

$$\begin{aligned} P_i^{\text{net}} &= \sum_{k=1}^n V_i V_k Y_{ik} \cos(\theta_i - \theta_k - \alpha_{ik}) = 0 & i = 1, \dots, n \\ Q_i^{\text{net}} &= \sum_{k=1}^n V_i V_k Y_{ik} \sin(\theta_i - \theta_k - \alpha_{ik}) = 0 & i = 1, \dots, n \end{aligned} \quad (6.45)$$

and

$$\begin{aligned} P_L(V_i) &= P_{L_{oi}} \left(\frac{V_i}{V_{oi}} \right)^{p_o} \\ Q_L(V_i) &= Q_{L_{oi}} \left(\frac{V_i}{V_{oi}} \right)^{q_o} \end{aligned} \quad (6.46)$$

The parameter vector p_L can be defined in terms of $P_{L_{oi}}$, $Q_{L_{oi}}$, n_{pi} , n_{qi} , etc.

The equilibrium point is calculated for a given set of reference points V_{oi} , T_M , V_{oi} , and a given demand P_{Li} and Q_{Li} . The load flow equations are extracted from Eqs. (6.45) and (6.46) as follows

1. Specify bus voltage magnitudes numbered 1 to m .
2. Specify bus voltage angle number 1 (slack bus).
3. Specify net injected real power $P_i^{\text{net}} = P_{Li}$ and $Q_i^{\text{net}} = Q_{Li}$ at all buses numbered $m+1$ to n .

Solve the following equations for the variables

$$\theta_2, \dots, \theta_n, \quad V_{m+1}, \dots, V_n,$$

$$\begin{aligned} 0 &= -P_i^{\text{net}} + \sum_{k=1}^n V_i V_k Y_{ik} \cos(\theta_i - \theta_k - \alpha_{ik}) = 0 & i = 2, 3, \dots, m \quad (\text{PVbuses}) \\ 0 &= -P_{Li} + \sum_{k=1}^n V_i V_k Y_{ik} \cos(\theta_i - \theta_k - \alpha_{ik}) = 0 & i = m+1, \dots, n \quad (\text{PQbuses}) \\ 0 &= -Q_{Li} + \sum_{k=1}^n V_i V_k Y_{ik} \sin(\theta_i - \theta_k - \alpha_{ik}) = 0 & i = m+1, \dots, n \quad (\text{PQbuses}) \end{aligned} \quad (6.47)$$

The standard load-flow Jacobian matrix involves the linearization of Eq. (6.47) with respect to $\theta_2, \dots, \theta_n, V_{m+1}, \dots, V_n$. After the solution using Newton's method, compute

$$\begin{aligned} P_i^{\text{net}} + j Q_i^{\text{net}} &= \sum_{k=1}^n V_i V_k Y_{ik} e^{j(\theta_i - \theta_k - \alpha_{ik})} \\ Q_i^{\text{net}} &= \sum_{k=1}^n V_i V_k Y_{ik} e^{j(\theta_i - \theta_k - \alpha_{ik})} & i = 2, \dots, m \end{aligned} \quad (6.48)$$

In the above load flow problem one can include inequalities on Q generation at P - V buses, switching Var sources, etc. From the load flow solution, the initial conditions of state variables in Eq. (6.48) can be computed systematically. The initial value of V_i is V_{i0} .

Linearization

Define $\hat{V}^T = [\hat{V}_g^T \hat{V}_l^T]$ corresponding to generator and load buses. Also define

$$x^T = [x_s^T \mid x_l^T] = [x_s^T, x_1^T, \dots, x_m^T]$$

where

$$x_s^T = [n_1, \dots, n_p]$$

and

$$x_i^T = [\delta_i, \omega_i, E'_q, E_{di}, E_{fi}, V_{ri}, R_{ri}] i = 1, \dots, m$$

and the algebraic variables as I_g , V_g , V_l . Also let

$$S_L^T = (P_{Lg}(V_i), Q_{Lg}(V_i))$$

The linearized equations corresponding to Eqs. (6.42)–(6.44) can be expressed as

$$\begin{bmatrix} \Delta \dot{x}_s \\ \Delta \dot{x}_l \\ 0 \\ 0 \\ 0 \end{bmatrix} = \begin{bmatrix} A_{s1} & 0 & 0 & 0 & A_{s5} \\ 0 & \bar{A}_1 & \bar{A}_2 & \bar{A}_3 & 0 \\ 0 & \bar{B}_1 & \bar{B}_2 & \bar{B}_3 & 0 \\ 0 & \bar{C}_1 & \bar{C}_2 & \bar{C}_3 & \bar{C}_4 \\ 0 & 0 & 0 & \bar{D}_1 & \bar{D}_2 \end{bmatrix} \begin{bmatrix} \Delta x_s \\ \Delta x_l \\ \Delta I_g \\ \Delta \hat{V}_g \\ \Delta \hat{V}_l \end{bmatrix} + \begin{bmatrix} 0 \\ 0 \\ 0 \\ \Delta S_{Lg} \\ \Delta S_{Ll} \end{bmatrix} + \begin{bmatrix} 0 \\ 0 \\ 0 \\ H_3 \\ H_4 \end{bmatrix} \Delta p_l$$

$$+ \begin{bmatrix} 0 \\ E \\ 0 \\ 0 \\ 0 \end{bmatrix} \Delta u \quad (6.49)$$

In Eq. (6.48) the variations corresponding ΔV_i in the nonlinear load characteristic is contained in ΔS_{Lg} and ΔS_{Ll} .

6.11.3 Static Stability (Type I Instability)

In Eq. (6.46), suppose that both $\Delta \dot{x}_s = \Delta \dot{x}_l = 0$. Then we have a static situation with all equations being algebraic. Let all the voltage deviations in $\Delta \hat{V}_g$ and $\Delta \hat{V}_l$

be denoted by $\Delta\hat{V}$, then the rest of the algebraic variables can be eliminated (assuming constant power load) to express $\Delta\hat{V} = J^{-1} H \Delta p_L$. If $\det(J_s) \rightarrow 0$ as load is increased it is referred to as Type I static instability, i.e., the system is not able to handle the increased load.

6.11.4 Dynamic Stability (Type II Instability)

Eliminating the algebraic variables in Eq. (6.49) and assuming $\Delta u \equiv 0$, it can be expressed as

$$\begin{bmatrix} \Delta\dot{x}_S \\ \Delta\dot{x}_I \end{bmatrix} = \begin{bmatrix} A_{SS} & A_{SI} \\ A_{IS} & A_{II} \end{bmatrix} \begin{bmatrix} \Delta x_S \\ \Delta x_I \end{bmatrix} + [H_1] \Delta p_L \quad (6.50)$$

Two types of dynamic instability (Type II) can be distinguished, slow and fast. In both cases we assume $\Delta p_L = 0$.

6.11.5 Slow Instability

Theoretically it should be possible to eliminate Δx_I in Eq. (6.50) using the singular perturbation theory and obtain the linearized slow system as $\Delta\dot{x}_S = A_S \Delta x_S$. The time scale of the phenomena is so large that linearized results may not reflect the true picture. For such a time intensive phenomena, nonlinear simulation is recommended.

6.11.6 Fast Instability

First we rearrange the variables $\{\Delta I_g, \Delta\hat{V}_g, \Delta\hat{V}_i\}$ as $\{\Delta I_g, \theta_1, \Delta V_1, \dots, \Delta V_m, \Delta\theta_2, \Delta\theta_3, \dots, \Delta\theta_n, \Delta V_{m+1}, \dots, \Delta V_n\} = [\Delta z, \Delta v]$. Next we assume x_S as constant and load parameters as constant which implies $\Delta p_L = 0$. We get

$$\begin{bmatrix} \Delta\dot{x}_I \\ 0 \\ 0 \end{bmatrix} = \begin{bmatrix} A_1 A_2 A_3 \\ B_1 B_2 B_3 \\ C_1 C_2 C_3 \end{bmatrix} \begin{bmatrix} \Delta x_I \\ \Delta z \\ \Delta v \end{bmatrix} + \begin{bmatrix} 0 \\ \Delta S_1 \\ \Delta S_2 \end{bmatrix} + \begin{bmatrix} E \\ 0 \\ 0 \end{bmatrix} \Delta u \quad (6.51)$$

For the constant power case, both ΔS_1 and ΔS_2 are $\equiv 0$. Otherwise, $\Delta S_1 = \Delta S_1(V_i)$ and $\Delta S_2 = \Delta S_2(V_i)$. For a given voltage-dependent load, ΔS_{1i} and ΔS_{2i} can be computed. Only the appropriate diagonal elements of B_2 , C_2 , and C_3 will be modified and we obtain the system

$$\begin{bmatrix} \Delta\dot{x}_I \\ 0 \\ 0 \end{bmatrix} = \begin{bmatrix} \tilde{A}_1 \tilde{A}_2 \tilde{A}_3 \\ \tilde{B}_1 \tilde{B}_2 \tilde{B}_3 \\ \tilde{C}_1 \tilde{C}_2 \tilde{C}_3 \end{bmatrix} \begin{bmatrix} \Delta x_I \\ \Delta z \\ \Delta v \end{bmatrix} + \begin{bmatrix} E \\ 0 \\ 0 \end{bmatrix} \Delta u \quad (6.52)$$

Now \tilde{C}_3 is the load flow Jacobian J_{LF} and $\begin{bmatrix} \tilde{B}_2 & \tilde{B}_3 \\ \tilde{C}_2 & \tilde{C}_3 \end{bmatrix} = J_{AE}$. The system matrix, A is obtained as

$$\Delta \dot{x}_t = A_{yy} \Delta x_t + E \Delta u$$

Using drastic assumptions about voltage control and load characteristics that the steady-state stability associated with the system matrix, A_{yy} can be determined by examining the load flow Jacobian, J_{LF} .

6.11.7 Voltage Stability Assessment

The algorithm for voltage collapse/voltage stability assessment includes static and dynamic assessment. The algorithm for dynamic stability assessment is shown in Fig. 6.7.

6.11.8 VSTAB—Voltage Stability Assessment (EPRI)

A more promising method with the trade name VSTAB, uses power flow and modal analysis techniques. It provides assessment of the proximity to voltage instability and determines the mechanism of voltage instability. In this method, the proximity to voltage instability is evaluated by conducting a series of power flow solutions with load increase until load flow divergence is encountered. When load flow divergence is encountered, the step size for load increase is reduced and the power flows are continued. The voltage stability limit is considered to have been reached when the step size reaches the cutoff value specified by the user. The load level at this point is the maximum loadability. This procedure is carried out simultaneously for the intact system as well as for contingencies. Load increase can be carried out with or without generation scaling. The slack bus generation is not scaled. Loading can be by area or by zone.

The mechanism of voltage instability is studied in VSTAB by using modal analysis. Modal analysis employing $V-Q$ sensitivities can identify areas that have potential problems and provide information regarding the mechanism of voltage collapse. The method is briefly discussed as follows.

The usual power flow equations can be expressed in the linearized form,

$$\begin{bmatrix} \Delta P \\ \Delta Q \end{bmatrix} = \begin{bmatrix} J_{p\theta} & J_{pv} \\ J_{q\theta} & J_{qv} \end{bmatrix} \begin{bmatrix} \Delta \theta \\ \Delta V \end{bmatrix} \quad (6.53)$$

where

ΔP = incremental change in bus real power

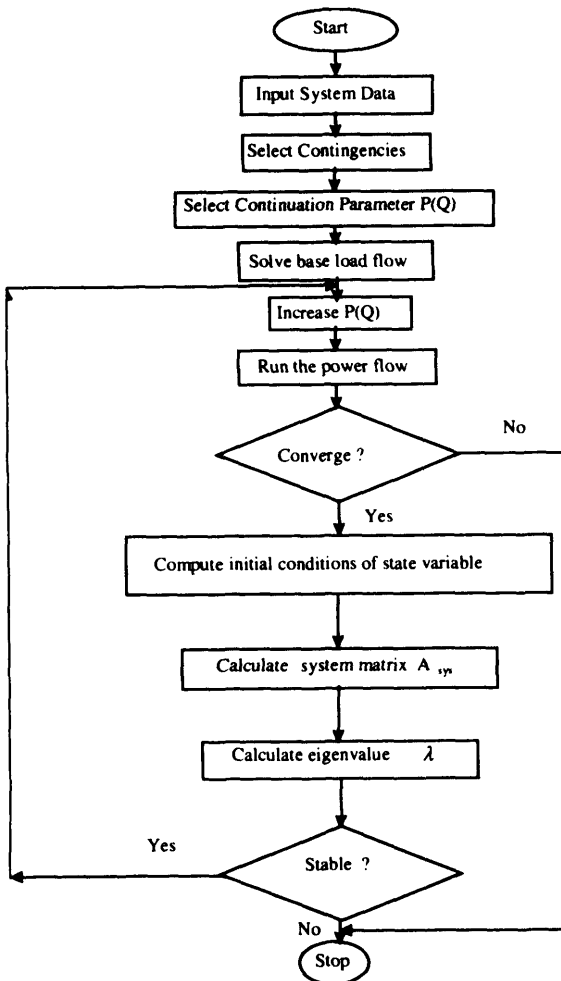


Figure 6.7 Summary of the dynamic voltage stability assessment technique.

ΔQ = incremental change in bus reactive power injection

$\Delta\theta$ = incremental change in bus voltage angle

ΔV = incremental change in bus voltage magnitude

The system dynamic behavior can be expressed by the first order differential equation,

$$X = f(X, V) \quad (6.54)$$

where

X = state vector of the system

V = bus voltage vector

For the steady-state condition $X = 0$, using the enhanced device models used in Eq. (6.54). Equation (6.53) can be rewritten as:

$$\begin{bmatrix} \Delta P_d \\ \Delta Q_d \end{bmatrix} = \begin{bmatrix} A_{11} & A_{12} \\ A_{21} & A_{22} \end{bmatrix} \begin{bmatrix} \Delta \theta_d \\ \Delta V_d \end{bmatrix} \quad (6.55)$$

where

ΔP_d = incremental change in device real power output

ΔQ_d = incremental change in device reactive power output

ΔV_d = incremental change in device voltage magnitude

$\Delta \theta_d$ = incremental change in device voltage angle

The terms A_{11} , A_{12} , A_{21} , and A_{22} represent a modified form of $J_{P\theta}$, J_{PV} , $J_{Q\theta}$, J_{Q-V} in the terms associated with each device. We can study the Q -V sensitivity while keeping P constant. For this analysis we can substitute $\Delta P = 0$ in Eq. (6.53) to give us upon simplification,

$$\frac{\Delta V}{\Delta \theta} = J_R^{-1} \quad (6.56)$$

where

$$J_R = J_{Q-V} - J_{Q\theta} J_{P\theta}^{-1} J_{PV} \quad (6.57)$$

By analyzing the eigenvalues and eigenvectors of the reduced Jacobian J_R , we arrive at

$$v = \Lambda^{-1} \times q \quad (6.58)$$

or

$$v_i = \frac{1}{\lambda_i} q_i \quad (6.59)$$

where

$$\Lambda^{-1} = \begin{bmatrix} \cdot & & \\ \cdot & & \\ & 1/\lambda_1 & \\ & & \cdot \end{bmatrix}$$

λ is the i^{th} modal voltage.

$$v = \eta \Delta V$$

$$q = \eta \Delta Q$$

Using modal analysis, these relative bus participation and branch participation factors can be computed for the i^{th} mode. The complete procedure for static voltage stability assessment via modal analysis is outlined in Fig. 6.8.

6.11.9 Preventive Control of Voltage Stability

There are two levels of voltage stability enhancement, the first level with device based control, the second level is in the form of operation-based control. The

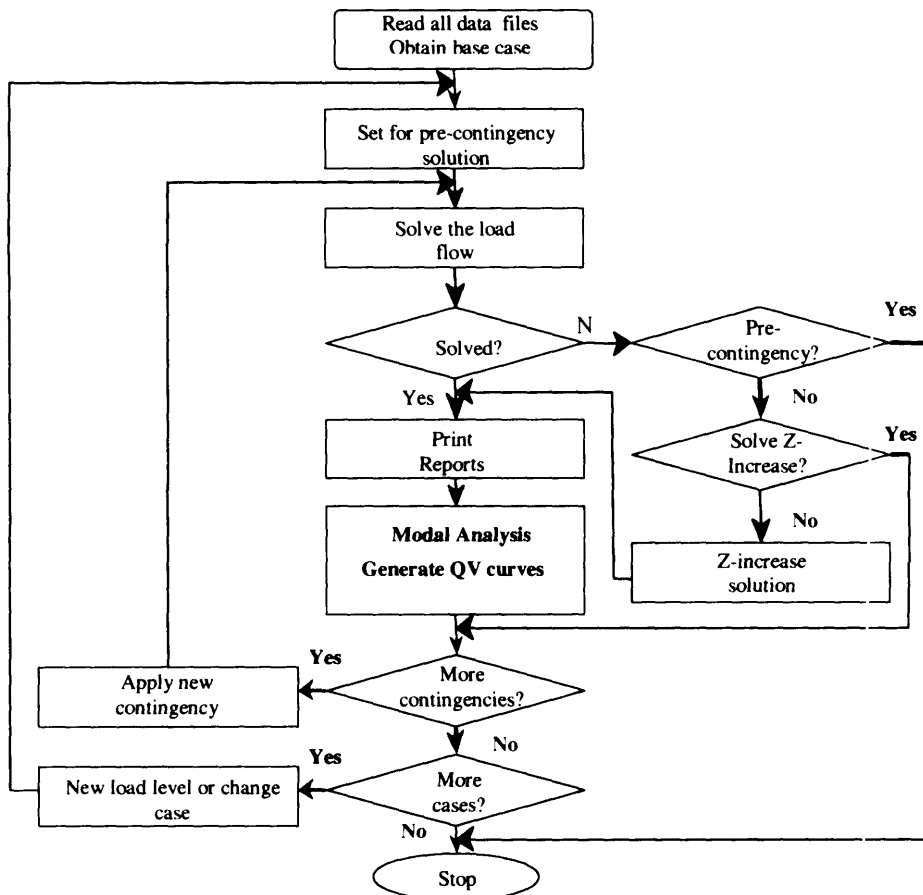


Figure 6.8 The VSTAB algorithm (© EPRI).

voltage stability is improved by optimal system operation conditions. The static analysis method is used for the determination of preventive control scheme. System operation conditions are determined by $F(\theta, V, \lambda) = 0$. The design of a voltage stability preventive control scheme includes the steps outlined in Fig. 6.9.

CONCLUSION

Power system voltage stability involves generation, transmission and distribution. So to maintain the voltage stability is crucial for the normal operation

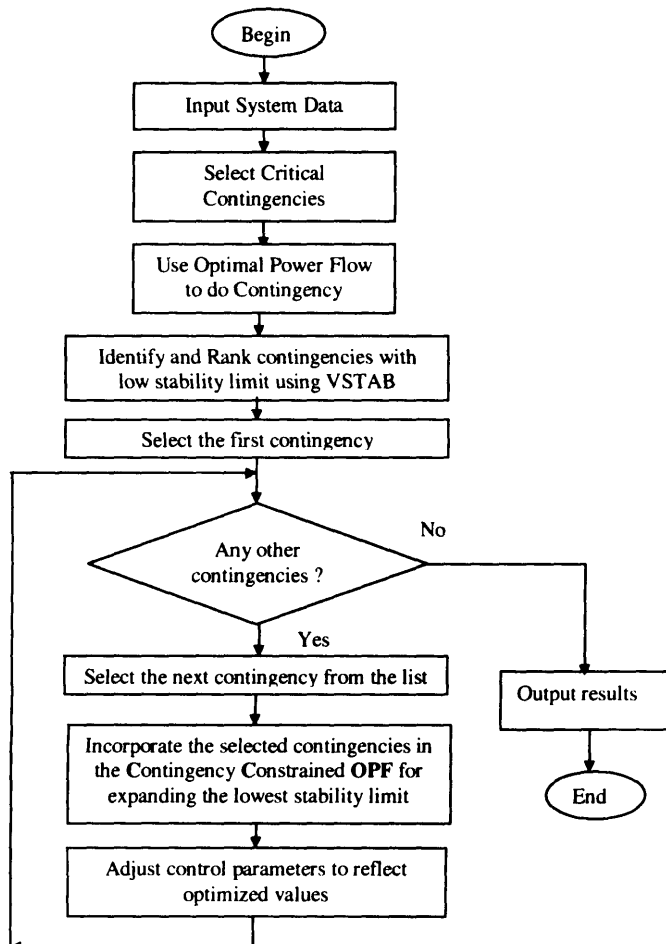


Figure 6.9 Voltage stability preventive control scheme.

of a power system. In adequate reactive power support from generators and transmission lines lead to voltage instability or voltage collapse which have resulted in several major system failures (blackouts) such as the massive Tokyo blackout in July 1987.

In order to prevent the stability limit being reached or exceeded during a given contingency, remedial actions need to be recommended. It is well known that in all cases, voltage instability is caused by inadequate transmission capacity at a given operating condition due to a contingency, which the system cannot withstand. Based on contingencies that occur, the distribution of plant generators, transmission flows and load to meet given stability criteria is usually done by using effective/economical control actions.

Future work in the determination of adequate remedial measures for stability enhancement have been proposed in past publications, where the corrective control action is handled as an optimization problem. The two-stage formulation to achieve the desired stability enhancement utilizes the concepts of Chapter 5 and this chapter. The first stage handles voltage stability enhancement while the second-stage optimization scheme deals with angle stability enhancement. The process will lead to a unified index. Hence, when carrying out stability enhancement based on a selected list of contingencies, only enhancement of the appropriate problem (either voltage or angle) needs to be carried out, thus saving labor and computational time. Future work in unifying the indices while incorporating the various available controls is still a challenge. The reader is invited to research further literature in selected references located at the end of the book. Also, the annotated glossary of terms supports the chapter.

MODAL ANALYSIS: WORKED EXAMPLE

Consider the 500 kV, 322 km (200 miles) lines transmission system shown in Fig. 10(a) below supplying power to a radial load from a ‘strong’ power system represented by an infinite bus. The line parameters, as shown in Fig. 10(b), are expressed in their respective per unit values on a common system base of 100 MVA and 500 kV.

1.1 Compute the full admittance matrix of the two-bus system and write the power flow equations from the sending end to the receiving end in the form:

$$P = f(\theta, V)$$

$$Q = g(\theta, V)$$

1.2 Hence or otherwise, write down the expressions for the four (4) sub-matrices of the Jacobian in the linearized load flow equations as defined by:

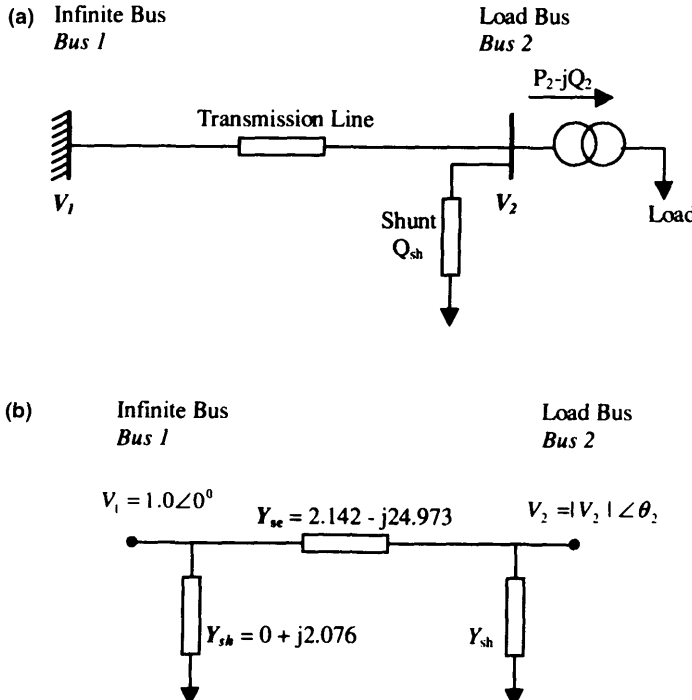


Figure 6.10 The 550 kV, 370 km (230 miles) line transmission system supplying a radial load: (a) schematic diagram of the transmission system and (b) the equivalent WYE circuit representation of the transmission line.

$$\begin{bmatrix} \Delta P \\ \Delta Q \end{bmatrix} = \begin{bmatrix} J_{P\theta} & J_{PV} \\ J_{Q\theta} & J_{QV} \end{bmatrix} \begin{bmatrix} \Delta \theta \\ \Delta |V| \end{bmatrix}$$

1.3 When $P_2 = 1500$ MW, calculate the eigenvalues of the reduced Q - V Jacobian matrix and the V - Q sensitivities with the following different reactive power injections for each of the corresponding two voltages on the Q - V curve.

- a. $Q_2 = 500$ MVAR.
- b. $Q_2 = 400$ MVAR.
- c. Values of Q_2 close to the bottom of the V - Q curve.

1.4 Determine the voltage stability of the system by computing the eigenvalues of the reduced V - Q Jacobian matrix for the following cases:

- a. $P = 1500 \text{ MW}, Q_i = 450 \text{ MVAR.}$
- b. $P = 1900 \text{ MW}, Q_i = 950 \text{ MVAR.}$

(Assume that the reactive power Q_i is supplied by a shunt capacitor).

Solution

From the figure, the admittance matrix of the 2-bus system is

$$Y = \begin{bmatrix} 2.142 - j22.897 & -2.142 + j24.973 \\ -2.142 + j24.973 & 2.142 - j22.897 \end{bmatrix}$$

The expression for P and Q at any bus k are given by:

$$\begin{aligned} P_k &= V_k \sum_{m=1}^n (G_{km} V_m \cos\theta_{km} + B_{km} V_m \sin\theta_{km}) \\ Q_k &= V_k \sum_{m=1}^n (G_{km} V_m \sin\theta_{km} - B_{km} V_m \cos\theta_{km}) \end{aligned}$$

where

$$\theta_{km} = \theta_k - \theta_m$$

For the 2-bus system we have:

$$P_1 = V_1 [(2.142V_1 \cos\theta_{11} - 22.897V_1 \sin\theta_{11}) + (-2.142V_2 \cos\theta_{12} + 24.973V_2 \sin\theta_{12})]$$

$$P_2 = V_2 [(-2.142V_1 \cos\theta_{21} + 24.973V_1 \sin\theta_{21}) + (2.142V_2 \cos\theta_{22} - 22.897V_2 \sin\theta_{22})]$$

$$Q_1 = V_1 [(2.142V_1 \sin\theta_{11} + 22.897V_1 \cos\theta_{11}) + (-2.142V_2 \sin\theta_{12} - 24.973V_2 \cos\theta_{12})]$$

$$Q_2 = V_2 [(-2.142V_1 \sin\theta_{21} - 24.973V_1 \cos\theta_{21}) + (2.142V_2 \sin\theta_{22} + 22.897V_2 \cos\theta_{22})]$$

where

$$\theta_{11} = \theta_{22} = 0.00 \text{ rads, and } \theta_{12} = -\theta_{21}$$

Hence, we are interested in only P_2 and Q_2 with $V_1 = 0 \text{ p.u.}$

$$P_2 = -2.142V_2 \cos\theta + 24.973V_2 \sin\theta + 2.142V_2^2$$

$$Q_2 = -2.142V_2 \sin\theta - 24.973V_2 \cos\theta + 22.897V_2^2$$

Hence the expressions for the Jacobian terms are give by:

$$J_{P\theta} = \frac{\partial P_2}{\partial \theta} = 2.142V_2 \sin\theta + 24.973V_2 \cos\theta$$

$$J_{PV} = \frac{\partial P_2}{\partial V_2} = -2.142\cos\theta + 24.973\sin\theta + 4.284V_2$$

$$J_{Q\theta} = \frac{\partial Q_2}{\partial \theta} = -2.142V_2\cos\theta + 24.973V_2\sin\theta$$

$$J_{QV} = \frac{\partial Q_2}{\partial V_2} = -2.142\sin\theta - 24.973\cos\theta + 45.794V_2$$

(a) The linearized power flow equations are

$$\begin{aligned}\Delta P_2 &= J_{P\theta}\Delta\theta + J_{PV}\Delta V_2 \\ \Delta Q_2 &= J_{Q\theta}\Delta\theta + J_{QV}\Delta V_2\end{aligned}$$

with

$$\Delta P_2 = 0.$$

$$\Delta Q_2 = (J_{QV}J_{Q\theta}J_{P\theta}^{-1}J_{PV})\Delta V_2 \quad \text{or} \quad \Delta Q_2 = J_R\Delta V_2$$

where

$$J_R = J_{QV} - J_{Q\theta}J_{P\theta}^{-1}J_{PV}$$

The expression for J_{QV} , $J_{Q\theta}$, $J_{P\theta}$, and J_{PV} were given before. For this simple system, J_R is a 1×1 matrix. The eigenvalue lambda of the matrix is the same as the matrix itself. The Q - V sensitivity is equal to the inverse of the eigenvalue.

For each of the Q 's, there are two solutions for the receiving end voltage. Table 6.2 summarizes the V , θ , λ , and dV/dQ with $P = 1500$ MW and $Q = 500$, 400, 306, and 305.9 MVar. For each case the eigenvalue and V - Q sensitivity are both negative at the low voltage solutions, and are both positive at high voltage solutions. With $Q = 305.9$ MVar close to the bottom of the Q - V curve dV/dQ is large and λ is very small.

Table 6.2 Results for Modal Analysis Worked Example

| Q (MVar) | High Voltage Solution | | | | Low Voltage Solution | | | |
|---------------|-----------------------|----------------|-----------|-----------------|----------------------|----------------|-----------|-----------------|
| | V (p.u.) | θ (deg) | λ | $\frac{dV}{dQ}$ | V (p.u.) | θ (deg) | λ | $\frac{dV}{dQ}$ |
| 500.0 | 1.024 | -37.3 | 17.03 | 0.059 | 0.671 | -66.7 | -39.87 | -0.025 |
| 400.0 | 0.956 | -40.1 | 12.41 | 0.081 | 0.706 | -60.3 | -20.96 | -0.048 |
| 306.0 | 0.820 | -48.2 | 0.52 | 1.923 | 0.812 | -48.8 | -0.950 | -1.055 |
| 305.5 | 0.184 | -48.7 | 0.02 | 50.10 | 0.815 | -48.6 | -0.700 | -1.434 |

(b) With the shunt capacitor connected at the receiving end of the line, the self admittance is:

$$Y_{22} = 2.142 - j(22.897 - B_c)$$

- (i) with $P = 1500$ MW and A 450 MVar reactive shunt capacitor, $V_2 = 0.981$, $\theta = -39.1$ degrees. Since $B_c = 4.5$ p.u., then $Y_{22} = 2.142 - j(22.897 - 4.5) = 2.142 - j18.397$. With this new value of Y_{22} , the reduced Q - V Jacobian matrix is $J_R = 5.348$, and J_R is positive indicating that the system is voltage stable.
- (ii) with $P = 1900$ MW and a 950 MVar reactive shunt capacitor, $V_2 = 0.995$, $\theta = -52.97$ degrees. Since $B_c = 9.5$ p.u., then $Y_{22} = 2.142 - j(22.897 - 9.5) = 2.142 - j1.397$. With this new value of Y_{22} , the reduced Q - V Jacobian matrix is $J_R = -13.683$, and J_R is negative indicating that the system is voltage unstable.

7

Technology of Intelligent Systems

INTRODUCTION

The previous chapters on voltage and angle stability assessment represent rich techniques for the analytical solutions of large interconnected systems. Several important and notable successes have been achieved in solving general simulation based calculations of stability for off-line studies. There remains a large amount of problems in power systems that are largely solved by human experts either in conjunction with results from numerical analysis and decision support systems. The following features frequently characterize these problems:

1. Inadequate model of the real world.
2. Complexity and size of the problems which prohibit timely computation.
3. Solution method employed by the human is not capable of being expressed in an algorithm or mathematical form. It usually involves many rules of thumb.
4. The operator decision making is based on fuzzy linguistics description.
5. Analysis of security such as voltage or angle is based on human judgement and experience.

These drawbacks have motivated the power system community to seek alternative solutions techniques through the use of artificial intelligence systems and variants of its techniques. In this chapter, we present a brief summary of

such techniques including expert systems decision trees, artificial neural networks, fuzzy logic systems, and their hybrids. These techniques have been employed for solving various power system operation and planning problems and especially for the assessment of transient and voltage stability prediction, instability prevention, and contingency ranking, etc.

Some commonality exists among intelligent systems approaches. The system requirements for developing or assessing intelligent systems approaches are as follows:

1. Ability to identify system states.
2. Selectivity of controls.
3. Learning ability to update knowledge.
4. Coordination of tasks.
5. Flexibility.
6. Ability to handle uncertainty.

An expert system (ES), also referred to as Knowledge Based System, embodies human expertise in a narrow field or domain in a machine implementation form. It utilizes elements of human knowledge to provide decision support at a level comparable to the human expert and is capable of justifying its reasoning. It separates the inference mechanism from the knowledge and uses one or more knowledge structures such as production rules frames, semantic nets, predicate calculus, and objects to represent knowledge.

The function of the expert system consists of its ability to collect and store an expert's ability to solve a problem so that a nonexpert can use it. The functional components of an expert system are represented and defined here.

1. Knowledge Base: Contains all relevant information about the system under study.
2. User interface: Input/output or so called man-machine interface gives the necessary information and decision rules to the user.
3. Inference Engine: Analyzes the system using if then rules based on goal/data oriented strategy called forward/backward chaining.

Other modules such as control mechanism and modification loop are usually excluded from expert systems to achieve robustness.

In the knowledge base, for example in a power system, the database gives the operating characteristics of the system through state estimation. The results from off-line studies are used as sets of rules in the knowledge base.

Three special features distinguish Expert Systems from traditional power system analysis:

1. The expert system allows easy flexibility of manipulation of domain specific knowledge without having to watch for the impact of changes on the way we are reasoning it.

2. The expert system is concerned with manipulating symbolic information rather than the numerical information directly.
3. The expert system addresses problems where knowledge may be deterministic and more imprecise and allows for certainty in reasoning.

7.1 FUZZY LOGIC AND DECISION TREES

Fuzzy set theory was developed by Prof. Zadeh in 1965 as a mathematical means of describing vagueness in linguistics. A fuzzy set is a generalization of ordinary sets that allows assigning a degree of membership for each element to range from $[0, 1]$ interval.

A fuzzy set differs from a crisp set which has a unique binary membership fraction in that the fuzzy set has an infinite number of membership functions that may represent it. Fuzzy reasoning offers a way to understand system behavior through interpolation approximately between input and output situations. Fuzzy logic is based simply on the way the brain deals with inexact information. A fuzzy system combines and applies sets with fuzzy rules to problems with overall complex nonlinear behavior. As a structured normal estimator, it expresses fuzzy if the rules of some expert knowledge.

Fuzzy set theory offers a new method for modeling the inexactness and uncertainty concerning decision-making. Fuzzy logic improves the potential for modeling human reasoning and for presenting and utilizing linguistic descriptions in a computerized inferencing environment.

The two methods of developing fuzzy models are based on:

1. Laws of cause and effect which use rules of relations described by reasoning in variable sets theory.
2. Laws of transition, which use ordinary equations to express, cause and effect relationship.

Fuzzy set theory uses the concept of possibility defined as a number between one (completely possible) and zero (totally impossible) instead of probability which measures the appropriate uncertainty of available statistical information. Where probability fails without statistical data, fuzzy set theory does a better job than other intelligent systems such as neural nets and expert systems.

7.2 ARTIFICIAL NEURAL NETWORKS

While fuzzy, expert system, and decision tree techniques are rule-based, there are certain AI techniques that use Artificial Neural Network (ANN) pattern recognition clustering strategies. An ANN is considered a machine that is designed to model the work the brain performs in dealing with a particular task of inter-

est. The neural network is usually implemented using electronic components or simulated in a software computation. A neural network performs computation through learning. It is a massively parallel distributed computation that is trained with the appropriate data and reproduces trained strategies and adapts according to changing situations.

Pattern recognition techniques on the other hand, act as classifiers depending on the pattern of interest. Clustering is also one of the unsigned ANN learning techniques. Instead of selecting a training set, we construct a set of unlabeled trial factors. These techniques use Euclidean distance to estimate the membership in a pattern group or to classify according to some prevailing rates.

Of the three intelligent systems approaches discussed here neural networks are best suited to problems where voluminous data and a complex nonlinear relationship exists between the input and output patterns, such as instability assessment and load forecasting problems. Artificial neural network schemes share the ability to identify the model structure of unknown systems with input/output data and efficiently solve combinational problems, which define their relationships. An overview of artificial neural networks and some significant neural learning algorithms is provided in this chapter.

The evaluation of intelligent systems has shown that neural-based approaches are most beneficial for power system stability assessment, due to their ability to generalize and "learn" from historical information. A basic overview of neural computing practices and methods is provided in the next section. In comparison to neural nets, expert system approaches are rather system specific and rigid. Fuzzy set theory is relatively new as a power system analysis tool. Further validation of membership functions and the use of network operation support using real fault situations warrants further investigation of fuzzy logic as a power system analysis tool. A review of the salient points defining the three intelligent systems discussed here is provided in Table 7.1.

ANNs are parallel distributed processing systems composed of nonlinear processing elements that perform in a manner similar to the most elementary functions of biological neurons. For instance, ANNs possess the ability to learn from experience, generalize from previous examples to new ones, and to abstract pertinent information from examples containing irrelevant or incomplete data. ANNs are not suited to simple mathematical tasks, such as computing voltage drops along a feeder. However, ANNs are beneficial in solving a great number of pattern recognition problems, that are either computationally burdensome or impossible for conventional iterative programs to solve.

Neural networks offer the following advantages:

ANNs have the ability to learn and construct a complex nonlinear mapping through a set of input/output examples. The network architecture allows for easy training without a need for a structured model.

Table 7.1 Features of Intelligent Systems Approaches

| Intelligent systems | System components | Functionality | Application areas |
|----------------------------|---|--|--|
| Artificial neural networks | Neurons Weighted connections between neurons Learning algorithm | Learning a mapping (relationship) from examples Self-organization into classes or clusters Associative memory Optimization General | Classification Estimation |
| Expert systems | Knowledge base User interface Inference engine | Learning from inference Data structure Linkage to external applications Distributed knowledge Specific | Estimation Decision making |
| Fuzzy logic | Crisis sets Membership functions Fuzzy sets | Handling of human subjectivity Human Knowledge in "thinking" machine Handling of human ambiguity in communication | Decision making in cases of inexact or ambiguous data sets |

Input variables can be easily added or deleted. Correlated or uncorrelated data can be utilized.

Neural networks have a superior noise rejection capability that can effectively deal with uncertainties of the actual process.

Neural networks execute very quickly. Most of the calculation overheads occur during the initial off-lines training.

Neural networks consist of a large number of parallel processing units which can be implemented using general or special purpose hardware.

Hence neural networks can relieve the burden of computation from the Energy Management System computers.

Before neural networks can gain the necessary recognition as useful problem solving tools in the power industry, certain fundamental issues have to be addressed. Some are associated with neural network fundamentals and others are problem dependent and are listed below:

Determining the proper consistency of the training and testing data sets including, the number of patterns, input dimensions, and statistical properties, in order to provide adequate generalization and knowledge retention.

Neural network decomposition in order to find the optimal stage or location for the use of neural networks. This is an important consideration in dealing with large-scale systems.

The use of feature selection and clustering techniques for data preprocessing. This can help achieve reduction in both dimensional and combinatorial complexity.

Neural networks must not be allowed to memorize the training data nor become saturated.

ANNs have been developed in numerous configurations. Despite their diversity, some commonality exists among the various network paradigms. In the following sections some fundamentals of network computing are presented.

7.2.1 Fundamentals of ANN

We review a specific neural network architecture, its activation function and elements of training. This is followed by a discussion of some of the factors of learning algorithms including back-propagation, counter propagation and clustering learning algorithms.

Architecture

The artificial neuron, also known as the processing element, is modeled to reflect the configuration of the biological neuron (Fig. 7.1). A set of inputs are applied, each representing the output of another neuron. Each input to a neuron is multiplied by a weight, corresponding to the input's connection strength or importance to that neuron.

The relationship described above is illustrated in Fig. 7.2. Here, a set of inputs, are applied to the neuron. The inputs, collectively defined as the vector \mathbf{X}_j , are multiplied by their associated weights (\mathbf{W}_{ij}) before being applied to the summation block, Σ . The inputs \mathbf{X}_j , now multiplied by the weights, collectively defined as the vector \mathbf{W}_i , are summed at the summation block, Σ to produce the activation level A_i of the j^{th} neuron in the next layer, subject to a threshold value, θ . This relationship can be stated in vector notation as follows:

$$A_i = \sum \mathbf{X}_j \mathbf{W}_{ij} \quad (7.1)$$

Activation Functions

The activation level, A_i , is further processed by an activation function, F , to produce the output signal of the j^{th} neuron, Out_i . The activation function may be a simple linear function, such as a gain, K :

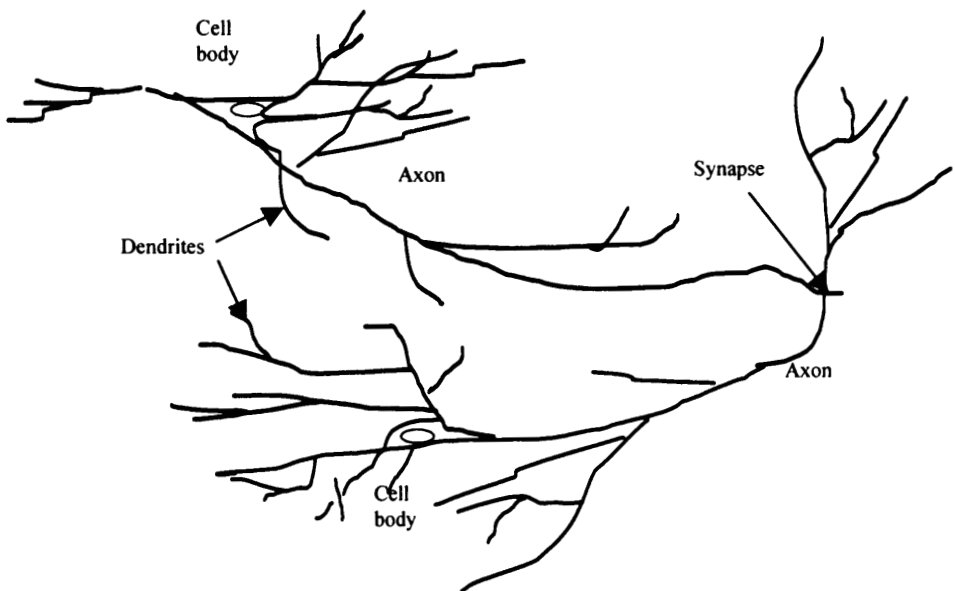


Figure 7.1 Components of biological neurons.

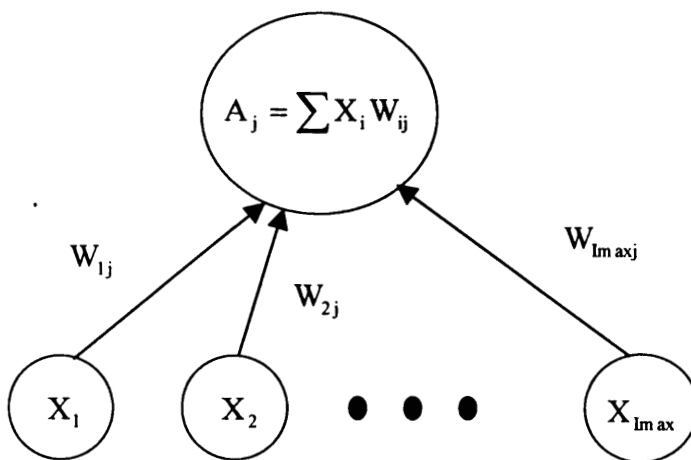


Figure 7.2 Components of an artificial neuron.

$$\text{Out}_j = KA_j \quad (7.2)$$

Where, K is a constant. Or it can be a threshold function, such as:

$$\begin{aligned} \text{Out} &= 0 \text{ if } A_j < \theta \\ &= 1 \text{ if } A_j \geq \theta \end{aligned} \quad (7.3)$$

Where θ is a constant threshold value. Alternately, F may be a function that more accurately simulates the nonlinear characteristics of a biological neuron, and permits more general network functions. One such function is the sigmoid activation function, which is the activation of choice for the majority of contemporary neural systems.

$$\text{Out}_j = \frac{1}{1 + e^{-A_j + \theta}} \quad (7.4)$$

The sigmoid function is known as a “squashing function,” since it compresses the range of A_j , so that the value of Out_j never exceeds some low boundaries. The boundaries are defined as 0 and 1 in the case of the sigmoid function. For a large value of A_j , the denominator in Equation 7.4 would approach 1, and thus produce an output close to 1. Likewise, for a value of A_j equal to $-\infty$, the denominator in Equation 7.4 would approach $+\infty$, and thus produce an output approaching zero.

In order to provide a clearer understanding of the role of the activation function in neural computing, we think of the activation function as defining a nonlinear gain in an analog electronic system. The gain is calculated by computing the ratio of the change in Out_j to a small change in A_j . Thus, the gain is the slope of the curve at a specific activation level. The gain may vary from a low value at large negative activation levels, to a high value at the zero point, and back to a low value at large positive levels. The central high gain region of the sigmoidal activation function solves the problem of processing small signals, while its regions of lower gains at positive and negative extremes are appropriate for large activation levels. Thus a neuron can perform adequately over a wide range of input levels.

Training the Neural Network

A neural network is trained so that a given stimulus (set of inputs) will produce a desired response (output set). Each input or output set is referred to as a vector. Training is the process by which input vectors are continuously applied to a network, while adjusting the unknown network components, until each input vector produces the desired output vector.

Training algorithms can be classified as supervised or unsupervised. Supervised training requires pairing each input vector with a desired output, or target vector, together these are called a training pair. Usually, neural networks are trained with a large number of these training pairs. A rule-of-thumb is to have at least 100 such training pairs for each input neuron, in order to represent a wide variety of system conditions. In the supervised training process an input vector is applied, the actual output of the network is determined and compared to the target value. The difference between the actual and target values is the error that is then fed back through the network to update the interconnection weights, and thus, minimize the error. The entire process is repeated until the error for the entire training set has met an acceptable tolerance level.

For unsupervised training, the training set consists solely of input vectors. These types of training processes group similar input sets into classes according to the statistical properties of the training set. There is no way to predetermine which output classes will be produced by a given input vector. Therefore, unsupervised training generally requires some postprocessing of data to transform the output classes into some meaningful format. Usually, all that is required is a simple identification of the input-output relationships defined by the network. Some significant training algorithms are presented and discussed in the next section.

7.2.2 Back Propagation Learning Algorithm

Of the existing neural network paradigms, the back propagation learning algorithm is an interesting approach to the solution of classification problems. The back propagation learning algorithm is a technique for optimizing the interconnection weights in an ANN by minimizing the global error between the desired and actual output of all the cases evaluated during the training session.

The procedure begins with the presentation of the input stimuli and the desired output of all the training cases and the initialization of all the interconnection weights to random values. The input stimuli are fed forward through the network to compute the actual output values. The error between the desired and actual outputs are computed and propagated back through the network to adjust the weights. This process is repeated until the global error satisfies a prespecified tolerance value.

7.2.3 Counter Propagation Learning Algorithm

The counter propagation network is not as robust as the back propagating techniques, but it can provide quick solutions for applications that cannot tolerate long training sessions. The network functions as a look-up table capable of generalization. The training process associates input vectors with their corre-

sponding output vectors, that may be either, in binary or continuous form. The generalization capability of the counter propagation network allows it to extract a desired output response even when presented with partially incomplete or incorrect input data. This makes the counter propagation network useful for pattern recognition, pattern completion, and signal enhancement applications. In its simplest form the counter propagation network is a combination of two well-known training algorithms, the Kohonen, and the Grossberg Outstar.

The Kohonen layer functions in a winner take all fashion. That is, for a given input vector only one output neuron in the Kohonen layer is activated (outputs a logical one), all of remaining outputs of the Kohonen layer are held at zero. The net output of each Kohonen neuron is the weighted sum of the inputs, therefore, the net output with the highest value is the "winner."

The Grossberg layer functions in a similar manner with its net output equal to the sum of the weighted values from the Kohonen layer. Since there is only one nonzero term from the Kohonen layer the calculation is simple. In fact, the only action of each neuron in the Grossberg layer is to output the value of the weight that connects it to the single nonzero Kohonen neuron.

The limitations of the counter propagation network make it inferior to back propagating techniques for most mapping network applications. However, the counter propagation network has been found to be useful for rapid prototyping of systems that can eventually yield to the greater accuracy and robustness of back propagating algorithms.

7.2.4 Clustering Learning Algorithm

A clustering-based ANN was implemented for applications to power system problems. The clustering ANN is similar in nature to the ART1 ANN developed by Carpenter and Grossberg and Kohonen's self-organizing map. The algorithm includes a feature extraction scheme for statistical derivation of a more robust set of feature variables than those that could be provided through purely heuristic methods.

The clustering ANN utilizes both the supervised and unsupervised training methodologies. The supervised module was used to synthesize the mapping between the input stimuli and the desired output clusters formed by the unsupervised module. Continuous handshaking between the two modules takes place until a prespecified tolerance is satisfied.

7.3 ROBUST ARTIFICIAL NEURAL NETWORK

Back propagation ANNs are well suited to enhancement of the conventional Transient Energy Function (TEF) procedure for many reasons. First, they can

be trained by the results of off-line TEF studies. Second, they can be quickly called on-line to classify a system subject to disturbance as secure or potentially insecure. Third, they can generalize from cases that were used in training to classify cases that were not previously evaluated. Fourth, they are robust enough to handle a variety of systems. And finally, the multi-layer perceptron networks can be used to overcome nonlinearly separable problems.

The development of the robust ANN involves the selection of an appropriate network architecture to determine how the neurons are connected, and the selection of an appropriate learning algorithm to determine how neurons process their information and how the connection strengths between layers were optimized, and the application of training data acquired from off-line.

7.3.1 Network Configuration

The basic neuron model for the back propagation algorithm contains inputs, x_i , that are adjusted by weights, w_{ij} , and summed. After which, a bias or threshold value, θ_j , is added, and the total is passed through the activation function $F(x)$ as an output. Mathematically this process can be represented by:

$$F(x, \theta) = F\left(\sum_{i=1}^{I_{\max}} x_i w_{ij} + \theta_j\right) \quad (7.5)$$

Where W_{ij} is the weight applied between i^{th} neuron of input layer and j^{th} neuron of hidden layer and I_{\max} represents the total number of input neurons.

Before starting the training process, all of the weight must be initialized to small random numbers ($-0.5 < w_{ij} < +0.5$). This ensures that the network is not saturated by large values of the weights. The random nature of the initial weights also allows the network to learn unequal final values of the weights if that is what is required for optimal performance.

7.3.2 Overview of Training

Training the robust artificial neural network requires the following step-by-step procedure:

1. Apply all the input vectors from the training set to the network.
2. Calculate the output of the network for each input vector.
3. Compute the error between the actual network output and the desired output for each input vector.
4. Calculate the global error as the averaged sum of the squared errors for the entire training set.

5. Adjust the weights and thresholds in a manner that minimizes the error.
6. Repeat steps 1–5 until the global error is acceptably low.

Upon completion of the training procedure the network is used for recognition and the weights are not changed. It may be seen that steps 1 and 2 constitute a “forward pass” through the network, in that the signal propagates from the network input to its output. Steps 3–5 are a “reverse pass,” where the global error propagates backwards through the network and is used to adjust the weights and thresholds.

The first two steps in the training procedure can be expressed as follows: an input vector, \mathbf{X} , is applied and an output vector, Out, is produced. The input-target vector pair, \mathbf{X} and \mathbf{T} , comes from the training set. The output vector, Out, is produced as a result of the application of \mathbf{X} to the network. Calculations in multi-layer neural nets are performed on a layer by layer basis, beginning with the hidden layer closest to the input layer. The weighted values of the input vector are summed in the form:

$$A_j = \sum_{i=1}^{I_{\max}} \mathbf{x}_i \mathbf{w}_{hi} \quad (7.6)$$

Where

A_j = active level of neuron j in the hidden layer

\mathbf{x}_i = i^{th} input from the input vector \mathbf{X}

\mathbf{w}_{hi} = interconnected weight applied between i^{th} neuron of input layer and j^{th} neuron of hidden layer.

The nonlinear sigmoidal activation function is applied to the activation level, A , in Eq. (7.7), to drive the value of hidden neurons toward one of the two states (0 or 1; stable or unstable).

$$H_j = \frac{1}{1 + e^{-(A_j + \theta_j)}} \quad (7.7)$$

Where: H_j = output of neuron j in the hidden layer

θ_j = dynamic threshold value of neuron j in the hidden layer

The addition of the threshold value, θ , increases training efficiency. The same process is applied for networks with additional hidden layers with the output of the preceding layer serving as inputs to the next layer in the network.

In the output layer the output nodes are defined as the weighted sum of the outputs from the preceding layer. No activation function is applied at the output node. The output neurons are computed as follows:

$$\text{Out}_k = \sum_{j=1}^{J_{\max}} H_j w_{Hjk} \quad (7.8)$$

Where: Out_k = output of k^{th} neuron in the output layer

W_{Hjk} = interconnected weight applied between j^{th} neuron in the hidden layer and k^{th} neuron of the output layer.

Therefore, the calculation of the outputs of the final layer requires the application of Eq. (7.6) to each layer, from the network's input to its output. In the reverse pass, defined by steps 3–5, two tasks must be accomplished. First, the weight of the output layer must be adjusted. And second, the weight and thresholds of the hidden layers must be adjusted.

In order to adjust the weights in the output layer an update factor for each weight must be computed. First, the global error, E , for the entire training set is computed using Eq. (7.9) as the average sum of the squared differences between the actual network outputs $\{\text{Out}_k\}$ and the target, or desired values, $\{T_k\}$.

$$E = \frac{1}{2k} \sum_{k=1}^K (T_k - \text{Out}_k)^2 \quad (7.9)$$

The error signal is multiplied by the derivative of the sigmoid function $[\text{Out}_k(1 - \text{Out}_k)]$ for the k^{th} neuron of the output layer, thereby producing the δ value for the neuron.

$$\delta_k = \text{Out}_k(1 - \text{Out}_k)(T_k - \text{Out}_k) \quad (7.10)$$

the δ is then multiplied by the output value from the previous layer that corresponds to the weight being adjusted.

$$\Delta w_{Hjk} = \delta_k H_j \quad (7.11)$$

where: Δw_{Hjk} = update factor for interconnection weight between the j^{th} neuron in the hidden layer and the k^{th} neuron in the output layer.

An identical process is performed for each weight proceeding from a neuron in the hidden layer to a neuron in the output layer.

Adjustment of the weights between the input layer is slightly different, since the hidden layers have no target vectors. Therefore, the update process described above cannot be used for this set of weights. Equation (7.11) is used for all of the weights, regardless of location, however, the δ term for the weight between the input layer and hidden layer must be calculated without the benefit of the target vector.

Instead, the δ values from the output layer are used to adjust the δ values

in the first hidden layer and the δ 's are propagated backwards to all of the preceding layers.

Consider a neuron in the hidden layer immediately behind the output layer. During the forward pass the output values of each layer are processed forward to the next layer via the interconnection weights, in terms of the δ , values are passed in the reverse direction from the output layer to the hidden layer, during the training period. Each weight between the hidden and output layers is multiplied by the δ value of the output neuron to which it is attached. The value of δ for the weights in the hidden layer preceding the output layer is produced by summing all of the products from the output layers and multiplying them by the derivatives of the sigmoidal function, at that particular hidden node. Thus,

$$\delta_j = H_j(1 - H_j) \left(\sum_{k=1}^K \delta_k w_{kj} \right) \quad (7.12)$$

The δ values are calculated for each neuron in a given hidden layer, and all of the weights in that layer are adjusted accordingly using the expression below:

$$\Delta w_{ij} = \delta_j x_i \quad (7.13)$$

for a multi-layer network this process is repeated layer by layer, until the input layer is reached and all of the unknowns have been adjusted.

7.3.3 Summary of Learning via Robust Back Propagation ANN

In summary, the learning period consists of a given network with a random set of weight values being simulated by all of the input vectors in a training set. A global system error is computed, which is usually quite large initially, thus requiring adjustment of the interconnection weights via a process known as training. A variety of training algorithms exist, of which a Robust Back propagation has significant advantages over classical Back propagation algorithms. Using the robust procedure, update factors for all of the weights in the network are computed based on the global system error between the actual network outputs and the target values. A gradient descent method is used to track the global error within an acceptable tolerance level by optimizing the interconnection weights. The conjugate gradient procedure possesses the advantages of simplicity and minimal storage requirements in mapping a given input to its corresponding output state. A successful learning exercise will yield a stable set of weights, which exhibit only minor fluctuations in the value if further learning is attempted.

Precautions should be taken against "over training," which occurs when the network has become too specific to the training data and is no longer able to

generalize to previously unseen data. To prevent this occurrence the network is periodically presented with test data during the training procedure. If the global system error increases from one checkpoint to the next then the training process was halted. A comparison of the robust tool to classical Back propagation paradigms is presented in Table 7.2.

Table 7.2 Classical Back Propagation Versus Robust ANN

| Feature | Classical back propagation | Robust ANN | Advantages of robust ANN |
|-------------------|--|-----------------------------------|---|
| Update scheme | Arbitrary threshold | Dynamic threshold | Streamlines learning process by updating dynamic threshold during every iteration of learning session Individual dynamic threshold for each hidden node increases accuracy |
| Data presentation | Stochastic presentation | Batch presentation | Batch data presentation order can remain sequential which is much less computationally intensive than stochastic data presentation, that must be random |
| Error function | Local error function | Global error function | Global error function represents true system wide error for each iteration in the learning session Weights are updated for entire training data at each iteration |
| Speed | Neural Ware Professional II/Plus: Over 4000 iterations for the XOR problem. Rumelhart, Hinton & Williams 245 iteration for XOR problem | 152 iteration for the XOR problem | Significant speed enhancement over classical methods |

The benefits in speed and accuracy of the Robust ANN over classical Back propagation methods can be traced back to three main characteristics. First, the Robust ANN utilizes a dynamic (adaptive) threshold value for each hidden node during the training session that is updated along with the interconnection weights as opposed to the arbitrary thresholds that allow for greater individuality in the learning process for each hidden node and thus have a positive impact on the accuracy of the final output.

The second and third beneficial traits of the Robust ANN are coupled. Since the Robust ANN utilizes a global error function that updates the weights and thresholds based on the average error of the entire data set, the training data can be presented in an identical sequential order for each pass. In contrast, the classical Back propagation method utilizes a local error function that updates the data after each training vector and thus the data must be presented in a different random order for each pass, which increases the computational complexity and thus, the required time for convergence.

7.3.4 Conclusions

Several different types of neural nets have been discussed in this section. This is by no means an exhaustive list. A selection has been made based on applicability to power system problems. While these have been inspired by biological neurons, the issue is not their ability to exactly model biological systems, but their importance as another solution paradigm for power system problems.

The area of artificial networks is a very active field of research. For instance, it includes neural smithing for optimal architecture and learning design. Pruning techniques are used to determine the optimal number of neurons to solve a specific problem, and adaptive learning algorithms to avoid retraining for large data sets. Training with noise can be used in order to overcome overfitting problems.

There are continuing efforts to combine and enhance ANN methods with regularization theory, stochastic, Bayesian, or other statistical and pattern recognition techniques in order to define optimality criteria for ANN performance. In fact, ANNs might be considered a set of highly adaptive statistical tools. Information-theoretic concepts are introduced in order to measure how ANNs generalize, i.e., how they will perform on unknown test data.

Finally, the combination of neural networks with other AI techniques like symbolic structures from expert systems, fuzzy logic, and genetic algorithms is being explored for many technical applications. Here complex problems are described with fuzzy techniques or expert rules and the subsequent classification, regression, or optimization tasks are solved with ANNs.

7.4 EXPERT SYSTEMS

It is not easy to give a precise definition of an *expert system*, because the concept of the expert system itself is changing as technological advances in computer systems take place and new tasks are incorporated into the old ones. In simple words, it can be defined as a computer system that models the reasoning and action processes of a human expert in a given problem area. Expert systems, like human experts, attempt to reason within specific knowledge domains.

An expert system allows the knowledge and experience of one or more experts to be captured and stored in a computer. This knowledge can then be used by anyone requiring it. The purpose of an expert system is not to replace the experts, but simply to make their knowledge and experience more widely available. Typically there are more problems than there are experts available to handle them. The expert system permits others to increase their productivity, improve the quality of their decisions, or simply to solve problems when an expert is not available.

Valuable knowledge is a major resource and it often lies with only a few experts. It is important to capture that knowledge so others can use it. Experts retire, get sick, move on to other fields, and otherwise become unavailable. Thus the knowledge is lost. Books can capture some knowledge, but they leave the problem of application to the reader. Expert systems provide direct means of applying expertise.

An expert system has three main components: a *knowledge base*, an *inference engine*, and a *man-machine interface*. The knowledge base is the set of rules describing the domain knowledge for use in problem solving. The prime element of the man-machine interface is a working memory which serves to store information from the user of the system and the intermediate results of knowledge processing. The inference engine uses the domain knowledge together with the acquired information about the problem to reason and provide an expert solution.

7.4.1 A Working Definition

An expert system is an artificial intelligence (AI) program incorporating a knowledge base and an inferencing system. It is a highly specialized piece of software that attempts to duplicate the function of an expert in some field of expertise. The program acts as an intelligent consultant or advisor in the domain of interest, capturing the knowledge of one or more experts. Nonexperts can then tap the expert system to answer questions, solve problems, and make decisions in the domain.

The expert system is a fresh new, innovative way to capture and package

knowledge. Its strength lies in its ability to be put to practical use when an expert is not available. Expert systems make knowledge more widely available and help overcome the age-old problem of translating knowledge into practical results. It is one more way the technology is helping us to get a handle on the oversupply of information. All AI software is knowledge-based as it contains useful facts, data, and relationships that are applied to a problem.

Expert systems, however, are a special type of knowledge based system as they contain heuristic knowledge. Heuristics are primarily from real world experience, not from textbooks. It is knowledge that comes directly from those people—the experts—who have worked for many years within the domain. It is knowledge derived from learning by doing. It is perhaps the most useful kind of knowledge, specifically related to everyday problems. It has been said that knowledge is power. Certainly there is truth in that but in a more practical sense, knowledge becomes power only when it is applied. The bottom line in any field of endeavor is RESULTS, some positive benefit or outcome. Expert systems are one more way to achieve results faster and easier.

7.4.2 Characteristics of Expert Systems

One advantage of the expert system is its permanence. Human expertise can quickly fade, regardless of whether it involves mental or physical activity. An expert must constantly practice and rehearse to maintain proficiency in some problem area. A significant period of disuse can seriously affect the expert's performance. Once expertise is acquired in an expert system, it is around forever, barring catastrophic accidents related to memory storage. Its permanence is not related to its use.

Another advantage of the expert system is the ease with which it can be transferred or reproduced. Transferring from one human to another is the laborious, lengthy, and expensive process called education (or in some cases, knowledge engineering). Transferring an expert system is the trivial process of copying or cloning a program or data file. An expert system is also much easier to document. Documenting human expertise is extremely difficult and time consuming. Documenting an expert system is a straight forward mapping between the way in that the expertise is represented in the system and the natural language description of that representation.

An expert system produces more consistent, reproducible results than does the human expert. A human expert may make different decisions in identical situations because of emotional factors. For example, a human may forget to use an important rule in a crisis situation because of time pressure or stress. An expert system is not susceptible to these distractions.

A final advantage of the expert system is its low cost. Human experts, especially the highly skilled ones, are very scarce and hence very expensive.

Expert systems, in contrast, are relatively inexpensive. They are costly to develop but relatively inexpensive to operate. Their operating cost is just the nominal computer cost of running the program. Their high development cost (years of effort of high-priced knowledge engineers and domain experts) is offset by their low operating cost and the ease of making new copies of the system.

Although expert systems tend to perform well, there are important areas in which human expertise is clearly superior to the artificial kind. This does not reflect a fundamental limitation of expert systems or AI, just the current state-of-the-art.

One such area is creativity. People are much more creative and innovative than even the smartest programs. A human expert can reorganize information and use it to synthesize new knowledge, while an expert system tends to behave in a somewhat uninspired routine manner. Human experts handle unexpected events by using imaginative and novel approaches to problem solving, including drawing analogies to situations in completely different problem domains. Programs have had little success in doing this.

Another area where human expertise excels is learning. Human experts adapt to changing conditions; they adjust their strategies to conform to new situations. Expert systems are not particularly adept at learning new concepts or rules, probably because it is a very difficult task that has always been made in developing programs that learn, but these programs tend to work in extremely simple domains and do not do well when confronted with the complexity and details of real-world problems.

Human experts can make direct use of complex sensory input, whether it be sight, sound, taste, or smell. But expert systems manipulate symbols that represent ideas and concepts, so sensory data must be transformed into symbols that can be understood by the system. Quite a bit of information may be lost in translation, especially when visual scenes are mapped into sets of objects and the relations between them.

Human experts can look at the big picture, examine all aspects of a problem, and see how they relate to the central issue. Expert systems, on the other hand, tend to focus on the problem itself, ignoring issues relevant to, but separate from, the basic problem. This happens because it takes a huge amount of expertise just to handle the basic problem, and it would take almost as much expertise to handle each of the hundreds of tangential problems that could arise. In the future, when faster and cheaper techniques for acquiring expert knowledge are developed, this situation may change.

7.4.3 Applications in Power System Operations

The focus of expert system research in the power systems operations area has been to help the system operator to function more effectively. Specific objectives include:

1. Understanding the interface requirements to integrate databases, various computer architectures, full graphics systems, and applications software expected in future control centers;
2. Defining the appropriate applications of expert systems (e.g., as a routine aid to operators, providing action plans during emergencies, or the rebuilding of a system after a major disturbance);
3. Building domain specific knowledge for general purpose expert systems (e.g., rules and techniques used by today's experienced operators to handle the daily operation of a power system);
4. Developing and evaluating specific expert systems (e.g., replacing tedious jobs done by humans);
5. Demonstrating expert systems that aid the operators in the most cost effective areas.

Control center operators benefit from using expert systems because such systems not only identify a problem, but they can also provide the underlying reasoning used to define the problem, and a set of recommended actions to ameliorate the problem. The best applications of expert systems have been in diagnostic situations where information about the system being studied is held in static tables. For application in power systems, information about the system can be taken from the real time database or a simulator.

7.4.4 Rule-Based System

There is a lot of confusion about terminology in the artificial intelligence literature because there are few standardization efforts. So in the following paragraph we present the definitions used in this chapter. A knowledge-based system is 'a program in which the domain knowledge is explicit and separate from the program's other knowledge.' It consists of the following five components: the knowledge base, the knowledge acquisition module, the inference engine, the explanation module, and the user interface (Fig. 7.3).

The Knowledge Base Contains Facts and Rules

Like any database, the knowledge base contains the data, called facts, which describe fixed properties of the problem. In addition, a knowledge base contains instructions describing how to process these data. If these instructions are given in an IF . . . THEN . . . rule format, then we are talking about a rule-based system.

For the rule IF A THEN B, A is called the left-hand side (LHS) and B the right hand side (RHS) of the rule. If A and B are logical expressions which can be true or false, A is called the premise and B the conclusion. But as we will

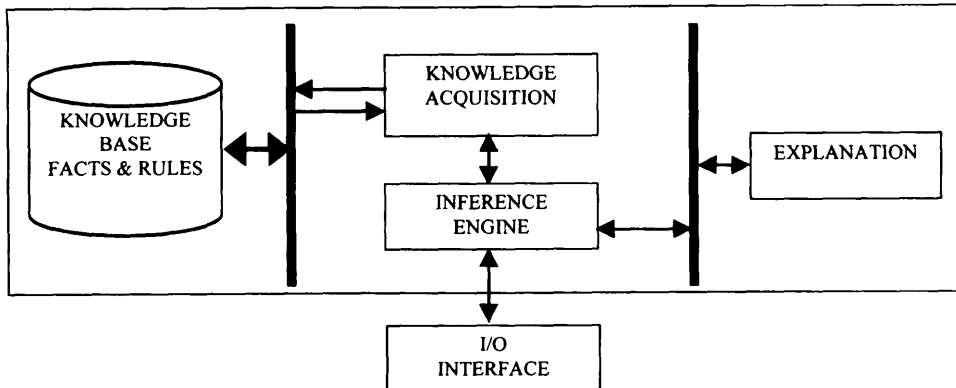


Figure 7.3 Knowledge-based system.

see later, we will also include actions like closing an element in the LHS or the RHS of a rule. These actions will change the initial facts. They cannot be considered as simple logic expressions.

These facts and instructions represented as rules may already have been formulated and written down explicitly because they are common invariable knowledge of the domain. In our case there exist manuals describing the possible actions which can be performed on different elements and normally everyone familiar with these manuals can manipulate these elements. In particular these manuals describe the problem completely. Nevertheless this work in control centers is done by operators who are certainly experts in this domain and who know their domain by heart.

In other cases, there is a human expert who uses heuristic or complex knowledge acquired during years of work. Often this kind of knowledge is incomplete and the reasoning mechanism applied by the human expert cannot be replaced by pure logic rules. For instance, intuition or so called common sense cannot be formalized this way. The main reason why we call our system a rule-based system and not an expert system is due to the fact that in principle our knowledge is complete. It can easily be formulated as rules. Also we do not want to contribute the misunderstanding that in any domain where a human expert explains his knowledge by IF . . . THEN . . . rules, this reasoning can be efficiently implemented by an expert system. This misunderstanding leads to hundreds of unsatisfying feasibility studies on expert system applications which can be found in the literature today. In short, a rule-based system is a special case of a knowledge-based system.

Knowledge Base Acquisition Module and I/O Interface are User Friendly

The knowledge base is built up using a program called a knowledge acquisition component. Depending on the nature of facts and rules this component may be a sophisticated rule editor generating ASCII or binary files or a program extracting relevant data from another database or even from a real-time process and storing it in the predefined format on mass storage medium.

The knowledge acquisition module as well as the user interface should be user friendly. Menu-driven and/or mouse-driven dialogue, graphic output multi-windowing all help to achieve this goal. These techniques are already well known.

The Inference Engine Provides Control

Whereas rules describe how to process data, the instructions of the inference engine describe how to process these rules. They fix for instance the order in which two rules concerning the same element are executed or fired. One possibility concerns the enumeration of the rules, where the numbers fix the priority of the rule. Another possibility is to process the youngest mentioned rule first. The processing protocol may be specific for the problem. Then it is called meta-knowledge with meta-rules. In order to keep the inference engine as general as possible it is sometimes convenient to store this meta-knowledge in the knowledge base.

The instructions also define the general problem solving strategy. There are two important techniques, backward chaining and forward chaining. The goal-driven strategy backward chaining tries to prove a goal, while data-driven control forward chaining deduces new data from existing facts.

The Explanation Module Explanation of the Inference Chain

The **explanation module** provides a trace facility for the end user in order to comment on the reasoning process.

Shells and Programming Languages are not Identical

An "empty" knowledge-based system which provides control and data structures but no knowledge is called a shell. Any shell is written in a certain programming language for instance Pascal, LISP, OPS83, or PROLOG. All these languages have their advantages and disadvantages. We note that OPS83 provides the data type "rules" and the forward chaining control strategy, whereas PROLOG is especially suited to implement backward chaining control, because of its backtracking facilities. Neither procedural languages like Pascal nor functional ones like LISP provide these facilities that therefore have to be programmed explic-

itly. Although they may be more efficient for a final implementation they are not suited for rapid prototyping in order to test concepts and methodologies.

We should emphasize however that PROLOG does not fit in our definition of a knowledge-based system shell because neither a control strategy nor an explanation facility are not provided but have to be programmed.

Using PROLOG facts as knowledge base facts and PROLOG predicates as rules does not permit the explicit separation of the inference engine and knowledge base. Although it may be tempting to quickly implement a prototype in pure PROLOG in order to test the concept, this prototype cannot be enhanced without changing the code of the program (except for those cases where only pure predicate calculus is used and no extra control is needed in order to enhance efficiency). Note however that the PROLOG trace facility does not automatically provide an explanation module. Depending on the PROLOG-interpreter, the output of this facility is more or less unreadable for nonprogrammers (e.g., variables are simply denoted by numbers). Furthermore, predicates used for building up strategies have to be hidden to the trace procedure because showing them will produce a lot of redundant information. The user-interface provided by standard CPROLOG is rather poor for our application. Similar arguments concerning control, explanation, and user-friendliness are valid for OPS83.

Let us have a look at the reasoning process of the human substation operator. The operator asks whether it is possible to close an element or to supply power to a certain load and how to do it. He therefore proves a hypothesis instead of looking at the substation configuration and collecting all possible conclusions and actions based on the initial state of the station. For this reason, many power oriented rule base systems have been written in PROLOG because this goal-driven strategy reflects the reasoning process of the end user better.

7.4.5 Reasoning with Uncertainty in Rule Based Systems

One of the important features of expert systems is their ability to deal with incorrect or uncertain information. There will be times when an expert system, in gathering initial inputs, will ask a question for which there is no answer. In such a case, simply say so. Expert systems are designed to deal with cases such as this. Because one may not have a particular fact, the search process will undoubtedly take a different path, it may take longer to come up with an answer, but the expert system will.

Traditional algorithmic software simply cannot deal with incomplete information. If one leaves out a piece of data, one may not receive an answer at all. If the data is incorrect, the answer will be incorrect. This is where artificial intelligence programs, particularly expert systems, are particularly useful when the inputs are ambiguous or completely missing, the program may still find a

solution to the problem. The system may qualify that solution, but at least it is an answer that can in many cases be put to practical use. This is consistent with expert level problem solving where one rarely has all the facts before making a decision. Common sense or knowledge of the problem tells us what is important to know and what is less important. Experts almost always work with incomplete or questionable information, but this doesn't prevent them from solving the problem.

Thus, increasingly in the design of expert systems, there been a focus on methods of obtaining an approximate solution to a problem when there is no clear conclusion from the given data. Logically, as expert system problems become more complex, the difficulty of reaching a complete conclusion certainty increases, so in some cases, there must a method of handing uncertainty. Researchers report that a classical expert system gave incorrect results due to the sharpness of the boundaries created by the if-then rule of the system; however, once a method for dealing with uncertainty (in these two cases fuzzy set theory) was used, the expert system reached the desired conclusions.

The successful performance of expert systems relies heavily on human expert knowledge derived from domain experts based on their experience. The other forms of knowledge include causal knowledge and information from case studies, databases, etc. Knowledge is typically expressed in the form of high level rules. The expert knowledge takes the form of heuristics, procedural rules, and strategies. It inherently contains vagueness and imprecision because experts are not able to explicitly express their knowledge. The process of acquiring knowledge is also quite imprecise, because the expert is usually not aware of all the tools used in the reasoning process. The knowledge that one reasons with may itself contain uncertainty. Uncertain data and incomplete information are other sources of uncertainty in expert systems.

Uncertainty in rule based expert systems occurs in two forms. The first form is linguistic uncertainty which occurs if an antecedent contains vague statements such as the level is "high" or "the value is near 20." The other form of uncertainty, called evidential uncertainty, occurs if the relationship between an observation and a conclusion is not entirely certain. This type of uncertainty is most commonly handled using conditional probability which indicates the likelihood that a particular observation leads to a specific conclusion. The study of making decisions under either of these types of uncertainty will be referred to as plausible or approximate reasoning. Several methods of dealing with uncertainty in expert systems have been proposed, including:

- Subjective probability
- Certainty factors
- Fuzzy measures
- Fuzzy set theory

The first three methods are generally used to hand evidential uncertainty, while the last method, fuzzy set theory is used to incorporate linguistic uncertainty.

As expert assessments of the indicators of the problem may be imprecise, fuzzy sets may be used for determining the degree to which a rule from the expert system applies to the data that is analyzed. When applying a method of reasoning with uncertainty to a rule based expert system, there must be a method of combining or propagating uncertainty between rules. A method of propagating uncertainty for the method of reasoning with uncertainty will be discussed next.

Subjective Probability and Statistics

One method of dealing with uncertainty is to use conventional statistics and probability. For example, with the use of statistics, sufficient data may be available to compute the mean (average), median, and standard deviations. These new figures derived from original data provide additional knowledge which will help in making a decision. Recall that probability is simply a ratio of the number of times that a particular action will occur for a given number of attempts. It is really a ratio as shown below:

$$P(x) = \text{Number of occurrence of an event/total number of events that take place}$$

The probability of x occurring, stated as $P(x)$, is the ratio of the number of times x occurs to the total number of event that takes place. For example, in rolling a standard die, the probability is one-sixth that any one of numbers, one through six, will come up. This may also be expressed as a fraction 0.16667, or as a percentage, 16.67%. In many knowledge representation cases, the probability for a certain condition or action may be known or can be estimated. For the probability of a certain even taking place is 70%, then one may initiate some action if the probability is equal or greater than 70%. If the probability is less than 70%, then perhaps an action may not be taken. For example, the production rule below uses the probability:

IF the stone is clear, without color
THEN it is diamond (probability 60%)

An example will illustrate this. Suppose we ask ten engineers whether they can program in the BASIC language. Out of the ten, three say they can. We can use these figures to compute the probability:

$$P(\text{BASIC}) = \frac{3}{10} = 0.3$$

What this says is that the probability of an engineer to be able to program in BASIC is 0.300. We can also express this—a percentage by simply multiplying the probability by 100. We say that the probability of engineers being able to program in BASIC is 30%. Probability figures like this can be used to determine rule strength if they fit the problem.

Multiple probability values will occur in many systems. For example, a rule may have three parts to its antecedent, each with a probability value. The overall probability of the value then becomes the product of the individual probabilities, if the parts of the antecedent are independent of one another. In a three part antecedent, the probabilities may be 0.90, 0.70, and 0.65. The overall probability is

$$P = (0.9)(0.7)(0.65) = 0.4095$$

The combined probability is about 41%. But this is true only if the individual parts of the antecedent do not affect or depend on one another.

Sometimes one rule references another. Here the individual rule probabilities can propagate from one to another. There is a need to evaluate the total probability of a sequence of rules or a path through the search tree to determine if a specific rule fires. Or one may be able to use the combined probability to predict the best path through the search tree. In other words, the probabilities become the “costs” of the individual arcs in the tree.

There are numerous methods of computing combined probabilities. If the rules are independent, a simple product can be used as described before. However, most events and rules are dependent upon one another. In that case, a special procedure called Bayes’ Rule or Theorem can compute the probability of event A occurring given that event B has already occurred. This is expressed as $P(A|B)$. Bayes’ Theorem is:

$$P(A|B) = \frac{P(B|A) P(A)}{P(B|A) P(A) + P(B|\sim A) P(\sim A)}$$

We will not attempt to explain this rule, but one should be aware of the fact that many expert systems use Bayes’ Theorem instead of certainty factors to deal with uncertainty. Several major expert system development tools use Bayesian probability.

Measures of Belief and Disbelief

Measures of belief and disbelief arose from the desire that evidence should incrementally increase the belief or disbelief in a hypothesis. The formal definition of the measure of belief was based on the idea that if a prior probability, $P(h)$ is defined, then the maximum amount of belief that can be added to $P(h)$

from a new piece of evidence is $1 - P(h)$. If a piece of evidence confirms $P(h|e)$, then this would amount to, adding $P(h|e) - P(h)$ to the previous belief, so the belief in h has been increased by

$$\Delta P(h) = \frac{P(h|e) - P(h)}{1 - P(h)}$$

The measure of increased disbelief can be defined similarly. Now with this idea, let the measure of increase belief (MB) given some evidence e about a hypothesis h be defined as:

$$MB[h,e] \rightarrow [0,1] \text{ with}$$

$$MB(h,e) = \begin{cases} 1 & \text{if } p(h) = 1 \\ \max \left\{ 0, \frac{P(h|e) - p(h)}{1 - p(h)} \right\} & \text{otherwise} \end{cases}$$

and let the measure of increased disbelief (MD) be defined as

$$MD[h,e] \rightarrow [0,1] \text{ with}$$

$$MD(h,e) = \begin{cases} 1 & \text{if } p(h) = 0 \\ \max \left\{ 0, \frac{P(h|e) - p(h)}{1 - p(h)} \right\} & \text{otherwise} \end{cases}$$

Note that when evidence e is assigned to a hypothesis h , only one of the MD or MB functions will be greater than zero so that a single piece of evidence cannot be used as both a measure of the confirmation and negation of a hypothesis. As the measures of belief and disbelief were used in the design of an expert system, it was found that a representation of the uncertainty in terms of a single measure would be more convenient in making comparisons of different hypotheses.

Certainty Factors

There are several methods of dealing with uncertain information. In rule based expert systems, numerical factors indicating the truth or probability of a premise or conclusion are used as a measure for uncertainty. These numerical factors are known as certainty factors (CF) and probability.

In a high percentage of expert system rules, there will be no ambiguity or uncertainty. We will know with confidence whether or not a particular premise or conclusion is true or false. If the information is not known at all, then the

rule requesting it will not fire. In cases where there is the possibility that the information is not known, special rules can be created to deal with this problem. The rule might state that if a particular piece of information is not available, then a certain action will be initiated.

Still, there are many cases where the information is known but we have less than 100% confidence in its truthfulness. Just as weather forecasters use a number to predict the likelihood of rain, so can a confidence number be used with production rules. A forecaster may say that there is a 80% probability of rain. They are saying that they don't know for sure whether or not it is going to rain. On the other hand, they have enough information to be able to say that 80% of the time under similar circumstances it rains. While a certainty or confidence factor is not really a probability, it is a number that helps to represent the uncertainty. A certainty factor is simply a measure of the confidence that a particular fact or rule is true or not true. It is usually a number between 0 and 1, where zero indicates no confidence and one means full or complete confidence. We also hear certainty factors called confidence factors or rule strength.

Certainty factors are used with both the premise (IF) and conclusion (THEN) portions of a rule. The two examples given below show how confidence factors are used.

IF the patient has the fever, CF = 0.6
THEN prescribe rest in bed

IF the patient is sneezing
AND has a runny nose
AND has watery eyes
THEN the patient has a cold, CF = 0.5

Figure 7.4 shows several ways to use certainty factors. The scale is up to the programmer. In Fig. 7.4A, a scale of 0 to 1 is used where 1 = absolute certainty; that is, 100% truthfulness or validity of the premise or conclusion of a rule. The 0, of course, indicates absolute uncertainty or falsity. Intermediate values have varying degrees of truthfulness or uncertainty. A scale of 0 to 10 or 0 to 100 can also be used with the same result. The + and - scale shown in Fig. 7.4B is another approach. A +5 indicates absolute certainty while a -5 indicates 100% contradiction. The 0 in the center of the scale indicates unknown. One could also use a -1/0/+1 scale as well.

Determining whether a particular rule is to fire requires the inference engine to look at the confidence factor and evaluate it. For example, if one is using the 0 to 1 scale, we might want the rule to fire if the confidence factor is above a certain threshold level, say at 0.2, you may assign a threshold of +1 or -1

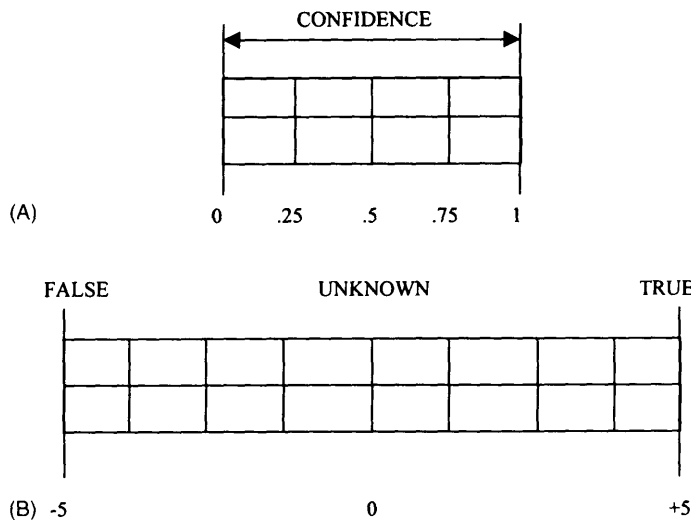


Figure 7.4 Confidence and certainty factor scales.

depending upon the circumstances at the minimum acceptable level for determining whether something is true or false. Other levels may be set depending upon the problem.

In rules with compound premise clauses connected by AND or OR, each clause may have its own CF. For such situations, there must be a way to compute a CF for the rule. This is done by using the minimum CF of all clauses connected by AND or the maximum CF of all clauses connected by OR. Some examples will illustrate this.

RULE 1:

```
IF      X(0.4)
AND    Y(0.75)
THEN   Z
Composite CF = 0.4
```

RULE 2:

```
IF      D(0.3)
AND    E(0.8)
THEN   F
Composite CF = 0.8
```

If each rule in a reasoning chain has a CF, each will, of course, affect the other. The outcome has to be decided based upon some composite evaluation. One way this is done is with a special formula.

$$\text{CF} = \text{CF}(X) + \text{CF}(Y) - \text{CF}(X) * \text{CF}(Y)$$

This says that the CF for rule X is added to the CF for rule Y and from that is subtracted the product of the CFs for rules X and Y . Below are two rules that illustrate this point:

RULE 3:

IF P
 AND Q
 THEN $R(0.65)$

RULE 4:

IF R
 THEN $S(0.20)$

The composite CF is then:

$$0.65 + -2.00 - (0.65)(0.20) = 0.85 - 0.13 = 0.72$$

Of course, there will usually be more than two rules in a chain. The above formula can be used by taking the composite CF of two rules and combining it with the CF of a third rule. That new composite CF is then combined with a fourth, and so on.

Fuzzy Logic

Fuzzy set-based techniques can provide an excellent framework for systematically representing the imprecision inherent in an expert's knowledge. We use the following example to illustrate,

IF the temperature is high (0.8)
 AND system is operating in heavy load period (0.9)
 THEN system is high stressed

The parameters in the premise and consequent temperature, load period, and system stress can be represented using simple fuzzy membership functions. In this case, the fuzzy information is contained in the terms high and heavy.

Although, there are situations where membership grades probabilities can take on similar values, they are not the same. One distinguishing factor between probability fuzzy membership grades is that the summation probabilities on a finite universal set must equal 1.

The main drawback of nonfuzzy methods in dealing with uncertainty is their handling of linguistic terms. Fuzzy theory provides a natural framework for dealing with linguistic terms used by experts. Imprecision in numeric data can be easily dealt with by expressing it as a fuzzy number. Fuzzy sets can be conveniently incorporated in expert systems to better deal with uncertainty imprecision.

Structure of the Expert Stability Assessment System

The fuzzy expert system structure is shown in Fig. 7.5. Its database contains the power system topology.

The knowledge base of the fuzzy expert system contains all the data of the contingencies. The information is based on known statistics of protection performance used in the system. If these data are not available when a fault occurs, the fuzzy expert system asks the dispatcher to provide them and then saves them in a database for future use. Models for estimation of possible contingencies, and heuristic rules about the relay characteristics for actual fault determination are also include.

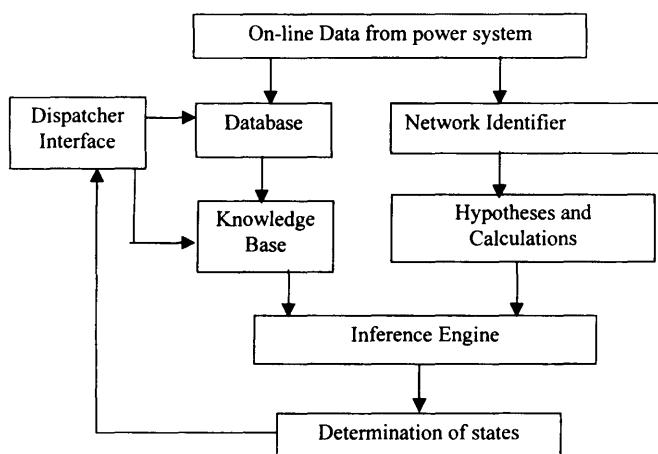


Figure 7.5 Fuzzy expert system structure.

7.5 FUZZY SETS AND SYSTEMS

In 1965, L. A. Zadeh laid the foundation of fuzzy set theory as a method to deal with the imprecision of practical systems. Bellman and Zadeh write: “Much decision making in the real world takes place in an environment in which the goals, the constraints and the consequences of possible actions are not precisely known.” This “imprecision” or fuzziness is the core of fuzzy sets or fuzzy logic. Fuzzy sets were proposed as a generalization of conventional set theory. Partially as a result of this fact, fuzzy logic remained the purview of highly specialized and mathematical technical journals for many years. This changed abruptly in the late 1980s.

7.5.1 Fuzzy Sets

In a conventional (nonfuzzy, hard, or crisp) set, an element of the universe either belongs to or does not belong to the set. That is, the membership of an element is crisp—it is either yes (in the set) or no (not in the set). A fuzzy set is a generalization of an ordinary set in that it allows the degree of membership for each element to range over the unit interval [0,1]. Thus, the membership function of a fuzzy set maps each element of the universe of discourse to its range of space, which, in most cases, is assumed to be the unit interval.

One major difference between crisp and fuzzy sets is that crisp sets always have unique membership functions, whereas every fuzzy set has an infinite number of possible membership functions that may represent it. This enables fuzzy systems to be adjusted for maximum utility to a given situation.

7.5.2 Fuzzy Systems, Complexity, and Ambiguity

Zadeh’s principle of incompatibility was given in 1973 to explain why there is a need for a fuzzy systems theory. The principle states, in essence, that as the complexity of a system increases, our ability to make precise and yet significant statements about its behavior diminishes until a threshold is reached beyond which precision and significance (or relevance) become almost mutually exclusive characteristics. This suggests that complexity and ambiguity (imprecision) are correlated: “The closer one looks at a real-world problem, the fuzzier becomes its solution.”

It is characteristic of the way a human thinks to treat problems involving complexity and ambiguity in a subjective manner. Complexity generally stems from uncertainty in the form of ambiguity: these are features of most social, technical, and economic situations experienced on a daily basis. In considering a complex system, humans reason approximately about its behavior (a capability that computers do not have) and thus maintain only a generic understanding of

the problem. This generality and ambiguity are adequate for a human to perceive and understand complex systems.

As one learns more and more about a system, its complexity decreases and understanding increases. As complexity decreases, the precision afforded by the computational methods becomes more useful in modeling the system. For less complex systems, thus involving little uncertainty, closed-form mathematical expressions offer precision descriptions of the system's behavior. For systems that are slightly more complex but for which significant data exist, model-free methods, such as computational neural networks, provide powerful and effective means to reduce some uncertainty through learning based on patterns in the available data.

Basic statistical analysis is founded on probability theory or stationary random processes, whereas most experimental results contain both random (typically noise) and nonrandom processes. One class of random processes or stationary processes exhibits the following three characteristics:

1. The sample space on which the processes are defined cannot change from one experiment to another, that is, the outcome space cannot change.
2. The frequency of occurrence, or probability, of an event within that sample space is constant and cannot change from trial to trial or experiment to experiment.
3. The outcomes must be repeatable from experiment to experiment. The outcome of one trial does not influence the outcome of a previous or future trial.

However, fuzzy sets are not governed by these characteristics.

The fundamental difference between fuzziness and probability is that fuzziness deals with deterministic plausibility, while probability concerns the likelihood of nondeterministic, stochastic, events. Fuzziness is one aspect of uncertainty. It is the ambiguity (vagueness) found in the definition of a concept or the meaning of a term such as *comfortable temperature* or *well cooked*. However, the uncertainty of probability generally relates to the occurrence of phenomena, as symbolized by the concept of randomness. In other words, a statement is probabilistic if it expresses some kind of likelihood or degree of certainty or if it is the outcome of clearly defined but randomly occurring events. For example, the statements "There is a 50-50 chance that he will be there," "It will be sunny tomorrow," and "Roll the dice and get a six" demonstrate the uncertainty of randomness.

Hence, fuzziness and randomness differ in nature: that is, they are different aspects of uncertainty. The former conveys "subjective" human thinking, feelings, or language and the latter indicates an "objective" statistic in the natural sciences.

From the modeling point of view, fuzzy models and statistical models also possess philosophically different kinds of information: Fuzzy memberships represent similarities of objects of imprecisely defined properties, while probabilities convey relative frequencies. The quest for a method of quantify nonrandom uncertainty (imprecision, vagueness, fuzziness) in physical processes is the basic premise of fuzzy system theory, for to understand uncertainty in a system is to understand the system itself. As understanding improves, the fidelity in modeling improves.

Whenever precision is evident, for example, fuzzy systems are less efficient than more precise algorithms in offering a better understanding of the problem. Requiring precision in engineering models and products translates to requiring high cost and long lead times in production and development. For other than simple systems, expense is proportional to precision: More precision entails higher cost. When considering the use of fuzzy logic for a given problem, an engineer or scientist should ponder the need for exploiting the tolerance for imprecision. Not only does high precision dictate high costs but it also entails low tractability in a problem.

On the other hand, fuzzy systems can focus on modeling problems characterized by imprecise or ambiguous information. The following are situations where it is appropriate to formulate system problems within a fuzzy system framework:

1. In processes involving human interaction (e.g., human descriptive or intuitive thinking)
2. When an expert is available who can specify the rules underlying the system behavior and the fuzzy sets that represent the characteristics of each variable
3. When a mathematical model of the process does not exist, or exists but is too difficult to encode, or is too complex to be evaluated fast enough for real-time operation, or involves too much memory on the designated chip architecture
4. In processes concerned with continuous phenomena (e.g., one or more of the control variables are continuous) that are not easily broken down into discrete segments
5. When high ambient noise levels must be dealt with or it is important to use inexpensive sensors and/or low-precision microcontrollers.

The ability to use fuzzy system tools will allow one to address the vast majority of problems that have the preceding characteristics. Fuzzy formulations can help to achieve tractability, robustness, and lower solution costs.

Any field can be fuzzified and hence generalized by replacing the concept of a crisp set in the target field by the concept of a fuzzy set. Therefore, we can fuzzify some basic fields such as graph theory, arithmetic, and probability theory

to develop fuzzy graph theory, fuzzy arithmetic, and fuzzy probability theory, respectively, moreover, we can also fuzzify some applied fields such as neural networks, pattern recognition, and mathematical programming to obtain fuzzy neural networks, fuzzy pattern recognition, and fuzzy mathematical programming, respectively. The advantages of fuzzification include greater generality, higher expressive power, an enhanced ability to model real-world problems, and a methodology for exploiting the tolerance for imprecision.

7.5.3 Fuzzy Theory in Electric Power Systems

With the remarkable and successful penetration of fuzzy systems into manufacturing, appliances, and computer products, their applications in power systems are beginning to mature and receive wider acceptance in the electric power community. The application of fuzzy set theory to power systems is a relatively new area of research.

Concepts of fuzzy set theory were first introduced in solving power system long-range decision-making problems in the late 1970s. However, substantial interest in its applications to power areas is fairly recent. While conventional analytical solution methods exist for many problems in power system operation, planning, and control, their formation of real-world problems suffers from restrictive assumptions. Even with these assumptions, solving large-scale power system problems is not trivial. Moreover, many uncertainties exist in a significant number of problems because power systems are large, complex, widely spread geographically, and influenced by unexpected events. These factors make it difficult to deal effectively with many power system problems through strictly conventional approaches alone. Therefore, areas of computational (artificial) intelligence emerged in recent years in power systems to complement conventional mathematical approaches and proved to be effective when properly coupled together.

In conceptualizing power system problems, the expert's empirical knowledge is generally expressed by language containing ambiguous or fuzzy descriptions. As a result, classical Boolean logic may not be a valid tool to represent such expertise. Fuzzy logic, on the other hand, is a natural choice for this purpose.

The growing number of publications on applications of fuzzy-set-based approaches to power systems indicates its potential role in solving power system problems. Results obtained thus far are promising, but fuzzy set theory is not widely accepted. The reasons for its lack of acceptance include the following:

- Misunderstanding of the concept
- Excessive claims of some researchers
- Lack of implemented and available systems
- Its status as a new theory

Unexpected events and their uncertainties are traditionally represented by probability. However, it has recently been made clear that some of the uncertain facts are intrinsically of a fuzzy nature and are difficult to manage properly using probabilistic approaches.

There are problems in power systems that contain conflicting objectives. In power system operation, economy and security, maximum load supply, and minimum generating cost are conflicting objectives. The combination of these objectives by weighting coefficients is the traditional approach to such problems. Fuzzy set theory offers a better compromise and obtains solutions that cannot be easily found by weighting methods. The benefits of fuzzy set theory over traditional methods are as follows:

- Provides alternatives for the many attributes of objectives selected
- Resolves conflicting objectives by designing weights appropriate to a selected objective
- Provides the capability for handling ambiguity expressed in diagnostic processes, which involves symptoms and causes

Power system components have physical and operational limits that are usually described as hard inequality constraints in mathematical formulations. Enforcing minor violations of some constraints (practically acceptable) increases the computational burden and decreases the efficiency and may even prevent finding a feasible solution. In practice, certain slight violations of the inequality constraints are permissible. This means that there is not a clear constraint boundary and the constraints can be made soft. Traditionally, this problem has been managed by modifying either the objective function or the underlying iterative process. The fuzzy set approach inherently incorporates soft constraints and thus simplifies implementation of such considerations.

The following steps are recommended when fuzzy set theory is used to solve power system problems:

Description of original problem: The problem to be solved should first be stated mathematically and linguistically.

Defining thresholds for variables: For a given variable, there is a specific value with the greatest degree of satisfaction evaluated from empirical knowledge, and a certain deviation is acceptable with decreasing degree of satisfaction until there is a value that is completely unacceptable. The two values corresponding to the greatest and least degree of satisfaction are termed thresholds.

Fuzzy quantization: Based on the threshold values already determined, proper forms of membership functions are constructed. The functions should reflect the change in degree of satisfaction with the change in variables evaluated by experts.

Selection of the fuzzy operations: In terms of the practical decision-making process by human experts, a proper fuzzy operation is selected so that the results obtained are like those obtained by experts. The interpretation of results using fuzzy systems is based on domain experts' reasoning. Therefore, at this level a hybrid fuzzy set-expert system scheme is desirable. It helps to remove any ambiguity that may occur in problem solving.

7.5.4 Membership Functions: Definitions

Let X be a set of objects, called the universe, whose elements are denoted x . Membership in a subset A of X is the membership function, μ_A from X to the real interval $[0,1]$. The universe is all the possible elements of concern in the particular context. A is called the fuzzy set and is a subset of X that has no sharp boundary. μ_A is the grade of membership x in A . The closer the value of μ_A is to 1, the more x belongs to A . The total allowable universe of values is called the *domain* of the fuzzy set. The domain is a set of real numbers, increasing monotonically from left to right where the values can be both positive and negative. A is completely characterized by the set of pairs

$$A = \{(x, \mu_A(x)), x \in X\} \quad (7.14)$$

Support of a fuzzy set A in the universal set X is the crisp set that contains all the elements of X that have a nonzero membership grade in A . That is

$$\text{Supp } A = \{x \in X | \mu_A(x) > 0\} \quad (7.15)$$

Fuzzy sets with a finite support assume that x_i is an element of the support of fuzzy set A and that μ_i is its grade of membership in A . Then A is written as

$$A = \frac{\mu_1}{x_1} + \dots + \frac{\mu_n}{x_n} = \sum_{i=1}^n \frac{\mu_i}{x_i} \quad (7.16)$$

When X is an interval of real numbers a fuzzy set A is expressed as

$$A = \int_x \frac{\mu_A}{x} \quad (7.17)$$

An *empty* fuzzy set has an empty support which implies that the membership function assigns 0 to all elements of the universal set.

A technical concept closely related to the support set is the alpha-level set or the “ α -cut.” An alpha-level is a threshold restriction on the domain of the

fuzzy set based on the membership grade of each domain value. This set, A_α , is the α -cut of A which contains all the domain values that are part of the fuzzy set at a minimum membership value of α . There are two kinds of α -cuts: weak and strong. The weak α -cut is defined as $A_\alpha = \{X, \mu_A(x) \geq \alpha\}$ and the strong α -cut as $A_\alpha = \{X, \mu_A(x) > \alpha\}$. Also, the alpha-level set describes a power or strength function that is used by fuzzy models to decide whether or not a truth value should be considered equivalent to zero. This is an important facility that controls the execution of fuzzy rules as well as the intersection of multiple fuzzy sets.

The degree of membership is known as the membership or truth function since it establishes a one-to-one correspondence between an element in the domain and a truth value indicating its degree of membership in the set. It takes the form,

$$\mu_A(x) \leftarrow f(x \in A) \quad (7.18)$$

The triangular membership function is the most frequently used function and the most practical, but other shapes are also used. One is the trapezoid which contains more information than the triangle. A fuzzy set can also be represented by a quadratic equation (involving squares, n^2 , or numbers to the second power) to produce a continuous curve. Three additional shapes which are named for their appearance are: the S-function, the PI-function, and the Z-function.

7.5.5 Set Operations

Union and Intersection of Fuzzy Sets

The classical union (\cup) and intersection (\cap) of ordinary subsets of X are extended by the following formulas for intersection, $A \cap B$ and union, $A \cup B$:

$$\forall x \in X, \mu_{A \cup B}(x) = \max(\mu_A(x), \mu_B(x)) \quad (7.19)$$

$$\forall x \in X, \mu_{A \cap B}(x) = \min(\mu_A(x), \mu_B(x)) \quad (7.20)$$

where $\mu_{A \cup B}$ and $\mu_{A \cap B}$ are respectively the membership functions of $A \cup B$ and $A \cap B$.

For each element x in the universal set, the function in Eq. (7.19) takes as its argument from the pair consisting of the element's membership grades in set A and in set B and yields the membership grade of the element in the set constituting the union of A and B . The disjunction or union of two sets means that any element belonging to either of the sets is included in the partnership which expresses the maximum value for the two fuzzy sets involved.

The argument to the function in Eq. (7.20) returns the membership grade of the element in the set consisting of the intersection of A and B . A conjunction or intersection makes use of only those aspects of set A and set B that appear in both sets which expresses the minimum value for the two fuzzy sets involved.

7.5.6 Complement of a Fuzzy Set

The complement of A , $\sim A$, which is the part of the domain not in a set, can also be characterized by *Not-A*. This is produced by inverting the truth function along each point of the fuzzy set and is defined by the membership function

$$\forall x \in X, \mu_{\sim A}(x) = 1 - \mu_A(x) \quad (7.21)$$

The complement registers the degree to which an element is complementary to the underlying fuzzy set concept. That is, how compatible is an element's value $[x]$ with the assertion, x is NOT y , where x is an element from the domain and y is a fuzzy region. A fuzzy complement is actually a metric. It measures the distance between two points in the fuzzy regions at the same domain. The linear displacement between the complementary regions of the fuzzy regions determines the degree to which one set is a counter example of the other set. We can also view this as a measure of the fuzziness or information entropy in the set.

Defining Fuzzy Sets

The steps below give general guidelines in defining fuzzy sets.

1. *Determine the type of fuzzy measurement.* Fuzzy sets can define:
 - Orthogonal mappings between domain values and their membership in the set (“ordinary fuzzy set”);
 - Differential surfaces which represent the first derivative of some action, degree of change between model states, or the force of control that must be applied to bring a system back to equilibrium;
 - A proportional metric which reflects a degree of proportional compatibility between a control state and a solution state;
 - A proportionality set which reflects a degree of proportionality between a control state and a solution state.
2. *Choose the shape (or surface morphology) of the fuzzy set.* The shape maps the underlying domain back to the set membership through a correspondence between the data and the underlying concepts. Some possible shapes are triangular, trapezoidal, PI-curve, bell-shaped, S-curves, and linear. Every base fuzzy set must be normal.
3. *Select an appropriate degree of overlap.* The series of individual

fuzzy sets, associated with the same solution variable, are converted into one continuous and smooth surface by overlapping each fuzzy set with its neighboring set. The degree of overlap depends on the concept modeled and the intrinsic degree of imprecision associated with the two neighboring states.

4. *Ensure that the domains among the fuzzy sets associated with the same solution variables share the same universe of discourse.*

7.6 EXPERT REASONING AND APPROXIMATE REASONING

7.6.1 Fuzzy Measures

The fuzzy measure assigns a value to each crisp set of the universal set signifying the degree of evidence or belief that a particular element belongs in the set. For example, we might want to diagnose an ill patient by determining whether this patient belongs to the set of people with, pneumonia, bronchitis, emphysema, or a common cold. A physical examination may provide us with helpful yet inconclusive evidence. Therefore, we might assign a high value, 0.75, to our best guess, bronchitis, and a lower value to the other possibilities, such as 0.45 to pneumonia, 0.30 to a common cold, and 0 to emphysema. These values reflect the degree to which the patient's symptoms provide evidence for one disease rather than another, and the collection of these values constitutes a fuzzy measure representing the uncertainty or ambiguity associated with several well-defined alternatives.

A fuzzy measure is a function

$$g: \beta \rightarrow [0, 1]$$

where $\beta \subset P(x)$ is a family of subsets of X such that:

1. $\emptyset \in \beta$ and $X \in \beta$.
2. If $A \in \beta$ then $\bar{A} \in \beta$.
3. If β is closed under the operation of set union, that is if $A \in \beta$ and $B \in \beta$, then also $A \cup B \in \beta$.

The set β is called a Borel field, since $A \cup B \supseteq A$ and $A \cup B \supseteq B$. We have $\max[g(A), g(B)] \leq g(A \cup B)$ due to the required monotonicity. Similarly, since $A \cap B \subseteq A$ and $A \cap B \subseteq B$, we have $g(A \cap B) \leq \min[g(A), g(B)]$.

Two large classes of fuzzy measures are referred to as belief and plausibility measures which are complementary (or dual) in the sense that one of them can be uniquely derived from the other. Given a basic assignment m , a belief measure and a plausibility measure are uniquely determined by the formulas

$$\text{Bel}(A) = \sum_{B \subseteq A} m(B) \quad \text{and} \quad \text{Pl}(A) = \sum_{B \cap A \neq \emptyset} m(B)$$

which are applicable for all $A \in \beta(x)$. Also $m(A)$ refers to the degree of evidence or belief that a specific element of X belongs to the set A alone. The *belief measure*, $\text{Bel}(A)$, represents the total evidence or belief that the element belongs to the set A as well as to the various special subsets of A . The *plausibility measure*, $\text{Pl}(A)$, represents not only the total evidence or belief that the element in question belongs to the set A or to any of its subsets but also the additional evidence or belief associated with sets that overlap with A . There are also three important special types of plausibility and belief measures, *probability measures* and a pair of complementary measures referred to as *possibility and necessity* measures.

7.6.2 Approximate Reasoning

The root mechanism in a fuzzy model is the proposition. These are statements of relationships between mode variables and one or more fuzzy regions. A series of conditional and unconditional fuzzy associations or propositions is evaluated for its degree of truth and all those that have some truth contribute to the final output state of the solution variable set. The functional tie between the degree of truth in related fuzzy regions is called the method of implication. The functional tie between fuzzy regions and the expected value of a set point is called the method of defuzzification. Taken together these constitute the backbone of approximate reasoning. Hence an approximate reasoning system combines the attributes of conditional and unconditional fuzzy propositions, correlation methods, implication (truth transfer) techniques, proposition aggregation, and defuzzification.

Unlike conventional expert systems where statements are executed serially, the principal reasoning protocol behind fuzzy logic is a parallel paradigm. In conventional knowledge-based systems pruning algorithms and heuristics are applied to reduce the number of rules examined, but in a fuzzy system all the rules are fired.

7.6.3 The Role of Linguistic Variables

Fuzzy models manipulate linguistic variables. A linguistic variable is the representation of a fuzzy space which is essentially a fuzzy set derived from the evaluation of the linguistic variable. A linguistic variable encapsulates the properties of approximate or imprecise concepts in a systematic and computationally useful way.

The organization of a linguistic variable is:

$$L_{\text{var}} \leftarrow \{q_1, \dots, q_n\} \cup \{h_1, \dots, h_n\}f, \quad (7.22)$$

where predicate q represents usuality or frequency qualifiers, h represents a hedge and f , is the core fuzzy set. The presence of qualifier(s) and hedge(s) is optional. Hedges change the shape of fuzzy sets in predictable ways and function in the same fashion as adverbs and adjectives in the English language. Frequency and usuality qualifiers reduce the derived fuzzy set by restricting the truth membership function to a range consistent with the intentional meaning of the qualifier. Although a linguistic variable may consist of many separate terms, it is considered a single entity in the fuzzy proposition.

7.6.4 Fuzzy Propositions

A fuzzy model consists of a series of conditional and unconditional fuzzy propositions. A proposition or statement establishes a relationship between a value in the underlying domain and a fuzzy space. *Proposition* is one that is qualified as an “if” statement. The proposition following the if term if, is the antecedent or predicate and is an arbitrary fuzzy proposition. The proposition following the *then* term is the consequent and is also any arbitrary fuzzy proposition

If w is Z **then** x is Y

interpreted as x is a member of Y to the degree that w is a member of Z . An unconditional fuzzy proposition is one that is not qualified by an if statement.

X is Y

where X is a scalar from the domain and Y is a linguistic variable.

Unconditional statements are always applied within the model and depending on how they are applied, serve either to restrict the output space or to define a default solution space. We interpret an unconditional fuzzy proposition as X is the minimum subset of Y when the output fuzzy set X is empty, then X is restricted to Y , otherwise, for the domain of Y , X becomes the $\min(X, Y)$. The solution fuzzy space is updated by taking the intersection of the solution set and the target fuzzy set.

If a model contains a mixture of conditional or unconditional propositions, then the order of execution becomes important. Unconditional propositions are generally used to establish the default support set for a model. If none of the conditional rules executes, than a value for the solution variable is determined from the space bounded by the unconditionals. For this reason they must be executed before any of the conditionals. The effect of evaluating a fuzzy proposition is a degree or grade of membership derived from the transfer function

$$\mu \leftarrow (x \in Y) \quad (7.23)$$

where x is a scalar from the domain and Y is a linguistic variable. This is the essence of an approximate statement. The derived truth membership value establishes a compatibility between x and the generated fuzzy space. This truth value is used in the correlation and implication transfer functions to create or update fuzzy solution space. The final solution fuzzy space is created by aggregating the collection of correlated fuzzy proposition.

7.6.5 Fuzzy Implication

The *monotonic* method is a basic fuzzy implication technique for linking the truth of two general fuzzy regions. When two fuzzy regions are related through a simple proportional implication function.

if x is Y then z is W

functionally represented by the transfer function

$$z \leftarrow f((x, Y), W) \quad (7.24)$$

then under a restricted set of circumstances, a fuzzy reasoning system can develop an expected value without going through composition and decomposition. The value of the output is estimated directly from a corresponding truth membership grade in the antecedent fuzzy regions. While the antecedent fuzzy expression might be complex, the solution is not produced by any formal method of defuzzification, but by a direct slicing of the consequent, fuzzy set at the antecedent's truth level. Monotonic reasoning acts as a proportional correlating function between two general fuzzy regions. The important restriction on monotonic reasoning is its requirement that the output for the model be a single fuzzy variable controlled by a single fuzzy rule (with an arbitrary complex predicate).

The multiplication space generated by the general composition *rules of inference* is derived from the aggregated and correlated fuzzy spaces produced by the interaction of many statements. In effect all the propositions are run in parallel to create an output space that contains information from all the propositions. Each conditional proposition whose evaluated predicate truth is above the current α -cut threshold contributes to the shape of the output solution variable's fuzzy representation. There are two principal methods of inference in fuzzy systems: the min-max method and the fuzzy additive method. These methods differ in the way they update the solution variable's output fuzzy representation.

For the *min-max inference* method the consequent fuzzy region is restricted to the minimum of the predicate truth. The output fuzzy region is updated by

taking the maximum of these minimized fuzzy sets. The consequent fuzzy set is modified before it is used to set each truth function element to the minimum of either the truth function or truth of the proposition's predicate. The solution fuzzy set is updated by taking, for each truth function value, the maximum of either the truth value of the solution fuzzy set or the fuzzy set that was correlated to produce the minimum of consequent. These steps result in reducing the strength of the fuzzy set output to equal the maximum truth of the predicate and then, using this modified fuzzy region, applying it to the output by using the OR (union) operator. When all the propositions have been evaluated, the output contains a fuzzy set that reflects the contribution from each proposition.

The fuzzy additive compositional inference method updates the solution variable's fuzzy region in a slightly different manner. The consequent fuzzy region is still reduced by the maximum truth value of the predicate, but the output fuzzy region is updated by a different rule, the bounded-sum operation. Instead of taking the $\max(\mu_A[x_i], \mu_B[y_i])$ at each point along the output fuzzy set, the truth membership functions are added. The addition is bounded by [1, 0] so that the result of any addition cannot exceed the maximum truth value of a fuzzy set. The use of the fuzzy additive implication method can provide a better representation of the problem state than systems that rely solely on the min-max inference scheme.

7.6.6 Correlation Methods

The process of correlating the consequent with the truth of the predicate stems from the observation that the truth of the fuzzy action cannot be any greater than the truth of the proposition's premise. There are two principal methods of restricting the height of the consequent fuzzy set: correlation minimum and correlation product. The most common method of correlating the consequent with the premise truth truncates the consequent fuzzy region at the truth of the premise. This is called correlation minimum, since the fuzzy set is minimized by truncating it at the maximum of the predicate's truth. The *correlation minimum* mechanism usually creates a plateau since the top of the fuzzy region is sliced by the predicate truth value. This introduces a certain amount of information loss. If the truncated fuzzy set is multi-modal or otherwise irregular, the surface topology above the predicate truth level is discarded. The correlation method, however, is often preferred over the correlation product (which does preserve the shape of the fuzzy region) since it intuitively reduces the truth of the consequent by the maximum truth of the predicate, involves less complex and faster arithmetic, and generates an aggregated output surface that is easier to defuzzify using the conventional techniques of composite moments (centroid) or composite maximum (center of maximum height).

While correlation minimum is the most frequently used technique, the cor-

relation product offers an alternative and, in many ways, better method of achieving the correlation. With *correlation product*, the intermediate fuzzy region is scaled instead of truncated. The truth membership function is scaled using the truth of the predicate. This has the effect of shrinking the fuzzy region while still retaining the original shape of the fuzzy set. The correlation product mechanism does not introduce plateaus into the output fuzzy region, although it does increase the irregularity of the fuzzy region and could affect the results obtained from composite moments or composite maximum defuzzification. This lack of explicit truncation has the consequence of generally reducing information loss. If the intermediate fuzzy set is multimodal, irregular, or bifurcated in other ways this surface topology will be retained when the final fuzzy region is aggregated with the output variable's under generation fuzzy set.

7.6.7 Aggregation

The evaluation of the model proposition is handled through an aggregation process that produces the final fuzzy regions for each solution variable. This region is then decomposed using one of the defuzzification methods.

Methods of Defuzzification

Using the general rule of fuzzy inference, the evaluation of a proposition produces one fuzzy set associated with each model solution variable. Defuzzification or decomposition involves finding a value that best represents the information contained in the fuzzy set. The defuzzification process yields the expected value of the variable for a particular execution of a fuzzy model. In fuzzy models, there are several methods of defuzzification that describe the ways we can derive an expected value for the final fuzzy state space.

Defuzzification means dropping a “plumb line” to some point on the underlying domain. At the point where this line crosses the domain axis, the expected value of the fuzzy set is read. Underlying all the defuzzification functions is the process of finding the best place along the surface of the fuzzy set to drop this line. This generally means that defuzzification algorithms are a compromise with a tradeoff between the need to find a single point result and the loss of information such as a process entails.

The two most frequently used defuzzification methods are composite moments (centroid) and composite maximum. *The centroid* or center or gravity technique finds the balance point of the solution fuzzy region by calculating the weighted mean of the fuzzy region. Arithmetically, for fuzzy solution region A , this is formulated as

$$R \leftarrow \frac{\sum_{i=0}^n d_i \mu_A(d_i)}{\sum_{i=0}^n \mu_A(d_i)} \quad (7.25)$$

where d is the I^{th} domain value and $u(d)$ is the truth membership value for that domain point. A centroid or composite moment defuzzification finds a point representing the fuzzy set's center of gravity. A *maximum decomposition* finds the domain point with the maximum truth. There are three closely related kinds of composite maximum techniques: the average maximum, the center of maximum, and the simple composite maximum. If this point is ambiguous (that is, it lies along a plateau), then these methods employ a conflict resolution approach such as averaging the values or finding the center of the plateau.

Also there are other techniques for decomposing a fuzzy set into an expected value. The *average of maximum value* defuzzification method finds the mean maximum value of the fuzzy region. If this is a single point, then this value is returned; otherwise, the value of the plateau is calculated and returned. The *average of the nonzero* region is the same as taking the average of the support set for the output fuzzy region. The *far and near edge of the support set* technique selects the value at the right fuzzy set edge and is of most use when the output fuzzy region is structured as a single-edge plateau. The *center of maximums* technique, in a multimodal or multiplateau fuzzy region, finds the highest plateau and then the next highest plateau. The midpoint between the centers of these plateaus is selected.

CONCLUSION

In this chapter, we offer the reader a glimpse of the main set of tools from the emerging area of intelligent systems. While there are excellent books and other forms of literature on the subject treated, the attempt of the coverage is to offer a brief summary of the ingredients of artificial neural networks (ANN), expert systems (ES), and fuzzy logic (FL) systems.

The coverage is intended to provide the necessary background for the following two chapters. Once again, the reader is invited to consult the list of references and the annotated glossary of terms in the back of the textbook, as a source of further information.

8

Application of Artificial Intelligence to Angle Stability Studies

INTRODUCTION

The computational requirements associated with dynamic security analysis (DSA) by conventional methods are two or three orders of magnitude more than the requirements for static security analysis. Therefore comprehensive on-line DSA is infeasible in present power system control centers. The exploitation of novel techniques to solve the problem of DSA is essential for on-line implementation. The interest in application of artificial intelligence (AI) to dynamic security analysis has been increasing steadily. The following advantages are addressed through using these methods:

1. A decomposition of the on-line DSA problem into manageable subproblems.
2. The need for an integrated environment for expert systems, neural networks and conventional programs working together.
3. Identification of the subproblem for which the neural networks are most suitable.
4. Feature variables of the power system and its dynamic security attributes to be used as the training inputs to the neural network.
5. Procedure to select appropriate contingency and check security of system using expert system.

8.1 ANN APPLICATION IN TRANSIENT STABILITY ASSESSMENT

The comprehensive on-line DSA is infeasible in present power system control centers. The exploitation of novel techniques to solve the problem of DSA is essential for on-line implementation. Neural network (NN) is one of the state-of-the-art methods used to perform dynamic security analysis in power systems. The interest in NN methods has been increasing in various fields because they can work well where rule-based expert systems and conventional algorithms are inadequate. For example, quantitative rules based on subjective inputs can be better implemented as a neural network classifier which can be trained on precisely defined training examples.

8.1.1 Robust ANN-Based Transit Energy Function

Earlier in this book, the formulation of the dynamic stability problem for multi-power systems was presented. As previously stated, the process by which operators and planners monitor the behavior of power systems, screen the various random and scheduled contingencies that may occur, and recommend corrective control action(s) to maintain or regain system stability, is known as dynamic security assessment (DSA). A hybridized tool, that incorporates the beneficial aspects of a structured preserving energy function and a robust artificial neural network, has been implemented to solve the contingency screening problem of DSA. It is more accurate than conventional transient energy function (TEF) methods, since the load buses will be modeled as nonlinear voltage dependent components instead of being absorbed into the admittance matrix, while maintaining the robust ANN properties of both speed and flexibility. Development of the ANN-enhanced TEF tool involves the construction of two modules, corresponding to the training/testing mode of one operation and the recall mode of the other operation respectively.

An implementation scheme for both modules of the integrated tool is provided here. Specific emphasis is placed on the training of the robust ANN, the handling of the “over-training” issue and the evaluation of network performance.

Description of Learning Process for the Robust ANN-Based TEF

Every neural system is subject to a learning process, through which a relationship is established between a set of known inputs and a known result. The learning algorithm for the robust ANN tool is shown in Fig. 8.1. The sums of the weighted inputs at each node of the hidden layer of the net were computed. The sigmoidal activation was then applied to the sum of each hidden node in order to represent a better representation of the effects of the input stimuli. The weighted sum of the hidden nodes was then computed as the initial output of

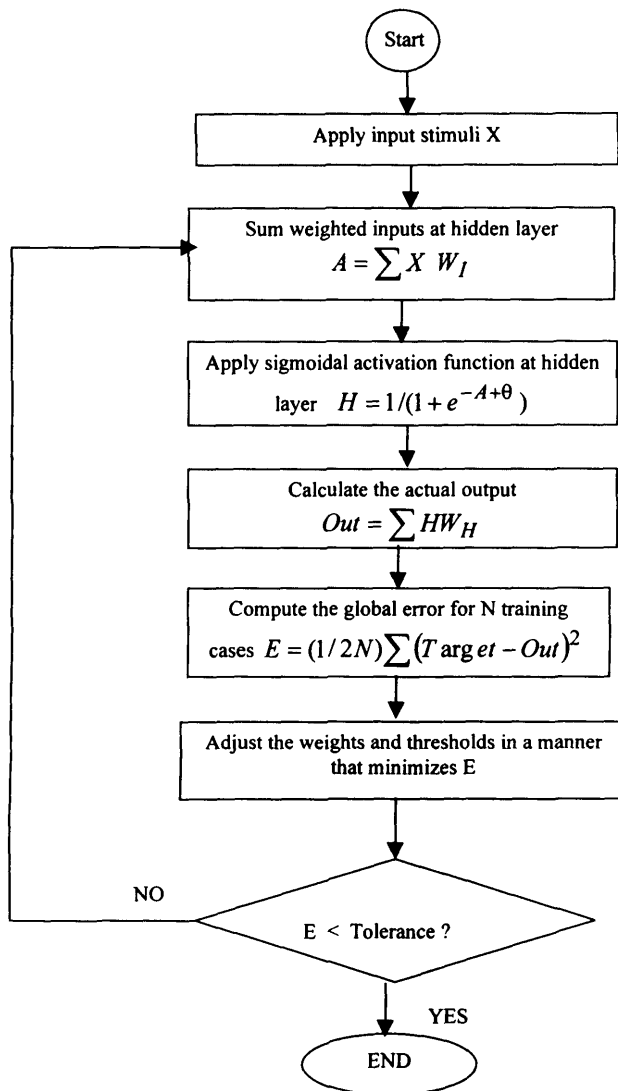


Figure 8.1 Learning algorithm for robust ANN tool.

the ANN. The error for each case was computed as the sum of the squares of the differences between the desired and the actual outputs. For each iteration, the global error was computed as the average of the sum of the errors for the cases evaluated.

The minimization routine, shown in Fig. 8.2, was then used to determine the gradient of the unknowns (weights and thresholds) with respect to the global error. These values were then used to update unknowns and the input stimuli were presented to the network over and over again, until the tolerance limit was satisfied. The final values of the weights and thresholds were then used by the recall module of the ANN enhanced energy function (TEF) tool to map the relationship between components of the energy of the system and the stability/instability of the system.

The data generated by the TEF program was then presented to the robust ANN, until the specified criteria was satisfied. Approximately 1000 cases were evaluated, with close to 60% of those dedicated to training the ANN tool. The reason for the vast number of training cases was to ensure that a diverse representation of the system, under various conditions, was provided to the ANN.

Again, the learning algorithm utilized a conjugate gradient search procedure to compute the minimum value of the error function and thus optimize the interconnection weights and threshold values. The initial weights and the threshold values were set to random values between -0.5 and $+0.5$.

The goal of any ANN application is to provide an accurate response to a given stimulus in a timely and efficient manner. Therefore, simple network architecture was utilized as a base case and more complex topologies were evaluated in turn. The accuracy of the training session was defined by a user-specified tolerance of 10^{-4} . Once the convergence criteria had been realized the network was tested using data not presented during training. The results of the testing phase demonstrated the ability of the ANN to generalize.

An additional routine was included to prevent the network from “over-training” or becoming too specific to the training set. This was accomplished by evaluating the global error function with respect to the test data (data not used for training) subject to the weights and thresholds at every twenty-fifth iteration of the learning process. If the global error of the test data increased from one check point to the next then the training process was stopped.

Recall Module

For the recall mode of operation the TEF program and the robust ANN were integrated into a unified program to compute the security state of the given system for a selected contingency. The initial prefault conditions were computed using a generic Newton–Raphson load flow method, as before. The clearing energy were calculated in the traditional manner to represent the conditions of the power system at fault clearing time. These values were then applied to the Robust ANN, using the weights and thresholds obtained in the training session, to determine the security state of the power system. A description of the algorithm for the recall module of the robust ANN-based TEF tool is presented in Fig. 8.3.

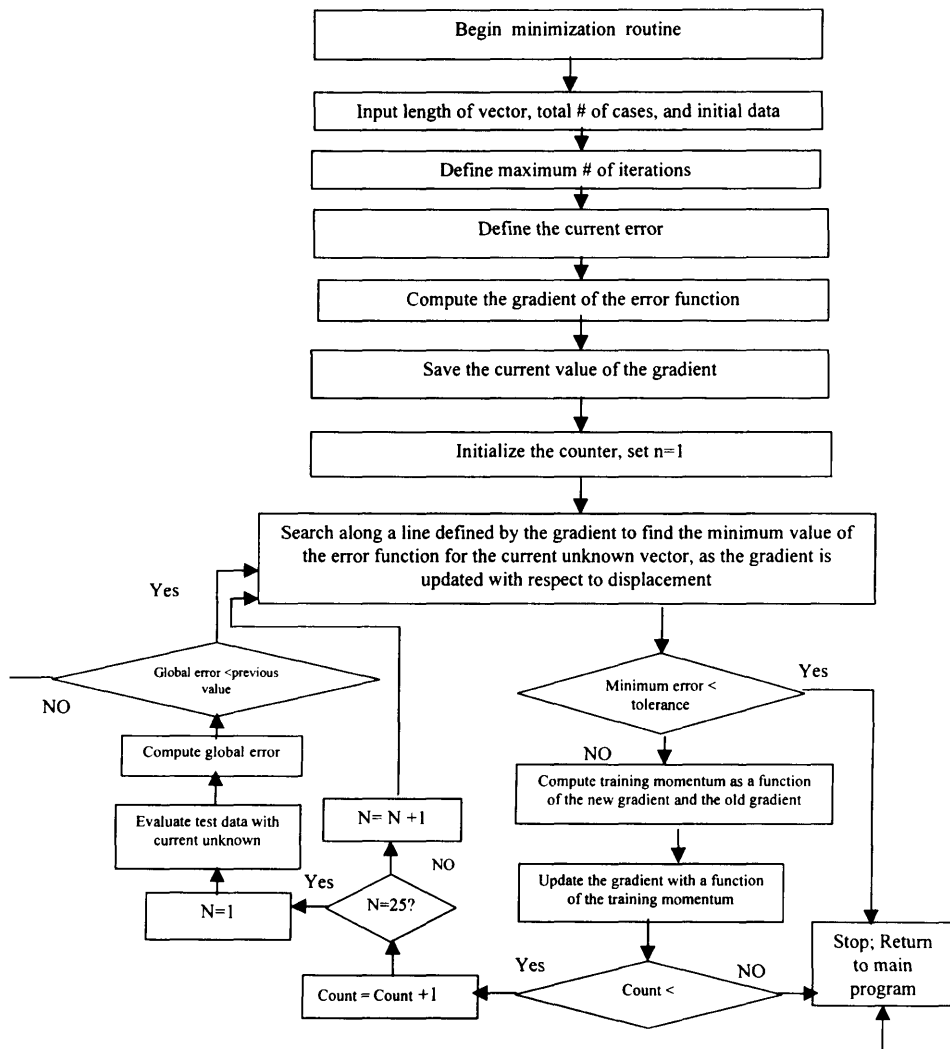


Figure 8.2 Minimization routine.

The results obtained by the training procedure were presented to the robust ANN as training data, with the clearing energy functioning as the input stimuli and the stability assessment computed by the TEF method functioning as the desired output value. The input stimuli were weighted and summed at the hidden layer of the net. The sigmoidal activation function was then applied to each

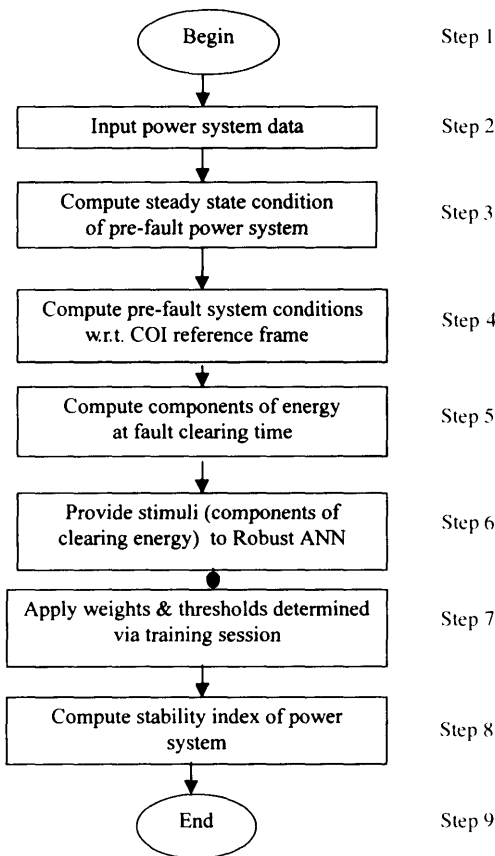


Figure 8.3 Recall Module of the robust ANN-based TEF tool.

hidden node, and the resulting values at each hidden node were weighted and summed as the stability index of the system. A block diagram of the recall module 3 of the robust ANN-based TEF tool is shown in Fig. 8.3.

Steps 1–4 of Fig. 8.3 follow the procedure for computation of the clearing energy. In step 5 the six components of the clearing energy were applied to the input layer of the robust ANN as shown in Fig. 8.4. The inputs were then multiplied by the interconnection weights computed during and summed at the hidden layer. The sigmoidal activation function was then applied to summation at each hidden node, subject to the threshold value determined by the training session. The final values of each hidden node were then weighted and summed to compute the stability index of the power system for the given contingency

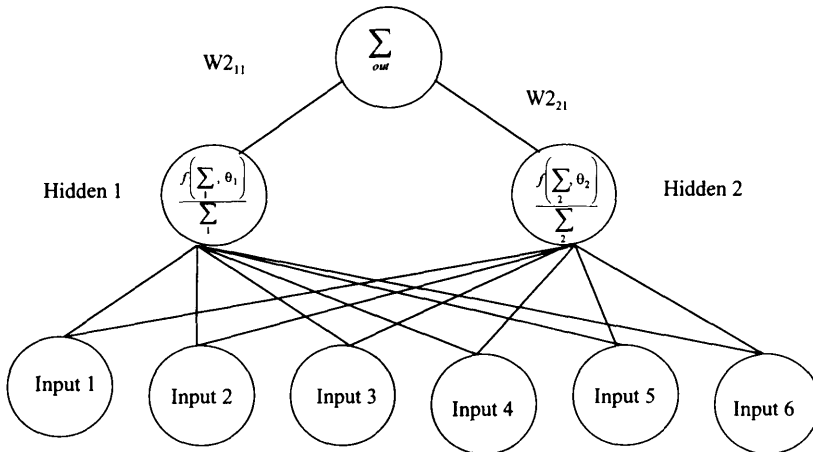


Figure 8.4 Robust ANN-based TEF network architecture.

The number of iterations required for training and the percentage of correct/incorrect classifications were the contributing factors in the determination of the optimal network architecture and significant input features for the solution of the robust ANN-based TEF.

8.1.2 Results

The ANN-enhanced TEF program defined in Sec. 8.2.2 was tested on the IEEE 39-bus 10-generator power system. As previously stated, simulation by the ANN-enhanced TEF program involved two stages of work. In the first stage simulation studies were conducted on the TEF program to collect data defining the effects of close to 1000 different contingencies on the IEEE 39-bus test system. A robust learning algorithm was then used to synthesize the relationship between the faulted systems, caused by the various contingencies, and the post-fault system, by optimizing the interconnection weights and thresholds in the network. In the second stage the robust ANN was integrated into the TEF tool to alleviate the computational burden caused by the determination of the critical energy.

In this section the ability of a robust ANN-based TEF tool to solve the DSA problem for electric power systems is demonstrated. The results of studies on the IEEE 39-bus test system using robust ANN-based TEF tool, were validated via comparison to results from an industrial grade TEF program and conventional time domain simulation studies. The comparison of results is preceded by a description of the IEEE 39-bus system.

The analysis of the results presented here clearly demonstrates the ability of the ANN-enhanced scheme to significantly decrease the time necessary for dynamic security assessment.

Input Data and System Diagram for the IEEE 39-Bus Power System

In order to verify the accuracy of the TEF tool, the results of case studies on the IEEE 39-bus system using the robust ANN-based TEF were compared to results generated by an industrial grade program on the same system. The power system generation and load data for the IEEE 39-bus network are presented in Tables 8.1 and 8.2. A schematic diagram of the 39-bus power system is provided in Fig. 8.5.

Comparison of Robust ANN-Based TEF to Classical TEF

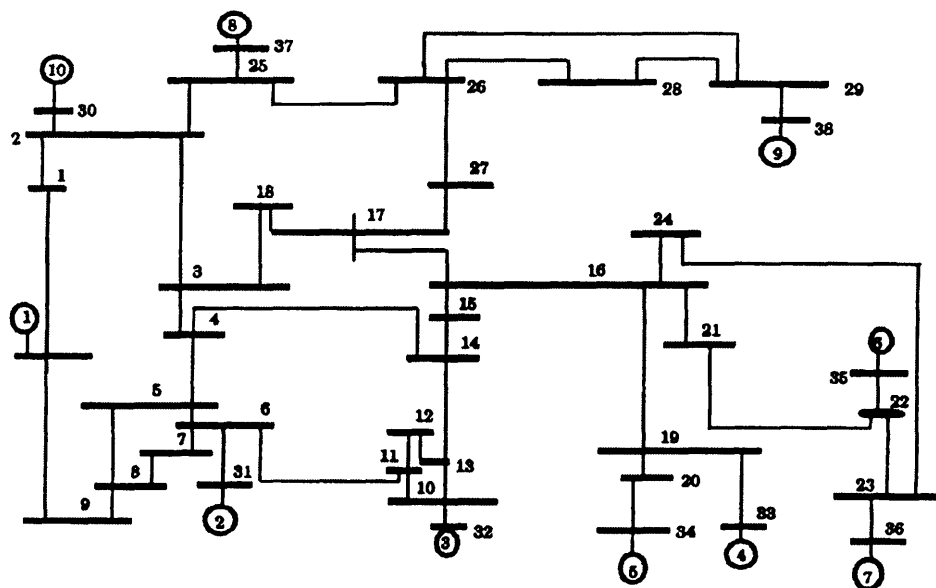
The robust ANN-based TEF procedure was used to solve the contingency screening problem for DSA. Validation of the security assessment determined by the robust ANN-based TEF was achieved through comparison to the results generated using the industry grade TEF3.0 program, developed by Ontario Hy-

Table 8.1 39-Bus System Load Data

| Load no. | Bus no. | P_d (MW) | Q_d (MVAR) |
|----------|---------|------------|--------------|
| 1 | 3 | 322.00 | 2.40 |
| 2 | 4 | 500.00 | 184.00 |
| 3 | 7 | 233.80 | 84.00 |
| 4 | 8 | 522.00 | 176.00 |
| 5 | 12 | 8.50 | 88.00 |
| 6 | 15 | 320.00 | 153.00 |
| 7 | 16 | 329.40 | 32.30 |
| 8 | 18 | 158.00 | 30.00 |
| 9 | 20 | 680.00 | 103.00 |
| 10 | 21 | 274.00 | 115.00 |
| 11 | 23 | 247.50 | 84.60 |
| 12 | 24 | 308.60 | -92.20 |
| 13 | 25 | 244.00 | 47.20 |
| 14 | 26 | 139.00 | 17.00 |
| 15 | 27 | 281.00 | 75.50 |
| 16 | 28 | 206.00 | 27.60 |
| 17 | 29 | 283.30 | 26.90 |
| 18 | 31 | 9.20 | 4.60 |
| 19 | 39 | 1104.00 | 250.00 |

Table 8.2 39-Bus System Generator Data

| Gen no. | Bus no. | P_G (MW) | $ V $ (Volt) |
|---------|---------|------------|--------------|
| 1 | 39 | 1000.00 | 1.0300 |
| 2 | 31 | N/A* | 0.9820 |
| 3 | 32 | 650.00 | 0.9831 |
| 4 | 33 | 632.00 | 0.9972 |
| 5 | 34 | 508.00 | 1.0123 |
| 6 | 35 | 650.00 | 1.0493 |
| 7 | 36 | 560.00 | 1.0635 |
| 8 | 37 | 540.00 | 1.0278 |
| 9 | 38 | 830.00 | 1.0265 |
| 10 | 30 | 250.00 | 1.0475 |

**Figure 8.5** Diagram of 39-bus power system.

dro under EPRI project RP2206-1, and classical time domain simulation studies using the trapezoidal numerical integration technique. A comparative analysis of the results of simulation tests on the IEEE 39-bus system with respect to accuracy is presented here.

A three-phase fault occurring at generator 30, was used as a basis for comparison. The fault clearing time and assessment for each case are listed below in Table 8.3.

Evaluation of the results in Table 8.3 clearly demonstrate that the security assessments provided by the robust ANN-based TEF tool are generally in good agreement with the security assessments provided by the results of conventional energy function and time domain simulation methods.

Testing of Robust ANN-Based TEF on IEEE 39-Bus System

In order to generate enough training/testing data for the robust ANN the effects of over 1000 contingencies were tested on the IEEE 39-bus system and evaluated using the TEF method. Close to 60% of these cases were randomly selected for training with the remaining 40+% reserved for testing. The contingencies represented three-phase faults at the terminal of each generator in the system, with fault clearing times varying between .0001 seconds and 0.5 seconds. Each input file contained the energy components at clearing time and the desired final output for each case.

In complex pattern classification problems, such as this one, the success of the training session is highly dependent on the initial weights and thresholds and the topology of the network. For all of the studies conducted the weights and thresholds were initialized at random values between -0.5 and +0.5. Since there is no general rule for the determination of the optimal number of nodes in the hidden layer many topologies were evaluated.

Table 8.3 Comparison of Results for 3 ϕ Fault at Bus 30

| Critical clearing time, t_c | TEF 3.0 ΔW | TEF 3.0 assessment | Robust ANN-based TEF ΔW | Robust ANN-based TEF assessment |
|-------------------------------|--------------------|--------------------|---------------------------------|---------------------------------|
| 0.1 | 5.9047 | Stable | 0.102538 | Stable |
| 0.12 | 5.3756 | Stable | 0.102539 | Stable |
| 0.14 | 4.7045 | Stable | 0.102540 | Stable |
| 0.16 | 3.8742 | Stable | 0.102542 | Stable |
| 0.18 | 2.8703 | Stable | 0.102543 | Stable |
| 0.20 | 1.6831 | Stable | 0.102543 | Stable |
| 0.22 | 0.1702 | Stable | 0.102544 | Stable |
| 0.24 | -1.2373 | Unstable | 0.867565 | Unstable |

Table 8.4 Description of Test Cases

| Case | No. of variables in input vector | Description of test case |
|------|----------------------------------|--|
| A | 6 | Input vector contains all six variables |
| B | 5 | Kinetic energy component excluded from the input vector |
| C | 5 | Component of potential energy w.r.t. position excluded from the input vector |
| D | 5 | Component of potential energy consumed in the real power load excluded from the input vector |
| E | 5 | Component of potential energy consumed in the reactive power load excluded from the input vector |
| F | 5 | Component of potential energy consumed in the generator reactance excluded from the input vector |
| G | 5 | Component of potential energy consumed in the transmission line excluded from the input vector |

Selection of Relevant Features of Robust ANN-Based TEF

In all, twenty-nine different network architectures were trained and tested to determine the optimal topology for the ANN-enhanced TEF tool. In order to determine which of the six components of the energy of the faulted system featured significantly in the assessment of system security, each of the variables was alternately deleted from the training/testing set. The studies are defined as cases A–G for simplicity (see Table 8.4). The training performance (number of presentations of input data) and accuracy (testing error percentage) were used to evaluate the studies.

A decrease in the number of presentations for training coupled with similar or improved classification of the test data would give a good indication that a certain component did not feature prominently in the learning process, and thus in the assessment of security.

The training/testing results (Tables 8.5–8.11) clearly showed that the net-

Table 8.5 Case A

| Architecture | No. of presentations | Testing error % |
|--------------|----------------------|-----------------|
| 6-2-1 | 504 | 0.45 |
| 6-3-1 | 18096 | 5.86 |
| 6-4-1 | 252 | 19.14 |
| 6-5-1 | 5014 | 4.95 |

Table 8.6 Case B

| Architecture | No. of presentations | Testing error % |
|--------------|----------------------|-----------------|
| 5-2-1 | 387 | 0.68 |
| 5-3-1 | 60000 | 0.68 |
| 5-4-1 | 24641 | 3.83 |
| 5-5-1 | 40669 | ~0 |

works with two neurons in the hidden layer generally converged with the fewest number of presentations. In most cases, testing accuracy was significantly affected by the exclusion of any one of the input variables. However, when the kinetic energy component was excluded from the training set (Case B [Table 8.6]) there was a clear improvement in the speed of the network, while testing accuracy was maintained at close to 100%. Thus, the optimal network architecture for the IEEE 39-bus system was the configuration with the kinetic energy component deleted from the training set and only two neurons in the hidden layer.

Therefore, it was established that the kinetic energy component was not a major contributor to the assessment of the dynamic stability of the 39-bus system, when using the robust ANN-based TEF tool. Evaluation of the results of the clearing energy module on a 3-bus 2-generator system, as well as the 39-bus 10-generator IEEE test system provided some interesting observations. In the 2-generator system the kinetic energy term was one of three components that dominated the SPEF at fault clearing time. For a 3-phase fault, lasting for a duration of 0.2 seconds, on the first machine of the system the magnitude of the kinetic energy term comprised close to 28% of the magnitude of the total energy. In comparison, for a 3-phase fault lasting 0.2 seconds on the largest machine in the 39-bus system the magnitude of the kinetic energy component of the SPEF at fault clearing time only constituted 0.002% of the magnitude of the total clearing energy term (Table 8.12). This may be partially due to the fact that the kinetic energy component is computed as a function of the ratio of the

Table 8.7 Case C

| Architecture | No. of presentations | Testing error % |
|--------------|----------------------|-----------------|
| 5-2-1 | 754 | 17.79 |
| 5-3-1 | 3960 | 19.14 |
| 5-4-1 | 1359 | 9.91 |
| 5-5-1 | 13695 | ~0 |

Table 8.8 Case D

| Architecture | No. of presentations | Testing error % |
|--------------|----------------------|-----------------|
| 5-2-1 | 846 | 16.44 |
| 5-3-1 | 46247 | 20.05 |
| 5-4-1 | 3120 | 6.53 |
| 5-5-1 | 573 | 6.98 |

Table 8.9 Case E

| Architecture | No. of presentations | Testing error % |
|--------------|----------------------|-----------------|
| 5-2-1 | 1069 | 16.22 |
| 5-3-1 | 1678 | 5.63 |
| 5-4-1 | 10373 | 13.51 |
| 5-5-1 | 756 | 19.82 |

Table 8.10 Case F

| Architecture | No. of presentations | Testing error % |
|--------------|----------------------|-----------------|
| 5-2-1 | 60000 | 3.15 |
| 5-3-1 | 60000 | 3.38 |
| 5-4-1 | 60000 | 5.86 |
| 5-5-1 | 58810 | ~0 |

Table 8.11 Case G

| Architecture | No. of presentations | Testing error % |
|--------------|----------------------|-----------------|
| 5-2-1 | 1304 | 24.77 |
| 5-3-1 | 60000 | 20.05 |
| 5-4-1 | 410 | 12.16 |
| 5-5-1 | 3144 | 0 |

Table 8.12 Magnitude of Components of TEF at Fault Clearing Time

| System | W_1 | W_{12} | W_{22} | W_{23} | W_{24} | W_{25} |
|--------------|----------|----------|----------|----------|----------|----------|
| 3-bus | 8.72 E-2 | 0.2001 | 9.78 E-6 | 2.73 E-2 | 1.26 E-3 | 1.79 E-4 |
| 2-generator | | | | | | |
| 39-bus | 1.90 E-5 | 3.50 E-5 | 9.54 E-2 | 2.38 E-2 | 0.9338 | 6.35 E-2 |
| 10-generator | | | | | | |

moment of inertia of the critical generator, M_k , to the moment of inertia of the entire system, M_t . Therefore, for systems containing a greater number of generators, the kinetic energy term will decrease in magnitude.

The dominance of each component in the TEF term had a significant effect on the selection of the feature variables for an assessment of system stability. Therefore, a more extensive study is needed, with detailed machine models and a variety of test systems, before a general statement can be made on the feature variables for DSA of electric power systems by energy function techniques.

8.1.3 ANN-Based Critical Clearing Time Assessment

Critical clearing time (CCT) – t_c is defined as maximal fault duration for which the system remains transiently stable. Mathematically, CCT is a complex function of prefault system conditions (operating point, topology, system parameters), fault structure (type and location) and postfault conditions that themselves are dependent on the protective relaying policy employed. It would be highly desirable to define this relation analytically but the diversity of variables involved makes this task extremely complicated.

In practice, CCT can be obtained in one of two ways: (1) by trial and error analysis of system postdisturbance equations or (2) by integrating fault-on equations and checking the value of the Lyapunov or energy function until it reaches a previously determined critical level V_c . In either approach, a numerical integration process is involved. From the point of view of on-line implementations of CCT assessment, this presents a major difficulty.

Application of ANNs is a promising alternative. The capabilities of neural-nets enable them to readily synthesize the complex mappings that transform the numerous input attributes or features of a power system into the single valued space of CCTs.

We examine the generalization capabilities of neural nets, focusing on their ability to deal with a large range of operating conditions and changes in network topology. For CCT assessment, each synchronous generator is represented by three features derived from the measurable parameters of the power system.

The first feature, A_{1i} , is the rotor angle relative to the inertial center of angle (COA) measured at the instant of fault initiation.

$$A_{1i} = \delta_i(0^+) - \delta_o(0^+) \quad i = 1, 2, \dots, N \quad (8.1)$$

The second feature, A_{2i} , represents the acceleration parameter of the synchronous generator during the fault. Because the mechanical output in the period immediately following the disturbance remains unchanged, the machine fault dynamics may be described by:

$$A_{2i} = \frac{P_{mi} - P_{fi}}{M_i} \quad i = 1, 2, \dots, N \quad (8.2)$$

where P_{fi} is the output of the i^{th} generator during the fault, when it remains almost constant.

The third feature, A_{3i} , is proportional to the kinetic energy each generator stores during the fault.

$$A_{3i} = \frac{(P_{mi} - P_{fi})^2}{M_i} \quad i = 1, 2, \dots, N \quad (8.3)$$

It is important to observe that all three attributes can be evaluated without solving any differential equations. They are expressed in terms of the operating parameters of the system prior to the fault and include the structure of the fault. Selected features are related to the fault on dynamics, however, and thus can provide a good representation of system behavior during the first transient swing.

The example four-machine power system shown in Fig. 8.6 will be used to illustrate an ANN approach to CCT assessment. Three-phase short-circuit faults are simulated at line 2-3 near bus 3. The fault-clearing policy is to restore the prefault system topology. Two different system topologies are used to generate the training set patterns: topology 1 with all seven lines in service; topology 2 with the line 3-4 removed. Fifteen different loading conditions are selected for each topology, all with the loading level of the system in the range 0.6–2.0 relative to the nominal operating point. The power factors of the loads are maintained at their nominal values.

The training set consists of 30 twelve-dimensional patterns (4 generators times 3 features) labeled with corresponding CT values. The latter are obtained by numerically integrating the posdisturbance system equations.

The neural network used for this study is shown in Fig. 8.7. It consists of an input layer with twelve units and a single hidden layer with six units. After training, the mapping learned by the net is represented by the weights and

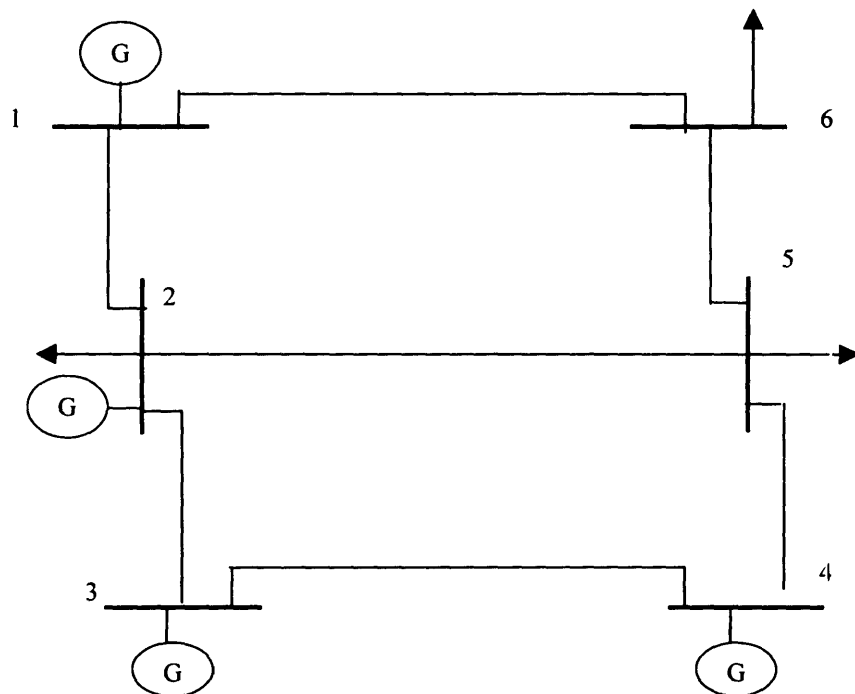


Figure 8.6 One-line diagram of the four-machine power system.

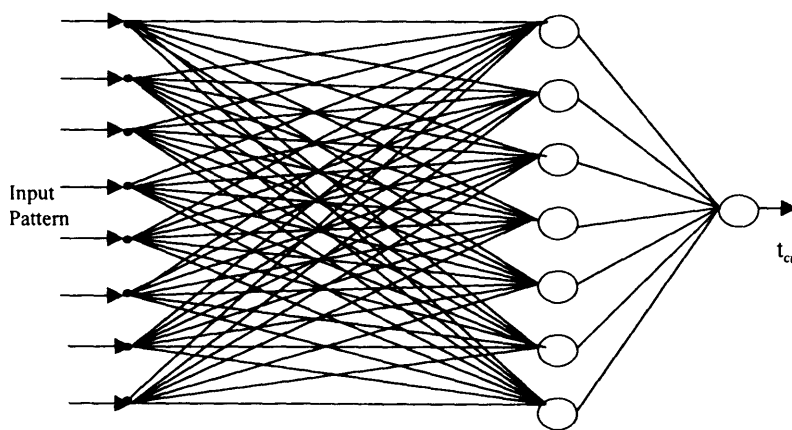


Figure 8.7 Multi-layered neural-net based assessment of critical clearing time.

thresholds; the least squares error was reduced to 2×10^{-4} after 5010 presentations of the training set. The other parameters of the learning process were the learning rate $\eta = 0.3$ and the momentum $\xi = 0.4$.

The performance of the neural network in new test cases, i.e., cases not seen during the training session, is illustrated in Table 8.13. Examples 1–7 correspond to power system topology 2, a topology used in the learning session. Examples 8–20 correspond to a new system topology obtained by removing lines 2–5.

The critical clearing times estimated by the neural network agree with the analytical values. Provided that a few different topologies appear in the training session, the network is able to operate generally, handling new topologies as well as new operating conditions. This performance improves over conventional nonadaptive pattern recognition in which every new topology requires a completely new set of discrimination rules.

Table 8.13 Comparison of CCTs Obtained with Numerical Integration of Differential Equations (Actual CCT) and Estimated with a Neural Net (Estimated CCT)

| Example | Load level pu | Actual CCT sec | Estimated CCT sec |
|---------|------------------|-------------------|----------------------|
| 1 | 0.65 | 0.59 | 0.59 |
| 2 | 0.85 | 0.49 | 0.49 |
| 3 | 0.95 | 0.46 | 0.45 |
| 4 | 1.15 | 0.39 | 0.39 |
| 5 | 1.45 | 0.33 | 0.33 |
| 6 | 1.65 | 0.29 | 0.29 |
| 7 | 1.95 | 0.25 | 0.25 |
| 8 | 0.80 | 0.53 | 0.53 |
| 9 | 0.90 | 0.49 | 0.49 |
| 10 | 1.00 | 0.46 | 0.46 |
| 11 | 1.10 | 0.43 | 0.43 |
| 12 | 1.20 | 0.40 | 0.40 |
| 13 | 1.30 | 0.38 | 0.38 |
| 14 | 1.40 | 0.36 | 0.36 |
| 15 | 1.50 | 0.34 | 0.34 |
| 16 | 1.60 | 0.32 | 0.32 |
| 17 | 1.70 | 0.31 | 0.31 |
| 18 | 1.80 | 0.29 | 0.29 |
| 19 | 1.90 | 0.28 | 0.25 |
| 20 | 2.00 | 0.23 | 0.22 |

8.2 A KNOWLEDGE-BASED SYSTEM FOR DIRECT STABILITY ANALYSIS

Identifying the safe operating regimes requires analysis of a large number of combinations of outages and the associated derivation and manipulation of the massive data and related sensitivity information. It is an extremely difficult and time consuming process when conventional computation methods are used. Such methods are implemented in the form of traditional computer programs with no direct provision for exploiting the operator knowledge of the system and without utilizing proper reasoning techniques and inferring logics (expert systems) to process such "operator knowledge." The use of expert systems in TEF method applications would therefore enable the security assessment programs to perform the required cognitive tasks.

The expert system methodology appears to be uniquely suited to take advantage of the following important attributes of the TEF method: (1) The ability to generate, organize, store, and retrieve a large amount of information required for power system transient analysis to be used for planning and operating a stability-limited power network, and (2) to use this information for intelligent decision-making to assess the dynamic security status of a given power network.

8.2.1 Expert System Development in DSA

In order to develop a TEF-expert system, the following information is needed.

- (a) General formation and application concepts
- (b) TEF knowledge base structure and configuration
- (c) Application rules

In dynamic security assessment, the knowledge base and application rules should include the contingency data and operating security information. Therefore, the rules can be constructed as follows:

- (1) Rules derived based on theoretical concepts
- (2) Rules and data constructed from detailed off-line computation
- (3) Rules established from operator knowledge and experience
- (4) Rules and data collected from previous on-line computed scenarios
- (5) Rules established from analyst knowledge and experience in the analysis of multiple TEF cases and comparisons with comparable numerical integration cases.

8.2.2 Role of the Expert in DSA

At present, most of the work in DSA is performed off-line. It requires an extensive amount of interaction from the expert who uses a time-domain simulation

program to identify the response of the power system to a number of postulated disturbances. The role of the expert involves:

- (a) Significant amount of human interaction
- (b) Use of human intuition, judgement and expertise and cognitive skills repetitively
- (c) Routine actions by the engineer or system operator

Select the Base Case

In the operations planning environment, the base system configuration is obtained from real-time operating conditions or by manual adjustments to a full system base case. The need for the study is identified by the system operator whenever the system configuration reaches a state for which operating limits are not prespecified by previous studies. The operator may also initiate a study before approving scheduled maintenance on major equipment.

Of all the possible study cases, the engineer selects only a few as base cases worthy of detail study. The base case selected represents a credible worst case scenario during the period of interest.

Selecting the Relevant Contingencies

For a base case obtained in the previous section, the engineer identifies appropriate credible outages which are potentially dangerous to the system based on past experience, and system configuration deviations from the full system and base case power flow solution. In general, the contingencies most commonly studied involve the following:

- Loss of a single generator
- Three-phase-to-ground fault cleared by the primary protection by opening the faulted line
- Single-phase-to-ground fault cleared by backup protection by delayed opening resulting in multiple equipment outages
- Three-phase-to-ground fault cleared by the primary protection by opening multiple transmission lines sharing the same transmission towers.

It is impossible to enumerate all possible outages. Therefore, only the most severe credible outages of important components of the system are considered. The dynamically important components in the system are identified by the explicit or implicit use of rules.

Operator Actions

After examining the results for a number of selected case studies and contingencies the engineer determines the operating constraints for the system such that

they will be valid for a number of operating conditions not explicitly studied. The system operators are required to operate the system within the security constraints.

In the cases of minor security violations for which timely postcontingency corrective actions are available, the operator may choose to continue the operation of the system in its current condition. In the cases of other security violations, the operator may choose to do the following:

- Reschedule generation
- Reschedule interchanges
- Arm or disarm remedial actions such as generation rejection, load shedding, and system separation.

8.2.3 Rule Base Structure

Based on the acquired knowledge, it is found that solution of the dynamic security assessment problem fits naturally with a rule-based system combined with procedures. Therefore, the rule-based technique is applied to demonstrate the feasibility of an expert system approach. In the process of knowledge base development, the attempt was made to maintain generality of rules while minimizing the system specific features.

Modules of Rule Base Structure

There are five modules in the developed rule base. Each module contains a number of rules performing a specific task in the dynamic security assessment. For convenience, each module of the rule base will be referred to as a "task."

First Task: Monitor System Conditions

Analyze system operation conditions for given system status. Check if the changes in system conditions since the last assessment are significant enough to warrant a new assessment. If there are significant changes then DSA is needed. The decision processes involved here have to rely completely on the precontingency steady-state condition of the power system and its relationships with previously analyzed base case(s).

Second Task: Contingency Analysis and Selection

Select contingencies relevant to the current system state. Rules in this task include examining the importance of each component to the dynamic security of the system and selecting the outage of the more important components for further study. Check whether the current system state is secure with respect to a given contingency. This task may use available information regarding the base case, given contingency, and the transient condition of the system immediately following fault-clearing.

Third Task: Acceptability Judgement

Using results of security and invulnerability assessment, rules in this task can make a judgement on the overall acceptability of the operating conditions. Another function of rules in this task is to perform a direct judgement of acceptability based on qualitative assessment of the system operating point (generation, load, and transmission), the external condition (weather, etc.), and disturbance (outages, etc.), and reactions (line tripping, etc.). Rules for the direct acceptability judgement in the first task provide a sufficient condition for acceptability.

Fourth Task: Security and Invulnerability Assessment

If the direct acceptability assessment task does not give a positive answer, then the next task will be initiated. This task contains rules, which compare security margins to the specified thresholds. The security margins are obtained by comparing the current operating value of a critical parameter such as line flow to the maximal flow value at which instability occurs. Invulnerability assessment is also performed in this task. At present, invulnerability refers to a "sensitive" operating condition that involves a severe drop in security margin in terms of the transient energy function (TEF) if a perturbation of the operating condition occurs.

Fifth Task: Remedial Actions

This is a collection of rules, which can be used to suggest change in the operating conditions in order to regain system security. If the security margin drops to a negative value (or below a specific threshold), then controls must be chosen to eliminate the abnormality. The selection of control is based on sensitivity of the control with respect to the security margin and the amount of available controls. The controls necessary to fully correct the insufficiency of security margin are suggested.

In addition to the tasks mentioned above, it is necessary to modify the security knowledge base through adding significant new information about the contingency and the initial operating conditions to the existing security archive in the knowledge base. Modification occurs only if the present analysis requires a change in the security region of the system as implied by the knowledge already available in the knowledge base. The structure of DSA with rule base is presented in Fig. 8.8.

Task 1: System State Monitor

This task consists of rules 1., 1.1, and 1.2. It serves as a fast monitor of the system base state. This task can only give a "yes" answer or a "not-sure" answer. If the answer is "not-sure," further analysis is needed, such as analysis of Tasks 2 and 3.

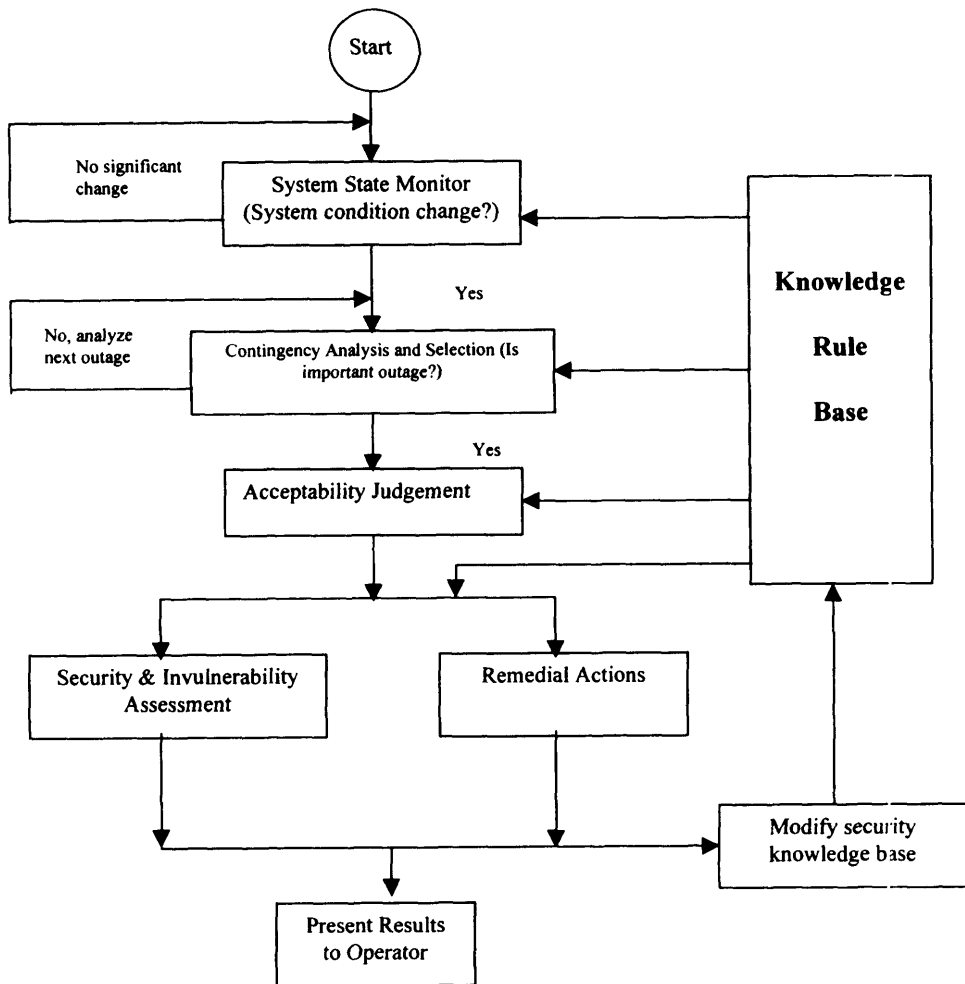


Figure 8.8 DSA structure with rule base.

1. IF the system S is in the base case.
THEN S certainly satisfies the dynamic security requirement.
Data: System base case data.
Output: S_dynamic security.
 - 1.1 IF system condition has only a small change around the base case.
THEN system can maintain dynamic security.

- Data: System base case data with small change.
 Output: S_dynamic security.
- 1.2 IF system condition has significant change.
 THEN system may not satisfy the dynamic security criterion, and further analysis is needed.
 Data: System base case data with big change.
 Output: System may have the problem of dynamic security.

Task 2: Contingency Analysis and Selection

This task also consists of rules 1., 1.1, and 1.2. This task is involved if the system condition analysis in Task 1 gives a “not-sure” answer under the significant change of system condition, especially under the outage cases. It offers a fast analysis of the system contingency scenarios. Only the important contingency scenarios are selected for further dynamic security analysis.

1. IF the outage scenario OC is not important.
 THEN OC will not be selected.
 Data: System data and outage parameters.
 Output: OC_neglected.
- 1.1 IF the contingency performance index (PI) is less than the threshold (PI_T) for a given outage scenario OC.
 THEN OC will not be selected.
 Data: system data, outage parameters, PI, and PI_T .
 Output: OC_neglected.
- 1.2 IF the contingency performance index (PI) is greater than the threshold (PI_T) for a given outage scenario OC.
 THEN OC will be selected for further dynamic security analysis.
 Data: system data, outage parameters, PI, and PI_T .
 Output: OC_selected.

Task 3: Acceptability Judgement

This task can be considered as having 2 subtasks. One subtask consists of the rule numbered 2 and its subordinates (i.e., rules 2.1, 2.1.1 and 2.1.2, 2.2 and 2.2.1). It serves as a faster analyzer of the system conditions (e.g., weather, load trend, etc.), and tries to draw a conclusion about acceptability. This task can only give a “yes” answer or a “not-sure” answer. If the answer is “not-sure,” the other subtask (represented by rules 1., 1.1, and 1.1.1) will be invoked. This task gives a “yes/no” answer to the acceptable or unacceptable question depending on the output of Task 4.

1. IF every operating condition in C satisfies the security and invulnerability constraints and policies,
THEN C is acceptable.

Data: security and vulnerability evaluation results (satisfied_ or_not), all cases in C, policy descriptions

Output: C_acceptability

- 1.1 IF SF(C) = yes and CF-SF(C) is greater than a threshold for every operating condition in C.

THEN the system satisfies the security and invulnerability constraints.

Data: SF(C), CF-SF(C) for all cases in C, threshold.

Output: security, invulnerability constraints satisfied or not.

- 1.2 IF every operating condition in C is secure and invulnerable
THEN SF(C) = yes.

Data: "secure" or "vulnerability" status of all cases in C.

Output: SF(C).

2. IF (Mode of Operation M is NORMAL, and Disturbance D is medium or large), or (M is High-Risk and Disturbance is Small).

THEN C is acceptable.

Data: Mode of Operation, Disturbance.

Output: C acceptability.

- 2.1 IF System S is SUSCEPTIBLE and External condition E is THREATENING THEN the Mode of Operation M is High-Risk.
Otherwise, M is NORMAL.

Data: S, E.

Output: M.

- 2.1.1 IF LoaD (LD) is STEADY and Transmission (TR) is NORMAL, or LoaD is PICK UP and GeneratioN (GN) is LOW and TR is Normal, or LoaD is STEADY and GeneratioN (GN) is LOW and TR is WEAK and Generation Inertia (GI) is LARGE.

THEN the System S is ROBUST.

Otherwise, it is SUSCEPTIBLE.

Data: LD, TR, GN, GI.

Output: S.

- 2.1.2 IF WEather (WE) is OF CONCERN,
or WEather is OF NO CONCERN and INterconnection (IN) has INSUFFICIENT SUPPLY.

THEN External Condition E is THREATENING.

Data: WE, IN.

Output: E.

- 2.2 IF the UPSET is MINOR and the REACTION is ADEQUATE.
 THEN the Disturbance is Small.
 Date: UPSET, REACTION.
 Output: D.
- IF the UPSET is SEVERE and the REACTION is ADEQUATE.
 THEN the Disturbance D is Medium.
 Data: UPSET, REACTION.
 Output: D.
- IF the UPSET is MINOR and the REACTION is INADEQUATE.
 THEN the Disturbance D is Medium.
 Data: UPSET, REACTION.
 Output: D.
- IF the UPSET is SEVERE and the REACTION is INADEQUATE.
 THEN the Disturbance D is Large.
 Date: UPSET, REACTION.
- 2.2.1 IF the Corrective Action is LINE TRIPPING and the TIMING is not FAILED, or the Corrective Action is GENERATION REJECTION and TIMING is ON TIME.
 THEN the Reaction R is ADEQUATE.
 Otherwise, it is INADEQUATE.
 Data: Corrective Action, Timing.
 Output: R.

Task 4: Security and Vulnerability Assessment

Rules for Security Assessment

This task is invoked if the system condition analysis in Task 3 gives a “not-sure” answer. As the name implies, this task consists of two parts. In one the security is assessed based on the use of energy margin (or security margin). In the other part, the sensitivity of the energy margin with respect to parameter variations is considered, i.e., how vulnerable the system is to parameter changes.

1. IF a family of regimes in a class have not crossed zero at a parameter value I, and the total probability of this family is higher than or equal to p.
 THEN the system is secure with probability p for this class of contingencies as long as the parameter is bounded by the value I.
 Data: probabilities of the given class of contingencies, I, p, family of regimes.
 Output: secure w Prob p.
- 1.1 IF an operating regime crosses the parameter (horizontal) axis at

a value IMAX.

THEN the system operating point is secure as long as the parameter is less than IMAX.

Data: IMAX, zero-crossing of the given regime.

Output: Operating point secure or not.

2. IF the normalized energy margin (NEM) is greater than a threshold (zero), or the Strength SG is HIGH and Stress is LOW or MEDIUM, or the Strength SG is Medium and Stress is LOW.

THEN the operating condition C is secure.

Otherwise, it is insecure.

Data: NEM, Threshold, SG, Stress.

Output: C secure or not.

3. IF (Security Margin > Threshold).

THEN (System is Secure).

Otherwise, System is Insecure.

Data: Security Margin, Threshold.

Output: Secure (YES/NO).

- 3.1 IF (Decision on updating Security Margin is YES).

THEN (Call Procedure Update Security Margin).

(see Task 5 for procedure).

Data: Decision on updating Security Margin, Mismatches between base case and current generations/interchanges, sensitivity of each generation/interchange to Security Margin, base case Security Margin

Output: (current) Security Margin.

- 3.1.1 IF (current generations are NOT equal to base case generations) AND (current tie interchanges are NOT equal to base case interchanges).

THEN (Update = YES).

Data: current (real-time) generation/interchange profile, base case generation/interchange profile.

Output: Decision on updating Security Margin (YES/NC).

Rules for Vulnerability Assessment

1. IF the degradation of energy margin (DEM) is larger than a threshold for any of the specified variations v, or the IMPRESSIONABILITY (IM) is HIGH, or the IM is LOW and UNSETTLEMENTS (US) is LARGE.

THEN the operating condition C is vulnerable. Otherwise, it is invulnerable.

Data: DEM, Threshold, "Variations", IM, US.

Output: C_vulnerable_or_not.

- 1.1 IF Sensitivity of Energy Margin (SEM) is higher than a threshold.
THEN IMPRESSIONABILITY (IM) is high.
Otherwise, it is LOW.
Data: SEM, Threshold.
Output: IM.
IF Delta Parameter Change (DPA) is larger than a threshold.
THEN the UNSETTLENESS is LARGE.
Otherwise, it is SHALL.
Data: DPA, Threshold.
Output: US.

Task 5: Remedial-Actions

This Task is invoked only if the security assessment of Task 4 gives a negative answer. The objective here is to adjust the available controllers in such a way that the system becomes secure.

1. IF (Corrected-Security-Margin < Threshold) AND (there are available control actions).
THEN (Select next control action in priority list) AND (Determine amount of threshold violation).
Data: Corrected-Security-Margin, Threshold, available controls ordered in priority.
Output: Highest priority control c, Amount of Security Margin Violation.
 - 1.1 IF (control action c is available) AND (control action c has the highest priority).
THEN (Determine the necessary amount of c for correction) AND (Calculate the Corrected-Security Margin).
Data: availability of control c, the current control c selected from rule 2.
Output: amount of control c, needed, corrected-security-margin.
 - 1.2 IF (control action c is at its limit).
THEN (set status of c to UNavailable) AND (remove c from the priority list).
Data: control c and its limit.
Output: updated availability status of control c
 - 1.3 IF (control action c is the current remedial control) AND (necessary amount of control c is not at its limit).
THEN (no more remedial action is needed)

- Data: control c, necessary amount of c.
Output: stop choosing remedial actions.
2. IF (Security Margin < Threshold) AND (there are NO available control actions.
THEN (no remedial action is possible).

8.2.4 Summary

In this section fundamental concepts and basic requirements for a dynamic security assessment expert system have been introduced for a stability-limited power network. The computerized procedure uses power system data provided by the TEF method as input data to the expert system.

For a given contingency the TEF method provides energy margins and energy margin sensitivities to operating parameters. The energy margins provide a measure of the system security. The energy margin sensitivities provide a measure of system vulnerability to changes in operating parameters. This data is suitable for providing the logic needed by an expert system for dynamic security assessment.

A framework for identifying and organizing the knowledge base requirements for the various tasks involved in dynamic security assessment has been presented. A multilevel tree structure for the TEF-expert system is proposed for the analysis associated with decisions concerning the power system's security/vulnerability status. It is important to note that the procedure outlined above provides a suitable framework in which to implement a much needed dynamic contingency classification and selection algorithm.

8.3 FUZZY-LOGIC-BASED POWER SYSTEM STABILIZATION

Development of a fuzzy-logic-based power system stabilizer to maintain stability and enhance closed-loop performance of a power system is described in this chapter. Simulation studies on a single-machine infinite-bus system and on a multi-machine power system model show very satisfactory performance.

The fuzzy-logic-based PSS (FLPSS) has been implemented on a low-cost micro controller and tested in the laboratory on a physical model of a single-machine infinite bus system. Experimental tests and results are also described.

8.3.1 FLC Structure

In conventional control, the amount of control is determined in relation to a number of data inputs using a set of equations to express the entire control process. Expressing human experience in the form of a mathematical formula is

a very difficult task, if not an impossible one. Fuzzy logic provides a simple tool to interpret this experience into reality.

Fuzzy logic controllers are rule-based controllers. The structure of the FLC resembles that of a knowledge-based controller except that the FLC utilizes the principles of fuzzy set theory in its data representation and its logic. The basic configuration of the FLC can be represented simply in four parts, as shown in Fig. 8.9:

Fuzzification module, the functions of which are, first, to read, measure, and scale the control variable (e.g., speed, acceleration) and, second, to transform the measured numerical values to the corresponding linguistic (fuzzy) variables with appropriate membership values.

Knowledge base, which includes the definitions of the fuzzy membership functions defined for each control variable and the necessary rules that specify the control goals using linguistic variables.

Inference mechanism, which is the kernel of the FLC. It should be capable of simulating human decision making and influencing the control actions based on fuzzy logic.

Defuzzification module, which converts the inferred decision from the linguistic variables back to numerical values.

8.3.2 Fuzzy Logic Controller (FLC) Design

The design process of an FLC may be split into the five steps described below.

Selection of Control Variables

The selection of control variables (controller inputs and outputs) depends on the nature of the controlled system and the desired output. It is more common to

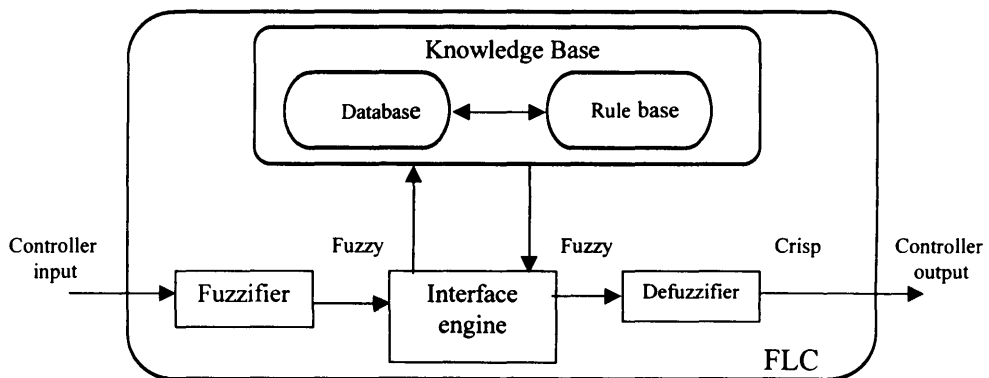


Figure 8.9 Schematic diagram of the FLC building blocks.

use the output error (e) and the rate or derivative of the output (e') as controller inputs. Some investigators have also proposed the use of error and the integral of error as an input to the FLC.

Membership Function Definition

Each of the FLC input signals and output signals, fuzzy variables ($X_i = \{e, e', u\}$), has the real line R as the universe of discourse. In practice, the universe of discourse is restricted to a comparatively small interval ($X_{\min}, X_{\max}, 1$). The universe of discourse of each fuzzy variable can be quantized into a number of overlapping fuzzy sets (linguistic variables). The number of fuzzy sets for each fuzzy variable varies according to the application. A common and reasonable number is an odd number (3, 5, 7 . . .). Increasing the number of fuzzy sets results in a corresponding increase in the number of rules.

A membership function is assigned to each fuzzy set. The membership functions map the crisp values into fuzzy values. A set of membership functions defined for seven linguistic variables NB , NM , NS , Z , PS , PM , and PB , which stand for Negative Big, Negative Medium, Negative Small, Zero, Positive Small, Positive Medium, and Positive Big, respectively. Membership functions can be of a variety of shapes, the most unusual being triangular, trapezoidal, or a bell shape. The triangular shape is used for the controller.

For simplicity, it is assumed that the membership functions are symmetrical and each one overlaps with the adjacent functions by 50%. In practice, the membership functions are normalized in the interval $[-L, L]$, which is symmetrical around zero. Thus, control signal amplitudes (fuzzy variables) are expressed in terms of controller parameters (gains).

Rule Creation and Inference

In general, fuzzy systems, as function estimators, map an input fuzzy set to an output fuzzy set $S: I' - I'$. Fuzzy rules are the relations between the fuzzy sets. They usually are in the form "if A , then B ," where A is the rule antecedent and B is the rule consequence. Each rule defines a fuzzy patch in the Cartesian product $A \times B$ (system state space). The antecedents of each fuzzy rule describe a fuzzy input region in the state space. This enables one to effectively quantize continuous state space so that it can cover a finite number of these regions. In terms of associative memory definition (FAM), each rule represents an association ($A_i; B_i$). The structure proposed firing all the rules at the same time (analogous to neural networks). This enables easier, faster, and very large scale integrated (VLSI) analogue and digital designs. A fuzzy system using two antecedents and one consequence (A_i, B_i, C_i) is shown in Fig. 8.10.

The association (A_i, B_i, C_i) or the rule of A_i , and B_i then C_i maps inputs A_i ,

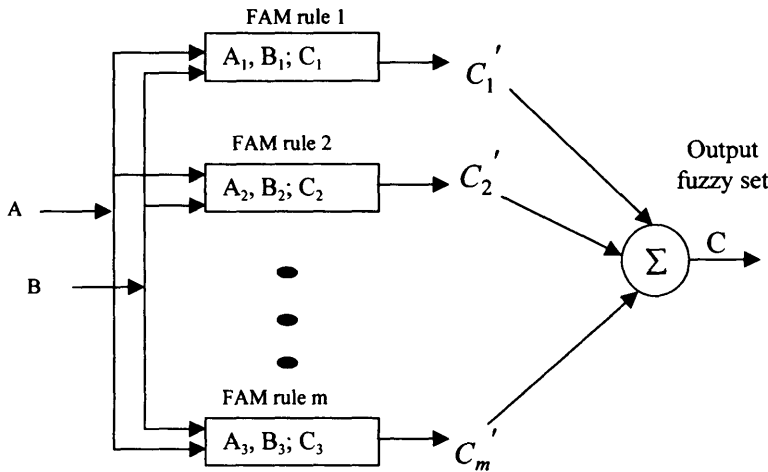


Figure 8.10 FAM system architecture for two fuzzy antecedent and one consequence.

B , to C' , a partially activated version of C . The corresponding output fuzzy set C combines the partially activated sets C'^1, \dots, C'^m , that is,

$$C = \sum_i^m C'^i \quad (8.4)$$

Fuzzy Inference

The well-known inference mechanisms in fuzzy logic are the correlation-minimum encoding and the correlation-product encoding. Consider fuzzy sets A and B to be fuzzy subsets of X, Y . The geometric set-as points interpretation of finite fuzzy sets A and B as points in unit cubes allows the representation of the sets of vectors. Thus, A and B can be represented by numerical fit vectors $A = (a_1, \dots, a_n)$ and $B = (b_1, \dots, b_m)$, where $a_i = m_A(x_i)$ and $b_i = m_B(u_i)$. Let the relation between A and B be governed by the FAM rule (A, B) . Using the definitions, the correlation-minimum encoding and the correlation-product encoding can be expressed follows.

1. The correlation minimum encoding is based on the fuzzy outer product notation. Expressed in matrices, the pairwise multiplication is replaced by the pairwise minima and the column sums with the column maxima. This max-min composition relation is denoted by the composition operator \odot . Thus the fuzzy outer product of the fit row vectors A and B , which forms the FAM matrix M , can be given by

$$M = A^T \odot B \quad (8.5)$$

Where

$$m_{ij} = \min(a_i, b_j) \text{ or } a_i \wedge b_j \quad (8.6)$$

and the cap operator \wedge indicates the pairwise minima.

2. The correlation-product encoding uses the standard mathematical o product of the fit vectors A and B to form the FAM matrix M :

$$M = A^T B \quad (8.7)$$

where

$$m_{ii} = a_i b_i$$

Correlation-minimum encoding produces a matrix of clipped B sets, while correlation-product encoding produces a matrix of scaled B sets.

Defuzzification Strategy

Defuzzification is a process of converting the FLC inferred control actions from fuzzy values to crisp values. This process depends on the output fuzzy set, which is generated from the fired rules. The output fuzzy set is formed by either a correlation-minimum encoding or the correlation-product encoding.

8.3.3 Fuzzy Rules

Fuzzy rules play a major role in the FLCs and have been investigated extensively. However, rules usually can be generated using knowledge and operating experience with the system or through the understanding of system dynamics.

In most cases, fuzzy rules map two input fuzzy variables, for example, the error e and the derivative of error e' , into one output fuzzy variable the control signal u . In such a system each fuzzy variable can be easily quantized to a number of fuzzy sets.

8.3.4 FLC Parameter Tuning

Parameter tuning for the FLC plays an important role in achieving the controller goals. Previous experience with the controlled system is helpful in selecting the initial values of the FLC parameters. If sufficient information is not available about the controlled system, the selection of suitable FLC parameters can be-

come a tedious trial-and-error process. Some efforts have been reported in the literature to automate the tuning of the FLC parameters at the design stage to get an optimal or near optimal system performance.

Another algorithm to tune the FLC parameters off-line is proposed in this section. The objective of the proposed parameter tuning algorithm is to change the controller gains in an organized manner to achieve desired system response. The tuning algorithm tries to minimize three system performance indices (PIs). These indices are the system overshoot (OS) and the performance indices J_1 , J_2 , are given as

$$OS = \frac{r - y}{r} \times 100\% \quad (8.8)$$

$$J_1 = \sum e^2 \quad (8.9)$$

$$J_2 = \sum te^2 \quad (8.10)$$

where r is the system reference, y is the system output, e is the system error, and t is the time.

An FLC with two inputs and a single output has two input parameters K_c , $K_{c'}$ and one output parameter K_u . The three parameters K_c , $K_{c'}$, and K_u , are tuned using the guided search algorithm.

The algorithm changes the three parameters in overlap loops, simulates the system with the new parameters, and calculates the performance index. It also detects if one of the parameters degrades the performance indices or leads to instability. In this case it stops incrementing this parameter. If the desired performance indices are achieved, the search stops. Otherwise, it continues over the specified search range of the FLC parameters.

In case of a complete lack of information about the parameters, the search for the best parameters may require a large number of iterations in searching for a proper minimum. Using some practical information about signal levels, it is easy to set an operating range to the FLC parameters.

8.3.5 Automatic Rule Generation

In some cases the dynamic behavior of the controlled system is unpredictable and difficult to understand. This situation imposes the need to automate the rule generation process. A lot of effort has been devoted to achieve this goal. In some cases an upper hierarchical set of rules has been chosen to generate the controller rules. This technique requires some understanding of the system dynamics to build these types of supervisory rules.

In some other cases, the rules were generated using an artificial neural network. The generation of rules is achieved by training the neural network

using sampled data sets. Although effective, this method requires some neural network background and long training time.

In this section two effective automatic rule generation (ARG) methods are proposed. These methods are very similar to the neural network technique. They also use sampled data ensemble but employ a fuzzy system to generate the rules instead of a neural network. The rules can be obtained easily from the known desired performance (input-output data pairs) of the system when controlled by another well-designed controller, for example, an adaptive controller or a proportional-integral-derivative (PID).

In the case of a two-input, one-output FLC, the controller requires two fuzzy variables, and using a fuzzy mapping function (fuzzy rules), it generates one-output fuzzy control action. Instead, the ARG is a reverse process. It uses the three fuzzy variables (e , e' , u) and generates the mapping function (fuzzy rules).

ARG Using Highest Match Method

The highest match (HM) algorithm properly fuzzifies the three input variables (e , e' , u). Each fuzzy variable matches in two fuzzy subsets. The algorithm considers only the subsets with highest match (highest membership value). Thus if e matches in both X and PS with membership values 0.75 and 0.25, respectively, it will consider that e matches only in the Z subset. Similarly the e' and u subsets will be PS and NS , respectively. Thus for this sample data, the rule having the antecedents $e = Z$ and $e' = PS$ will be assigned to a consequence $U = NS$; that is, the generated rule will be:

$$\text{If } e = Z \text{ and } e' = PS, \text{ then } u = NS$$

This process is repeated for the whole set of sampled data ensemble. At the end of the above-mentioned process, the same rule may be assigned to different consequences. To resolve this problem, the final rule consequence is generated by weighing all the consequences assigned to this rule by their number of occurrences.

ARG Using Fuzzy Inference Reverse Engineering

The algorithm mentioned in Sec. 5.6.1 focuses the information derived from the input-output data set on a single rule (the highest match) and ignores the effect on the other fired rules. This may lead to a considerable number of unassigned (empty) rules. The fuzzy inference reverse engineering (FIRE) technique avoids this drawback considering the aggregated effect of all fired rules.

8.3.6 Fuzzy-Logic-Based Power System Stabilizer

A FLPSS with a set of FAM rules and continuous membership functions as discussed earlier has been designed. An organized method is followed to generate the rule base and to tune the parameters of the FLPSS.

The performance of the FLPSS is first studied using a simulation model of a synchronous machine connected to an infinite bus. The FLPSS has been tested on the power system under various fault and load disturbances to ensure its effectiveness, robustness, and reliability as a power system stabilizer.

Single-Machine Power System Model

A power system model consisting of a synchronous machine connected to a constant voltage bus through a double-circuit transmission line is used in the simulation studies. A schematic diagram of the model is shown in Fig. 8.11.

The system is represented by a ninth-order nonlinear model including the governor and the automatic voltage regulator (AVR) exciter. The state equations representing the power system and the synchronous machine, governor, and AVR model parameters are given in the referenced literature. The solution of the model differential equations was obtained using a fourth-order Runge–Kutta method with a simulation time step of 1 ms.

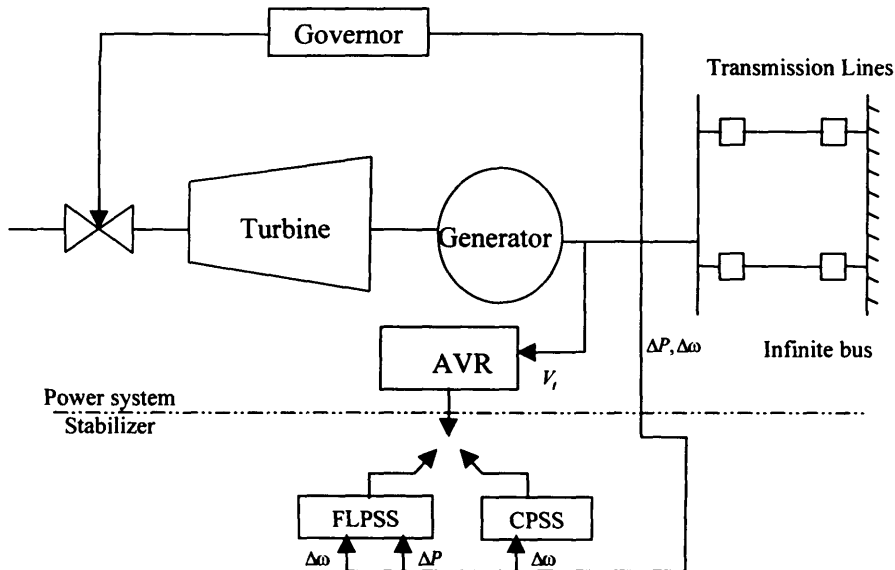


Figure 8.11 A schematic diagram of a synchronous machine model with stabilizers.

The control signal generated by the PSS is injected as a supplementary stabilizing signal to the AVR summing point. The system model has been designed to support both the CPSS and the FLPSS and can be easily extended to support other types of PSS.

Fuzzy Logic Power System Stabilizer

Using the description given in Sec. 8.4.3 for FLC design, a power system stabilizer based on the FLC algorithm has been developed. Since the goal of this application is to stabilize and improve the damping of the synchronous machine, speed deviation $\Delta\omega$ and active power deviation ΔP_e , have been selected as the controller inputs. The controller output is then injected into the AVR summing point.

This configuration implies that the FLC has two input parameters, K_{ω} and K_p , and one output parameter, K_u , as seen in Fig. 8.12. The selection of these parameters is usually subjective and requires previous knowledge of the fuzzy control variables (input and output signals). Also previous experience of the controlled system dynamics is commonly used in the creation of the fuzzy control rules. However, an organized approach as described in the next section has been adopted for the generation of rules and tuning of parameters for the FLPSS.

FLPSS/Rule Generation and Parameter Tuning

Using the FIRE ARG method and a sampled data set generated by using the CPSS, a proper set of rules was obtained. The rules used in all the following

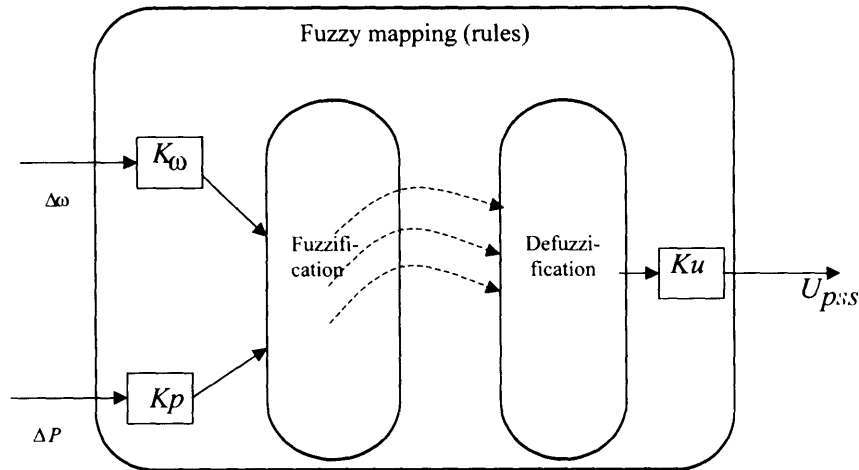


Figure 8.12 Schematic diagram of the FLPSS.

Active Power

| | | NB | NM | NS | Z | PS | PM | PB |
|--|--|----|----|----|----|----|----|----|
| | | NB | NB | NB | NB | NM | NS | Z |
| | | NB | NB | NM | NM | NS | Z | PS |
| | | NB | NM | NS | NS | Z | PS | PM |
| | | NM | NM | NS | Z | PS | PM | PM |
| | | NM | NS | Z | PS | PS | PM | PB |
| | | NS | Z | PS | PM | PM | PB | PB |
| | | Z | PS | PM | PB | PB | PB | PB |

Figure 8.13 FLPSS rules generated by fire algorithm.

experiments are shown in Fig. 8.13. The correlation-product inference mechanism is used to generate the output fuzzy set for the FLPSS. The defuzzification process is based on the center-of-gravity method.

Once the proper rules are obtained, the proper parameter tuning should be d in order to achieve good performance. Tuning of FLPSS parameters can be a tedious trial-and-error process if not enough information is available about the range of controller variables and how they change with different disturbances. The objective of the off-line tuning algorithm is to determine the controller parameters that provide the desired system response.

The tuning algorithm tries to minimize three system PIS by varying the FLPSS parameters. In the present case, the output parameter is set to give the maximum allowable control action, while the other two parameters K_o , K_p , were tuned using the guided search algorithm.

The selected values of the FLPSS parameters are those that minimize the use of the guided blind search. Once the FLPSS had been tuned, the parameters were kept unchanged throughout subsequent studies. The tuned parameters of the FLPSS are

$$K_o = 100 \quad K_p = 0.21 \quad K_u = 0.1$$

CONCLUSIONS

Unlike the classical design approach, which requires a deep understanding of the system, exact mathematical models, and precise numerical values, a basic feature of the fuzzy logic controller is that a process can be controlled without the knowledge of its underlying dynamics. The control strategy learned through experience can be expressed by a set of rules that describe the behavior of the

controller using linguistic terms. Proper control action can be inferred from this rule base that emulates the role of the human operator or a benchmark control action. Thus, fuzzy logic controllers are suitable for nonlinear, dynamic processes for which an exact mathematical model may not be available.

Using the principles of fuzzy logic control, a PSS has been designed to enhance the operation and stability of a power system. Results of simulation and experimental studies look promising.

The reader is reminded that further information on the contents of this chapter can be found in the referenced articles and transaction papers, at the end of this volume.

9

Application of Artificial Intelligence to Voltage Stability Assessment and Enhancement of Electrical Power Systems

INTRODUCTION

Most of the voltage collapse related incidents are believed to be related to heavily stressed systems where large amounts of real and reactive power are transported over long EHV transmission lines while appropriate power resources are not available to maintain normal voltage profiles at receiving end buses. In some cases, however, voltage profiles show no abnormality prior to undergoing voltage collapse because of load variations. Operators may observe no advance warning signals until sudden significant changes in the voltage magnitude result in actions of automatic protective equipment to crash the network. This phenomenon is caused by large and small disturbances. Large disturbances consist of the loss of generators, transmission lines, and transformers. Small disturbances on the other hand consist of slow variation in the system load.

The common analytical techniques used for voltage stability assessment during these disturbances are:

1. Minimum singular value decomposition which determine the singularity of the Jacobian matrix of the system under study;
2. The concept of multiple load flow solutions which are used for determining the proximity of a particular voltage collapse point. This method derives the variation of load change for specified bus voltage degradation;

3. The concept of energy margin developed as an indicator to voltage stability by computing the system stable equilibrium points, SEPs, and unstable equilibrium points, UEPs;
4. The condition number of power flow Jacobian matrix used to estimate the voltage collapse point; and
5. The continuation method, which computes the neighborhood of voltage collapse for variation in load. The scheme is based on the solution of the load flow equations by suitable modification of the Jacobian using a continuation parameter to avoid singularity of the Jacobian near the collapse point.

There are a lot of reservations about the results, accuracy, difficulties, and the computational burden involved in using these techniques. Therefore, a tool which can provide timely evaluation of voltage stability of the system under diversified operating conditions would be very useful.

In recent years, efforts to improve on speed, accuracy, and ability to handle stressed/ill-conditioned systems have led to the development of intelligent systems-based tools. The potential application of ANN, and ES as alternative approaches for solving certain difficult power system problems, where the conventional techniques have not achieved the desired speed, accuracy, or efficiency is quite promising.

This chapter deals with the application of ANN and ES to voltage stability assessment.

9.1 ANN-BASED VOLTAGE STABILITY ASSESSMENT

The purpose of ANN-based voltage stability assessment is to obtain the maximum MW loading of the system for a given contingency without conducting *PV* studies. The proposed scheme for ANN-based voltage stability assessment utilizes a multi-layer feed forward network employing back propagation algorithm for the training process. Details of constructing the network architecture, preparation of the training data, and testing process will be done in the following sections.

9.1.1 Mechanism for Generating Training Data Based on Modal Analysis

The mechanism used for the production of the data needed for training the proposed network is based on modal analysis, employing *VQ* sensitivities that have the ability to identify areas that have potential problems and provide information regarding the mechanism of voltage collapse. The method can be described as follows:

The system dynamic behavior can be expressed by the first order differential equation,

$$\dot{X} = f(X, V)$$

where X = state vector of the system

V = bus voltage vector

Under the steady state condition $\dot{X} = 0$, using enhanced device models, the linearized power flow equations can be written as:

$$\begin{bmatrix} \Delta P_d \\ \Delta Q_d \end{bmatrix} = \begin{bmatrix} J_{P\theta} & J_{PV} \\ J_{Q\theta} & J_{QV} \end{bmatrix} \begin{bmatrix} \Delta \theta_d \\ \Delta V_d \end{bmatrix}$$

where:

ΔP_d : Incremental change in device real power output;

ΔQ_d : Incremental change in the device reactive power output;

$\Delta \theta_d$: Incremental change in the device voltage angle;

ΔV_d : Incremental change in the device voltage magnitude;

$J_{P\theta}$, J_{PV} , $J_{Q\theta}$, and J_{QV} represent a modified form of the power flow Jacobian elements in the terms associated with each device.

We can study the QV sensitivity while keeping P constant, and substitute $\Delta P = 0$ in the linearized power flow equations to give after some simplification,

$$\Delta V = J_R^{-1} \Delta Q$$

where

$$J_R = J_{QV} - J_{Q\theta} J_{P\theta}^{-1} J_{PV}$$

We examine the eigen values and the eigen vectors of the reduced Jacobian J_R to arrive at:

$$v = \Lambda^{-1} q \text{ or } v_i = \frac{1}{\lambda_i} q_i$$

where Λ^{-1} is a diagonal matrix with entries $1/\lambda_i$, λ_i is the i^{th} modal voltage, $v = \eta \Delta V$ and $q = \eta \Delta Q$.

The bus participation factors determine the contribution of each λ_i to VQ sensitivity at bus k . They can be expressed in terms of the left and right eigen vectors of J_R , as:

$$P_{ji} = \xi_{ji} \eta_{ji}$$

The branch participation factors P_{ji} which give the relative participation of branch j in mode I are given by:

$$P_{ji} = \frac{\Delta Q \text{ loss for branch } j}{\max \Delta Q \text{ for all branches}}$$

The ΔQ loss can be found by calculating the ΔV and $\Delta \theta$ change at both ends of the branch.

The generator participation factors P_{mi} that give the relative participation of machine m in mode i are given by:

$$P_{mi} = \frac{\Delta Q \text{ for machine } m}{\max \Delta Q \text{ for all machines}}$$

The machine participation factors can be used to determine the generators that supply the most reactive power on demand. The reactive reserve at these generators can contribute heavily to voltage stability. The modal analysis algorithm is utilized in the EPRI VSTAB program.

9.1.2 Suggested Neural Networks Architecture

The ANN-based voltage stability assessment process is designed to predict the critical system loading, expressed in MW, for a given contingency without conducting *PV* simulations. The network architecture, as shown in Fig. 9.1, is as follows:

The input layer consists of 12 neurons that represent the 12 input variables, namely:

1. $Q_s^{\text{total}}/Q_s^{\text{installed}}$ (ignoring slack bus reactive generation).
2. Q_s at most critical generator/Max Q_s at that generator. The most critical generator is the one with the lowest voltage.
3. The Q_s reserve at generator with least Q_s reserve.
4. The number of generators sitting at limiting Q_s .
5. Lowest voltage at base case loading.
6. Number of buses with voltage below 1pu.
7. Total active power demand in MW.
8. Total reactive power demand in MVAR.
9. Total active power loss in MW.
10. Total reactive power losses in MVAR.
11. Ratio of the most critical branch MVA flows, to total MVA demand (from the power flow solution for the intact system).

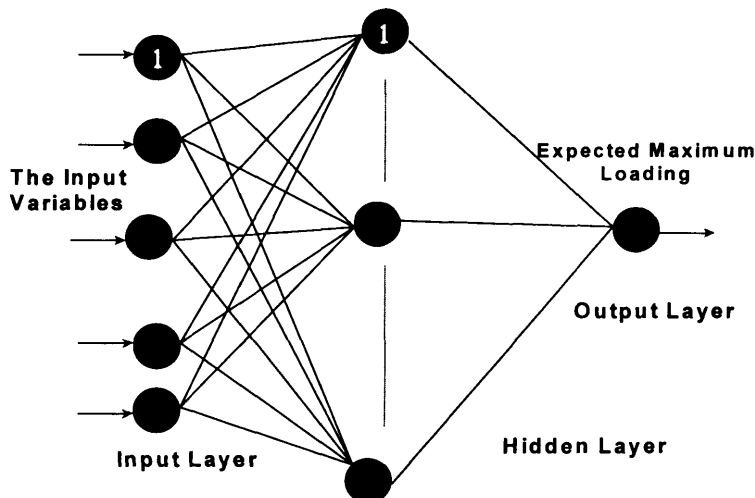


Figure 9.1 Suggested network design.

12. Ratio of the most critical branch MVA flows to the maximum total MVA demand before collapse (intact system only).

The number of the neuron in the hidden layer was obtained experimentally i.e., this number was determined from studying the network behavior during the training process taking into consideration some factors like convergence rate, error criteria, etc. In this regard, different configurations will be tested and the best suitable configuration will be selected based on the accuracy level required.

The output layer consists of one neuron representing the predicted maximum MW loading in MW.

9.1.3 Training Process

The data needed for the training process is obtained from the simulation results using EPRI VSTAB. Next the results from VSTAB are analyzed and processed for training and testing. The training data exploited about 75% of the simulation results. Finally, the data sets, set aside for testing, were presented for the trained network for the testing process.

The data was modified to satisfy the input requirements of the neural network for better discrimination between data sets. One thousand cases were produced by the VSTAB program for the training and testing process. The accuracy during the training process was set to 1.0E-03. The configuration with 5 neurons achieved a convergence tolerance below 1.E-03 in about 1000 iterations. The

configuration with 7 neurons in the hidden layer achieved the same accuracy level with a higher number of training iterations. The configuration with 3 neurons in the hidden layer did not achieve an accuracy below 1.0E-3 in about 6000 iterations possibly reaching a local minimum. The training error showed more variation with change in the architecture than in the previous studies.

It was observed that the critical branch loading makes a significant contribution toward voltage collapse. The lower the total Q_c reserve, the lower the allowable maximum MVA loading on the system. The Q_c reserve at the most critical generator is very instrumental in maintaining high maximum loadability. Conversely, improvements in the voltages and/or reactive reserve via compensation at such buses can increase the stability margin. The cases with low voltages during contingencies at base case loading have a lower maximum MVA loading before collapse. The total active and reactive losses for the contingencies at the base case loading signify the degree of change in the network flows due to contingencies.

9.1.4 Case Study: New England 39-Bus System

The voltage stability studies were conducted on the New England 39-bus system, shown in Fig. 9.2, which is slightly adapted to the study. The existing base case was used to create a variety of cases with different load distributions with near-base case loading, different generation patterns, generator voltage patterns, and transformer tap ratio settings. This was achieved through randomly varying relevant parameters about the original base case values. In some cases economic dispatch and loss minimization were used to make the solution comply with voltage and flow limits. Contingencies consisting of different branch outages and different generator outages giving rise to different Q_c reserves were implemented on all of the above data sets. In total, a few thousand different cases were generated. For each case the 12 parameters used as inputs to the ANN were produced with the corresponding maximum system loadability. 75% of the simulation results were used to train the network while the remaining 25% were used for the testing process.

Based on the training error statistics, there were 5 neurons in the hidden layer architecture for the testing process. A sample test result for the back propagation algorithm using the selected ANN architecture is shown in Fig. 9.3.

Figure 9.3 shows the difference between the desired and computed output for the test data expressed in MW. The global normalized test error was 2.07E-03, which correspond to 50 MW. The minimum error is less than 100 MW. The difference between the maximum load at collapse and base load is in the neighborhood of 1000 MW indicating an accuracy better than 90% in the ANN test results.

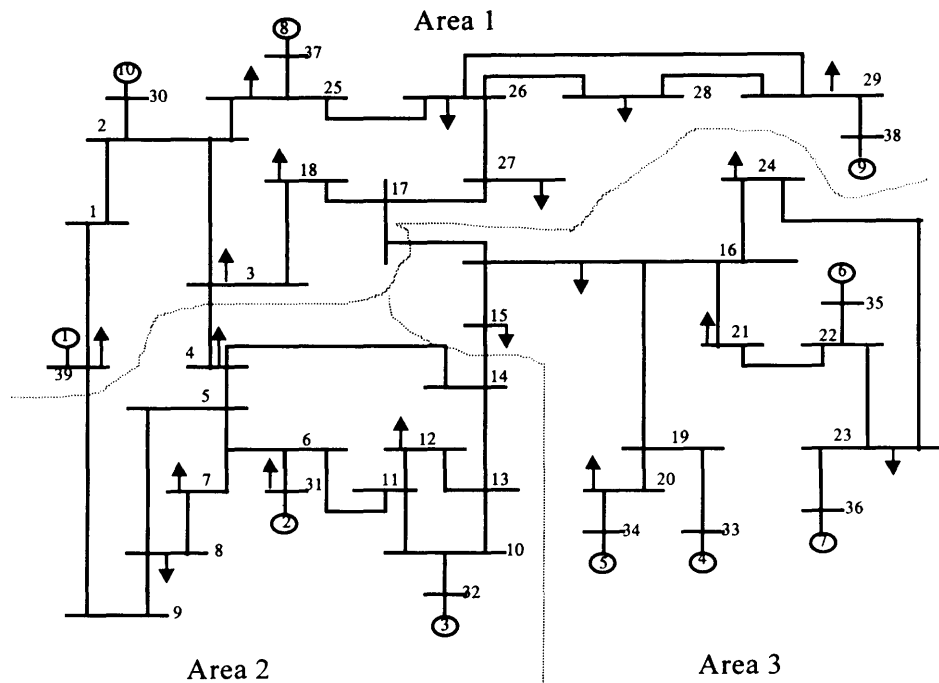


Figure 9.2 New England 39-bus system.

9.2 ANN-BASED VOLTAGE STABILITY ENHANCEMENT

The work of Sec. 9.1 is extended to accommodate voltage stability enhancement using switchable shunt compensators. The buses sensitive to reactive compensation are identified via modal analysis and used as candidate buses for applying compensation. Key physical parameters contributing toward voltage collapse such as reactive generation reserve and reactive compensation at base load are used as key input variables. The ANN output provides the enhanced maximum demand at collapse and the reactive compensation needed to achieve the enhanced stability margin. The New England 39-bus system is used for the study.

9.2.1 Voltage Stability Enhancement Using Shunt VAR Compensation

The voltage stability enhancement using shunt VAR compensation modifies the network power flow equations at base load to the form given by:

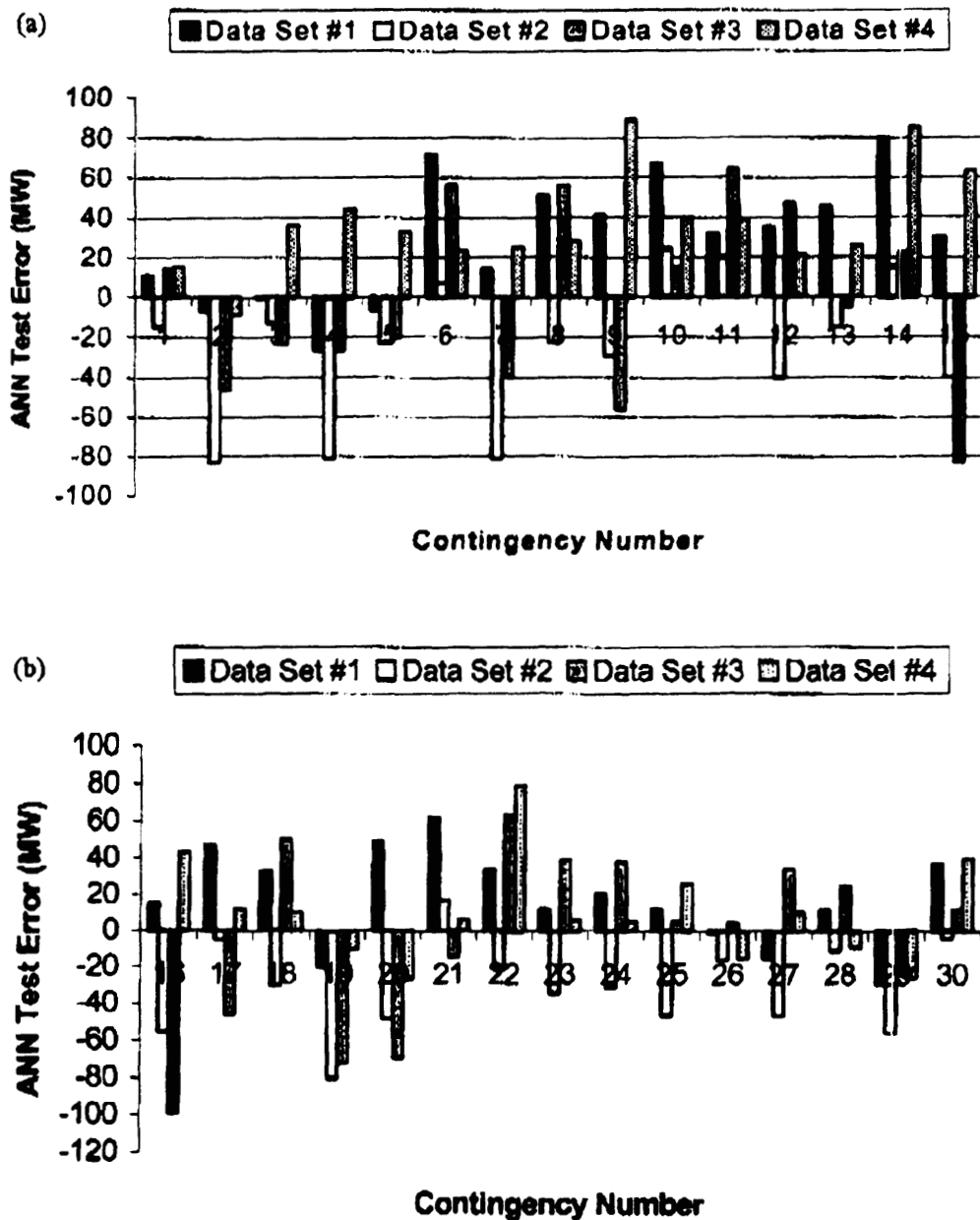


Figure 9.3 A sample test result.

$$P_i^k - P_{gi}^k + P_{di} = 0 \quad i = 1, 2, \dots, Nb \quad i \in \text{gen} \quad k = 0, 1, \dots, Nk$$

$$Q_i^k - Q_{gi}^k - Q_{ci}^k + Q_{di} = 0$$

The collapse state power flow equations are:

$$P_i' - P_{gi}' + P_{di}' = 0 \quad i = 1, 2, \dots, Nb \quad i \in \text{gen} \quad k = 0, 1, \dots, Nk$$

$$Q_i' - Q_{gi}' - Q_{ci}' + Q_{di}' = 0$$

The symbol (') represents the state collapse point, Q_c represents the shunt VAR compensation, and k represents the contingent cases. One form of shunt VAR compensation is via static VAR compensators (SVC). The optimal value of SVC at collapse point can be obtained through optimization where the generator voltages and transformer tap ratios can be optimized. An alternative, using VSTAB, employing power flow without optimization is used in the current study.

9.2.2 Suggested Neural Networks Architecture

The ANN-based voltage stability enhancement is designed to predict the enhanced maximum demand at collapse and the reactive compensation needed to achieve the enhanced stability margin. The network architecture, as shown in Fig. 9.4, is as follows:

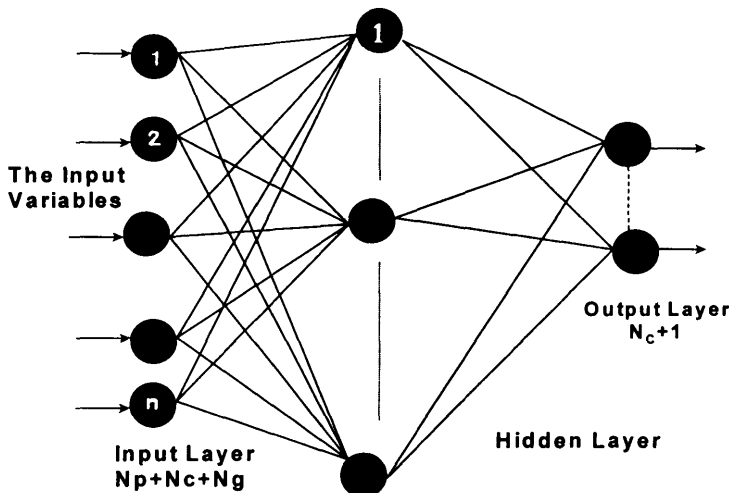


Figure 9.4 Suggested artificial neural network (ANN) design.

The Input Layer

Voltage stability assessment requires identification of the collapse point based on load variation commonly employing a property such as singularity of the load flow Jacobian matrix at the collapse point. The load at buses participating in collapse, the reactive compensation at base load at selected buses, and the reactive reserve at each generator are used as input to the neural network.

The number of neurons in the hidden layer is determined by:

$$N_p + N_c + N_g$$

where

N_p is the number of buses participating in the collapse;

N_c is the number of VAR sites; and

N_g is the number of generators.

Hidden Layer

In the study, 1–2 hidden layers with multiple hidden node are tested. For each proposed network architecture, the number of the hidden neurons varies from 2–30.

Output Layer

In this study we assess reactive compensation at collapse and the maximum power demand at the collapse point. Hence the number of the output nodes is determined by: $N_c + 1$.

9.2.3 Studies Conducted

For the New England 39-bus system, 5 VAR sites were chosen based on the participation factors. Voltage stability studies were then carried out with these buses treated as VAR sites containing switchable shunts. The load at buses participating in the collapse and the magnitude of the shunts required to maintain the voltage within an acceptable range (0.95–1.05 pu) at base load and at the collapse point were noted along with the Q_g reserve at base load and the total maximum power demand at collapse. The load at buses numbered 12, 15, 16, 20, 21, 23, and 24 were used as part of the input while buses numbered 12, 15, 20, 21, and 24 were selected as VAR sites based on their high participation. A few hundred load configurations were generated using a random perturbation around the base load and the preceding procedure was repeated for all different load configurations.

Different ANN architectures were constructed with hidden nodes ranging from 2–20, and hidden layers from 1–2. The different ANN were trained with

the 85% of the simulated data results. The stability margin was computed as the ratio of the maximum power demand at collapse to the base load providing an index in the range of 1.0–2.0. All other data was converted to per unit during training and testing.

The ANN training statistics are presented in Table 9.1. This table shows the approximate number of presentations required to achieve an error below the tolerance 1.0E-04. The training process is terminated if convergence was not reached with 100,000 presentations. The following remarks are made:

1. The different ANN architectures with one hidden layer and with less than 6 hidden nodes did not converge below the tolerance error for over 100,000 presentations.
2. All architectures with one hidden layer and with less than 6 hidden nodes did not converge below the tolerance error for over 100,000 presentations.
3. All architecture with 1 hidden layer and with more than 5 hidden nodes converged below the tolerant error in less than 4000 presentations.
4. Within the scope of the architectures tested, those with 11, 14, and 30 hidden nodes converged with the least number of presentations, i.e., 600–700 presentations.

Table 9.1 Training Statistics for Different ANN Architectures

| ANN architecture | | |
|-------------------------|------------------------|--------------------------------------|
| Number of hidden layers | Number of hidden nodes | Number of iterations for convergence |
| 1 | 3–5 | >100,000 |
| | 6 | 3800 |
| | 7 | 1600 |
| | 8–9 | 2200 |
| | 10 | 1000 |
| | 11 | 600 |
| | 12–13 | 1500 |
| | 14 | 600 |
| | 15 | 1700 |
| | 20 | 1100 |
| | 30 | 700 |
| | 2–5; 2–5 | >100,000 |
| | 6; 6 | 10,000 |
| 2 | 10; 10 | 3600 |

5. The addition of an extra hidden layer did not improve the performance of the ANN.
6. With 2 hidden layers and with less than 6 hidden nodes in each layer, the ANN did not converge below the tolerance within 100,000 presentations.
7. For architectures comprising 6 hidden nodes in each layer, the number of presentations required for convergence was about 10,000.
8. For 10 hidden nodes in each layer, the ANN converged in about 3600 presentations.

A comparison of the test results using the different architectures with 1 hidden layer are shown in Tables 9.1–9.3.

The errors are expressed in MW and MVAR for better readability. From these tables the following remarks are made:

1. The maximum error is in its maximum value for the network with 3 and 4 hidden nodes.
2. The error starts decreasing at 5 hidden nodes and stabilizes for 6 hidden nodes and higher.
3. The lowest average error is with 7 hidden nodes or with 30 hidden nodes.
4. Since a smaller architecture is naturally preferred, the architecture with 7 hidden nodes is recommended for the study.

Table 9.2 Maximum Test Error for Various ANN Architectures

| Number of hidden nodes | Maximum error in reactive compensation at collapse expressed in MVAR | | | | | Maximum error in estimated maximum demand MW |
|------------------------|--|----------|----------|----------|----------|--|
| | Q_{12} | Q_{15} | Q_{20} | Q_{21} | Q_{24} | |
| 3 | 37.9 | 86.0 | 66.7 | 58.6 | 31.3 | 121.6 |
| 4 | 33.7 | 47.4 | 33.2 | 35.4 | 23.4 | 113.1 |
| 5 | 39.7 | 28.7 | 15.1 | 10.1 | 16.1 | 34.8 |
| 6 | 11.2 | 17.9 | 9.1 | 10.5 | 15.3 | 29.2 |
| 7 | 9.2 | 13.6 | 8.2 | 13.0 | 11.9 | 26.9 |
| 8 | 8.4 | 28.0 | 10.9 | 11.0 | 16.9 | 25.5 |
| 9 | 10.0 | 13.9 | 7.8 | 8.2 | 14.8 | 32.9 |
| 10 | 13.5 | 22.2 | 9.0 | 8.5 | 15.2 | 28.9 |
| 11 | 9.7 | 28.8 | 8.2 | 10.5 | 16.5 | 35.0 |
| 12 | 12.0 | 17.4 | 10.9 | 11.1 | 10.9 | 30.3 |
| 30 | 10.0 | 18.8 | 8.6 | 8.1 | 11.4 | 29.8 |

Table 9.3 Average Test Error for Various ANN Architectures

| Number of hidden nodes | Average error in reactive compensation at collapse expressed in MVAR | | | | | Average error in estimated maximum demand MW |
|------------------------|--|----------|----------|----------|----------|--|
| | $Q_c 12$ | $Q_c 15$ | $Q_c 20$ | $Q_c 21$ | $Q_c 24$ | |
| 3 | 19.6 | 31.9 | 20.9 | 19.0 | 12.2 | 39.6 |
| 4 | 15.3 | 18.3 | 11.0 | 14.1 | 10.7 | 39.1 |
| 5 | 12.0 | 8.9 | 5.7 | 3.9 | 8.3 | 15.9 |
| 6 | 5.1 | 8.7 | 4.8 | 5.1 | 5.2 | 16.0 |
| 7 | 3.9 | 8.3 | 5.5 | 6.3 | 5.3 | 9.8 |
| 8 | 4.8 | 12.2 | 5.2 | 4.5 | 6.3 | 12.8 |
| 9 | 5.1 | 7.9 | 3.9 | 4.2 | 5.7 | 11.1 |
| 10 | 5.2 | 9.5 | 3.7 | 4.3 | 6.2 | 10.3 |
| 11 | 4.1 | 13.1 | 4.0 | 5.6 | 6.9 | 10.0 |
| 12 | 5.5 | 8.7 | 3.8 | 5.0 | 6.2 | 11.4 |
| 30 | 4.9 | 9.7 | 2.6 | 3.5 | 4.9 | 7.9 |

A sample set of results for the chosen architecture (i.e., 1 hidden layer and 7 hidden nodes) is shown in Tables 9.4 and 9.5. Table 9.4 shows the difference between the desired and the computed output for the test data expressed in MW and MVAR.

Table 9.5 shows the desired output for reactive power compensation and

Table 9.4 Sample ANN Test Error for Architecture that Has 7 Hidden Nodes

| Number of hidden nodes | Error in estimated reactive compensation at collapse expressed in MVAR | | | | | Maximum error in estimated maximum demand MW |
|------------------------|--|-----------|----------|----------|----------|--|
| | $Q_c 12$ | $Q_c 15$ | $Q_c 20$ | $Q_c 21$ | $Q_c 24$ | |
| 1 | 0.28 | 1.35 | 1.77 | 1.52 | 2.76 | 2.01 |
| 2 | 9.18 | 10.85 | 5.8 | 2.18 | 6.86 | 2.92 |
| 3 | 4.31 | 4.28 | 6.41 | 6.95 | 2.77 | 16.46 |
| 4 | 0.46 | 13.6 | 7.32 | 12.98 | 0.85 | 1.24 |
| 5 | 0.80 | 5.32 | 5.21 | 12.03 | 7.74 | 26.92 |
| 6 | 4.89 | 2.26 | 6.13 | 3.18 | 11.87 | 11.96 |
| 7 | 1.85 | 9.81 | 8.16 | 6.99 | 4.58 | 17.89 |
| 8 | 5.8 | 11.52 | 7.16 | 0.84 | 10.53 | 16.36 |
| 9 | 2.47 | 10.63 | 5.04 | 9.75 | 1.34 | 0.66 |
| 10 | 8.79 | 13.813.18 | 2.31 | 6.47 | 3.82 | 1.93 |

Table 9.5 Desired Output for Test Cases (from VSTAB)

| Case | Desired reactive compensation at collapse expressed in MVAR | | | | | Desired demand at collapse in MW |
|------|--|-----------|-----------|-----------|-----------|---|
| | $Q_{.12}$ | $Q_{.15}$ | $Q_{.20}$ | $Q_{.21}$ | $Q_{.24}$ | |
| 1 | 0.28 | 1.35 | 1.77 | 1.52 | 2.76 | 2.01 |
| 2 | 9.18 | 10.85 | 5.8 | 2.18 | 6.86 | 2.92 |
| 3 | 4.31 | 4.28 | 6.41 | 6.95 | 2.77 | 16.46 |
| 4 | 0.46 | 13.6 | 7.32 | 12.98 | 0.85 | 1.24 |
| 5 | 0.80 | 5.32 | 5.21 | 12.03 | 7.74 | 26.92 |
| 6 | 4.89 | 2.26 | 6.13 | 3.18 | 11.87 | 11.96 |
| 7 | 1.85 | 9.81 | 8.16 | 6.99 | 4.58 | 17.89 |
| 8 | 5.8 | 11.52 | 7.16 | 0.84 | 10.53 | 16.36 |
| 9 | 2.47 | 10.63 | 5.04 | 9.75 | 1.34 | 0.66 |
| 10 | 8.79 | 13.813.18 | 2.31 | 6.47 | 3.82 | 1.93 |

the power demand at collapse. For the reactive compensation, we see that the error ranges from about 0.28 MVAR to 13.6 MVAR. From Table 9.3 we see that the average error is in the neighborhood of 3–8 MVAR. For the estimated demand at collapse, the error ranges from about 0.66 MW to about 26.9 MW. The desired demand being in the range of 10,000 MW. Hence, the relative percentage error is less than approximately 0.3% indicating good ANN prediction.

9.3 A KNOWLEDGE-BASED SUPPORT SYSTEM FOR VOLTAGE COLLAPSE DETECTION AND PREVENTION

9.3.1 Voltage Collapse Using Expert System Technology

The scheme for expert system-based voltage collapse detection and prediction includes the decision procedure, knowledge acquisition about how to select and rank indicators affecting voltage collapse (VC), preventive measures to handle various violations, and selection of appropriate models for voltage collapse detection and prevention.

Specifically, it should be able to handle the following tasks:

1. Selection for performance index for contingencies;
2. Selection of optimization models for prevention;
3. Recommendation of prevention measures for voltage problems; and
4. Selection of procedure for conducting experiments that lead to voltage collapse.

9.3.2 Knowledge Acquisition and Presentation

The knowledge about the system performance variables and sensitivity parameters may be acquired off-line. The knowledge that needs to be acquired is as follows:

1. Load history;
2. System configurations and critical outages;
3. Control variables: generator taps, VAR, etc.;
4. List of facts on generator data, bus data, capacitor data, line data, and interchange data; and
5. Solution models and techniques.

The identification variables involve the relevant parameters associated with load history, critical line outages, control variables, and other modeling techniques. From the voltage collapse detection schemes reviewed, it was found that load history is not taken into account, the selection of critical lines depends on the system conditions and that prioritization of control parameters affects system behavior. Therefore, currently used mathematical predictive techniques cannot be used to ascertain adequate voltage collapse detection and preventive measures.

The proposed work reported here basically considers the static model using multiple-solution and divergence evaluation of power flow calculation to predict VC and the dynamic model for studying the effects of governors, exciters, etc. The preventative measures used are the VAR planning technique and optimum power flow (OPF) for correcting violations of voltages and flows at an optimum cost.

It is intended that the proposed expert system should be able to identify the type of data encountered, choose the best model for voltage collapse detection and use the appropriate model of OPF for prevention. The knowledge/experience regarding the determination of the best protection for given impact parameters should be appropriately acquired off-line before implementation.

9.3.3 Structural Design of KBVCDP Scheme

The estimation of voltage collapse phenomena is performed in three major tasks, namely (1) power flow base established or divergence control, (2) selection of detection schemes, and (3) correction of violations. This framework developed in numerical methods is designed and enhanced by using KB strategies to achieve optimal performance. Figure 9.5 depicts the implementation logic of interdependent models required to build the knowledge base voltage collapse detection and prevention (KBVCDP) scheme. It consists of a detection and prevention scheme enhanced by the KB support, as described in the proceeding sections.

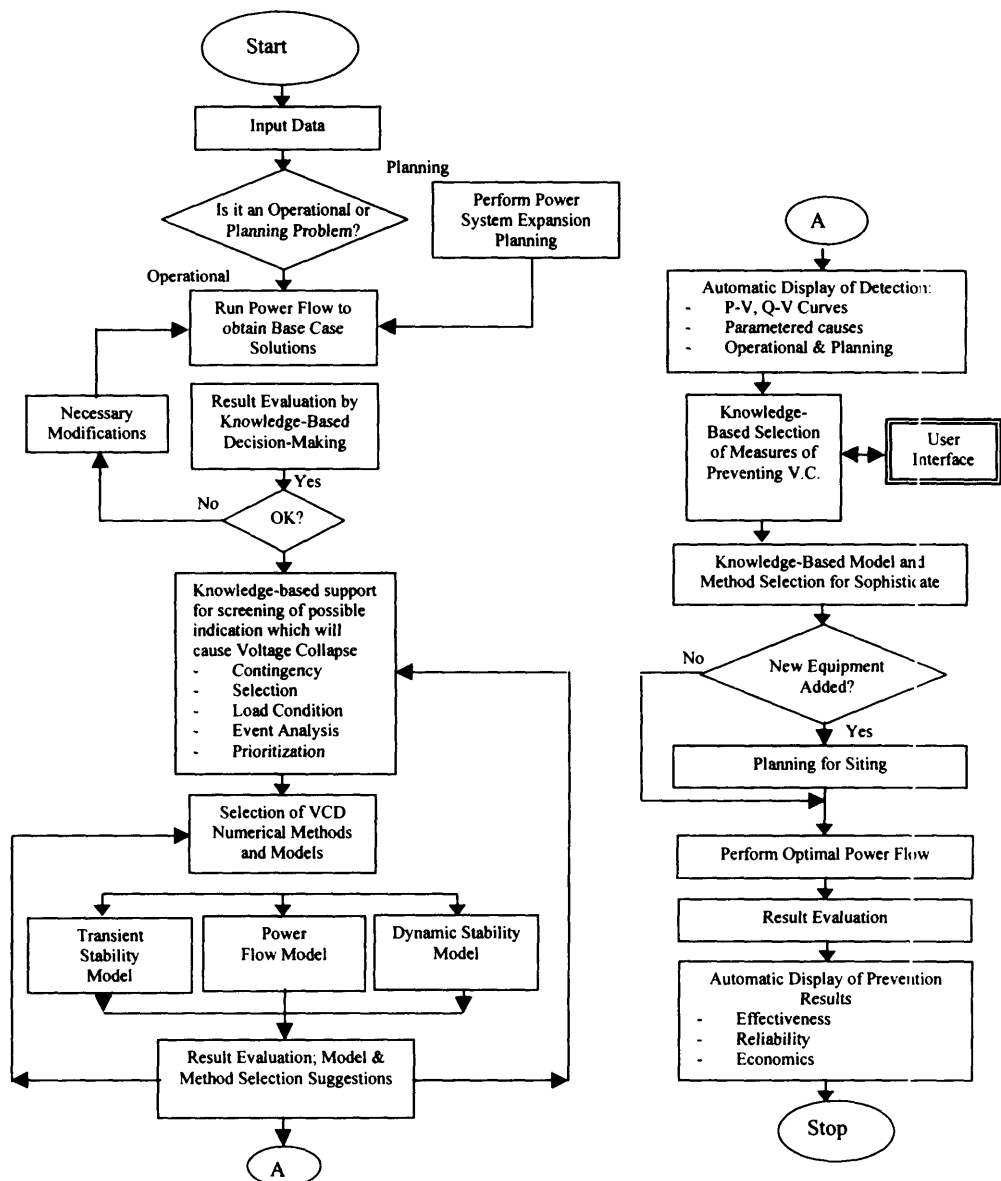


Figure 9.5 Flowchart of the KBVCDP implementation.

Power Flow Divergence Monitoring (KBPFDM)

The program modules utilize heuristic rules to identify cases of load flow run that may diverge due to bad data, telemetering error, method of solution, etc. Suggested corrective measures are also given by the expert system.

Indicator Selection (KBIS)

For an off-line type of study, VC estimation may be detected by evaluating the impact of different indicators on the system that will predict limit violations, thereby causing VC. The KBIS provides prioritized parameters for detection schemes, which can be any of the numerical methods or improved power flow techniques such as an automatic power flow technique.

The automatic power flow technique is a self-contained power flow approach that gives the sensitivity of voltage measurement with respect to parameter changes and make *QV* and *PV* plots to identify the knee point. Other selectable detection schemes developed within KBVCDP include other numerical techniques such as Barbier's and Schlueter's.

KBVC Prevention Scheme (KBVCP)

The identified critical VC points and measures for preventing VC are handled effectively by the KBVCP. It selects appropriate controls as constraints for the optimization algorithm, minimizes relevant objective functions and includes other conditions and models in seeking an optimum corrective measure that is economical and effective. The display of VC knee point and the indicators are given in graphical form. Using the KB system, the corrective measures and the rules fixed are tabulated in matrix forms.

9.3.4 Structural Design of Expert System

A preliminary prototype of the expert system used to verify the feasibility of the KBVCDP has been designed in PROLOG. Its structure is shown in Fig. 9.6. It consists of the following parts: knowledge base, blackboard, inference engine and user interface, and application programs.

Knowledge Base

A knowledge base in the expert system (ES) is the principal source of knowledge used for the KBVCDP implementation. It consists of a fact base and a rule base. The first base consists of fact statements and contains the basic description and record of all power system components, status and configurations and knowledge needed for describing power system states, conditions for selecting measures and methods for interpretation of results. The knowledge contained in

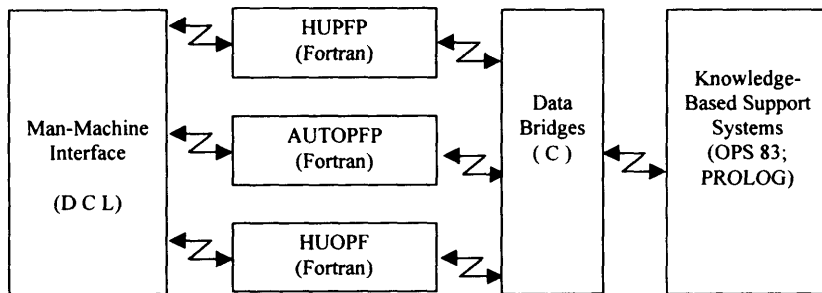


Figure 9.6 Prototype structure of the knowledge-based support system.

the rule base is used to describe the cause-effect relationship between facts in the fact base and perform the basic decision making that will lead to a good decision support scheme. These rules are used in forming the KBPFDM, KBIS, KBMS, KBCM, etc.

Blackboard

The blackboard is designed for database management and communication between the expert system and other units. Messages to prompt new rules or start new evaluation, terminate a study, select relevant data, or improve qualitative reasoning are stored within the blackboard. With results reasoning completed output modules and user access modules are fetched to complete the study.

Inference Engine

The inference engine is dedicated to making effective use of domain knowledge in the knowledge base and to perform message interaction on the blackboard, based on data driven, forward-chaining, and modular procedures.

Rules for Detecting Power Flow Divergence

The rules for detection are developed based on the experience of the operators, literature review, and interviews with experts. The rules detect bad system data, check errors in telemetering, and evaluate the erroneous results due to numerical methods used. Forming those rules and their combinations is designed to indicate specific load flow runs that lead to divergence.

Rules for Selecting VC Parameters (Indicators)

Rules development for prioritizing parameters that may lead to VC are constructed. They consider the impact of events such as line outage, generation

outage, load transformer taps, excitation effects, and other combinations along with other system conditions. The severity of indicators causing VC are ranked.

Rules for Selecting Models and Approaches for VC Detection

Rule development for selecting VC detection methods are based on choice of models, desired options (speed, accuracy, and display), and other major events causing VC.

The expert system selects the indicators that have a higher priority for VC. Several system parameters, limits, and violations are stored in the database. The detection system condition and events causing VC are based on the skills and experience of the operator. Very often the operator's decision will change according to the severity of the contingency or other factors.

The detection and prevention of voltage collapse (VC) based on the KB approach is fast and accurate. The system reads the data, performs manipulations, prioritizes the indicators causing VC and selects appropriate measures, models, and methods for detection and correction.

9.3.5 Knowledge Organization for KBVCDP System

The development of a KB support system for KBVCDP requires the determination of a knowledge organization scheme for the VC detection and prevention. Using a matrix format, the heuristic rules describing detection strategies are formalized. The rules are divided into each of the subtasks. With appropriate data, the prototype KB system will be tested.

Rules for Preventive Measures Selection

Rules for selecting preventive measures are developed based on the following aspects:

1. Rules for ranking corrective measures in terms of the economic evaluation. The effects of system conditions such as loading, generation, length of lines, and seasons of the year are employed to select appropriate measures.
2. Rules for evaluating reactive power, LTC, and others constrain effectiveness. These rules evaluate the effectiveness of LTC, and other controls as constraints for the optimization algorithm. The role of LTC as detrimental or beneficial is evaluated by using system conditions. The selection of appropriate objective functions is identified by using system conditions and limit violations based on the type of violation, ranking of indicators causing the violations, and other system conditions.

9.4 IMPLEMENTATION FOR KBVCDP

The algorithm described in Fig. 9.5 was programmed on a VAX 11/780 and IBM PC compatible computer. The numerical programs are coded in FORTRAN, while the symbolic computation programs are coded in PROLOG. The functional descriptions of each of the KB modules are discussed.

The data files and communication between these modules are also displayed in Fig. 9.7. The program runs on the IEEE 57-bus test system using the rules developed for each of the KB modules. These rules are simulated based on predetermined experiments.

When the experience and knowledge aspects are filled in the matrix according to different selections, different rules can then be developed. The rule matrix approach makes rule development both easier and faster. At the same time, the rule matrix method is also very useful for the new rule developed while the new experiences have been gained. Each column of the rule matrix is a knowledge unit for the rule condition or conclusion and suggestions that are identified. Tables 9.6–9.9 summarize some important results based on experience.

Other combinations of system conditions are checked and results will classify divergence of the power flow as critical, severe, or normal for the power flow divergent part of KBVCDP. Other parts of KBVCDP are developed by the same approach.

Rules are capable of prioritizing causes of power flow (PF) divergence, multiple solutions, and extraneous solutions. Other associated knowledge bases for voltage collapse detection include the development of rules that study the indicators for detecting voltage collapse and selecting the performance index for voltage collapse studies, and rules for selection of measures for voltage collapse periods.

9.4.1 Limitation of the Operator Assisted Expert System

When the human experts' heuristics are successfully encoded in the KB, a review of the literature indicates that the ES was comparable in performance with human expert to a certain extent. Creating the KB for the VCDP or for any of the operational problems (e.g., security-assisted, and voltage control) is a difficult problem. One must first define the problem to be solved and then encode it in a set of rules. However, the KB cannot solve the problem by itself. A human expert uses past experience together with the background of the whole problem to make the correct decision on causes of VC and preventive methods needed. Hence, in order to design an ES that can utilize the expertise of the human, we must find a way of integrating the human expert's empirical knowledge in one domain.

Successfully encoding the human expert's empirical knowledge into a set

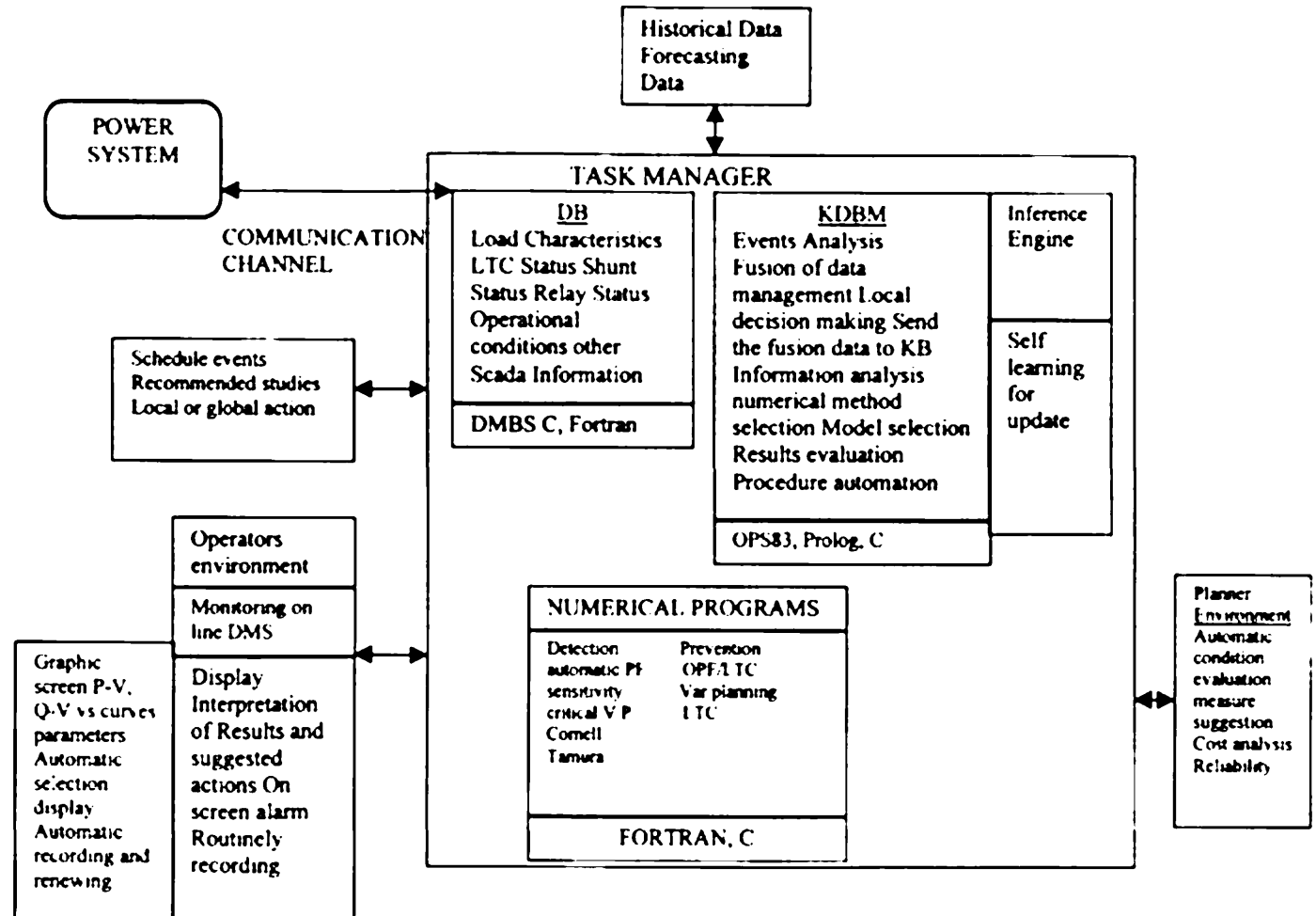


Figure 9.7 Model architecture for knowledge based support VCDP

Table 9.6a Matrix of Rules for Voltage Collapse: Method Selection

| Events | | | | | IF | | | | | | | | Then | | | | | |
|--------|---|---|---|---|-----------------|------|--------------|-----|----------------|-----|------|----|-----------------|-----|-----|------|-------|---|
| 1 | 2 | 3 | 4 | 5 | Choice of model | | | | Desired option | | | | Selected method | | | | | |
| L | S | L | S | L | Rank | Stat | Stat and Dyn | Dyn | Speed | Acc | Disp | HU | Tamura | BPA | Sch | Barb | Chang | |
| | X | | | | 1 | | | X | X | | | | X | | | X | | |
| | X | | | | 1 | | | X | | X | | | X | | | | | |
| | X | | | | 1 | | | X | | | | | X | | | | | |
| | X | | | | 2 | | X | | X | | | | X | | | | | |
| | X | | | | 2 | | X | | | X | | | | | | X | | |
| | X | | | | 3 | X | | | X | | | | | | X | | X | |
| | X | | | | 3 | X | | | | X | | | X | | | | | |
| | X | | | | 3 | X | | | | | X | | X | | | X | | |
| | X | | | | 1 | | X | | X | | | | | | | | | X |
| | X | | | | 1 | | X | | | X | | | | | | | X | |
| | X | | | | 2 | X | | | X | | | | | | X | | X | |
| | X | | | | 2 | X | | | | X | | X | | | | X | | |
| | X | | | | 2 | X | | | | | X | X | | | | | | |
| | X | | | | 1 | X | | | | X | | | | | | X | | |
| | X | | | | 2 | | | | | X | | | | | | X | | |
| | | X | | | 1 | X | | | | | X | | | | | X | | |
| | | X | | | 1 | X | | | | | X | | | | | X | | |
| | X | | | | | | | | | | | | | | | | | |

of production rules might also prove to be a difficult task. The knowledge base is likely to be incomplete and may be inconsistent. These limitations are justified in VCDP since the cause of VC are system-dependent. The model used involves the interaction of system parameters, system conditions, etc. The ES designed may have the problem of portability and inconsistent knowledge.

The traditional nonknowledge-based approaches for voltage collapse detection and prevention can be used to solve the problems in VCDP. At the same time, the following are common problems:

The divergence reason for the power flow, automatic series run power flow, and optimal power flow programs are always difficult to identify especially for the less experienced power engineers. Even the judgement of experienced engineers can be wrong because voluminous input and output data are involved. At the same time, the divergence of the iteration procedure may be caused by reasons in the program other than in the data.

Table 9.6b Matrix of Rules for Voltage Collapse: Method Selection

| Events | | | | | IF | | | | | | | | Then | | | | | | | |
|--------|---|---|---|---|-----------------|---|---|------|----------------|--------------|-----|-------|-----------------|------|----|--------|-----|-----|------|-------|
| 1 | 2 | 3 | 4 | 5 | Choice of model | | | | Desired option | | | | Selected method | | | | | | | |
| L | S | L | S | L | S | L | S | Rank | Stat | Stat and Dyn | Dyn | Speed | Acc | Disp | HU | Tamura | BPA | Sch | Barb | Chang |
| | | X | | 3 | X | | | | | | | X | | X | | | | | | |
| | | | X | 2 | X | | | | | | | X | | X | | | | | | |
| | | | | X | 1 | | | | | X | X | | | | | X | | | | |
| | | | | X | 2 | | | | | | X | | | | | X | | | | |
| | | | | X | 2 | | | | X | | | | X | | | | | X | X | |
| | | | | X | 3 | X | | | | | X | | | X | | | | | | |
| | | | | X | 3 | X | | | | | | X | | | | | | X | | |
| | | | | | 1 | X | | | | | X | | | | | | X | | | |
| | | | | | 1 | X | | | | | | X | | X | | | | | | |
| | | | | | 1 | X | | | | | | | X | X | | | | X | | |
| | | | | | 2 | X | | | | | X | | | | | | | X | | |
| | | | | | 2 | X | | | | | | X | | X | | | | | X | |
| | | | | | 2 | X | | | | | | X | | X | X | | | | | |
| | | | | | 3 | X | | | | | | | | | | | | X | | |
| | | | | | 3 | X | | | | | | X | | X | | | | | X | |
| | | | | | 3 | X | | | | | | | X | X | | | | | | |
| | | | | | | | | | | | | | | | | | | | | |
| | | | | | | | | | | | | | | | | | | | | |
| | | | | | | | | | | | | | | | | | | | | |
| | | | | | | | | | | | | | | | | | | | | |

Table 9.7 Corrective Measures and Economical Ranking

| No. | Measures | If | Then |
|-----|--|----|-----------------------------|
| | | | Economical condition number |
| 1 | Capacitor dispatch | | 2 |
| 2 | Dispersed generation control | | 1 |
| 3 | Demand-side management | | 6 |
| 4 | Voltage reduction for load relief | | 5 |
| 5 | LTC and distribution voltage regulator | | 4 |
| 6 | Load shedding | | 7 |
| 7 | Series compensation | | 8 |
| 8 | Parrallel compensation | | 3 |
| 9 | Network expansion | | 9 |
| 10 | New plants | | 10 |

Table 9.8 Matrix of Rules for Power Flow Divergence Indicators
(Solutions Methods)

| Rule number | If | | | | Then | |
|-------------|-------------|-----|----------------|----|---|---|
| | Mis-matches | | Initial values | | For Newton-Raphson (NR) divergence due to | For Gauss-Seidel (GS) divergence due to |
| | Incr | Dec | Yes | No | | |
| 1 | X | | | | X | Ill-condition problem |
| 2 | | X | X | | | X |
| 3 | | X | X | | X | Data representation |
| 4 | X | | X | | | X |
| 5 | X | | | X | X | Initial values |

Table 9.9 Effective of LTC for Optimal Power Flow

| Network conditions | If | | | | Then | |
|--------------------|--|-------|-------------|---------|---------------------|-------------|
| | Power import $P_{\text{LOAD}} - P_{\text{GLOCAL}}$ | | VAR support | | Installation of LTC | |
| Key line outage | <Zero | >Zero | Deficit | Surplus | Beneficial | Detrimental |
| X | | X | X | | | X |
| X | X | | X | | | X |
| X | | X | | X | * | * |
| X | X | | X | X | X | |
| | | X | X | | | X |
| | X | | | X | * | X |
| | | X | | X | X | * |
| | X | | | | | |

*To be determined.

The voltage collapse indicator selection is very complicated. In power system voltage collapse studies, what causes the voltage collapse is the most important study aspect of the stable problem. Most of the time, there may be more than one cause, but determining the original and most important ones are difficult.

Because of the selection indicators, the preventive measure selection is also quite complicated. The selection of preventive measures involves consideration of economics, planning strategies, operational security and system feasibility for the measures. At this time, there are no acceptable strategies for this problem.

For certain study problems, the selection of study models and numerical methods is a complex one even for researchers who have been studying voltage collapse phenomena for a long time. Interpretation of the numerical program results usually require the judgement of an engineer.

To solve the above problems for the nonknowledge-based approaches, the knowledge-based approach has the following advantages:

The data bridge can transfer the quantitative data into qualitative data directly. Thus, the KB scheme can directly use the data for logical reasoning for determining any possible errors in the numerical data and making suggestions for correcting them. This procedure will save a considerable amount of time for indicator identification.

The knowledge-based voltage collapse indicator selection, study model, and method selection scheme can make more sophisticated and faster choices for the decision-making procedure. The selected indicators and study model is more suitable for the study. This is the same as in preventive measure selection, the KBVCDP gives more choice of measures rather than the right judgement at due time.

The KBVCDP also gives heuristic and clear guidance on how to detect and prevent voltage collapse in a more convenient way.

The approach, using knowledge-based technology, is suggested to enhance the detection and prevention scheme for voltage collapse. The suggested approach has been prototyped as an expert system program both on the IBM PC/AT using the PROLOG language and on the VAX 11/780 using OPS83 and C languages. The data bridge concept has been introduced, and data bridges for different numerical programs have been designed and implemented. Shorter reasoning time and more accurate results by using KBVCDP are verified by the results and the explanation.

9.4.2 Examples of KBVCDP Output

The KBVCDP developed has been tested on different systems under operational conditions. The program was initially developed under the VAX 11/780 and

Table 9.10a Test Results Number 1: Rule Matrix for Power Flow Divergence (57-Bus System)

| Test case number | Rule fired | T_p | V- δ position number | PV position number | R/X ratio | Lines loss number | System condition |
|------------------|------------|------------|-----------------------------|--------------------|-----------|-------------------|------------------|
| 1 | 1 | In limits | 1 | 12, 39 | Low | No | Severe |
| 2 | 3 | Out limits | 2 | 12, 39, 1 | High | No | Severe |
| 3 | 8 | Out limits | 1 | 27, 36, 42 | High | 1-5 | Critical |
| 4 | 12 | In limits | 3 | 27, 36, 42 | High | No | Critical |
| 5 | 15 | Out limits | 12 | 1, 39 | High | No | Critical |
| 6 | 16 | Out limits | 2 | 27, 36, 42 | Low | No | Critical |
| 7 | 20 | In limits | 39 | 1, 12 | High | 1-5 | Severe |
| 8 | 22 | Out limits | 1 | 12, 39 | Low | No | Severe |

IBM PC/AT environment using PROLOG, PASCAL, and FORTRAN. Later, the program was modified using OPS83, C, DCL, and FORTRAN languages entirely under the VAX 11/780 environment.

9.4.3 Tests of KBVCDP on the 57-Bus System

To demonstrate the capability of the KBVCDP, a series of tests were performed on the 57-bus system. Tables 9.10a-9.10f give the results of the rule matrix for

Table 9.10b Test Results Number 2: Rule Matrix for Power Flow Divergence Indicators (Solution Method)

| Test case number | Ruled fired | Mismatch | Initial values | Data precision | Tolerance | Newton-Raphson method | Gauss-Seidel method |
|------------------|-------------|---------------------------|---------------------------------|----------------|-------------|-----------------------|---------------------|
| 9 | 1 | Increase bus number 12 | Ok | Double | Not reached | Ill-conditional data | -- |
| 10 | 2 | Decrease | Ok | Single | Not reached | | -- |
| 11 | 4 | Increase bus number 29 | Ok | Double | Satisfied | Data precision | -- |
| 12 | 5 | Increase bus number 29 | Bus number 33 heavily loaded | Double | Satisfied | Initial value | -- |

Table 9.10c Test Results Number 3: Rule Matrix for VC Indicator Selection

| Test case number | Rule fired | Line outage number | LTC condition | Compensation | Rank |
|------------------|----------------------|--------------------|----------------|------------------------|------|
| 13 | Event load 1 | 1–15 | Off limit 4–18 | Series and parallel on | 1 |
| 14 | Event load 4 | 1–15 | Off limit 4–18 | Series and parallel on | 1 |
| 15 | Generation event 3 | 1–15 1–15 | In limits | Series and parallel on | 2 |
| 16 | LTC event 2 | | Off limit 4–18 | Series and parallel on | 2 |
| 17 | Compensation event 5 | 1–15 | Off limit 4–18 | Series on | 2 |

Table 9.10d Test Results Number 4: Rule Matrix for Detection Method Selection

| Test case number | Model selection | Speed | Accuracy | Display | Selected method |
|------------------|--------------------|-------|----------|---------|--------------------|
| 18 | Dynamic | X | | | Tamura and Barbier |
| 19 | Dynamic | | X | | Tamura |
| 20 | Static and dynamic | X | | | Tamura |
| 21 | Static | | X | | Hu and Schlueter |
| 22 | Static | X | | | Hu and Schlueter |
| 23 | Static | | | X | Schlueter |
| 24 | Static | | X | | Howard Uni |
| 25 | Static | X | | | BPA |

Table 9.10e Test Results Number 5: Rule Matrix for Preventive Measures Selection

| Test case number | Model selected | Q limits | V limits | Flow over | $Q_G > Q_{G\text{MAX}}$ | Corrective measure rank |
|------------------|--------------------|----------|----------|-----------|-------------------------|-------------------------|
| 26 | Dynamic | Out | Out | Out | Yes | 5 |
| 27 | Dynamic | | Out | Out | Yes | 4 |
| 28 | Dynamic | Out | Out | Out | | 1 |
| 29 | Static and dynamic | Out | Out | Out | | 2 |

Table 9.10f Test Results Number 5: Rule Matrix for OPF

| Test case number | V Constraints | P_e Constraints | Q_e Constraints | Flow Constraints | P_d Constraints | Security index | LTC Constraints | Q_e Constraints | Objective |
|------------------------|--------------------|----------------------|----------------------|---------------------|----------------------|-------------------|--------------------|----------------------|---------------------|
| 30 | X | X | X | X | X | X | X | X | Voltage and cost |
| 31 | X | X | X | X | X | X | X | X | Q_{losses} |

the power flow divergence indicator with respect to power flow data. Test cases number 1 and number 2 are with correct slack bus and control bus position. The RX ratio and data format results in the same system condition, that is, classified as "severe."

9.5 UTILITY ENVIRONMENT APPLICATION

The developed KBVCDP is numerical program-dependent. For different numerical programs, the data bridges from numerical program to knowledge-based program vary. The application of KBVCDP to different utility companies needs more implementation of the data bridges for special programs.

CONCLUSION

The use of artificial neural networks for voltage stability assessment and enhancement has been presented. The method utilizes modal analysis to obtain suitable buses for use as VAR sites. The ANN-based maximum loadability of the power system was demonstrated and the ANN-based maximum loadability of the power system with VAR compensation was demonstrated as well.

The maximum loadability of the power system and reactive power compensation at collapse used for training the ANN have been obtained using the EPRI VSTAB program. The sensitivity of the accuracy of the predicted output from the ANN has been investigated with different ANN architectures. The trained ANN has been tested with input data not previously seen by ANN.

It is concluded that the back propagation algorithm can be used with reasonable accuracy for providing an estimate for the reactive compensation at collapse as well as a measure of the voltage stability margin in the presence of switchable shunts. The appropriate ANN architecture needs to be determined based on the relevant system data.

The trained ANN provides reasonable results in an extremely short time, almost instantaneously, when compared with other existing methods utilizing successive power flow or optimization.

The inputs/outputs for training are easily obtained via successive power flows and do not require extensive computation when compared with certain other energy-based methods utilizing ANN for assessment of the voltage stability limit.

The design, analysis, and development of a knowledge-based expert system to detect and prevent voltage collapse has been demonstrated. The detection scheme selects parameters that cause voltage collapse and also evaluates available models of the power system. It uses rule-based techniques for prioritizing

indicators and choosing appropriate numerical methods. The prevention scheme identifies measures needed to correct violations of bus voltages and flows due to a loss of generating units or critical lines. Selected measures are under-load tap changers, capacitors, line switching, load shedding, and generation adjustment. The knowledge-based system ranks these measures in terms of their effectiveness in corrections. Subject to equipment and network constraints, a specialized optimal power flow scheme based on a reactive power model of a power system minimizes cost and power loss.

The expert system was tested on medium-sized power systems. Bonneville Power Administration's Puget Sound Area, and New England's Boston Area. Results reveal the need for adequate use of under-load tap changers and other control devices as a short-term measure to prevent voltage collapse. Such devices can obviate the need for the installation of a new generation of capacity and the expansion of transmission systems.

10

Epilogue and Conclusions

This book treated broad issues in power system dynamics with special emphasis on the twin subjects of angle and voltage stability. Both are essential tools for dynamic security assessment.

Dynamic security characterizes a power-system's ability to withstand disturbances and ensure continuity of service. In operational planning, dynamic security analysis encompasses a large class of problems, such as finding the security status of a network, the power transfer limit in a transmission corridor, the worst contingency in a specific area, or performing some complex sensitivity analyses. In practice, dynamic security is often measured in terms of a dynamic security limit, defined as the maximum power transfer for which the network cannot only survive the worst possible normal contingency, but also guarantee an acceptable level of service quality without loss of load.

Dynamic security analysis is dominated by the use of algorithmic software for off-line evaluation and control of load flow, transient stability, and other network characteristics. Even though simulations are readily performed, assessing and ensuring dynamic security across all possible topologies and contingencies remains a formidable challenge.

Power system networks currently operate more and more in a stressed state where conservative operation often results in significant financial consequences. The process for an on-line dynamic security assessment requires a reasonable level of built-in intelligence to detect and determine the following:

1. Assess the system dynamic performance
2. Determine the degree of stability or instability (margin)
3. Determine the sensitivity of the margin to key variables
4. Iteratively repeat the preceding steps to obtain the stability limit.

In order to do a credible job of security assessment, a large number of combinations of network configurations under contingency must be done. This is beyond the capability of the typical operational planning unit in an electric power system. There are three reasons for this:

1. Determining the power transfer limit is a complex, iterative process requiring the execution of many stability simulations and considerable expertise. To perform a single power transfer limit search, one begins by executing a power flow for a given topology and carrying out manual modifications to the input data until a satisfactory steady-state case is found. This is then used to initialize the network for a transient-stability simulation, also manually initiated by the user. Once the simulation is complete, we may resort to yet another tool to apply transient-stability criteria, determining what the next step will be (i.e., increase or decrease power transfer in the faulted corridor), to modify local-flow software inputs accordingly and re-enter the process. This is repeated until the required limit is found.
2. The process of computing transient stability simulation remains highly time-intensive due to expertise-related tasks. This is true for data collection, input validation, output postprocessing, and result analysis requiring a considerable amount of time.
3. Additional expertise is required to scale the problem down in such a way that the dynamic security limit of only a small set of topologies need to be found explicitly. This reduced set forms a basis for estimating the needed dynamic security limits. The price to pay is a lack of precision that translates into more conservative security limits.

In order to improve the efficiency and accuracy of off-line intelligence security analysis, the application of artificial intelligence techniques has been proposed. Alternatively, expert system, fuzzy logic and ANN usually in combination with energy based methods or simplified algorithms may be used. An interesting recent concept involves the use of a generalized shell for the purpose of mechanizing processes in dynamic security assessment. Marceau et al. (1993) demonstrate that semantic networks combined with frame-based structures can effectively model the process and provide a framework for constructing a highly powerful and user-friendly environment. Their research carried out on a production level prototype shows that it is possible to mechanize routines traditionally carried out by human experts. This mechanization greatly enhances the realization of complex processes.

The expectation of dramatic increases in the interconnection and complexity of power systems has raised concerns about the performance, security, and control of transmission and distribution networks. These increases are expected to result primarily from two developments:

1. New legal requirements allowing greatly expanded wheeling of power over existing networks, and
2. The wide-spread application of power-electronics-based active switching and control devices to raise the real power capacity of existing lines via local control of voltage, impedance, or phase angle.

We have already suggested that power systems are already becoming increasingly stressed. Unexpected behavior has been observed in many networks under unusual stress, behavior suggesting that some important system dynamics are not yet well understood and hence are not accounted for in simulations conducted for control and security purposes. Enhanced fundamental knowledge about system stability and nonlinear dynamics may be necessary in order to control existing and future power systems reliably and continuously under all contingencies. In addition to ensuring power network security under normal and exceptional stress, such improved understanding could yield substantial economic benefits by allowing secure operation closer to performance margins than is currently considered safe.

Interconnected power networks can be described as stressed, highly nonlinear, noncontinuous systems. Systems of this type are extremely difficult to accurately model, either mathematically or conceptually. Thus, current power system simulations generally aim to model the slow, quasi-continuous dynamics most significant to system dispatchers, such as excessive voltage and apparent power variation with respect to changing demand. The details of transient behavior, with which most computational complexity is associated, are for the most part neglected.

Typical network simulations are considerably simplified and approximate (although they still incorporate hundreds of complex equations). In addition, even the most comprehensive models include fundamental approximations to account for anticipated behavioral nonlinearity or noncontinuity and depend on critical assumptions about performance because we lack a complete understanding of the physical behavior of complex power systems. For example, to facilitate computation for conventional simulations, parameters like load values are held constant, even though these parameters are known to vary slightly. And the modeling of systems that incorporate active control devices requires the use of assumptions because complete descriptions of device behavior are not yet available.

Observing that all models do not use the same approximations and assumptions, their predictions of system behavior may differ strikingly, especially for

conditions of stress. Utility experts thus find it difficult to assess the validity of a given model's results. Nonetheless, as long as predictions indicate that control measures will maintain generation-load imbalances within a normal operating range, dispatchers assume that the system will remain stable, and they are almost always correct.

Recent studies of historical voltage collapse events suggest that traditional load simulations (such as those assuming constant load angle, constant impedance, and constant current) may not capture important voltage dynamics. For example, a voltage collapse may be initiated by the oscillatory behavior of generator exciters, but models that consider only the slow dynamics of the system ignore exciter dynamics and other transient behaviors. As a result, unsteady system states may be incorrectly assessed as stable, with continued operation possibly leading to local or systemwide failure.

Chaos theory, the study of nonlinear dynamics, may provide new approaches for understanding the transient behavior of complex power systems and for ensuring network stability. Mathematical research during the past 20 years indicates that any system involving feedback can exhibit chaos. It can be shown that chaos is present in simple power system models over a range of loading conditions. Recent research results suggest that events such as voltage collapse, low-frequency electromechanical oscillations, and transient stability may be linked to chaotic behavior.

It has been established that there is a relationship between voltage collapse and chaos-related bifurcations in voltage-reactive power solutions. Significant work has been carried out aimed at increasing our understanding of chaos and transient stability. In particular, researchers examined in detail certain unusual, possibly chaotic behaviors observed in small power systems and are looking at tools for evaluating system stability under parametric or structural variations. Efforts focus on improving the characterization of bifurcations in simple and complex power systems. Bifurcations, which represent qualitative transformations in a system's operational behavior (changes from stable to unstable states, for example, or the onset of multiple allowable solutions), can lead to chaos. Because fundamental power flow equations have multiple solutions (swing dynamics), bifurcations in power system behavior are always possible.

A three-bus model was enhanced to include generator dynamics, revealing several additional bifurcations, some of which lead to chaotic oscillation through period-doubling cascades. For these cases, an infinite number of power flow solutions occur in response to only a small change in reactive load, causing rapid fluctuations in voltage and load angle that could produce power flow oscillations exceeding the thermal limits of transmission lines and lead to system collapse.

Simulations focusing on these dynamic-generator-case bifurcations also indicate that voltage collapse may take place before the reactive power demand is increased to the system's steady-state operating limit, the point at which the

static-case, saddle-node bifurcation occurs. Thus, the model system, and probably actual power systems as well, may be less stable under fluctuating real-world conditions than under the steady-state cases assumed in conventional stability calculations.

Structural stability is a relatively new concept in power system analysis. Broadly speaking, a system is structurally stable if small variations in the model do not change qualitatively the set of trajectories originating from all initial conditions in the state space. For a given dynamic model, we examine system behavior subject to small disturbances in the domain of parameter space. This is different from Lyapunov stability where we wish to know if a perturbation in the state-of-the-system results in the trajectory returning to the equilibrium asymptotically. A dynamic system which is unstable in the sense of Lyapunov is structurally stable since the trajectories do not change for small changes in parameter values.

A complete characterization of structural stability for two-dimensional systems can be related to the nature of the equilibria and limit circles. For higher order systems such a complete characterization is not possible. Bifurcation theory is directly related to structural stability. Research work has been conducted that aims to provide dispatchers with a better understanding of the limits of all significant structural parameters (such as load angle, current, impedance, and reactive power demand) so that power systems can be operated to maximize cost-effectiveness without initiating harmful chaotic behavior.

Structural stability is important for power system security because key parameters are known to fluctuate slightly. For a system to be assessed as structurally stable, its behavior must return to its steady-state if perturbed. For example, a power network is considered structurally stable if slight changes in current or load angle do not appreciably affect the interactions between voltage and other system variables. (This differs from the more common notion of Lyapunov stability, which assesses stability on the basis of the initial values of system variables.) Structural stability defines the parameter range within which system behavior is qualitatively similar; multiple ranges may exist for a given parameter. Little work has been done in this area for nonlinear models of power systems.

Research has revealed that for systems characterized by more than two parameters, no complete description of structural stability is possible. But parametric limits of structural stability can be related conceptually and mathematically to bifurcations. Both indicate qualitative changes in system behavior and can be seen in phase portraits of a system. Thus, bifurcation analysis of system behavior can partially characterize structural stability ranges.

It was observed that if control actions are taken into account, the critical values of parameters that influence voltage collapse may be lower than those predicted by static criteria. They postulate that the range over which a dynamic system is structurally stable is always smaller than the range for the same system

considered under static conditions only. Thus, parameter margins identified by conventional, static-case power system models to ensure safe system behavior may be overly permissive for dynamic, real-world networks.

Results suggest that knowledge of dynamic stability limits is key for reliable control of modern power systems. These margins must be satisfactory at all system buses for the varying load demands typical over a 24 hr period. To identify the margins, an enhanced understanding of active power networks is required. Particularly important are physical and mathematical descriptions of the behavior of active control devices that fully account for their fast-switching dynamics.

There is a need for better analytic capabilities in both the areas of system planning and operations. Promising techniques include the use of energy function methods, which are based upon the use of Lyapunov's direct method for assessing the stability of systems of nonlinear differential equations. After many years of research, energy functions are now successfully used to assess system transient stability in the planning context, and are on the verge of being used on-line to determine the transient stability limits. More recently, energy methods have also been employed for assessing the system's quasi-static voltage security. The relationship between the use of energy functions in these two different contexts, was examined by Overbye et al. (1991).

The key points for energy function usage in the transient stability problem is that the energy is used to determine whether the postfault is within the region of attraction of the postfault stable equilibrium point (SEP), and that the determination of the critical boundary of stability depends on the faulted system trajectory.

In contrast, for the voltage security problem the system state is assumed to vary quasi-statically (i.e., not subject to a large disturbance) in response to the slow (with a time scale of min to hr) variation in system parameters, such as the aggregate loads. Loss of the system stability in this context would occur not through a large disturbance providing the system state with enough "energy" to escape the SEPs energy "well," but rather through the coalescing of the SEP with one of the type-one UEPs contained on the boundary through a saddle node bifurcation as the energy "well" flattens out. Because of the need to model nonimpedance loads and to retain the network topology, the SPM has been used exclusively in voltage security assessment.

It has been proposed that the UEP energy, which is a measure of the distance between the SEP and UEP, be used as a measure for the system quasi-static voltage security. Numerical testing has shown that the energy measures tend to change in a manner proportional to the change in the system's maximum steady loadability. System steady-state voltage security could thus be assessed by monitoring these energy measures, with decreasing energy values indicating

increased vulnerability to voltage instability; a value of energy approaching zero would indicate an imminent loss of system operating point.

There is, however, a significant difference in the use of these UEP energies from their transient stability use. In transient stability the goal is to determine a *single critical energy value*, which depends upon the fault-on system trajectory. In contrast with the steady-state voltage problem one is concerned with maintaining system voltage security while facing an imprecisely known future system parameter variation. While a future voltage collapse would be characterized by the coalescing of the SEP with a particular UEP, there is no need to determine precisely this UEP *a priori*. Rather the energies associated with a number of UEPs would be monitored. It is shown that each UEP energy can be used to quantify the voltage stability in a particular portion of the system and that only the small subset of UEPs with low associated energies need to be calculated. This is because in a large system, there is a need to simultaneously monitor the voltage security in a number of separate areas.

Two major similarities in the application of energy methods to the transient and voltage problems is that the same energy formulation can be used in both, and that both make use of the energy of the UEPs on the boundary of the region of attraction. In general for a three bus system, it is shown that the power flow equations have an SEP solution and another type-one UEP solution. Energy methods could then be used for transient analysis by determining if the energy after a fault is cleared is less than that of a specific threshold.

Whether the system possesses other solutions depends on the load model used. If the load is modeled as constant impedance then there are no other solutions to the power flow equations, since the network is linear and could be replaced by a Thevenin equivalent impedance. However, if the load is modeled as constant power, then the system has two additional solutions.

Phase portraits can be used to illustrate a number of the mechanisms that could cause the system to lose its stable operating point; and that would thus need to be considered in security analysis. For the transient analysis, stability would be assessed by determining if the energy at the time the fault is cleared is less than ϑ^* . The value of ϑ^* depends on the exit point (i.e., the point where the critically cleared trajectory would cross the stability boundary $\partial\Omega$). Since this value would typically be by a large generator angle, the exit point would be in the vicinity of the transient stability UEP. A new use of the energy function would be for dynamic voltage security assessment. As in the case of transient analysis, stability would be assessed by determining if the energy after some disturbance is less than some critical value. However, the disturbance here would be one that would tend to cause the system trajectory to exit the SEPs UEP. Such a disturbance would be characterized by low voltage magnitudes (as opposed to large generator angles), and may have a substantially longer time

frame than the transient stability problem (on the order of min as opposed to s). Examples of such disturbances are the effects of LTC transformers, generators hitting reactive power limits, and load dynamics.

Quasi-steady voltage security could be monitored by noting the variation in the UEP energy as the system state changes in response to the slow (on the order of min to hr) variation in system parameters, such as the aggregate loads.

The second segment of this book introduces a relatively new technology and its direct applications and future to power system engineers. Over the past few decades, the topic of artificial intelligence (AI) has gained the interest of researchers and scientists in many fields. The applications span many disciplines including electrical engineering extending its way to electrical power system analysis, protection, and enhancement. The resulting advantages will inherently depend on the specific applications of the existing methods that are available to the engineering sector.

As discussed in previous chapters of the book, the primary branches in artificial intelligence are Fuzzy Logic, Artificial Neural Networks, and Expert Systems. The obvious benefits of using Fuzzy Logic and/or Fuzzy Logic Expert Systems include the enhancement of the assessment criteria used in the study of large power systems, and also as decision support systems. This mode of AI application as a support tool to the existing technique provides clearer solution alternatives to problems, in which case there are many variants with multi-levels of uncertainties. Therefore the assessment of the power system is improved and the appropriate control actions to be exercised in the event of contingencies are more efficiently allocated, especially in a utility where the resources are either limited or expensive to use. Furthermore, the use of Fuzzy Logic and/or Expert Systems in power system stability studies can significantly reduce computational burden in some algorithms, as the human or engineering judgment is exploited in determining redundancies of choice. The classic example is contingency analysis of a power system, whereby it may not be necessary to consider *all* possible cases, but rather *all* (sufficiently) *probable* cases.

The area of Artificial Neural Networks (ANN) has its place as a planning and operation tool or support tool also, especially in light of some of the more recent restructuring developments that has occurred in the power industry. These changes, such as deregulation of the power industry, have been a result of changes in the markets for electricity both as a commodity and service. The challenge in the application of ANN lies in the unanswered questions that we have come face to face with as both engineers and power system tools and policy makers. For instance, what are the impacts of artificial intelligence support tools on power system reliability and stability? Can the technology improve the desired goals of the classical integration techniques (Runge-Kutta, Modified Euler, Trapezoidal, and so forth) making them better assessment methods? How

can we perform detailed security assessment of the power system with the introduction of this enhancement method?

In conclusion, we have realized the capabilities and limitations of the existing methods utilized in performing comprehensive analysis on the power system, both in the areas of steady state and transient stability studies. Maintaining power system stability is one challenge, but it is the flip-side of the coin that motivates us to go to work, which are the problems associated with power system instability. The severity of the faults resulting from voltage and/or angle instability has led to the development of many methods of monitoring and preventing these unwanted results. Such methods, some of which were highlighted and discussed in detail in this book, are currently being enhanced via the application of state of the art technologies. The cost-benefit analysis of such tools is yet to be done for large-scale power system applications, for both planning and operational purposes. In this light, continued research and the use of artificial intelligence as an enhancement to the computational and decision tool will introduce much benefit to the power industry.

Glossary

Accelerating torque: The difference between the input torque to the rotor and the sum of the load and loss torques; the net torque available for accelerating the rotating parts.

Activation function: Hidden units that are needed to introduce nonlinearity into a neural network.

Active power: The average power in an electric power circuit is referred to as the active power.

Admittance: The term admittance (symbol Y) is used in a transform network (s-domain or complex, for sinusoidal steady state operation) to denote the inverse of the impedance parameter. The current through an element is the product of the element's admittance and the voltage across it.

Angle stability: Stability of an electric power system evaluated on the basis of the analysis of the dynamics of the rotor angle dynamics and the coupled electric network.

Angular acceleration: The rate of change of angular rotor speed.

Angular speed: The rate of change of the rotor angle.

Approximate reasoning: A computational modeling of any part of the process used by humans to reason about natural phenomena.

Artificial Neural Network (ANN): Physical cellular systems that can be used to acquire, store, and utilize experiential knowledge.

Back propagation learning algorithm: The back propagation algorithm modifies synaptic connection strengths with nonlocal error information. The algorithm propagates the instantaneous squared error backward from the output through the hidden layers to the input at each iteration.

Back propagation or counter propagation neural networks: A neural network training method that uses the generalized delta rule that uses a gradient descent method to minimize the total squared error of the output computed by the net.

Capacitor bank: An assembly at one location of capacitors and necessary accessories required for a complete operating installation.

Capacitive reactance: The imaginary part of the impedance of a predominantly capacitive element.

Certainty factors: Guesses or projections by the domain expert about the relevance of evidence to support the recommendations passed by the inference engine of the rule-base system to the user.

Clearing angle: The angle corresponding to the time elapsed from the beginning of overcurrent to the final circuit interruption.

Conductance: The following are not equivalent but are supplementary: (1) The real part of admittance and (2) the physical property of an element that is the factor by which the mean square voltage must be multiplied to give the corresponding power lost as heat or as other permanent radiation or loss of energy from the circuit.

Continuation power flow: The Jacobian matrix of the power flow computation becomes singular at the voltage stability limit. Continuation power flow overcomes this problem by using locally the parametrized continuation method involving predictor and corrector steps.

Convergence: For an iterative process, convergence means that the successive differences between subsequent values of the unknown values have progressively become closer and are below a certain predefined convergence tolerance threshold.

Counter propagation: A neural network means that combine an unsupervised Kohonen layer with a teachable output layer.

Crisp sets: The fuzzy set term for traditional set theory. That is, whether or not an object belongs to a set.

Critical clearing angle: For a system of one machine connected to an infinite bus, and for a given fault and switching arrangement, the critical clearing angle is that switching angle for which the system is at the edge of instability.

Current: A generic term used where there is no danger of ambiguity to refer to any one or more currents specifically described. The use of certain adjectives before "current" is often convenient, as in conducting current.

Database: A collection of clauses with each clause on a database representing something that is known to be true.

Decision trees: Tools for making number-based decisions where a lot of complex information needs to be taken into account.

Direct method: The direct method is usually referred to as Lyapunov second method of stability assessment, which attempts to determine stability by using a suitable Lyapunov function.

Direct-axis: The axis that represents the direction of the plane of symmetry of the no-load magnetic flux density, produced by the main field winding, normally coinciding with the radial plane of symmetry of a field pole.

Direct-axis component of armature current: The component of the armature current that produces a magnetomotive force distribution that is symmetrical about the direct axis.

Direct-axis component of armature voltage: The component of the armature voltage of any phase that is in time phase with the direct axis component of current in the same phase. A direct axis component of voltage may be produced by: (1) rotation of the quadrature axis component of magnetic flux, (2) variation (if any) of the direct axis component of magnetic flux, and (3) resistance drop caused by the flow of the direct axis component of armature current.

Direct-axis component of magnetomotive force: The component of magnetomotive force that is directed along the direct axis.

Direct-axis current: The current that produces direct-axis magnetomotive force.

Direct-axis magnetic-flux component: The magnetic-flux component directed along the directed axis.

Direct-axis subtransient impedance: The magnitude obtained by the vector addition of the value for the armature resistance and the value for direct axis subtransient reactance. The resistance value to be applied in this case will be a function of frequency depending on rotor iron losses.

Direct-axis subtransient reactance: The quotient of the initial value of a sudden change in that the fundamental alternating current component of armature voltage, that is produced by the total direct-axis primary flux, and the value of this simultaneous change in fundamental alternating current component of direct axis armature current, the machine running at rated speed.

Direct-axis subtransient voltage: The direct-axis component of the terminal voltage which appears immediately after the sudden opening of the external circuit when the machine is running at a specified load, before any flux variation in the excitation and damping circuits has taken place.

Direct-axis synchronous impedance: The magnitude obtained by the vector addition of the value for armature resistance and the value for direct axis synchronous reactance.

Direct-axis synchronous reactance: The quotient of a sustained value of that fundamental alternating current component of armature voltage that is produced by the total direct axis flux due to direct axis armature current and the value of fundamental alternating current component of this current, the machine running at rated speed. Unless otherwise specified, the value of synchronous reactance will be that corresponding to rated armature current. For most machines, the armature resistance is negligibly small compared to the synchronous reactance.

Direct-axis transient impedance: The magnitude obtained by the vector ad-

dition of the value for armature resistance and the value for direct axis transient reactance.

Direct-axis transient reactance: The quotient of the initial value of a sudden change in that fundamental alternating current component of armature voltage, which is produced by the total direct axis flux, and the value of the simultaneous change in fundamental alternating current component of direct axis armature current. The machine is assumed to be running at rated speed.

Direct-axis transient voltage: The direct axis component of the armature voltage that appears immediately after the sudden opening of the external circuit when running at a specified load, neglecting the components that decay in the first few cycles.

Direct-axis voltage: The component of voltage that would produce direct axis current when resistance is limited.

Distribution system: The distribution system is the final stage in the transfer of power to the individual customers.

Dynamic response: An output expressed as a function of time resulting from the application of a specified input under specified operating conditions.

Dynamic security assessment: The process of using tools of transient stability analysis in predicting the vulnerability of a power system to contingencies.

Electric power system: The function of an electric power system is to convert energy from one of the naturally available forms to the electrical form and to transport it to the points of consumption.

Equal area criterion: For a rotor that is accelerating, the condition for stability is that a maximum value of the rotor angle exists and that the area under accelerating power versus rotor angle curve is zero up to that maximum rotor angle.

Excitation control: The function of excitation control is to regulate the generator voltage and reactive power output.

Excitation system: The equipment providing field current for a synchronous machine, including all power, regulating, control, and protective elements.

Expert systems (ES): A computer program that processes problem-specific information in the working memory with a set of rules contained in the knowledge base system, using an inference engine to infer new information.

Fault: A physical condition that causes a device, a component, or an element to fail to perform in a required manner, for example, a short-circuit, a broken wire, an intermittent connection.

Feedback: The return of a fraction of the output to the input.

Feeder: A set of conductors originating at a main distribution center and supplying one or more branch circuit distribution centers, or any combination of these two types of equipment.

Fictitious voltage: Voltage terms introduced in transient equations to explain

the flux inertia linkages created by rapid changes in conditions external to the machine (*see Transient equations*).

Flux linkages: The sum of fluxes linking the terms forming the coil.

Forward chaining: The process used in an expert system for deriving new information from known information. In forward chaining of rules, all rules whose pre-conditions are fulfilled by the data set of the given observations and derived intermediate results are eventually triggered.

Frequency: The number of complete cycles of sinusoidal variation per unit time.

Frequency response: A characteristic, expressed by formula or graph, which describes the dynamic and steady-state response of a physical system in terms of the magnitude ratio and the phase displacement between a sinusoidally varying input quantity and the fundamental of the corresponding output quantity as a function of fundamental frequency.

Fuzzy expert system: An expert system that uses a collection of fuzzy membership functions and rules, instead of Boolean logic, to reason about data.

Fuzzy logic: Fuzzy logic deals with ambiguity in defining various variables involved in describing the operation of a system.

Fuzzy logic systems (FLS): These are systems which mathematically model complex relationships that are usually handled in a vague manner by language or linguistics.

Fuzzy quantization: A mathematical means of describing vagueness in linguistics. The membership functions defined on the input variables are applied to their actual values in order to determine the degree of truth for the premise of each rule.

Fuzzy reasoning: A formal mathematical procedure for the representation of uncertainty that is used in the management of real systems.

Fuzzy set theory: A mathematical formulation developed by Dr. Lotfi Zadeh of UC/Berkeley in the 1960s as a means to model the uncertainty of natural language. The theory is used to solve problems that contain vagueness or uncertainty in the representation of knowledge and factual statements.

Fuzzy subset: Fuzzy subset F of a set S can be defined as a set of ordered pairs, each with the first element from S , and the second element from the interval $[0,1]$, with exactly one ordered pair present for each element of S .

Governor: The assembly of fluid, electrical, or mechanical control equipment used for regulating the flow of water, steam, or other medium to the prime mover for such purposes as starting, holding speed or load, or stopping.

IF-THEN-ELSE Rule: A basic knowledge representation by means of which directional relationships between objects can be represented using a precondition and an action that is often supported by the certainty of the action.

Impedance: The term impedance (symbol Z) is used in a transform network (s -domain or complex, for sinusoidal steady state operation) to relate cur-

rent through an element and the voltage across it, via the extended Ohm's law $V = ZI$.

Inductance: The property of an electric circuit by virtue of which a varying current induces an electromotive force in that circuit or a neighboring circuit.

Induction motor: An ac motor in which a primary winding on one member (usually the stator) is connected to the power source and a polyphase secondary winding, or a squirrel cage secondary winding on the other member (usually the rotor) carries induced current.

Inertia constant: The energy stored in the rotor when operating at rated speed expressed as kilowatt-seconds per kilovoltampere rating of the machine.

Inference engine: The brain of the expert system as it contains the knowledge that is used to decide on how to apply the rules to infer new knowledge. It controls the firing of the rules in the expert system.

Infinite bus: A voltage source that maintains constant voltage and frequency regardless of the load connected to it.

Intelligent systems: These are man-made systems that emulate functions of living creatures and human mental faculties.

Iterations: Describes a process, which repeatedly executes a sequence of steps until some condition is satisfied.

Knowledge-based system (KBS): A sub-program for solving problems, in which the problem-solving methods and the knowledge are kept separate, which makes it amenable to modification by exchanging the knowledge with the same problem-solving method and contributes to the explainability by enabling the knowledge used for deriving the problem solution to be given.

Lag: The delay between two events.

Laplace transform: The quantity obtained by performing the operation:

$$F(s) = \int_0^{\infty} f(t)e^{-st} dt$$

where $s = \sigma + j\omega$.

Learning algorithm: These are computational procedures that are generally aimed at ill-defined and time-varying processes and use heuristics, adaptation and pattern recognition techniques to construct neural networks and rule-based systems.

Linear system: A system or element with the properties that if y_1 is the response to x_1 , and y_2 is the response to x_2 , then $(y_1 + y_2)$ is the response to $(x_1 + x_2)$, and ky_1 is the response to kx_1 .

Load: The electric power used by devices connected to an electrical generating system.

Load angle: The angular displacement, at a specified load, of the center line of a field pole from the axis of the armature magnetomotive force pattern.

Load angle curve: A characteristic curve giving the relationship between the rotor displacement angle and the load, for constant values of armature voltage, field current, and power factor.

Load center: A point at which the load of a given area is assumed to be concentrated.

Load model: A mathematical representation of the variation of the active and reactive power requirements of the load at a certain point in the system with voltage and frequency at that point.

Lyapunov function: A scalar differentiable function $V(x)$ defined in some open region including X_c such that in that region:

$$V(x) > 0 \text{ for } x \neq x_c$$

$$V(x_c) = 0$$

$$V'(x) \leq 0$$

Man-machine interface: A medium through which the user of the expert system is able to communicate with the computer allowing data transfer in the form of input data, reports, system maintenance, and results.

Mechanical power: The power imparted by the prime mover to the synchronous generator.

Membership function: It is a graphical representation of the magnitude of participation of each input to the fuzzy system and by computing the logical product of the membership weights for each active rule, a set of fuzzy output response magnitudes are produced.

Meta-knowledge: The knowledge that a system has about its own knowledge that characterizes its own workings. This could include probabilities of architectural module, efficiencies or dependabilities.

Monotonic reasoning: A deduction in the theory of classical logic that can be proven to be valid under all conditions for all time.

Neural network: Neural networks consist of numerous, simple processing units or “neurons” that we can globally program for computation. Neural networks are trained to store, recognize, and associatively retrieve patterns or database entries, to solve problems involving estimating sampled functions when we do not know the form of the functions.

Neuron: The neuron is the fundamental unit of the nervous system, particularly the brain. The neuron is a simple processing unit that receives and combines signals from many other neurons through filamentary input paths.

Newton's method: An iterative method for finding the solution to a set of nonlinear equations using first order derivatives.

Nonlinear system: A system described by a set of nonlinear equations. In this case the superposition principle does not apply.

Perception learning rule: An iterative learning procedure that usually converge to the correct weights that will ultimately give the correct output for all input training patterns.

Phase angle: The measure of the progression of a periodic wave in time or space from a chosen instant or position.

Positive definite: A quadratic form $V(x) = x^T Qx$ is positive definite if $V(x) > 0$ for all values of x different from zero.

Power factor: The cosine of the angle between the current through an electric circuit element and the voltage across it is referred to as the element's power factor.

Power flow equations: The system of equations relating the active and reactive power injections at each bus in an electric network in terms of voltage magnitudes and phase angles.

Power system stability: The term is used to define the ability of the bulk power electric system to withstand sudden disturbances such as electric short circuits or unanticipated loss of system components. For further details see Sec. 1.3.

Prime mover: The machine used to develop mechanical horsepower necessary to drive a generator to produce electrical power.

Prime mover control: The function of prime mover control is to regulate the speed and control energy supply variables such as boiler pressures, temperatures, and flows.

Quadrature axis transient impedance: The operator expressing the relation between the initial change in armature voltage and a sudden change in quadrature axis armature current component, under the following assumptions: (1) Only the fundamental frequency components considered for both voltage and current. (2) No change in the voltage applied to the field winding. (3) The rotor running at steady speed. (4) Considering only the slowest decaying component and the steady state component of the voltage drop. If no rotor winding is along the quadrature axis and/or the rotor is not made out of solid steel, this impedance equals the quadrature-axis synchronous impedance.

Quadrature axis: The axis that represents the direction of the radial plane along which the main field winding produces no magnetization, normally coinciding with the radial plane midway between adjacent poles. The positive direction of the quadrature axis is 90° ahead of the positive direction of the direct axis, in the direction of rotation of the field relative to the armature.

Quadrature axis component of armature current: The component of the armature current that produces a magnetomotive force distribution that is symmetrical about the quadrature axis.

Quadrature axis component of armature voltage: The component of the armature voltage of any phase that is in time-phase with the quadrature axis component of current in the same phase. A quadrature axis component of voltage may be produced by: (1) rotation of the direct axis component of magnetic flux, (2) variation (if any) of the quadrature axis component of magnetic flux, (3) resistance drop caused by the flow of the quadrature axis component of armature current.

Quadrature axis current: The current that produces quadrature axis magnetomotive force.

Quadrature axis magnetomotive force: The component of a magnetomotive force that is directed along an axis in quadrature with the axis of the poles.

Quadrature axis subtransient impedance: The operator expressing the relation between the initial change in armature voltage and a sudden change in quadrature axis armature current, under the following assumptions: (1) Only the fundamental frequency components considered for both voltage and current. (2) No change in the voltage applied to the field winding. (3) The rotor running at steady speed. If no rotor winding is along the quadrature axis and/or the rotor is not made out of solid steel, this impedance equals the quadrature axis synchronous impedance.

Quadrature axis subtransient reactance: The ratio of the fundamental component of reactive armature voltage, due to the initial value of the fundamental quadrature axis component of the alternating current component of the armature current, to this component of current under suddenly applied balanced load conditions and at rated frequency. Unless otherwise stated, the quadrature axis subtransient reactance is that corresponding to rated armature current.

Quadrature axis subtransient voltage: The quadrature axis component of the terminal voltage that appears immediately after the sudden opening of the external circuit when the machine is running at a specific load, before any flux variation in the excitation and damping circuits has taken place.

Quadrature axis synchronous impedance: The impedance of armature winding under steady state conditions where the axis of the armature current and magnetomotive force coincides with the quadrature axis. In large synchronous machines where the armature resistance is negligibly small, the quadrature axis synchronous impedance is equal to the quadrature axis synchronous reactance.

Quadrature axis synchronous reactance: The ratio of the fundamental component of reactive armature voltage, due to the fundamental quadrature axis

component of armature current, to this component of current under steady-state conditions and at rated frequency. Unless otherwise stated, the value of quadrature axis synchronous reactance will be that corresponding to the rated armature current.

Quadrature axis transient reactance: The ratio of the fundamental component of reactive armature voltage, due to the fundamental quadrature axis component of the alternating current component of the armature current, to this component of current under suddenly applied load conditions and at rated frequency. The value of current is determined by extrapolating the envelope of the alternating current component of the current wave to the instant of the sudden application of the load, neglecting the high-decrement current during the first few cycles. Note that usually the quadrature axis transient reactance equals the quadrature axis synchronous reactance except in solid-rotor machines, since in general there is no really effective field current in the quadrature axis.

Quadrature axis transient voltage: The quadrature axis component of the armature voltage that appears immediately after the sudden opening of the external circuit when running at a specified load, neglecting the components that decay in the first few cycles.

Quadrature axis voltage: The component of voltage that would produce quadrature axis current when resistance is limited.

Reactance, effective synchronous: An assumed value of synchronous reactance used to represent a machine in a system study calculation for a particular operating condition.

Reactive capability curve: A curve that identifies the reactive capability limits of a synchronous machine based on three considerations: (1) Armature current limit; (2) field current limit; and (3) end region-heating limits.

Reactive power: The reactive power Q is defined as the square root of the square of the apparent power S minus the square of the active power P .

$$Q = \sqrt{(S^2 - P^2)}$$

Reactive power is developed when there are inductive, capacitive, or nonlinear elements in the system. It does not represent useful energy that can be extracted from the system but it can cause increased losses and excessive voltage peaks.

Region of stability: A region in the state space, where the system is stable.

Regulator: An electric machine regulator that controls the excitation of a synchronous machine.

Regulator, excitation system: A regulator that couples the output variables of the synchronous machine to the input of the exciter through feedback and

forward controlling elements for the purpose of regulating the synchronous machine output variables.

Resistance: The physical property of an element, device, branch, network, or system that is the factor by which the mean square conduction current must be multiplied to give the corresponding power lost by dissipation as heat or as other permanent loss of energy from the circuit.

Simulation: The representation of the functioning of one system by another, for example to represent a physical system by a mathematical model.

Slip: The difference between the synchronous speed and the actual speed of a rotor to the synchronous speed.

Soft computing: A term coined by Zadeh to refer to the emerging area of computational intelligence such as fuzzy logic, neural networks, genetic algorithms, and expert systems.

Stability: An aspect of system behavior associated with systems having the general property that bounded perturbations result in bounded perturbations in the output.

Stability, absolute: Global asymptotic stability maintained for all given nonlinearities.

Stability, Lyabunov: For a solution $\phi(x(t_0), t)$, Lyabunov stability means that for every given $\varepsilon > 0$ there exists a $\delta > 0$ such that $\|\Delta x(t_0)\| \leq \delta$ implies $\|\Delta\phi\| \leq \varepsilon$ for $t \geq t_0$.

Stability, power system: In a system of two or more synchronous machines connected through an electric network, the conditions in which the difference of the angular positions of the rotors of the machines either remains constant while not subjected to a disturbance, or becomes constant following an aperiodic disturbance.

Stabilizer: An excitation system stabilizer is an element or group of elements that modify the forward signal by either series or feedback compensation to improve the dynamic performance of the excitation control system.

Stabilizer, power system: An element or group of elements that provide an additional input to the regulator to improve power system dynamic performance.

Static: Refers to a state in which a quantity exhibits no appreciable change within an arbitrarily long time interval.

Security assessment: In an operational environment, security assessment consists of predicting the vulnerability of the system to possible disturbances.

Steady state: That in which some specified characteristic of a condition such as value, rate, periodicity, or amplitude exhibits only negligible change over an arbitrarily long time.

Steady state contingency analysis: Steady state contingency analysis predicts power flows and bus voltage conditions following events such as transmission line outages, transformer outages and generator outages.

Steady state stability: A condition that exists in a power system if it operates with stability when not subjected to an aperiodic disturbance. In practice, a variety of relatively small aperiodic disturbances may be present without any appreciable effect upon the stability. This is valid as long as the resultant rate of change in load is relatively slow in comparison with the natural frequency of oscillation of the major parts of the system or with the rate of change in field flux of the rotating machines.

Steady state stability limit: The maximum power flow possible through some particular point in the system when the entire system or the part of the system to which the stability limit refers is operating with steady state stability.

Subtransient current: The initial alternating component of armature current following a sudden short-circuit.

Subtransient Reactance: The reactance of a generator at the initiation of a fault.

Subtransmission system: In contrast to the transmission system, the subtransmission system transmits power at a lower voltage and in smaller quantities from the transmission system to the distributions substations.

Susceptance: The imaginary part of admittance.

Synchronous generator: A synchronous alternating current machine that transforms mechanical power into electrical power.

Synchronous machine: A machine in which the average speed of normal operation is exactly proportional to the frequency of the system to which it is connected.

Synchronous reactance, effective: An assumed value of synchronous reactance used to represent a machine in a system study for a particular operating condition.

Synchronous speed: The speed of rotation of the magnetic flux produced by or linking the primary winding.

System generation control: The function of system generation control is to balance the total system generation against system load and losses so that the desired frequency and power interchange with neighboring systems is maintained.

Three phase system: A combination of circuits energized by alternating electromotive forces which differ in phase by one third of a cycle (120°).

Time delay: A time interval which is purposely introduced in the performance of a function.

Torque: The vector product of force and moment arm and is widely designated by the unit Newton meter.

Transient current: The current under nonsteady conditions. Also, the alternating component of armature current immediately following a sudden short circuit, neglecting the rapidly decaying component present during the first few cycles.

Transient energy function: This is a Lyapunov function used in the direct method for transient stability analysis.

Transient equations: Used whenever conditions in the modeled system change faster than a static representation of voltage and flow can accommodate. Under such conditions, flux inertia means these rapid changes cannot establish themselves throughout the machine immediately, and two new fictitious voltages, usually referred to as E'_q and E'_d must be introduced to represent the flux linkages in machine rotor windings, and used in the model equations.

Transient reactance: The reactance of a generator between the subtransient and synchronous states.

Transmission control: These include power and voltage control devices such as static VAR compensators, synchronous condensers, switched capacitors and reactors, tap-changing transformers, phase shifting transformers, and HVDC transmission controls.

Transmission line: A line used for power transmission.

Transmission system: A transmission system interconnects all major generating stations and main load centers in an electric power system.

Turbine-generator unit: An electric generator with its driving turbine.

Voltage: Voltage is synonymous with potential difference between two conductors.

Voltage collapse: It is the process by which the sequence of events accompanying voltage instability leads to a low unacceptable voltage profile in a significant part of the power system.

Voltage regulator: A synchronous machine regulator that functions to maintain the terminal voltage of a synchronous machine at a predetermined value, or to vary it according to a predetermined plan.

Voltage stability: A voltage stability study evaluates the ability of a power system to maintain acceptable voltages at all nodes under normal conditions and after being subjected to contingency conditions.

Voltage stability indexing: Many indices characterizing the proximity of an operating state to the voltage collapse point have been developed. The degeneracy of the load flow Jacobian matrix is used as an index of the power system steady state stability.

Appendix: Chapter Problems

PROBLEMS FOR CHAPTER 2

Problem 2.1

A single-phase source is connected to a two-terminal, passive circuit with equivalent impedance measured between the terminals given by:

$$Z = (2.0 - j2.0) \Omega$$

The source current is $i(t) = 4 \cos \omega t \text{ kA}$. Determine:

- a. The instantaneous power,
- b. The real power, and reactive power delivered by the source, and
- c. The source power factor.

Problem 2.2

Consider a single-phase load with an applied voltage:

$$v(t) = 120 \cos(\omega t + 10^\circ) \text{ volts}$$

and load current

$$i(t) = 8 \cos(\omega t - 50^\circ) \text{A.}$$

Determine the power triangle.

Find the power factor and specify whether it is lagging or leading. Calculate the reactive power supplied by capacitors in parallel with the load that corrects the power factor to 0.9 lagging.

Problem 2.3

A circuit consists of two impedances, $Z_1 = 20 \angle 30^\circ \Omega$ and $Z_2 = 30 \angle -45^\circ \Omega$ in parallel, supplied by a source voltage $V = 120 \angle 60^\circ$ volts. Determine the power triangle for each of the impedances and for the source.

Problem 2.4

An industrial plant consisting primarily of induction motor loads absorbs 1000 kW at 0.75 power factor lagging.

- Compute the required kVA rating of a shunt capacitor to improve the power factor to 0.9 lagging.
- If a synchronous motor rated 1000 hp with 90% efficiency operating at rated load and at unity power factor is added to the plant instead of the capacitor, calculate the resulting power factor. Assume constant voltage. (1 hp = 0.746 kW)

Problem 2.5

The real power delivered by a source to two impedances, $Z_1 = (3.0 + j5.0) \Omega$ and $Z_2 = 10.0 \Omega$ connected in parallel, is 1500 W. Determine:

- The real power absorbed by each of the impedances.
- The source current.

Problem 2.6

A single-phase source has a terminal voltage $V = 120$ volts and a current $I = 25 \angle 30^\circ$ A, which leaves the positive terminal of the source. Determine the real and reactive power, and state whether the source is delivering or absorbing each.

Problem 2.7

A source supplies power to the following three loads connected in parallel: (1) a lighting load drawing 10 kW, (2) an induction motor drawing 10 kVA at 0.90

power factor lagging, and (3) a synchronous motor operating at 10 hp, 85% efficiency and 0.95 power factor leading (1 hp = 0.746 M).

Determine the real, reactive, and apparent power delivered by the source. Also, draw the source power triangle.

Power 2.8

Three identical impedances of $(26 + j15) \Omega$ are connected in wye to a 460 V balanced three-phase source. Determine:

- a. The magnitude of the line currents.
- b. The total power dissipated for the three phases.

Problem 2.9

Three identical impedances of $(18 + j22.5) \Omega$ are connected in wye to a 550 V balanced three-phase source. Determine:

- a. The magnitude of the line currents.
- b. The total power dissipated for the three phases,
- c. The total reactive power, and
- d. The power factor.

Problem 2.10

Repeat Problem 2.9 for the case where the three impedances are connected in delta.

Problem 2.11

Current, voltage, and power to a balanced three-phase circuit are measured and found to be 20 A, 550 V, and 10.5 kW, respectively. Determine equivalent circuits per phase as follows:

- a. Wye-connected, series combination of resistance and reactance in each phase.
- b. Delta-connected, parallel combination of resistance and reactance in each phase.

Problem 2.12

Voltage, apparent power, and power to a balanced three-phase circuit are measured and found to be 460 V, 50 kVA, and 48.5 kW respectively. Determine equivalent circuits per phase as follows:

- a. Wye-connected, parallel combination of resistance and reactance in each phase.
- b. Delta-connected, series combination of resistance and reactance in each phase.

Problem 2.13

The current, voltage, and power factor of a balanced three-phase circuit are measured and found to be 15 A, 440 V, and 0.75 lagging respectively. Determine equivalent series-connected resistance and reactance circuits per phase if the phases are:

- a. Wye-connected.
- b. Delta-connected.

Problem 2.14

The voltage, apparent power, and power factor of a balanced three-phase circuit are measured and found to be 600 V, 150 kVA, and 0.9 leading respectively. Determine equivalent parallel connected resistance and reactance circuits per phase if the phases are:

- a. Wye-connected.
- b. Delta-connected.

Problem 2.15

Three impedances are connected in delta to a balanced 208 V, three-phase source of sequence *abc*. The impedances are

$$Z_{ab} = 10 + j20 \Omega$$

$$Z_{bc} = 20 - j10 \Omega$$

$$Z_{ca} = 20 + j10 \Omega$$

- a. What are the three-phase voltages?
- b. Calculate the three-phase currents.
- c. Calculate the three-line currents.

Problem 2.16

Three impedances are connected in delta to a balanced 460 V, three-phase source of sequence *abc*. The impedances are

$$\begin{aligned}Z_{ab} &= 25 + j15 \Omega \\Z_{bc} &= 17 - j18 \Omega \\Z_{ca} &= 20 + j20 \Omega\end{aligned}$$

- a. What are the three-phase voltages?
- b. Calculate the three-phase currents.
- c. Calculate the three line currents.

Problem 2.17

Two loads are connected to a 460 V, three-phase balanced source. One is a three-phase motor connected in delta and running such that the power is 25 kW with a line current of 35 A. The power factor is known to be lagging. The other is a single-phase 10 kW heater that takes a unity factor current of 22 A when connected between lines b and c. Using V_{ab} as a reference, determine the three line currents.

Problem 2.18

Two loads are connected to a 460 V, three-phase balanced source. One is a three-phase balanced load connected in wye and having a line current of 20 A with a power factor of 0.9 (lagging). The other is a single-phase load which has a current of 15 A at a power factor of 0.7 (leading) when connected between lines a and c. Using V_{ab} as a reference, determine the three line currents.

Problem 2.19

Two loads are connected to a 208 V, three-phase balanced source. One is a three-phase motor connected in delta and running such that the line current is 10 A with a power factor of 0.866 (lagging). The other is a single-phase heater which takes a current of 15 A at a power factor of 0.98 (lagging) when connected between lines a and b. Using V_{ab} as a reference, determine the three line currents.

Problem 2.20

Two inductive loads are connected to a 460 V, three-phase balanced source. One is a three-phase balanced load of 50 kW connected in wye and having a line current of 125 A. The other is a single-phase load of 5 kW and 10 kVA connected between lines a and c. Using V_{ab} as a reference, determine the three line currents.

Problem 2.21

A three-phase induction motor is connected to a balanced 550 V, 60 Hz supply. For a particular mechanical load the input is 100 kVA and 80 kW. The power factor is to be increased to 0.95 (lagging) by means of a delta-connected capacitor bank connected to the motor terminals. Determine the capacitance per phase required.

Problem 2.22

When a certain three-phase induction motor is operated at its rated load the current, voltage, and power are 70 A, 550 V, and 50 kW respectively. A second motor, when connected to the same source, takes a current of 50 A and a power of 30 kW. Normally both motors operate simultaneously. Assuming that the system frequency is 60 Hz.

- Determine the delta-connected capacitance per phase required to raise the power factor to 0.95 (lagging).
- With this value of capacitance remaining in the circuit, determine the resulting power factor when the second motor is disconnected.

Problem 2.23

A certain inductive, balanced three-phase load dissipates 60 kW with a current of 66 A when connected to a 550 V, 60 Hz supply.

- Obtain the parameters of the equivalent wye-connected circuit in which the reactance and resistance are connected in series.
- A set of three capacitors, each 500 μF , is connected in series with the load. Determine the current, voltage, and power of the original load.
- Obtain the overall power factor.

Problem 2.24

A synchronous machine has the following inductances associated with the stator windings:

$$L_{ab} = 3.3 + 0.05 \cos 2\theta \text{ mH}$$

$$L_{ac} = -1.6 - 0.05 \cos \left(2\theta + \frac{\pi}{3} \right) \text{ mH}$$

Use equations 2.26 and 2.30 to determine L_d and L_q in Henrys

Problem 2.25

A 500 MVA, 24 kV, 60 Hz three-phase synchronous machine has the following inductances in Henrys:

$$L_d = 5 \text{ mH}$$

$$L_q = 4.5 \text{ mH}$$

Determine the base impedance and inductance, and then find the per unit value of L_d and L_q .

Problem 2.26

A synchronous machine serves a load with:

$$V_t = 1 \angle 10^\circ \text{ pu}$$

$$I_t = 0.5 \angle -20^\circ \text{ pu}$$

Assume that $X_d = 1.2$ and neglect the armature resistance. Find the value of E' and δ based on the equivalent circuit of Fig. 2.10.

Problem 2.27

Consider a static load represented by the model of Eq. (2.40). It is known that a 10% increase in voltage magnitude results in a 15% increase in power. Predict the percentage change in power for a 10% decrease in voltage.

Problem 2.28

The model of Eq. (2.41) represents the dependence of the active power of a static load on voltage. The following measurements are available for increases in the voltage magnitude and the corresponding increase in active power:

| $\Delta V\%$ | $\Delta P\%$ |
|--------------|--------------|
| 10 | 58.5 |
| 15 | 68.13 |
| 20 | 78.00 |

Predict the change in active power for a 10% decrease in voltage magnitude.

PROBLEMS FOR CHAPTER 3

Problem 3.1

Consider the exciter model given by Eq. (3.1) with $K_L = 1.00$, $S_e = 0.8$, and $T_e = 0.5$ s. Assume that the voltage reference is a unit step. Find the exciter voltage output e_t as a function of time. Assume zero initial conditions.

Problem 3.2

Find the steady state value of the exciter voltage for Problem 3.1.

Problem 3.3

Use the block diagram of Fig. (3.5) for a typical stabilizer to establish a state space model of the system.

Problem 3.4

Assume that the input steps for the stabilizer of Fig. (3.5) are given by $\Delta\omega = 0.1$ and ΔP_e . Find the steady state value of ΔV_c . Assume that:

$$T_1 = 0.1 \quad T_2 = 0.05 \quad T_3 = 0.2$$

$$K_u = 0.6 \quad K_p = 0.8$$

Problem 3.5

Consider the model of Fig. (3.8) represented by Eq. (3.7). Write a state space model for the system in terms of four states. Define the control input as:

$$u(t) = \omega_{\text{ref}} - \omega_r$$

Assume that:

$$T_G = 0.2 \quad T_R = 5 \quad R_I = 0.4$$

$$T_p = 0.05 \quad K_s = 5 \quad R_p = 0.04$$

Find the response to a unit step input.

Problem 3.6

Repeat Problem 3.5 using a three state model involving x_1 , x_2 , and η .

Problem 3.7

Consider the model of Fig. (3.9). Write a state space model for the system in terms of the two states. Define the control input as:

$$u(t) = \omega_{\text{ref}} - \omega_r$$

Assume that:

$$T_o = 0.2 \quad K_i = 4 \quad R_p = 0.05$$

Find the eigenvalues of the system and the response to a unit step input.

PROBLEMS FOR CHAPTER 4**Problem 4.1**

Given a 60 Hz, four-pole turbo generator rated 20 MVA, 13.2 kV, with an inertia constant of $H = 7 \text{ kWs/kVA}$:

- Calculate the kinetic energy stored in the rotor at synchronous speed.
- Find the acceleration if the net mechanical input is 26,800 hp and the electric power developed is 16 MW.
- Assume that the acceleration in part b is constant for a period of 10 cycles. Find the change in δ in that period.

If this generator is delivering rated MVA at 0.8 PF lag when a fault reduces the electric power output by 50%, determine the accelerating torque at the fault time.

Problem 4.2

A 60 Hz alternator rated at 20 MVA is developing electric power at 0.8 power factor lagging with net mechanical input of 18 MW. Assume that acceleration is constant for a period 15 cycles, in which δ attains a value of 15° electrical from zero initial conditions. Calculate the inertia constant H for the machine.

Problem 4.3

Show that the speed of a generator subject to a constant decelerating power of 1 pu will be reduced from rated value to zero in 2 H seconds.

Problem 4.4

A 20 MVA, 13.8 kV, 60 Hz, two-pole, Y-connected three phase alternator has an armature winding resistance of 0.07 ohms per phase and a leakage reactance of 1.9 ohms per phase. The armature reaction EMF for the machine is related to the armature current by $E_{ar} = -j19.91 I_a$. Assume that the generated EMF is related to the field current by $E_t = 60 I_b$.

- Compute the field current required to establish rated voltage across the terminals of a load when rated armature current is delivered at 0.8 PF lagging.
- Compute the field current needed to provide rated terminal voltage to a load that draws 100% of rated current at 0.85 lagging.

Problem 4.5

A 10 MVA, 13.8 kV, 60 Hz, two pole, Y-connected synchronous generator is delivering rated current at rated voltage and unity PF. Find the armature resistance and synchronous reactance given that the field excitation voltage is 11935.44 V and leads the terminal voltage by an angle 47.96°.

Problem 4.6

A 1500 kVA, three-phase, Y-connected, 4160 V, 10-pole, 60 Hz synchronous generator has an armature resistance of 0.126 ohms per phase and a synchronous reactance of 3 ohms per phase. Find the full load generated voltage per phase at 0.8 PF lagging.

Problem 4.7

The synchronous reactance of a cylindrical rotor synchronous generator is 0.90 pu . If the machine is delivering active power of 1.00 pu to an infinite bus whose voltage is 1.00 pu , at unity PF, calculate the excitation voltage and the power angle.

Problem 4.8

A cylindrical rotor machine is delivering active power of 0.80 pu and reactive power of 0.60 pu at a terminal voltage of 1.00 pu . If the power angle is 22°, compute the excitation voltage and the machine's synchronous reactance.

Problem 4.9

A cylindrical rotor machine is delivering active power of 0.80 *pu* and reactive power of 0.60 *pu* when the excitation voltage is 1.20 *pu* and the power angle is 25°. Find the terminal voltage and synchronous reactance of the machine.

Problem 4.10

The reactances x_d and x_q of a salient-pole synchronous generator are 0.95 and 0.70 per unit, respectively. The armature resistance is negligible. The generator delivers rated kVA at unity PF and rated terminal voltage. Calculate the excitation voltage.

Problem 4.11

The reactances x_d and x_q of a salient-pole synchronous generator are 1.00 and 0.60 per unit respectively. The excitation voltage is 1.77 *pu* and the infinite bus voltage is maintained at 1.00 *pu*. For a power angle of 19.4°, compute the active and reactive power supplied to the bus.

Problem 4.12

A salient pole machine supplies a load of 1.20 *pu* at unity PF to an infinite bus. The direct axis and quadrature axis synchronous reactances are:

$$x_d = 0.9283 \quad x_q = 0.4284$$

The power angle δ is 25°. Evaluate the excitation and terminal voltages.

Problem 4.13

Consider the case of an electric machine connected to an infinite bus through a reactive electric network such that the magnitude of the power angle curve is unity. A change in the network results in a new power angle curve with magnitude x . Suppose the machine is delivering a power p before the change occurs, then show that the maximum value of p such that the system remains stable satisfies:

$$\frac{p}{x} \left[-\sin^{-1} \left(\frac{p}{x} \right) - \sin^{-1} p + \pi \right] = \sqrt{1 - \left(\frac{p}{x} \right)^2} + \sqrt{1 - p^2}$$

Verify that for $x = 0.5$, the maximum value of prefault power p is approximately 0.4245.

Problem 4.14

A generator is delivering 0.60 of P_{\max} to an infinite bus through a transmission line. A fault occurs such that the reactance between the generator and the bus is increased to three times its prefault value. When the fault is cleared, the maximum power that can be delivered is 0.80 of the original maximum value. Determine the critical clearing angle using the equal-area criterion.

Problem 4.15

A generator is delivering 0.50 of P_{\max} to infinite bus through a transmission line. A fault occurs such that the new maximum power is 0.30 of the original. When the fault is cleared, the maximum power that can be delivered is 0.80 of the original maximum value.

- Determine the critical clearing angle.
- If the fault is cleared at $\delta = 75^\circ$, find the maximum value of δ for which the machine swings around its new equilibrium position.

Problem 4.16

The power-angle curves for a single machine against an infinite bus system is $P = 2.8 \sin \delta$. Under fault conditions, the curve is described by:

$$P = 1.2 \sin \delta$$

Assume that the system is delivering a power of 1.0 pu prior to the fault and that fault clearing results in the system returning to the prefault conditions. If the fault is cleared at $\delta_c = 60^\circ$, would the system be stable? Find the maximum angle of swing δ , if the system is stable.

Problem 4.17

A generator is delivering 0.55 of P_{\max} to an infinite bus through a transmission line. A fault occurs such that the reactance between the generator and the bus is increased to three times its prefault value. When the fault is cleared, the maximum power that can be delivered is 0.75 of the original maximum value.

Determine the critical clearing angle using the equal-area criterion.

Problem 4.18

The 60 Hz synchronous machine shown in Fig. 1 is generating 235 MW and 90 MVAr of power. The voltage at the infinite bus q is $1.0 + j0.0$ pu, and the line

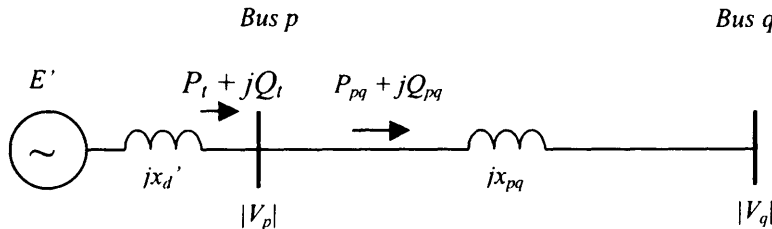


Figure 1. Impedance diagram of sample power system.

reactance is 0.065 pu on a 100 MVA base. The machine transient reactance is 0.22 pu and the inertia constant is 3.78 per unit on a 100 MVA base.

- Solve the initial power flow of the system.
- Using the Euler integration technique, calculate the changes in phase angle and speed of the generator for a three-phase fault at bus p , which is cleared after 0.06 second. Use a time step size of 0.02 second and a total time of 0.18 seconds.

- P_t : generator real terminal power
 Q_t : generator reactive terminal power
 P_{pq} : real power flow
 Q_{pq} : reactive power flow
 E' : voltage behind the transient reactance
 V_p : voltage at bus p
 V_q : voltage at bus q
 x_d' : generator transient reactance
 x_{pq} : transmission line reactance

Problem 4.19

- Draw a detailed flow chart of the Modified Euler technique, as applied to power system stability studies.
- For the problem given in No. 1, using the Modified Euler integration technique, calculate the changes in phase angle and speed of the generator for a three-phase fault at bus p , which is cleared after 0.06 second. Use a time step size of 0.02 second and a total time of 0.18 seconds.

Problem 4.20

The 100 MVA, 13.8 kV, 60 Hz synchronous machine has a transient reactance of 0.025 pu and an inertia constant of 4.00 per unit on its own base. It is

supplying a power of 95 MVA at a power factor of 0.895 lagging to an infinite bus. The voltage at the infinite bus is $1.0 + j0.0 \text{ pu}$ and the net reactance of the parallel lines is 0.30 pu on a 100 MVA base.

- Draw a single line diagram of the system and solve its initial power flow.
- Using the RK-3 (Runge–Kutta) integration technique to calculate the changes in phase angle and speed of the generator for a three-phase fault at the generator bus, which is cleared after 0.06 second. Use a time step size of 0.02 second and a total time of 0.18 seconds.

Problem 4.21

For the system given in Problem 4.3, consider the loss of one of the parallel branches whose impedance is 0.06 pu . If this fault occurred at $t = 0.0$ second and was cleared through breaker reclosure at $t = 0.50$ second, calculate the changes in phase angle and speed of the generator from $t = 0.00$ to $t = 0.12$ seconds. Use the Euler integration technique with a time step size of 0.02 second.

Problem 4.22

A synchronous machine in a power system has a swing or dynamic equation, which can be shown to be equal to:

$$\frac{2H}{\omega} \frac{d^2\delta}{dt^2} = T_m - T_e$$

$$T_e = (K_1 + K_2)\sin\delta$$

where T_e = electrical torque,

T_m = mechanical torque,

δ = angular speed of the machine, and

K_1, K_2 = constants that are functions of the network.

- Develop implementation algorithms for solving the swing equation by any two numerical methods.
- Comment on the computations efficiency of the two algorithms in a, especially for large multi-machine power systems.

PROBLEMS FOR CHAPTER 5

Problem 5.1

Define and briefly discuss the following terminologies, as applied to the topic of dynamic stability assessment (DSA) in electric power systems.

- Angle stability
- Center of inertia, COI
- Stable equilibrium point, SEP
- Unstable equilibrium point, UEP
- Critical energy V_{cr}
- Energy margin

Problem 5.2

Consider a simple power system as shown in Fig. 2, consisting of a generator delivering power to a large system represented by an infinite bus through two transmission circuits. The single generator represents a thermal generating plant consisting of four 600 MVA, 24.5 kV, 60 Hz units supplying power to the infinite bus. Bus B is the infinite bus, which can be represented by a voltage source of constant voltage magnitude and constant frequency. The initial operating conditions of the system, with quantities expressed in pu on a 2200 MVA, 24.5 kV base, are as follows:

$$\begin{aligned} P &= 0.953 \text{ pu} & Q &= 0.532 \text{ pu} \\ E_t &= 1.0 \text{ pu at } 15.50^\circ & E_b &= 0.935 \text{ pu at } 0.00^\circ \end{aligned}$$

The classical model of the generators has unitized parameters lumped to that of a single equivalent generator given as: $X_d' = 0.325 \text{ pu}$ and the machine constant, $H = 3.06 \text{ MW.s/MVA}$.

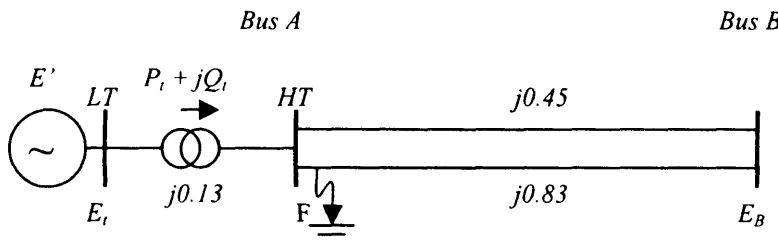


Figure 2. Single line diagram of the power system for problem 5.2.

If a solid three-phase fault occurs at point F as shown in Fig. 2, and is subsequently cleared by *isolating* the faulted circuit, then:

- Write the dynamic equations for the postfault system referred to the center of inertia, COI.
- Write the expression for the system energy function.
- Calculate the postfault system stable equilibrium point (SEP), unstable equilibrium point (UEP), and the critical energy V_{cr} .
- Calculate the energy at fault clearing with $t_c = 0.08, 0.12,$ and 0.16 second.
- Determine the system stability for each of the three fault durations.

In this problem, the network reactances shown are on a 2200 MVA base and the resistances are assumed to be negligible.

Problem 5.3

Re-visit the data given in Problem 5.2. Consider a loss of line contingency that was created due to an open circuit fault on the branch of the parallel transmission system whose reactance is 0.83 pu . If the fault was subsequently cleared by controlled breaker reclosure, then:

- Calculate the postfault system stable equilibrium point (SEP), unstable equilibrium point (UEP), and the critical energy V_{cr} .
- Calculate the energy at fault clearing with $t_c = 0.10, 0.20,$ and 0.30 second.
- Hence or otherwise, determine the system stability for each of the three fault durations.

In this problem, the network reactances shown are on a 2200 MVA base and the resistances are assumed to be negligible.

Problem 5.4

- Discuss Lyapunov's stability criteria, as applied to *stability assessment* studies performed on electrical power systems.
- Explain how the generalized expression of the transient energy function for a multi-machine power system can be used to determine the stability of the system.
- What are the challenges faced by engineers and researchers in attempting to obtain fast and useful solution to the transient energy function of part b? Also comment on the desired accuracy of the solution.

PROBLEMS FOR CHAPTER 6

Problem 6.1

Consider the 550 kV, 370 km (230 miles) line transmission system shown in Fig. 3a below supplying power to a radial load from a 'strong' power system represented by an infinite bus. The line parameters, as shown in Fig. 3b, are expressed in their respective per unit values on a common system base of 100 MVA and 55 kV.

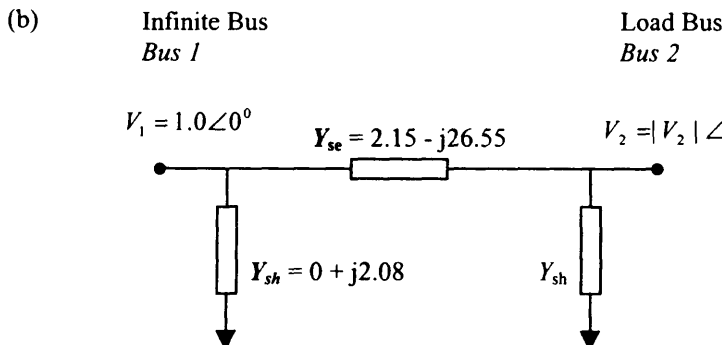
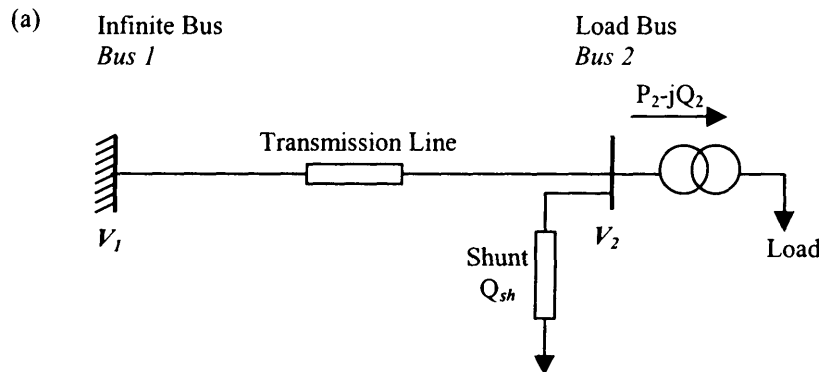


Figure 3. The 550 kV, 370 km (230 miles) line transmission system supplying a radial load. (a) The schematic diagram. (b) The equivalent wye circuit representation of the transmission line.

6.1.1 Compute the full admittance matrix of the two-bus system and write the power flow equations from the sending end to the receiving end in the form:

$$\begin{aligned} P &= f(\theta, V) \\ Q &= g(\theta, V) \end{aligned}$$

6.1.2 Hence or otherwise, write down the expressions for the four (4) submatrices of the Jacobian in the linearized load flow equations as defined by:

$$\begin{bmatrix} \Delta P \\ \Delta Q \end{bmatrix} = \begin{bmatrix} J_{P\theta} & J_{PV} \\ J_{Q\theta} & J_{QV} \end{bmatrix} \begin{bmatrix} \Delta \theta \\ \Delta |V| \end{bmatrix}$$

6.1.3 When $P_2 = 1600$ MW, calculate the eigenvalues of the reduced Q - V Jacobian matrix and the V - Q sensitivities with the following different reactive power injections for each of the corresponding two voltages on the Q - V curve.

- a. $Q_i = 510$ MVAR
- b. $Q_i = 405$ MVAR
- c. Values of Q_i close to the bottom of the V - Q curve.

6.1.4 Determine the voltage stability of the system by computing the eigenvalues of the reduced V - Q Jacobian matrix for the following cases:

- a. $P = 1600$ MW, $Q_i = 460$ MVAR
- b. $P = 1890$ MW, $Q_i = 965$ MVAR

Assume that the reactive power Q , is supplied by a shunt capacitor.

Problem 6.2

This problem demonstrates the concept of parameterization. Consider a simple 2-bus power system as shown in Fig. 4, where we are interested in the behavior on the bus voltage, V to the amount of reactive power demand at the bus under prespecified conditions.

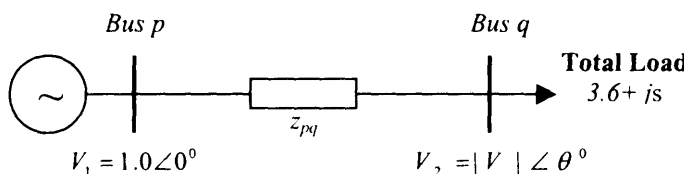


Figure 4. A simple 2-bus power system.

Given that s is the parameter of interest, which represents reactive power, and the following physically-meaningful parameterization equations:

$$0 = 3.6 - V \cos \theta + 10 V \sin \theta \quad \dots \dots \text{(i)}$$

$$0 = s + 10 V^2 - V \sin \theta - 10 V \cos \theta \quad \dots \dots \text{(ii)}$$

6.2.1 Solve the parameterization equations in Sec. 6.2.1 using values of s from 0.00 to s_{\max} in increments of 0.100 pu MVar.

6.2.2 What is the value of s_{\max} , at which point no real solutions are obtainable? Plot the resulting $|V|$ vs. s and θ vs. s traces on the same grid.

6.2.3 How safe is it to deduce the maximum reactive loadability limit of the given 2-bus power system?

Problem 6.3

This problem demonstrates the basic concepts of Modal analysis, as applied to voltage stability studies in power systems. A 4-Bus power system is shown in Fig. 5 and the operating conditions are summarized in Table 1.

6.3.1 Compute the full and reduced Jacobian matrices of the system.

6.3.2 Calculate the eigenvalues and eigenvectors of the reduced Jacobian matrix.

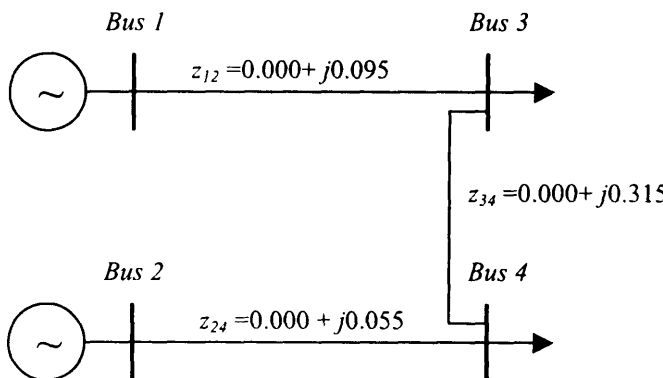


Figure 5. A 4-Bus power system for Modal analysis.

Table 1 Operating Conditions for the 4-Bus System

| Bus no. i | Complex bus voltages, \mathbf{V}_i | |
|-------------|--------------------------------------|-----------------------------------|
| | Voltage magnitude $ V_i $ (pu) | Voltage angle θ_i (deg) |
| 1 | 1.000 | +0.000 |
| 2 | 1.000 | -25.890 |
| 3 | 0.655 | -38.980 |
| 4 | 0.795 | -38.980 |

6.3.3 Determine the modal reactive power variation and modal voltage variation.

6.3.4 Determine the bus, branch, and generator participants.

Problem 6.4

Using the algorithm for static assessment, solve the following system of algebraic equations represented by:

$$\begin{aligned} 1.1x^2 - 1.1y &= 3.2 \quad \dots \dots \text{(i)} \\ 2.2x + 0.9y &= -k \quad \dots \dots \text{(ii)} \end{aligned}$$

where k is a parameter varying from $k = 0$ to k_{\max} .

Problem 6.5

The synchronous machine shown in Fig. 6 is generating 250 MW and 85 MVAR of power. The machine transient reactance is 0.200 pu, and the line reactance is

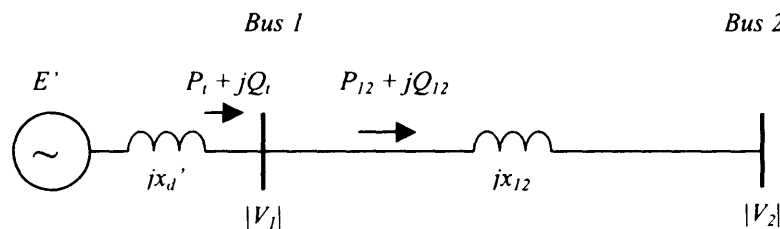


Figure 6. The impedance diagram of sample power system.

0.045 pu, both on a 100 MVA base. The value of the voltage at the infinite bus (node 2) is $1.000 + j0.000$ pu

6.5.1 Solve the power flow of the system for both low and high voltage power solutions.

6.5.2 Construct the necessary vectors required by the *VIPI* Method and compute this proximity index.

6.5.3 Consider a bolted three-phase fault occurring in the middle of the transmission line. Calculate the multiple power flow solutions (as in part 6.5.1), and the voltage instability proximity index.

6.5.4 Comment on the *VIPI* values obtained in 6.5.2 and 6.5.3.

Bibliography

- Abed, E. H. and Varaiya P. Nonlinear Oscillations in Power Systems. *Int. J. Elect. Power Energy Syst.*, 6, 1984, 37–43.
- Adkins, B., *The General Theory of Electrical Machines*. Chapman and Hall Ltd., London, 1962.
- Aggoune, M., Atlas, L. E., Cohn, D. A., El-Sharkawi, M. A., and Marks, R. J. Artificial Neural Networks for Power System Static Security Assessment, *IEEE Int. Symposium on Circuits and Systems*. Portland, OR (May 9–11 1989b) pp. 490–494.
- Aggoune, M., El-Sharkawi, M. A., Park, D. C., Damborg, M. J., and Marks II, R. J. Preliminary Results on Using Artificial Neural Networks for Security Assessment. *IEEE Proc. of 1989 PICA*. Seattle, WA, (May 1989) pp. 252–258.
- Alsac, O. and Stott, B. Optimal Load Flow with Steady-State Security, *IEEE Trans. PAS*, Vol. 94 (1974) pp. 745–751.
- Alvarado, F. L. Parallel Solution of Transient Problems by Trapezoidal Integration, *IEEE Trans. Power Appar. Syst.*, PAS-98, No. 3 (May/June 1989) p. 1080.
- Anderson, P. M. and Fouad, A. A. *Power System Stability and Control* Ames: Iowa State University Press, 1977.
- Antsaklis, P. J. Neural Networks in Control Systems, *IEEE Control Systems Magazine* (April 1989) pp. 3–5.
- Athay, T., Podmore, R., and Virmani, S. A Practical Method for Direct Analysis of Transient Stability, *IEEE Trans. Power Appar. Syst.*, PAS-98, 2, (Mar./Apr. 1979) pp. 573–584.
- Aylett, P. D. The Energy-Integral Criterion of Transient Stability Limits of Power Sys-

- tems, *Proc. of the Institution of Electrical Engineers (London)*, 105C, 8, (Sept. 1958) pp. 257–536.
- Ajjarapu, V. and Christy, C. The Continuation Power Flow: A Tool for Steady State Voltage Stability Analysis, *IEEE PICA Conference Proceedings*, (May 1991) pp. 304–311.
- Barisilal, D. Ilukaram, and Partlitasaradiy, K. An Expert System for Power System Voltage Stability Improvement, *Electrical Power & Energy Systems*, Vol. 19, no. 6, 1997, pp. 385–392.
- Bartle, R. G. *The Elements of Real Analysis*, John Wiley & Sons, Inc., New York, 1976.
- Begovic, M. and Phadke, A. G. Dynamic Simulation of Voltage Collapse, *IEEE Proceedings of PICA*. Seattle, WA (May 1–5, 1989).
- Bellman, R. and Giertz, M. On the Analytic Formalism of the Theory of Fuzzy Sets, *Information Science*, Vol. 5, 1973, pp. 149–156.
- Bergen, A. R. and Hill, D. J. Structure Preserving Model for Power System Stability Analysis, *IEEE Trans. Power Appar. Syst.*, PAS-100, Vol. 1, (Jan. 1981) pp. 25–35.
- Bergen, A. R. Analytical Methods for the Problem of Dynamic Stability, *Proc. International Symposium on Circuits and Systems*, 1977.
- Bergen, A. R. *Power System Analysis*, Prentice-Hall, Inc., Englewood Cliffs, NJ, 1986.
- Bergen, A. R., Hill, D. J., and DeMarco, C. L. A Lyapunov Function for Multi-Machine Power Systems with Generator Flux Decay and Voltage Dependent Loads, *Int. J. of Electric Power and Energy Syst.*, 8, 1, (Jan. 1986) pp. 2–10.
- Berggren, B. Transient Behavior in a Stressed Power System. MS Thesis, Iowa State University, Ames, 1988.
- Bhatia Neelu, G. Incorporation of Nonlinear Load Models and Identification of Inter-area Mode Phenomenon in the Transient Energy Function Method, Ph.D. Dissertation, Iowa State University, Ames, 1989.
- Boratyńska-Stadnicka, D. J., et al. Converting an Existing Computer Code to a Hypercube Computer, *Proceedings of the 199-9 PICA*, (May 1989) pp. 394–399.
- Braae, M. and Rutherford, D. A. Selection of Parameters for a Fuzzy Logic Controller, *Fuzzy Sets and Systems*, Vol. 2, No. 3, (1979) pp. 185–199.
- Brasch, F. M., Jr., et al. Design of Multiprocessor Structures for Simulation of Power System Dynamics, *Report No. EL-1756-1*, Palo Alto, CA.: EPRI, March 1981.
- Brown, J. E., Kovacs, K. P., and Vas, P. A Method of Including the Effects of Main Flux Path Saturation in the Generalized Equations of AC Machines, *IEEE Trans. Power Appar. Syst.*, PAS-102, No. 1, (Jan. 1983) pp. 96–102.
- Canay, I. M. Causes of Discrepancies on Calculation of Rotor Quantities and Exact Equivalent Diagrams of the Synchronous Machine, *IEEE Trans. Power Appar. Syst.*, PAS-88, No. 7, (July 1969).
- Canay, I. M. Determination of Model Parameters of Synchronous Machines, *IEE Proc.*, 130, Part B, No. 2, (March 1983) pp. 86–94.
- Cardozo, E. and Talukdar, S. N. A Distributed Expert System for Fault Diagnosis, *IEEE Transactions on Power Systems*, (May 1988) pp. 641–646.
- Carvalho, V. F. et al. Direct Analysis of Transient Stability for Large Power Systems, *EPRI Report No. EL-4980*, December 1986.

- Chandrashekhar, K. S. and Hill, D. J. Cutset Stability Criterion for Power Systems Using a Structure Preserving Model. *International Journal of Electric Power and Systems* 8, No. 3 (July 1986) pp. 146-157.
- Chang, C. S., Sutanto, D., and Lachs, W. Automatic Control of Voltage Instability by an Expert System Utilizing Pattern Recognition Techniques. *Proc. of the Tenth Power System Computation Conference*, Graz, Austria, (August 1990) pp. 1057-1064.
- Chen, G. P. and Malik, O. P. Tracking Constrained Adaptive Power System Stabilizer. *IEEE Proceedings on Generation, Transmission and Distribution*, Vol. 142, No. 2, (1995) pp. 149-156.
- Chen, G. P., Malik, O. P., Hope, G. S., Qin, Y. H., and Xu, G. Y. An Adaptive Power System Stabilizer Based on Self-Optimizing Pole-Shifting Control Strategy. *IEEE Transactions on Energy Conversion*, Vol. 8, No. 4, (1993) pp. 639-645.
- Chen, S. T., Yu, D. C., and Moghaddamjo, A. R. Weather Sensitive Short-Term Load Forecasting Using an Non-Fully Connected Artificial Neural Network. *IEEE Trans. on Power Syst.*, Vol. 7, No. 3, (Aug. 1992).
- Cheng, S.-J., Chow, Y. S., Malik, O. P., and Hope, G. S. An Adaptive Synchronous Machine Stabilizer, *IEEE Transactions on Power Systems*, Vol. PWRS-1, No. 3, (1986) pp. 101-109.
- Chiang, H. D. Analytical Results on Direct Methods for Power System Transient Stability Assessment, *Control and Dynamic Systems* (C. T. Leondes, ed.), 43, Academic Press, San Diego, CA (1991) 275-334.
- Chiang, H. D., Dobson, I., Thomas, R. J., Thorp, J. S., and Fekih-Ahmed, L. On Voltage Collapse in Electric Power Systems, *Proceedings of PICA*, (May 1-5 1989) Seattle, WA.
- Chiang, H. D., Wu, F. F., and Varaiya, P. P. Foundations of Direct Methods for Power System Transient Stability Analysis, *IEEE Trans. Circuits Syst., CAS-34* (Feb. 1987) pp. 160-173.
- Chow, J. H., (ed.). Time-Scale Modeling of Dynamic Networks with Applications to Power Systems, *Vol. 46 of lecture notes in Control and Information Sciences*, Springer-Verlag, New York, 1982.
- Chow, M. and Thomas, R. J. Neural Networks Synchronous Machine Modeling, *Proceedings of the 1989 ISCAS*, Vol. 1. Portland, OR (May 1989) pp. 495-498.
- Christie, R. D. and Talukdar, S. N. Expert Systems for On-Line Security Assessment: A Preliminary Design, *IEEE Transactions on Power Delivery*, (July 1986) pp. 736-743.
- Christie, S., Talukdar, N., and Nixon, J. C. CQR: A Hybrid Expert System for Security Assessment, *Proc. 1989 PICA*, pp. 267-273.
- Chua, L. O. and Lin, P. M. Computer-Aided Analysis of Electronic Circuits, Prentice-Hall, Inc., Englewood Cliffs, NJ, (1975).
- CIGRE Task Force 38-02-10. *Modeling of Voltage Collapse Including Dynamic Phenomena*, (1993).
- Concordia, C. Synchronous Machines, John Wiley & Sons, New York, 1951.
- Coultes, M. E. and Watson, W. Synchronous Machine Models by Standstill Frequency Response Tests, *IEEE Trans. Power Appar. Syst., PAS-100*, Vol. 4, (Apr. 1981) pp. 1480-1489.

- Cutsem, T. V. A Method to Compute Reactive Power Margins with Respect to Voltage Collapse, *IEEE Trans. on Power Systems*, Vol. 6, No. 2 (Feb. 1991) pp. 145–156.
- Cutsem, T. Van, Wchenkel, L., Pavella, M., Heilbronn, B., Goubin, M., and Gilliard, M. Decision Trees for Preventive Voltage Stability Assessment, *Proc. 2nd Int. Workshop On Bulk, Power System Voltage Phenomena—Voltage Stability and Security*. McHenry, USA, (August 1991) pp. 217–228.
- Dandeno, P. L. et al. Current Usage and Suggested Practices in Power System Stability Simulations for Synchronous Machines, *IEEE Trans. Energy Conversion*, EC-1, 1, (Mar. 1986) pp. 77–93.
- Dandeno, P. L., Kundur, P., and Schulz, R. P. Recent Trends and Progress in Synchronous Machine Modeling in the Electric Utility Industry, *IEEE Proc.*, Vol. 62, No. 7, (July 1974) pp. 941–950.
- Debs, A. Modern Power System Control and Operation, Kluwer Academic, Boston, MA (1988).
- DeMarco, C. L. and Overbye, T. J. An Energy Based Measure for Assessing Vulnerability to Voltage Collapse, *IEEE Trans. Power Syst.*, Vol. 5, No. 2, (May 1990) pp. 582–591.
- DeMarco, C. L. and Bergen, A. R. A Security Measure for Random Load Disturbances in Non-Linear Power System Models, *IEEE Trans. on CAS*, Vol. 34, No. 12, (Dec. 1987).
- DeMarco, C. L. and Overbye, T. J. An Energy Based Security Measure for Assessing Vulnerability to Voltage Collapse, *IEEE Trans. on Power Systems*, Vol. 5, No. 2, (May 1990).
- DeMarco, C. L. and Overbye, T. J. Low Voltage Power Flow Solutions and Their Role in Exit Time Based Security Measures for Voltage Collapse, *Proc. the 27th IEEE Conf. on Decision and Control*, Austin, TX, (Dec. 1988).
- Dembart, B., et al. Dynamic Stability Calculations Using Vector and Array Processors, *Report no. EL-3335*, Palo Alto, CA: EPRI, (January 1984).
- DeMello, F. P. and Concordia, C. Concepts of Synchronous Machine Stability as Affected by Excitation Control, *IEEE Trans.*, PAS-88, (Apr. 1969) pp. 316–329.
- DeMello, F. P. and Hannett, L. N. Determination of Synchronous Machine Stability Study Constants, *EPRI Report EL-1424*, 3, Electric Power Research Institute, Palo Alto, CA, (June 1980).
- DeMello, F. P. and Hannett, L. N. Representation of Saturation in Synchronous Machines, *IEEE Trans. Power Syst.*, PWRS-1, 4, (Nov. 1986) pp. 8–18.
- DeMello, F. P. and Laskowski, T. F. Concepts of Power System Dynamic Stability, *IEEE Trans. on Power Appar. and Syst.*, PAS-94 (3), (May/June 1975) pp. 827–833.
- DeMello, F. P., Nolan, P. J., Laskowski, T. F., and Undrill, J. M. Coordinated Application of Stabilizers in Multimachine Power Systems, *IEEE Trans. Power Appar. Syst.*, PAS-99, (May–June 1980) pp. 892–901.
- Dobson, I. and Chiang, H. Towards a Theory of Voltage Collapse in Electric Power Systems, *Systems & Control Letters*, (1989).
- Domme, H. W. Digital Computer Solution of Electromagnetic Transients in Single and Multiphase Networks, *IEEE Trans. PAS*, Vol. 88, No. 4, (April 1969) pp. 388–399.

- Downey, T. J., and Meyer, D. J. A Genetic Algorithm for Feature Selection, *Proceedings of the Artificial Neural Networks in Engineering Conference*, St. Louis, MO, (1994) pp. 363–368.
- Dubois, D. and Prade, H. Fuzzy Real Algebra, Some Results, *Fuzzy Sets and Systems*, Vol. 2, (1979) pp. 327–348.
- Duda, R. O. and Hart, P. E. *Pattern Classification and Scene Analysis*, John Wiley & Sons, New York (1973).
- Dynamic Security Assessment of Power Systems. In *Proceedings of the 10th Power System*
- Ebron, S., Lubkeman, D., and White, M. A Neural Network Approach to the Detection of Incipient Faults on Power Distribution Feeders, *IEEE Trans. on Power Delivery*, Vol. 5, No. 2, (April 1990) pp. 905–914.
- El-Abiad, A. H. and Nagappan, K. Transient Stability Region of MultiMachine Power Systems, *IEEE Trans. Power Appar. Syst., PAS-852*, (Feb. 1966) pp. 169–178.
- Electric Power Research Institute. Electromagnetic Transients Program (EMTP) Primer, *EPRI Report EL-4202*, Palo Alto, CA, (Sept. 1985).
- Electric Power Research Institute. Power System Planning and Operations: Future Problems and Research Needs, *EPRI Special Report EL-377-SR*, (Feb. 1977).
- Electric Power Research Institute. User Survey and Implementation Plan for EMTP Enhancements, *EPRI Report EL-3668*, Palo Alto, CA, (Sept. 1984).
- Elgerd, O. I. *Electric Energy System Theory, An Introduction*, McGraw-Hill Book Co., New York, (1982).
- El-Kady, M. A., Tang, C. K., Carvalho, V. F., Fouad, A. A., and Vittal, Dynamic Security Assessment Utilizing the Transient Energy Function Method, *IEEE Trans. Power Syst., PWRSI*, 3, (Aug. 19) pp. 284–291.
- El-Keib, A. A. and Ma, X. Application of Artificial Neural Networks in Voltage Stability Assessment, *IEEE/PES Winter Meeting*, (1995).
- El-Metwally, K. A. and Malik, O. P. Fuzzy Logic Power System Stabilizer, *IEEE Proceedings on Generation, Transmission and Distribution*, Vol. 143, No. 3, (1996) pp. 263–268.
- El-Metwally, K. A. and Malik, O. P. Parameter Tuning for a Fuzzy Logic Controller, *Proceedings of the IFAC Twentieth World Congress on Automatic Control*, Sydney, Australia, Vol. 2, (July 18–23, 1993) pp. 581–584.
- El-Sharkawi, M. A. and Huang, S. S. Query-Based Learning Neural Network Approach to Power System Dynamic Security Assessment, *Int. Symposium on Nonlinear Theory and its Applications*, Waikiki, HI (December 5–10, 1993).
- El-Sharkawi, M. A. and Huang, S. S. Application of Genetic-Based Neural Networks to Power System Static Security Assessment, *Int. Conf. On Intelligent Systems Application to Power Systems*, Montpellier, France (September 5–9, 1994a).
- El-Sharkawi, M. A., Marks, A., Damborg, R. J., Atlas, M. J., Cohn, L. E., D. A., and Aggoune, M. Artificial Neural Networks as Operator Aid for On-Line Static Security Assessment of Power Systems, *Power Systems Computation Conference*, Graz, Austria (August 19–24, 1990) pp. 895–901.
- El-Sharkawi, M. A. and Huang, S. S. Ancillary Techniques for Neural Network Applications, *IEEE World Congress on Computational Intelligence, ICNN '94*, Orlando, FL (June 28–July 2, 1994b).

- El-Sharkawi, M. A., Marks, R. J., Aggoune, M. E., Park, D. C., Damborg, M. J., and Atlas, L. E. Dynamic Security Assessment of Power Systems using Back Error Propagation Artificial Neural Networks, *Second Symposium on Expert System Application to Power Systems*, Seattle, WA (1989).
- El-Sharkawi, M. A., et al. Neural Networks and Their Application to Power Engineering, *Control and Dynamic Systems* 41, Academic Press, (1991).
- El-Sharkawi, M. A., Marks, R. J., and Weerasooriya, S. Neural Networks and Their Application to Power Engineering, in *Control and Dynamic Systems, Advances in Theory and Applications* (C. T. Leondes, ed.), Vol. 41, Part 1/4, Academic Press, San Diego, CA (1991), 2473-37 (March 1990).
- El-Sharkawi, M. A. and Atteri, R. Static Security Assessment of Power System Using Kohonen Neural Network, *Proc. Second Int. Forum on Neural Network Applications to Power Systems, ANNPS '93*, Yokohama, Japan (April 1993).
- Endrenyi, J. *Reliability Modeling in Electric Power Systems*, John Wiley & Sons, New York, (1978).
- EPRI Report. Extended Transient-Midterm Stability Package (ETMSP), EPRI EL-4610, Electric Power Research Institute, Palo Alto, CA (Jan. 1987).
- EPRI Report. Artificial Intelligence Technologies for Power System Operations, EPRI Project 1999-7, (1986).
- EPRI Report. Development of Expert Systems as On-Line Power System Operational Aids, No. EL-5635, (1987).
- EPRI Report. Power System Dynamic Analysis-Phase I, EPRI Report EL-484, Electric Power Research Institute, (July 1977).
- EPRI Project. Power System Dynamic Security Analysis Using Artificial Intelligent Systems, Phase Feasibility Evaluation, EPRI Project RP 3103-2 (1993).
- Feng, Z., Ajjarapu, V., and Long, B. Identification of Voltage Collapse Through Direct Equilibrium Tracing, *IEEE Trans. on Power Systems*, (submitted).
- Feng, Z., Ajjarapu, V., and Maratukulam, D. J. A Approach for Preventive and Corrective Control to Mitigate Voltage Collapse, *IEEE Trans. on Power Systems*, (submitted).
- Findlay, J. A., Maria, G. A., and Wong, V. R. Stability Limits for Bruce LGR Scheme, *Proc. 18th Power Systems Computation Conference*, Helsinki, Finland, (1984).
- Fischl, R., Kam, M., Chow, J. C., and Ricciardi, S. Screening Power System Contingencies Using a Back-Propagation Trained Multiperceptron, *Proc. of the 1989 ISCAS*, Vol. 1, Portland, OR (May 1989) pp. 486-489.
- Fitzgerald, A. E., Kingsley, C., and Umans, S. D. *Electric Machinery*, McGraw-Hill Book Co., New York, (1983).
- Fleming, P. J. Computer Aided Design of Regulations Using Multi Objective, In *Proceedings of IFAC Control Applications of Nonlinear Programming and Optimization*, Capri, Italy (1985) pp. 47-52.
- Forgy, C. *OPS83 User's Manual*, Computer Science Department, Carnegie-Mellon University, (1983).
- Fouad, A. A. and Stanton, S. E. Transient Stability of Multimachine Power System, Parts I and III, *IEEE Trans. Power Appar. and Syst.*, (July 1981) pp. 3408-3424.
- Fouad, A. A. and Vittal, V. Power System Transient Stability Assessment Using the Transient Energy Function Method, *Control and Dynamic Systems* (C. T. Leondes, ed.), 43, Academic Press, San Diego, CA (1991) 115-184.

- Fouad, A. A. et al. Calculation of Generation-Shedding Requirements of the B. C. Hydro System Using Transient Energy Functions, *IEEE Trans. Power Appar. and Syst.*, Vol. 1, No. 2 (May 1986) pp. 17–24.
- Fouad, A. A., et al. Transient Stability Margin as a Tool for Dynamic Security Assessment, EPRI Report No. EL-1755, March (1981).
- Fouad, A. A., et al. Transient Stability Program Output Analysis, Report no. EL-4192, Palo Alto, CA: EPRI, August (1985).
- Fouad, A. A., S. Venkataraman, and Davis, J. A. An Expert System for Security Trend Analysis of a Stability-Limited Power System, Paper no. 91WM216-2 PWRS presented at the 1991 Power Engineering Society Winter Meeting, New York, (February 1991).
- Fouad, A. A., Vittal, V., and Oh, T. Critical Energy for Transient Stability Assessment of a Multimachine Power System, *IEEE Trans. on Power Appar. and Syst.*, Vol. PAS-103, (1984) pp. 2199–2206.
- Fukunaga, K. and Koontz, W. L. G. Application of Karhunen-Loeve Expansion to Future Selection and Ordering, *IEEE Trans. Computers*, Vol. c-19, No. 4 (April 1970).
- Fukunaga, K. Introduction to statistical pattern recognition, Academic Press, New York (1972).
- Galiana, F. D. and Lee, K. On the Steady State Stability of Power Systems, *Proc. of PICA*, Toronto, (May 1977).
- Gate, E. C., Hemmaplardh, K., Manke, J. W., and Gelopoulos, D. P. Time Frame Notion and Time Response of the Models in Transient, Mid-Term and Long-Term Stability Programs, *IEEE Trans. Power Appar. Syst.*, PAS-103, 1, (Jan. 1984) pp. 143–150.
- Geeves, S. CIGRE TF 38.02.09, (conv.) *Assessment of Practical Fast Transient Stability Methods; State of the Art*, ELECTRA, No. 153 (April 1994).
- Gelopoulos, D. P. Midterm Simulation of Electric Power Systems, EPRI Report EL-596, Electric Power Research Institute, Palo Alto, CA, (June 1979).
- Glandy, M. G. and Pai, M. A. Analysis of Voltage Collapse in Power Systems, *Proc. of the 21st NAPS*, (Oct. 1989).
- Grainger, J. J. and Stevenson, W. D. *Power System Analysis*, McGrawHill, New York (1994).
- Greene, S., Dobson, L., and Alvarado, F. L. Sensitivity of the Loading Margin to Voltage Collapse with Respect to Arbitrary Parameters, *IEEE Trans. Power Syst.*, PWRS 1, (May 1996) pp. 845–850.
- Gross, C. A. *Power System Analysis*, John Wiley & Sons, Inc., New York, (1986).
- Guckenheimer, J. and Holmes, P. Nonlinear Oscillations, Dynamic Systems, and Bifurcation of Vector Fields, Springer-Verlag, New York, (1983).
- Hahn, W. *Stability of Motion*, Springer-Verlag, Berlin, (1967).
- Hakimimashhadi and Heydt, G. T. Fast Transient Security Assessment, *IEEE PWRS*, Vol. 102 (December 1983) pp. 3816–3824.
- Hammons, T. J. and Winning, D. J. Comparisons of Synchronous Machine Models in the Study of the Transient Behavior of Electrical Power Systems, *Proc. IEEE*, Vol. 118, No. 10, (Oct. 1971) pp. 1442–1458.
- Harris, M. R., Lawrenson, P. J., and Stephenson, J. M. Per-unit Systems with Special Reference to Electrical Machines, Cambridge University Press, Cambridge, England, (1970).

- Hartana, R. K. and Richards, G. G. Harmonic Source Monitoring and Identification Using Neural Networks, *IEEE PES 1990 Winter Meeting*, Paper No. 90 WM 238-6 PWRS, Atlanta, GA, (Feb. 1990).
- Hasan, A. R., Martis, T. S., and Sadral Ula, A. H. M. Design and Implementation of a Fuzzy Controller Based Automatic Voltage Regulator for a Synchronous Generator, *IEEE Trans. on Energy Conv.*, Vol. 9, No. 3, (1994) pp. 550–557.
- Hassan, M. A. M., Malik, O. P., and Hope, G. S. A Fuzzy Logic Based Stabilizer for a Synchronous Machine, *IEEE Trans. on Energy Conv.*, Vol. 6, No. 3, (1991) pp. 407–413.
- Hawing, J. N., Choi, J. J., Seho Oh, and Marks, R. J. 11. Query-Based Learning Applied To Partially Trained Multilayer Perceptrons, *IEEE Trans. Neural Networks*, No. 1 (January 1991) pp. 131–136.
- Heffron, W. G. and Phillips, R. A. Effects of Modern Amplitude Voltage Regulator in Under Excited Operation of Large Turbine Generators, *AIEE Trans.*, PAS-71, (Aug. 1952) pp. 692–697.
- Heydt, G. T. *Computer Analysis Methods for Power Systems*, Macmillan Publishing Co., New York, (1986).
- Hirsch, M. W. and Smale, S. *Differential Equations, Dynamical Systems, and Linear Algebra*, Academic Press, New York, (1974).
- Hiyama, T. Robustness of Fuzzy Logic Power System Stabilizers Applied to Multi Machine Power System, *IEEE Trans. on Energy*, Vol. 9, No. 3, (1994) pp. 451–459.
- Hsu, Y. Y. and Cheng, C. H. Design of Fuzzy Power System Stabilizers for Multi-Machine Power Systems, *IEEE Proceedings on Generation, Transmission and Distribution*, Vol. 137, Part C, No. 3, (May 1990), pp. 233–238.
- IEEE Committee Report. Computer Representation of Excitation Systems, *IEEE Trans. Power Appar. Syst.*, PAS-87, 6, (June 1968) pp. 1460–1464.
- IEEE Committee Report. Dynamic Models for Steam and Hydro Turbines in Power System Studies, *IEEE Trans. Power Appar. Syst.*, PAS-92, 6, (Nov/Dec 1973) pp. 1904–1915.
- IEEE Committee Report. Excitation System Models for Power System Stability Studies, *IEEE Trans. Power Appar. Syst.*, PAS-100, 2, (Feb. 1981) pp. 494–509.
- IEEE PES Engineering Education Committee. IEEE Tutorial Course: Digital Simulation of Electrical Transient Phenomena, *IEEE Tutorial 81 EHO 173-5-PWR*. IEEE, New York, (1980).
- IEEE Std 115A. IEEE Trial Use Standard Procedures for Obtaining Synchronous Machine Parameters by Standstill Frequency Response Testing, *Supplement to ANSI-IEEE Std. 115-1983*, IEEE, New York, (1984).
- IEEE. Symposium on Synchronous Machine Modeling for Power System Studies, *83TH0101-6-PWR, Tutorial at IEEE/PES 1983 Winter Meeting*, New York, (1983).
- IEEE. Special Publication 90TH0358-2-PWR, *Voltage Stability of Power Systems: Concepts, Analytical Tools and Industry Experience*, (1990).
- Ignizio, J. P. Generalized Goal Programming—An Overview, Computer and Ops. Research (Pergamon Press) 10, No. 4, (1983) pp. 277–289.
- Ilic-Spong, M., Crow, M. L., and Pai, M. A. Transient Stability Simulation by Waveform

- Relaxation Methods, *IEEE Trans. on Power Syst.* PWRS-2, No. 4 (November 1987) pp. 943-952.
- Ipakchi, K. R., Brandwajan, A., El-Sharkawi, M. A. and Cauley, G. Neural Works for Dynamic Security Assessment of Large-Scale Power Systems: Requirements Overview, *Proc. 1st International Forum on NNAPS*, Seattle, WA (1991) pp. 65-71.
- Iwan S. N. and Tan, O. T. Neural-Net Based Real-Time Control Capacitors Installed on Distribution Systems, *IEEE Trans. on Power Delivery*, Vol. 5, No. 1, (1990) pp. 266-272.
- IEEE Working Group on Dynamic System Performance of the System Planning Subcommittee, IEEE Power Engineering Society Power System Engineering Committee, Symposium on Adequacy and Philosophy of Modeling: Dynamic System Performance, *IEEE Publication 75 CHO 970-4-PWR IEEE*, New York, (1975).
- Jackson, W. B. and Winchester, R. L. Direct and Quadrature Axis Equivalent Circuits for Solid-Rotor Turbine Generators, *IEEE Trans. Power Appar. Syst.*, PAS-88, 7, (July 1969) pp. 1121-1136.
- Jaris, J. and Galiana, F. D. Quantitative Analysis of Steady-State Stability in Power Networks, *IEEE Trans. on PAS*, Vol. 100, (Jan. 1981).
- Jeyasurya, B. Power System Loading Margin Estimation Using Artificial Neural Network, *28th North American Power Symposium*, M.I.T., MA, (November 1996).
- Kakimoto, N., Ohsawa, Y., and Hayashi, M. Transient Stability Analysis of Electric Power Systems via Lure Type Lyapunov Functions, Parts II, and I, *IEEE Trans. of Japan*, 98, 5/6, (May/June 1978).
- Kam, F. R., Chow, M. J. C., and Ricciardi, S. An Improved Hopfield Model for Power System Contingency Classification, *Proc. of the 1990 ISCAS*, Vol. 3, New Orleans, LA (May 1990) pp. 2925-2928.
- Kessel, P. and Glavitsck, H. Estimating the Voltage Stability of a Power System, *IEEE Transactions*, 1986, PWRD-1(3), pp. 346-354.
- Kundur, P. *Power System Stability and Control*, McGraw Hill, New York, (1993).
- Kwanty, H. G., et al. Static Bifurcation in Electric Power Networks: Loss of Steady State Stability and Voltage Collapse, *IEEE Trans. on CAS*, Vol. CAS-33, No. 10, (Oct. 1986) pp. 981-991.
- Khorasani, K., Pai, M. A., and Sauer, P. W. Modal-Based Stability Analysis of Power Systems Using Energy Functions, *Int. J. of Electric Power and Energy Systems*, Vol. 8, No. 1, (January 1986) pp. 11-16.
- Kimball, E. W. *Power System Stability: Synchronous Machines*, Dover Publications, Inc., New York, (1956).
- Kohonen, T. Self-Organized Formation of Topologically Correct Feature Maps, *Biol. Cybernetics*, No. 43 (1982) pp. 59-69.
- Kokotovic, P. V. and Sauer, P. W. Integral Manifold as a Tool for Reduced Order Modeling of Nonlinear Systems: A Synchronous Machine Case Study, *IEEE Trans. Circuits Syst.*, Vol. 36, No. 3, (Mar. 1989) pp. 403-410.
- Kokotovic, P. V., Khalil, H. K., and O'Reilly, J. *Singular Perturbation Methods in Control: Analysis and Design*, Academic Press Inc., London, (1986).
- Komai, K., Sakaguchi, T., and Takeda, S. Power System Fault Diagnosis with an Expert

- System Enhanced by the General Problem Solving Method, *IASTED Conference*, Bozeman, Montana (Aug. 1986).
- Kosko, B. *Fuzzy Thinking*, Prentice-Hall, Englewood Cliffs, NJ, (1993).
- Kosko, B. *Neural Networks and Fuzzy Systems: A Dynamic Approach to Machine Intelligence*, Prentice-Hall, Englewood Cliffs, NJ (1992).
- Krause, P. C. *Analysis of Electric Machinery*, McGraw-Hill, New York, (1986).
- Kreyszig, E. *Advanced Engineering Mathematics*, John Wiley & Sons, Inc., New York, (1972).
- Kuffel, E. and Abdullah, M. *High-Voltage Engineering*, Pergamon Press, Oxford, England, (1970).
- Kundur, P. *Power System Stability and Control*, McGraw-Hill, New York, (1994).
- Kundur, P., Klein, M., Rogers, G. J., and Zywno, M. S. Application of Power System Stabilizer for Enhancement of Overall System Stability, *IEEE Trans. PWRS-4*, (May 1989) pp. 614-626.
- La Scala, M., et al. A Highly Parallel Method for Transient Stability Analysis, In *Proceedings of the 1989 PICA*, (May 1989) pp. 380-386.
- Larsen, E. V. and Swann, D. A. Applying Power System Stabilizers, Part I to III, *IEEE Trans. on Power Appar. and Syst.*, Vol. PAS-100, No. 6, (1981) pp. 3017-3046.
- Lee, B. H. and Lee, K. Y. A Study on Voltage Collapse Mechanism in Electric Power Systems, *IEEE Trans. on Power Appar. Syst.*, Vol. 6, No. 3, (Aug. 1991) pp. 966-974.
- Lee, B. H. and Lee, K. Y. Dynamic and Static Voltage Stability Enhancement of Power Systems, *IEEE Transactions on Power* Vol. 8, No. 1, (Feb. 1993) pp. 231-238.
- Lee, C. C. Fuzzy Logic in Control Systems: Fuzzy Logic Controller-Parts I and II, *IEEE Trans. on Syst. Man and Cybernetics*, Vol. 20, No. 2, (1990) pp. 404-435.
- Lee, S. Y., et al. Parallel Power System Transient Stability Analysis on Hypercube Multiprocessors, In *Proceedings of the 1989 PICA*, (May 1989) pp. 400-406.
- Lesieutre, B. C., Sauer, P. W., and Pai, M. A. Sufficient Conditions on Static Load Models for Network Solvability, In *Proc. 24th Annual North Amer. Power Symp.*, Reno, NV (Oct. 1992) pp. 262-271.
- Liu, C. C. and Dillon, T. S. State-of-the-Art of Expert System Applications to Power Systems, *Int. J. Electrical Power and Energy Systems*, (1989) in press.
- Liu, C. C. Dynamic Security Assessment: The Role of Expert Systems, minutes of the July 27, 1988 meeting of the Dynamic Security Assessment Working Group meeting, Power System Engineering Committee of the Power Engineering Society, IEEE.
- Liu, C. C., Lee, S. J., and Venkata, S. S. An Expert System Operational Aid for Restoration and Loss Reduction of Distributed Systems, *IEEE Trans. on Power Delivery*, (May 1988) pp. 619-626.
- Liu, C.-W., Chang, J.-S., Su, M.-C. Neuro-Fuzzy Networks for Voltage Security Monitoring Based on Synchronized Phaser Measurements, *IEEE Summer Meeting*, Berlin.
- Liu, C. C. and Vu, K. T. Analysis of Tap-Changer Dynamics and Construction of Voltage Stability Regions, *IEEE Trans. on CAS*, Vol. 36, (April 1989) pp. 575-590.
- Liu, C. C. Characterization of a Voltage Collapse Mechanism due to the Effects of On-Line Tap Changers, *Proceedings of IEEE International Symposium on Circuits and Systems*, San Jose, CA, Vol. 3, (May 1986) pp. 1028-1030.

- Lopes, J. A., Pecas, F. M., Fernandes, Matos, M. A. Fast Evaluation of Voltage Collapse Risk Using Pattern Recognition Techniques, *Paper APT 300-20-09 accepted for presentation at the IEEE/NTUA Athens Power Tech Conference*, Athens, Greece, (Sept. 5–8, 1993).
- Long, B. and Ajjarapu, V. The Sparse Formulation of ISPS and Its Application to Voltage Stability Margin Sensitivity and Estimation, *IEEE Trans. on Power Appar. Systems*, (Oct. 1997).
- Lyapunov, A. M. The General Problem of the Stability of Motion (in Russian), *The Mathematical Society of Kharkov, Russia, 1892*, English translation, Taylor and Francis Ltd., London, (1992).
- Medanic, M., Illic-Spong and Christensen, J. Discrete Models of Slow Voltage Dynamics for Under Load Tap-Changing Transformer Coordinations, *IEEE Trans. on Power Appar. Syst.*, Vol. 2, (Nov. 1987) pp. 873–882.
- Morison, G. K., Gao, B., and Kundur, P. Voltage Stability Using Static and Dynamic Analysis, *IEEE/PES Summer Meeting*, Seattle, WA, (July 12–16 1992) 92 SM 590-0-PWRS.
- Ma, X., El-Keib, A. A., Smith, R. E., and Ma, H. Estimation of Voltage Stability Margins Using Artificial Neural Networks, *Proc. Of the 26th NAPS*, (Sept. 1994).
- Maeda, M. and Murakami, S. A Self-Organizing Fuzzy Controller, *Fuzzy Sets and Systems*, Vol. 51, (1992) pp. 29–40.
- Magnusson, P. C. Transient Energy Method of Calculating Stability, *AIEE Trans.*, Vol. 66, (1947) pp. 747–755.
- Mansour, Y., Vaahedi, E., Chang, A. Y., Corns, B. R., Garrett, B. W., Demaree, K., Athay, T., Cheung, K., and Hydro, B. C. On-Line Transient Stability Assessment (TSA): Model Development, Analysis and Post-Processing, *IEEE Trans. Power Appar. Syst.*, Vol. 10, No. 1, (Feb. 1995) 241–253.
- Marathe, H. Y., Liu, C. C., Tsai, M. S., Rogers, R. G., and Maurer, J. M. An On-Line Operational Expert System with Data Validation Capabilities, *Proc. 1989 PICA*, pp. 56–63.
- Marceau, R. J., Mailhot, R., and Galiana, F.D. A Generalized Shell for Dynamic Security Analysis in Operation Planning, *IEEE Trans. on Power Systems*, Vol. 8, No. 3 (1993), pp. 1098–1106.
- Maria, G. A., Tang, C., and Kim, J. Hybrid Transient Stability Analysis, Paper no. 89SM684-2-PWRS, *IEEE Summer Power Meeting*, Longbeach, CA, (July 1989).
- McCalley, J. D., et al. Power System Security Boundary Visualization Using Neural Networks, *Bulk power system dynamics and Control IV-Restructuring*, (August 24–28, 1998) Santorini, Greece.
- McClelland, E. C. and Van Home, P. R. Fast Voltage Predication Using a Knowledge Based Approach, *IEEE Trans. PWRS*, (February 1983) pp. 315–319.
- Michel, A. N., Fouad, A. A., and Vittal, V. Power System Transient Stability Using Individual Machine Energy Functions, *IEEE Trans. Circuits Syst., CAS-30*, Vol. 5, (May 1983) pp. 266–276.
- Miller, R. K., and Michel, A. N. *Ordinary Differential Equations*, Academic Press, New York, (1983).
- Minnich, S. H. et al. Saturation Functions for Synchronous Generators from Finite Ele-

- ments, *Paper 87 WM 207-4, IEEE/PES 1987 Winter Meeting*, New Orleans, LA, (Feb. 1–6, 1987).
- Minnich, S. H. Small Signal, Large Signals and Saturation in Generator Modeling, *IEEE Trans. Energy Conversion, EC-1*, Vol. 1, (Mar. 1986) 94102.
- Mori, H., Tamaru, Y., and Tsuzuki, S. An Artificial Neural-Net Based Technique for Power System Dynamic Stability with the Kohonen Model, *IEEE Proc. of 1991 PICA*, Baltimore, MD, (May 1991) pp. 293–301.
- Miranda, V. and Saraiva, J. T. Fuzzy Modeling of Power Systems Optimal Load Flow, *IEEE Trans. on Power Appar. Systems*, Vol. 7, No. 2, (1992) pp. 843–849.
- Mori, H. and Tamura, Y. On Voltage Security On-Line Index in Electric Power Systems, *Power System Engineering Committee of IEEE of Japan*, Paper No. PE85-41, (June 1985) (in Japanese).
- Mori, H. and Tsuzuki, S. Determination of Power System Topological Observability Using the Boltzmann Machine, *IEEE Proc. of 1990 ISCAS*, New Orleans, LA, (May 1990) pp. 2938–2941.
- Mori, H. and Tsuzuki, S. Estimation of Critical Points on Static Voltage Stability in Electric Power Systems, *IFAC Proc. of 1990 Symp. on Power Systems and Power Plant-Control*, Seoul, Korea, (Aug. 1990) pp. 550–554.
- Mori, H. and Tsuzuki, S. Power System Topological Observability Analysis Using a Neural Network Model, *Proc. of Second Symposium on Expert Systems Application to Power Systems*, Seattle, WA (July 19) pp. 385–391.
- Mori, H. Decentralized Power System Voltage Control Using Artificial Neural Networks, *Proc. of 1992 IEEE ISCAS*, San Diego, CA, (May 1992) pp. 1701–1704.
- Mori, H. Monitoring and Control of Power System Voltage Stability Using an Artificial Neural Networks, *Preprints-of 1992 IFAC/IFIP/IMACS International Symposium on Artificial*
- Mori, H. and Tama-ru, Y. An Artificial Neural-Net Based Approach to Monitoring Power System Voltage Stability, *Proc. of Nulk Power System Voltage Phenomena II: Voltage Stability and Security*, Deep Creek Lake, MD, (Aug. 1991) pp. 347–358.
- Mori, H., Itou, K., Uematsu, H., and Tsuzuki, S. An Artificial Neural Net Based Method for Predicting Power System Voltage Harmonics, " *IEEE Trans. on Power Delivery*, Vol. 7, No. 1, (Jan. 1982) pp. 402–409.
- Mori, H., Uematsu, H., Tsuzuki, S., Sakurai, T., Kojima, Y., and Suzuki, K. Identification of Harmonic Loads in Power Systems Using an Artificial Neural Networks, *Proc. of Second Symposium on Expert Systems Application in Power Systems*, Seattle, WA, (July 1989) pp. 371–378.
- Niebur, D. and Germond, A. J. Power System Static Security Assessment Using Kohonen Neural Network Classifier, *IEEE Trans. Power Delivery* (May 1992) pp. 865–871.
- Nims, J. W., El-Keib, A. A., and Smitk, R. E. Contingency Ranking for Voltage Stability Using a Genetic Algorithm, *Electric Power Systems Research*, (October 1996).
- Nuhanovic, A., Glavic, M., and Prijaca, N. Validation of Clustering Algorithm for Voltage Stability Analysis on the Bosnian Electric Power System, *IEEE Proceedings on Generator Transmission and Distribution*, Vol. 145, No. 1, (1998) pp. 21–26.
- Obadina, O. O. and Berg, G. J. VAR Planning for Power System Security, *IEEE Trans. on Power Systems*, Vol. 4, No. 2, (May 1989).

- O'Grandy, M. G. and Pai, M. A. Analysis of Voltage Collapse in Power Systems, *Proc. of the 21st NAPS*, Rolla, MO, (Oct. 1989).
- Overbye, T. J. and Demarco, C. L. Improved Techniques for Power System Voltage Stability Assessment Using Energy Methods, *IEEE Trans. on Power Systems*, Vol. 6, No. 4, (Nov. 1991).
- Ojo, J. D. and Lipo, T. A. An Improved Model for Saturated Salient Pole Synchronous Motors, *Paper 88 SM 614-0, IEEE/PES 1988 Summer Meeting*, Portland, OR, (July 24-29, 1988).
- Olive, D. W. New Techniques for the Calculation of Dynamic Stability, *IEEE Trans. Power Appar. Syst., PAS-85*, Vol. 7, (July 1966).
- Ostojic and Heydt, G. T. Transient Stability Assessment by Pattern Recognition in the Frequency Domain, *IEEE Trans. Power Appar. Syst.*, Vol. 6, (February 1991) pp. 231-237.
- Osyczka, A. Multicriterion Optimization in Engineering, Ellis Horwood, Ltd. (Division of John Wiley), New York, (1984).
- Overbye, T. J. and DeMarco, C. L. Improved Techniques for Power System Voltage Stability Assessment Using Energy Based Sensitivities, *IEEE Trans. on Power Syst.*, Vol. 6, No. 3, (Aug. 1991).
- Overbye, T. J. and DeMarco, C. L. Voltage Stability Enhancement Using Energy Based Sensitivities, *IEEE Trans. on Power Syst.*, Vol. 6, No. 3, (Aug. 1991).
- Overbye, T. J. Application of an Energy Based Security Method to Voltage Instability in Electrical Power System, *Dissertation*, University of Wisconsin-Madison, (1991).
- Overbye, T. J., Dobson, I., and DeMarco, C. L. Q-V Curve Interpretations of Energy Measures for Voltage Security, *IEEE/PES 1993 Winter Meeting*, (Jan 31-Feb 5, 1993).
- Padiyar, K. R. and Chosh, K. K. Direct Stability Evaluation of Power Systems with Detailed Generator Models Using Structure Preserving Energy Functions, *Int. J. Electr. Power and Energy Syst.*, Vol. 11, No. 1, (Jan. 1989) pp. 47-56.
- Padiyar, K. R. and Sastry, H. S. Y. Topological Energy Function Analysis of Stability of Power Systems, *Int. Electr. Power and Energy Syst.*, Vol. 9, I-, (Jan. 1987) pp. 9-16.
- Pai, M. A. et al. Direct Method of Stability Analysis in Dynamic Security Assessment, *Paper No. 1.1/A4, IFAC World Congress*, Budapest, (July 1984).
- Pai, M. A. *Computer Techniques in Power System Analysis*, Tata McGraw-Hill, New Delhi, India, (1979).
- Prabhakara, F. and Heydt, G. T. Review of Pattern Recognition Methods for Rapid Analysis of Transient Stability, *IEEE-PES Technical Report on Rapid Analysis of Transient stability*, #87TH0169-3-PWR (1987).
- Pai, M. A. *Energy Function Analysis for Power System Stability*, Kluwer Academic Publishers, Boston, (1989).
- Pai, M. A. Power System Stability Studies by Lyapunov-Popov Approach, *Proc. 5th IFAC World Congress*, Paris, (1972).
- Pai, M. A., *Power System Stability*, North Holland Publishing Co., New York, (1981).
- Pai, M. A., Laufenberg, M., and Sauer, P. W. Some Clarification in the Transient Energy Function Method, *Int. J. of Elec. Power, and Energy Systems*, Vol. 18, No. 1, (1996), pp. 65-72.

- Pang, C., Kprabhakara, F. S., El-Abiad, A. H., and Koivo, A. I. Security Evaluation Power Systems Using Pattern Recognition, *IEEE Trans. PAS*, Vol. 93, (May/July 1974) pp. 969-976.
- Pao, Y. and Sobajic, D. J. Combined use of Unsupervised and Supervised Learning Dynamic Security Assessment, *Proc. of PICA*, Baltimore, MD, (May 1991) pp. 278-284.
- Park, D. C., El-Sharkawi, M. A., Marks, R. J., Aggoune, M. E., Atlas, L. E., and Damborg, M. J. Electric Load Forecasting Using an Artificial Neural Network, *IEEE PES 1990 Summer Meeting*, Paper No. 90 SM 377-2 PWRS, Minneapolis, MN, (July 1990).
- Patrick, E. *Fundamentals of Pattern Recognition*, Prentice-Hall Information and System Science Series, Englewood Cliffs, NJ, (1972).
- Pavella, M. and Murthy, P. C. *Transient Stability of Power Systems: Theory and Practice*, John Wiley & Sons, Inc., New York, (1994).
- Peng, T. M., Hubele, N. F., and Karady, G. G. Advancement in the Application of Neural Networks, for Short-Term Load Forecasting, *IEEE Trans. on Power Appar. Syst.*, Vol. 1, No. 1, (Feb. 1992).
- Peterson, T. S. *Calculus with Analytic Geometry*, Harper & Row Publishers, Inc., New York, (1960).
- Policy in a Fuzzy-Logic Controller. *Electronics Letters*, Vol. 11, (1975) pp. 625-626.
- Pottle, C. Array and Parallel Processors in On-Line Computations. Report No. EL-2363, Palo Alto, CA: EPRI, (April 1982).
- Prabhashankar, K. and Janischewsyj, W. Digital Simulation of Multimachine Power Systems for Stability Studies, *IEEE Trans. on Power Appar. Syst.*, PAS-87, Vol. 1, (Jan. 1968) pp. 73-79.
- Proceedings 8th Power Systems Computation Conference, Helsinki, Finland, (1984) pp. 1063-1069.
- Proceedings of Symposium on Expert Systems Application to Power Systems, Stockholm, Helsinki, (August 1988).
- Proceedings of the IEEE Third International Conference on fuzzy Logic, San Francisco, CA, (1993).
- Proceedings of the Workshop on Power System Security Assessment, Iowa State University, (1988). Library of Congress Catalog No 88-091408.
- R. I. II. Artificial Neural Networks for Power Systems Static Security Assessment, *Proc. of the ISCAS*, Vol. 1, Portland, OR (May 1989a).
- Rahimi, F. A., Lauby, M. C., Wrubel, J. N., and Lee, K. W. Evaluation of the Transient Energy Function Method for On-Line Dynamic Security Analysis, *IEEE Trans. on Power Appar. Syst.*, Vol. 8, No. 2, (May 1993) pp. 497-506.
- Rajagopalan, C. Dynamic of Power Systems at Critical Load Levels, Ph.D. Thesis, University of Illinois, Urbana-Champaign, (1989).
- Rajagopalan, C., Lesieutre, B., Sauer, P. W., and Pai, M. A. Dynamic Aspects of Voltage/Power Characteristics, *IEEE Trans. Power Appar. Syst.*, Vol. 7, (Aug. 1992) pp. 990-1000.
- Rajagopalan, C., Sauer, P. W., and Pai, M. A. An Integrated Approach to Dynamic and Static Voltage Stability, *Proc. 1989 American Control Conference*, Pittsburgh, PA, Vol. 3, (June 1989) pp. 1231-1235.

- Ribbens-Pavefla, M. And Evans, F. J. Direct Methods for Studying of the Dynamics of Large Scale Electric Power Systems—A Survey, *Automatica*, Vol. 21, No. 1, (1985) pp. 1–21.
- Ramey, D. G. and Skooglurid, J. W. Detailed Hydrogovernor Representation for System Stability Studies, *IEEE Trans. Power Appar. Syst., PAS-89*, Vol. 1, (Jan. 1970) pp. 106–112.
- Ramo, S., Whinnery, J. R., and Van Duzer, T. *Fields and Waves in Communication Electronics*, John Wiley & Sons, Inc., New York, (1965).
- Ranjan, R. K., Pai, M. A., and Sauer, P. W. Analytical Formulation of Small Signal Stability Analysis of Power Systems with Nonlinear Load Models, In *Sadhana Proc. in Eng. Sci.*, Indian Acad. Sci., Bangalore, India, Vol. 18, No. 5, (Sept 1993) 869–889, Errata, Vol. 20, No. 6, (Dec. 1995) p. 971.
- Rankin, A. W. Per-Unit Impedance of Synchronous Machines, *AIEE Trans.*, Vol. 64 (Aug. 1945).
- Rastgoufard, P., Yazdankhah, A., and Schlueter, R. A. Multi-Machine Equal Area Based Power System Transient Stability Measure, *IEEE Trans. on Power Appar. Syst.*, Vol. 3, No. 1, (February 1988) pp. 188–196.
- Russell, B. D. and Watson, K. Power Substation Automation Using a Knowledge Based System Justification and Preliminary Field Experiments, *IEEE Trans. on Power Delivery*, (October 1987) pp. 1090–1097.
- Sobajic, D. and Pao, Y. Artificial Neural Net based Dynamic Security Assessment Electric Power Systems, *IEEE Trans. PWRS*, Vol. 4, (February 1989) pp. 22–228.
- Sobajic, D., Pao, Y. H., and Dolce, J. On-Line Monitoring and Diagnosis of Power System Operating Conditions Using Artificial Neural Networks, *Proc. of the 19 ISCAS*, Vol. 3, Portland, OR, (May 1989) pp. 2243–2246.
- Stagg, G. W. and El-Abiad, A. H. *Computer Methods in Power System Analysis*, McGraw-Hill Book Co., New York, (1968).
- Stott, B. Power System Dynamic Response Calculations, *Proc. IEEE*, Vol. 67, (Feb. 1979), pp. 219–241.
- Su, C.-C. and Hsu, Y.-Y. Fuzzy Dynamic Programming: An Application to Unit Commitment, *IEEE Trans. on Power Appar. Syst.*, Vol. 6, No. 3, (1991) pp. 1231–1237.
- Systems Control Inc. Development of Dynamic Equivalents for Transient Stability Studies, Final Report EPRI EL-456, Electric Power Research Institute, Palo Alto, CA, (Apr. 1977).
- Tamura, Y., Iba, K., and Iwamoto, S. A Method for Finding Multiple Load Flow Solutions for General Power Systems, *IEEE/PES Winter Meeting*, NY, (1980) Paper 043-0.
- Tamura, Y., Mori, H., and Iwamoto, S. Relationship Between Voltage Instability and Multiple Load Flow Solutions in Electric Power Systems, *IEEE Trans. on PAS*, Vol. PAS-102, No. 5, (May 1983).
- Tamura, Y., Nakanishi, Y., and Iwamoto, S. On the Multiple Solution Structure, Singular Point and Existence Condition of Multiple Load Flow Solutions, *IEEE/PES Winter Meeting*, NY, (1980) Paper 043-0.
- Tamura, Y., Sakamoto, K., and Tayama, Y. Voltage Instability Proximity Index (VIPI)

- Based on Ill-Conditioned Power Systems, *Proc. of the 27th conf. on Decision and Control*, Austin, TX, (Dec. 1988).
- Tranuchit, A. and Thomas, R. J. A Posturing Strategy Against Voltage Instability in Electric Power Systems, *IEEE Trans. on Power Appar. Syst.*, (Feb. 1988) pp. 87-93.
- Tamura, Y., Mori, H., and Iwamoto, S. Relationship Between Voltage Instability and Multiple Load Flow Solutions in Electric Power Systems, *IEEE Trans. on Power Appar. Syst.*, Vol. PAS-102, No. 5, (May 1983) pp. 1115-1125.
- Tinney, W. F., Brandwajm, V., and Chan, S. M. Sparse Vector Methods, *IEEE Trans. Vol. PAS-104*, No. 2, (Feb. 1985).
- Tomsovic, K., Liu, C. C., Ackerman, P., and Pope, S. An Expert System Dispatchers' Aid for the Isolation of Line Section Faults, *IEEE Trans. on Power Delivery*, (July 1987) pp. 736-743.
- Treinen, R. T., Vittal, V., and Kliemann, W. An Improved Technique to Determine the Controlling Unstable Equilibrium Point in a Power System, *IEEE Trans. on Circuits and Systems-I, Fundamental Theory and Application*, Vol. 43, No. 4, (Apr. 1996) 313-323.
- Toomey, L. J. *IBM Systems Journal* Vol. 27, No. 4 (1988) pp. 416-435.
- Tou, J. T. and Gonzalez, R. C. *Pattern Recognition Principles*, Addison Wesly, MA (1974).
- Tranuchit, A. and Thomas R. J. A Posturing Strategy Against Voltage Instability in Electric Power Systems, *IEEE Trans. on Power Appar. Syst.*, (Feb. 1988).
- Tucker, S. G. The IBM 3090 System: An Overview, *IBM Systems Journal* Vol. 25, No. 1 (1986) pp. 4-20.
- Tylavsky, D. J., et al. Frequency Domain Relaxation of Power System Dynamics, In *Proceedings of the 1989 PICA*, (May 1989) pp. 387-393.
- U.S. Energy Research and Development Administration. Systems Engineering for Power: Status and Prospects, *Proceedings Engineering Foundation Conference, CONF-750867*, Henniker, NH, (Aug. 17-22, 1975).
- Varaiya, P. P., Wu, F. F., and Chen, R.-L. Direct Methods for Transient Stability Analysis of Power Systems: Recent Results, In *Proceedings IEEE* 73 (December 1985) pp. 1703-1715.
- Venckov, V. A., et al. Estimation of Electrical Power System Steady State Stability in Load Flow Calculations, *IEEE Trans. Power Appar. Syst.*, Vol. 94, (May/June 1975).
- Venkov, V. A., Stroev, V. A., Idelchick, V. I., and Trasov, V. I. Estimation of Electrical Power System Steady State Stability in Load Flow Calculations, *IEEE Trans. Power Appar. Syst.*, Vol. 94, (May/June 1975).
- Venkatasubramanian, V., Schattler, H., and Zaborszky, J. Voltage Dynamics: Study of a Generator with Voltage Control, Transmission and Matched MW Load, *IEEE Trans. Autom. Contr.*, Vol. 37, (Nov. 1992) pp. 1717-1733.
- Verghese, G. C., Perez-Arriaga, I. J., and Scheweppe, F. C. Selective Modal Analysis with Applications to Electric Power Systems, Part I and II, *IEEE Trans. Power Appar. Syst.*, PAS-101 (Sept. 1982) pp. 3117-3134.
- Vidyasagar, M. *Nonlinear Systems Analysis*, Prentice-Hall, Englewood Cliffs, NJ, (1978).

- Vittal, V., et al. Derivation of Stability Limits Using Analytical Sensitivity of the Transient Energy Margin, *Paper No. 89WM207-2 PWRS IEEE/PES 1989 Winter Meeting*, New York.
- Vittal, V., Bhatia, N., and Fouad, A. A. Analysis of the Inter-Area Mode Phenomenon in Power Systems Following Large Disturbances, *Paper No. 91WM228-7-PWRS presented at the 1991 Power Engineering Society Winter Meeting*, New York. (February 1991).
- Vittal, V., Fouad, A. A., and Kundur, P. Determination of Transient Stability-Constrained Plant Generation Limits, *Proceedings of the IFAC Symposium on Automation and Instrumentation for Power Plants*, Bangalore, India, (December 15–17, 1986) pp A-8-1 through A-8-5.
- Vittal, V., Prabhu, G. M., and Lim, S. L. A Parallel Computer Implementation of Power System Transient Stability Assessment Using the Transient Energy Function Method, *IEEE Trans. Power Syst.*, Vol. 6, No. 2, (February 1991) pp. 167–173.
- Vulnerability to Voltage Collapse. *IEEE Trans. on Power Appar. Syst.*, Vol. 5, No. 2, (May 1990).
- Wada, N. et al. A Real Time Expert System for Power System Faults Analysis, *IASTED Conference*, Bozeman, Montana (August 1986).
- Weerasooriya, S. and El-Sharkawi, M. A. Towards Static Security Assessment of Large Scale Power Systems Using Neural Networks, *IEEE Proc. C: Generation, Transmission and Distribution*, Vol. 139, No. 1 (January 1992) pp. 64–70.
- Weerasooriya, S. and El-Sharkawi, M. A. Dynamic Security Assessment of Power Systems Using Neural Networks, *Int. Conf. on Expert Systems Appl. for the Electric Industry*, Phoenix, AZ (December 8–10, 1993).
- Weerasooriya, S. and El-Sharkawi, M. A. Use of Karhunen Loeve Expansion in Training Neural Networks for Static Security Assessment, *Proc. 1st Int. Forum on NNA Ps.*, Seattle, WA (July 1991) pp. 59–64.
- Weerasooriya, S. Application of Neural Networks for Classification and System Identification in Power Systems, Ph.D. Thesis, University of Washington (1992).
- Wehenkel, L., Van Cutsem, Th., and Ribbens-Pavella, M. An Artificial Intelligence Framework for On-Line Transient Stability Assessment of Power Systems, *IEEE Trans. Power Appar. Systems*, (Ma 1989) pp. 789–800.
- Werners, B. Aggregation Models in Mathematical Programming, in *Mathematical Models for Decision Support*, G. Mitra (ed.), Birkhäuser, Berlin, (1988), pp. 295–319.
- Willems, J. Direct Methods for Transient Stability Studies in Power System Analysis, *IEEE Trans. Autom. Control, A C-16*, 4, (July–Aug. 1971) pp. 1469–1481.
- With Nose Curve using Homotopy Continuation Method, *IEEE/PES 1990 Summer Meeting*, Minneapolis, Minnesota, (July 15–19, 1990).
- Wollenberg, B. and Sakaguchi, T. Artificial Intelligence in Power System Operations, *Proceedings of the IEEE*, (Dec. 1987) pp. 1678–1685.
- Wollenberg, B. F. Feasibility Study for an Energy Management System Intelligent Alarm Processor, *IEEE Trans. Power Syst.*, (May 1986) pp. 241–247.
- Wood and Wollenberg, B. F. *Power Generation, Operation & Control*, John Wiley & Sons, Inc., New York, (1984).
- Woodson, H. H. and Melcher, J. R. *Electromechanical Dynamics Part I: Discrete Systems*, John Wiley & Sons, Inc., New York, (1968).

- Xie, G. and Ramshaw, R. S. Nonlinear Model of Synchronous Machines with Saliency. *Paper 85 SM 347-0, IEEE/PES 1985 Summer Meeting*, Vancouver, Canada, (July 14–19, 1985).
- Xue, Y., Gao, Z., Zhu, J., and Liu, J. A Planning Decision Support Expert System for Transient and Dynamic Security of Power Systems. *Proc. 1989 Expert Systems Application to Power Systems*, pp. 218–224.
- Young, C. C. and Webler, R. M. A New Stability Program for Predicting the Dynamic Performance of Electric Power Systems, *Proceedings of the American Power Conference*, Vol. 29, Chicago, (1967) pp. 1126–1138.
- Young, C. C. Equipment and System Modeling for Large Scale Stability Studies, *IEEE Trans. Power Appar. Syst.*, PAS-91, 1, (Jan./Feb. 1972) pp. 99–109.
- Young, C. C. The Synchronous Machine, *IEEE Tutorial Course on Modern Concepts of Power System Dynamics*, 70 M 62-PWR, Institute of Electrical and Electronics Engineers, New York, (1970).
- Young, T. and Fu, K. S. *Handbook of Pattern Recognition Image Processing*, Academic Press, New York, (1986).
- Yu, Y. N. *Electric Power System Dynamics*, Academic Press, New York, 1983.
- Zadeh, L. A. Fuzzy Sets as a Basis for a Theory of Possibility, *Fuzzy Sets and Systems*, Vol. 1, No. 1, (1978) pp. 3–28.
- Zadeh, L. A. Fuzzy Sets, *Information and Control*, Vol. 8, (1965) pp. 338–353.
- Zadek, Lofti A. *Knowledge Representation in Fuzzy Logic*, Kluwer Academic Publishers, (1992).
- Zhang, B. S. and Edmunds, J. M. Self-Organizing Fuzzy Logic Controller, *IEEE Proceedings D*, Vol. 139, No. 5, (1992) pp. 460–464.
- Zhang, Y., Chen, G. P., Malik, O. P., and Hope, G. S. An Artificial Neural Network-Based Adaptive Power System Stabilizer, *IEEE Transactions on Energy Conversion*, Vol. 8, No. 1, (1993) pp. 71–77.
- Zhou, Q., Davidson, J., and Fouad, A. A. Application of Artificial Neural Networks in Power System Security and Vulnerability Assessment, *IEEE/PES 1993 WM*, (Jan 31–Feb 5, 1993).
- Zimmermann, H.-J. and Zysno, P. Latent Connectives in Human Decision Making, *Fuzzy Sets and Systems*, Vol. 4, No. 1, (1980) pp. 37–51.

This page intentionally left blank

Index

- abc*-Phase sequence, 15, 16
- Accelerating power, 72
- Accelerating torque, 46
- Activation functions, 182
- Activation level, 182
- Active load, 5
- Active power, 12, 21
- AGC, 158
- AI (*see* Artificial Intelligence)
- Alpha cut, (α -cut), 211
- Angular momentum, 48
- ANN (*see* Artificial Neural Network)
- ANN-Based TEF, 222
 - algorithm, 223
 - learning process, 222
- Antecedents, 250
- Apparent power, 13
- Approximate reasoning, 214–215
- ARG (*see* Automatic Rule Generation)
- Armature windings, 22
- Artificial Intelligence, 221, 259, 296
- Artificial Neural Networks, 9, 177, 178
 - architecture, 180
- Artificial neuron (*see* Neuron)
- Automatic Rule Generation, 254
- Automatic Voltage Regulators (*see* AVR)
- Average power, 12
- AVR, 98, 255, 135
- Axon, 181
- Back propagation, 183, 188
- Balanced 3-phase systems, 15
- Base value, 26
- Belief measure, 215
- Bellman, 206
- Benefit-to-cost index, 9
- Bifurcation points, 148
- Bifurcation theory, 9, 141
- Branch switching, 87
- Bulk power system, 4
- Carpenter, 184
- CCT (*see* Critical clearing time)
- Cell body, 181
- Center of inertia, 122

- Certainty factors, 201
 Chaos theory, 292
 Clustering, 184
 Complex power, 11, 13
 COI (*see* Center of inertia)
 Condition number, 143
 Confidence scales (*see* Certainty factors)
 Conjugate current, 13
 Continuation method, 145, 147
 Control valve position, 42
 Corrector, 90, 149
 Counter propagation, 184
 Critical clearing time, 234
 Cylindrical rotor synchronous machine, 55
 Defuzzification, 215, 219, 249
 Delta-connection, 18
 Dendrites, 181
 Direct axis, 56
 Direct axis synchronous reactance, 54
 Distribution system, 4
 dq0 transformation, 24
 Dynamic security, 289
 Dynamic security assessment (DSA), 8, 221
 Dynamic stability, 164
 Dynamic voltage stability, 157
 algorithm, 166
 equilibrium point, 161
 fast subsystems, 161
 linearization, 163
 load flow, 161
 slow subsystems, 160
 Edison Electric, 1
 EHV (*see* Extra high voltage)
 Eigenvalues, 114, 156
 Electrical torque, 46
 Electric power system, 3
 fuzzy theory, 209
 Electromechanical transient, 109
 Energy function, 127, 130
 Energy Systems Network Laboratory, 97
 Equal area criteria, 73–75
 Error signal, 187
 ES (*see* Expert system)
 ESNL (*see* Energy systems network laboratory)
 Euclidean distance, 178
 Euclidean norm, 147
 Excitation control, 6
 Excitation control system, 37
 Excitation system, 40
 model, 36
 Exciter model, 37
 linear differential equations, 39
 Expert reasoning, 214
 Expert system, 9, 176, 191
 characteristics, 192
 definition, 191
 DSA, 238
 inference engine, 191
 knowledge acquisition, 273
 knowledge base, 191
 man-machine interface, 191
 measures, 200
 probability, 199
 rule-based structure, 240
 subjective probability, 199
 Extra high voltage, 2, 135, 259
 FACTs, 158
 FIRE (*see* Fuzzy Inference Reverse Engineering)
 FL (*see* Fuzzy logic)
 FLC (*see* Fuzzy Logic Controller)
 FLPSS (*see* Fuzzy Logic Power System Stabilizer)
 Flux, 55
 Flux linkages, 23
 Four-machine power system, 239
 Frequency dependent load, 34
 Fuzzification, 249
 Fuzzy inference, 251
 Fuzzy Inference Reverse Engineering, 254
 Fuzzy logic, 9, 177, 204
 correlation method, 218
 linguistic variable, 215
 monotonic method, 217

- [Fuzzy logic]
parameter tuning, 252
power system stabilizer, 248, 255
rules, 252
- Fuzzy Logic Controller, 248, 249
- Fuzzy proposition, 216
- Fuzzy sets, 206
definition, 213
operations, 212
- Fuzzy set theory, 177
- Gate opening, 40
- Generator
real power, 118
reactances, 54
short circuit current, 53
- Generator model, 52
- Generator voltage, 6
- Generic electric power system, 4
- Global error function, 189
- Grossberg Outstar algorithm, 184
- Hidden layer, 187
- Hidden node, 226
- High Voltage DC links, 133
- High-Voltage Direct Current, 2
- HVDC transmission control, 7
- HVDC (*see* High-Voltage Direct Current)
- Hydraulic turbine model, 40
- IEEE 57-bus test system, 278
- IEEE 39-bus system, 227, 229
- IEEE working group, 134
- Inductance
mutual, 23
self, 23
- Induction motor, 43
equivalent circuit, 44
slip, 44
torque, 43
- Inertia, 46
- Inertia constant, 28, 47–50
- Inference chain, 196
- Inference engine, 175, 196, 276
- Inference, rules, 217
- Infinite bus, 63, 68, 118
- Instantaneous current, 11
- Instantaneous power, 11
- Integral-square error, 125
- Integration methods, 9
- Integration techniques
Euler method, 91
modified Euler method, 91
predictor corrector, 89
Runge-Kutta method, 9, 94
sampling method, 97
trapezoidal method, 9, 94
waveform relaxation, 9
- Intelligent systems, 175
approaches, 179
- Jacobian matrix, 141, 143
reduced, 156
- KB (*see* Knowledge base)
- KBVCDP (*see* Knowledge-Based Voltage Collapse, Detection and Prevention)
- k-finite difference equations, 89
- Kinetic energy, 47–48
- Kirchoff's law, 16
- Knowledge base, 176, 194, 249
- Knowledge-based system, 195, 238
- Knowledge-Based Voltage Collapse, Detection and Prevention, 273
implementation, 274, 278
structural design, 275
- Kohonen layer, 184
- Learning algorithms, global error, 183
- L Index, 140
- Linear programming, 9
- Linear system
sensitivity, 144
- Line voltage, 16
- Load characteristics, 32
- Load models
constant power, 149
dynamic, 43, 158
linear model, 150
- Load parameters, 33

- Load representation, 85
 Local stability, 111
 LP (*see* Linear programming)
 LTC, 277
 LU decomposition, 148
 Lyapunov
 function, 115
 theorem, 112
- Machine models, 59
 Machine rating, 49
 Machine switching, 88
 Marceau, 290
 Maximum norm, 147
 Mechanical torque, 46
 Membership function, 211, 250
 Minimum singular value, 142
 Min-max inference, 217
 Mismatch, 145
 Modal analysis, 156
 Models
 exciter, 38
 generator, 52
 governing system, 40, 42
 hydraulic turbines, 40
 PSS, 39
 static electric network, 10
 static loads, 32
 synchronous machine, 21
 terminal voltage transducer, 39
 voltage regulator, 38
 Modified Euler method, 91
 Mutual inductance, 23
- Necessity measure, 215
 NERC (*see* North American Electric Reliability Council)
 Neural networks, 221
 learning algorithms, 183
 training, 183
 Neuron, 180
 New England 39-bus power system, 264
 Newton-Raphson, 145, 156
 New York power pool, 132
 n-Generator System Model, 117
 Nodal matrix method, 83
- Normalization (*see* per unit representation)
 North American Electric Reliability Council, 3
- OPF (*see* Optimal power flow)
 Optimal power flow, 9
- Parameterization, 151
 Participation factor, 157, 262
 Pendulum, 114
 kinetic energy, 115
 potential energy, 115
 Per unit representation, 25
 PF (*see* power factor)
 Phase diagram, 13, 56-60
 Phase-shift transformers, 7
 Phase voltage, 16
 PID (*see* Proportional-Integral Derivative)
 Plausibility measure, 215
 Post-fault curve, 81
 Power angle curve, 70, 120
 wound rotor machine, 66
 Power factor, 11, 12, 14
 Power failures, 132
 Power flow, 165
 linearized model, 165
 Power interchange, 6
 Power relationships, 20
 Power system
 basic elements, 5
 complex power concepts, 11
 security assessment, 45
 three-phase systems, 14-21
 Power system stability, 7
 Power system stabilizers, 38, 158
 Power triangles, 13
 Predictor, 149
 Predictor-corrector step, 147
 Pre-fault curve, 81
 Prime mover, 40
 Prime mover controls, 6
 Probability measure, 215
 Proportional-Integral Derivative, 254
 Proposition, 216
 PSS (*see* Power system stabilizers)

- p.u. (*see* Per unit representation)
P-V curve, 146, 151
- QP (*see* Quadratic programming)
Quadratic programming, 9
Quadrature axis, 56
Quality of power, 5
Quantization, 210
Q-V curve, 146
Q-V sensitivity, 156, 167
- Ray, James J., 97
- RBS (*see* Rule-based system)
Reactive capability limits, 31
Reactive load, 5
Reactive power, 6, 13, 21
Reactors, 7
Robust ANN, 222
Rotor voltage, 21
Rule-based system, 194
Rules
 divergence, 276
 selecting models for VC detection, 277
 selecting VC parameters, 276
Runge-Kutta, 9, 95
- Saliency effects, 65
Salient pole synchronous machine, 56, 57
- Self inductance, 23
Sensitivity analysis, 146
SEP (*see* Stable equilibrium point)
Sigmoidal activation function, 225
Sigmoidal function, 182
SIL, 135
Speed regulation, 6
Squashing function, 182
Stability
 angle, 8
 BCU, 131
 boundary, 127
 definitions, 111
 equal area method, 72
 lemma, 112
 Lyapunov's theorem, 112
 positive definite function, 112
- [Stability]
 SEPs, 260
 simple pendulum, 114
 single-machine system, 118
 UEP, 129
 voltage, 8
Stability assessment, 63, 71–82
 fuzzy expert systems, 205
 TEF method, 121
 voltage, 132
Stable equilibrium point, 69, 130, 260
Star connection (*see* WYE connection)
Static assessment
 algorithm, 153
Static load model, 32
Static security assessment, 8
Static stability, 163
Static var compensators, 6
Static voltage compensating devices, 133, 158
Static voltage stability assessment
 modal analysis, 158
Stator voltage, 21
Steam turbine, 42, 43
Steam turbine model, 42
Sub-transient equations 59
Sub-transient reactance, 50, 53
Sub-transmission system, 4
SVCs (*see* Static voltage compensating devices)
Swing equation, 46, 72
Switched capacitors, 6
Synapse, 181
Synchronous condensers, 6
Synchronous machine, 3
 classic model, 27
 dynamic model, 29
 equivalent circuits, 29–30
 modeling, 21–30
 network representation, 84
 rotor circuit, 22
 stator circuit, 22
 steady state model, 30
 subtransient model, 30
 transient equations, 58
 transient model, 30
 voltage equations, 22

- Synchronous machine modeling, 21
 System base, 26
 System faults, 86
- Tamura, Y., 141
 Tangent vector, 150
 Tap-changing transformers, 7
 Target value, 187
 Taylor expansion, 94
 TEF (*see* Transient energy function)
 Three-phase power, 20, 21
 Three-phase system, 14
 Threshold function, 182
 Time frames
 models, 139
 RLC components, 139
 Training algorithms, 184
 Grossberg Outstar, 184
 Kohonen, 184
 Training process, 263
 output vector, 183
 Transient droop, 41
 Transient energy function, 110, 120,
 185, 222
 flowchart, 128
 integral-squared error (ISE), 122
 stored energy, 123
 Transient equations, 58
 Transient reactance, 53, 50
 Transient stability, 68, 109
 algorithm, 92–93, 98–104
 concepts, 68
 Transient stability assessment, 222
 Transient swing, 121
 Transmission network, 4
 Trapezoidal rule, 9
 Truth functions (*see* Membership function)
 Turbo generator
 high pressure, 49
 low pressure, 49
- UEP (*see* Unstable equilibrium point)
 ULTCs, 135
 Uncertainty, 197
- Unstable equilibrium point, 69, 130, 260
 Unsupervised training, 183
- VAR, 265
 VC (*see* voltage collapse)
 VIPI, 141
 Voltage collapse, 134, 135
 classifications, 134
 definition, 134
 detection, 148, 272
 prediction methods, 138
 predictor step, 150
 prevention, 272
 time-frame, 136
 Voltage instability, 159 (*see* Voltage stability problems)
 classification, 159
 Voltage instability indicators, 140
 Voltage regulator, 37
 Voltage stability assessment, 132, 165,
 259
 ANN-based, 260
 techniques, 140
 time-frame, 139
 Voltage stability
 modeling, 136
 preventive control, 168
 time-frame (Carson Taylor), 137
 Voltage stability problems, 138
 classification, 138
 Voltage transducer, 38
 V-Q sensitivity, 157
 VSTAB, (EPRI), 165, 263
- Water hammer effect, 40
 Water starting time, 40
 Waveform relaxation, 9
 Wye-connection, 16
- Y-connection, 15 (*see* Wye-connection)
 Y-Bus or admittance matrix, 85,
 118
- Zadeh, 177
 ZIP load model, 34